ABSTRACT

Title of Dissertation: THE SIGNIFICANCE OF SEA ICE ALGAE IN THE PACIFIC ARCTIC DETERMINED BY HIGHLY BRANCHED ISOPRENOID BIOMARKERS

Chelsea Wegner Koch, Doctor of Philosophy, 2021

Dissertation directed by: Dr. Lee Cooper

Professor, University Maryland Center for Environmental Science

Our current understanding of ice algae as a carbon source at the base of the Arctic food web is limited because of difficulties unequivocally distinguishing sympagic (sea ice) from pelagic primary production once assimilated by consumers. For this study, I tested the utility of highly branched isoprenoids (HBI), which are unusual lipids produced by diatoms. This includes a biomarker found exclusively in Arctic sea ice termed the ice proxy with 25-carbon atoms (IP_{25}) and two other HBIs with sea ice and pelagic sources. HBI measurements in the Pacific Arctic (the northern Bering and Chukchi seas) were sparse compared to the rest of the Arctic prior to this investigation. Analysis of surface sediments and cores collected across the continental shelf revealed a latitudinal gradient of increasing sympagic HBIs. Some of the highest concentrations of IP_{25} recorded in the Arctic were found in the Chukchi Sea. Fluxes of IP_{25} indicated year-round export of ice algal lipids in this region. Persistent diatom fluxes and rapid burial of sympagic carbon are likely a sustaining resource for infaunal communities throughout the year. As such, HBIs were

measured in benthic primary consumers and indicated an elevated utilization of ice algae by surface and subsurface deposit feeders, while suspension feeders by contrast showed greater pelagic organic carbon utilization. Sympagic organic carbon signatures were largely influenced by the HBI content in local sediments. This led to the identification of two species with possible dependencies on ice algae. This method was extended to transient, higher trophic organisms by measurement of HBIs in Pacific walrus livers harvested during subsistence hunting activities. Relative HBI proportions were shown to relate to foraging location and revealed a higher reliance on sympagic organic carbon by female and juvenile Pacific walruses relative to males. This is likely due to a greater requirement for sea ice habitat by females and calves in the Bering and Chukchi seas. This study showed that HBI biomarkers can robustly track sea ice organic carbon contributions through the Pacific Arctic food web and should be considered alongside other trophic markers in future monitoring efforts in response to climate change.

THE SIGNIFICANCE OF SEA ICE ALGAE IN THE PACIFIC ARCTIC DETERMINED BY HIGHLY BRANCHED ISOPRENOID BIOMARKERS

by

Chelsea Wegner Koch

Dissertation submitted to the Faculty of the Graduate School of the
University of Maryland, College Park, in partial fulfillment
of the requirements for the degree of
Doctor of Philosophy
2021

Advisory Committee:
Professor Lee W. Cooper, Chair
Professor Jacqueline M. Grebmeier
Professor Andrew Heyes
Professor Ryan Woodland
Dr. Thomas A. Brown

Dedication

At the time of writing this dissertation, we were in the midst of a global pandemic with the novel coronavirus (COVID-19) causing over half a million deaths in the United States. This was the backdrop to months of political instability leading to an insurrection at the US Capitol and a summer of civil unrest driven by racial inequities, injustices and police brutality. This may all sound pretty depressing – and indeed it was. However, during all of this chaos and trying to finish my PhD, there was a silver lining. I brought a new life into this world.

I dedicate this dissertation to my daughter, Thalia. I was three months pregnant when Jackie, Lee and I traveled to St. Lawrence Island in the middle of winter, to discuss our research with the tribal councils in Savoonga and Gambell. We arrived in Savoonga on a tiny plane from Nome after waiting out blizzard conditions on the island. We had intended on visiting Gambell but never managed to make it due to weather. I will never forget that you were along for the adventure – as we rode on snow machines and trudged through the dark and blustery snow. I hope that this spirit of exploration stays with you. I also realize that the Arctic we know today will be unrecognizable when you grow up. I hope this will serve as a reminder to you that no matter how small you think your contributions are to the world, every little bit you can do counts.

Acknowledgements

None of this would have been possible without the support of my advisor, Lee Cooper. Lee is always willing to help other researchers improve their manuscripts or give advice, myself included. I have valued his support out at sea (helping me sample mud), in the lab, and improving my manuscripts. Lee has helped me become a more seasoned researcher. I also could not have done this without Jackie Grebmeier. Lee and Jackie have been great mentors that have helped me thrive throughout my PhD program. Jackie and Lee are tireless in their pursuits and have taught me firsthand all the hard work and grit required to get your fieldwork done. Their leadership in the Arctic research community is admirable – serving on so many different international research and planning committees – and have inspired me to pursue early career leadership positions in several Arctic organizations myself. I feel lucky to have worked alongside this dynamic duo.

Our lab is a fantastic group of people that have made this work enjoyable. Christina Goethel has been a supportive lab-mate, shipmate and travel buddy. Together we have learned that *Astarte* clams can survive anything and have had a good laugh or two about the priapulid worms we bring up in the Van Veen grabs. Needless to say, we have spent many hours together spraying mud off the back deck of the Laurier. Cédric Magen was instrumental in analyzing my stable isotope samples and generally anything else I needed help with in the lab. Laura Gemery was critical to getting this project together by sharing some of her mud from prior cruises and has also been a wonderful colleague and friend. I could always count on Alynne Bayard to discuss GIS and what shows were worth watching. I also thank Stephanie Soques for taking the time to teach me in the sorting lab.

My committee members supported my growth and development as a scientist. Dr. Tom Brown has been a sounding board throughout my PhD program. He taught me everything I needed to know about HBI analysis when I visited his lab in Scotland and was always willing to answer any question I had

along the way. Dr. Andrew Heyes and Cheryl Clark made it possible for me to set up this research at the Chesapeake Biological Laboratory and were always available to help. Cheryl taught me the skills to maintain and operate the gas chromatograph – mass spectrometer detector for which I am so grateful. Dr. Ryan Woodland was integral in setting up our clam HBI depuration experiment at the lab and providing the lawn chairs needed to hold it all together. While not officially committee members, Dr. Catherine Lalande and Dr. Karen Frey, have been important mentors for me on this PhD journey and it has been enriching to have collaborated with them on this research.

I had the privilege to sail with some amazing scientists that were helpful in a number of ways and I hope to continue working with. This group includes Luisa Young, Shea Wyatt, Sarah Ann-Questel, Dr. John Nelson, Sophie Spiliotopoulos, Clare Gaffey and Sarah Zimmerman. Our time on the CCGS *Sir Wilfrid Laurier* were some of my favorite memories from my PhD and I will never forget them. A special thanks to these people for always having a good sense of humor even though we were all tired and sore.

I also have to thank my dear friend, Dr. Emily Osborne, for all of her words of encouragement and our discussions about my research over coffee. Our science adventures together began in 2012 in South Carolina, the Knauss Fellowship reunited us in Washington, D.C. years later and then again we both wound up in the Arctic. Having had someone to navigate through all of this with and share these experiences has made it so much more meaningful. I was so grateful we had the opportunity to sail together on the *Healy*. She continuously exemplifies a strong, dedicated and professional female scientist and I sincerely hope our science careers continue to intersect.

And of course, none of this would have been possible without my husband, Dave. He has been unwavering in his support of me throughout this entire journey. He gave me the encouraging nudge I needed to leave my job at the US Antarctic Program to pursue this pesky idea that I wanted to get my PhD. He has also listened to me run through enough practice talks that he is able to almost accurately tell

you what IP_{25} is. Finding his little notes of encouragement hidden in my suitcase every time I had to do fieldwork always reminded me that I could count on him and made our time apart easier. He has helped me achieve everything I wanted and more. I am so grateful to have such a supportive partner in all of my aspirational pursuits.

I also acknowledge the Aleut/Unangan, Iñupiat and Yupik lands we visited during our field work in Unalaska, Utqiaġvik, Nome and Savoonga. Co-production of knowledge and Indigenous-led research is necessary to achieve truly inclusive work that meets the urgent needs and challenges Arctic residents face due to climate change. I have been learning what this means and trying to build these bridges during my PhD program, but recognize that additional efforts are needed to provide these communities stability and equity. I will always make this a priority in my future interactions and projects in the Arctic.

Table of Contents

List of Tables

List of Figures

List of Abbreviations

BARC	Barrow Canyon
CEO	Chukchi Ecosystem Observatory
CHIR	Chirikov Basin
CSIA	Compound specific isotope analysis
DBO	Distributed Biological Observatory
DMSP	Defense Meteorological Satellite Program
GC-MS	Gas chromatograph–mass spectrometer
HBI	Highly branched isoprenoid
HLY	United States Coast Guard Cutter *Healy*
HTLP	High trophic level prey
IP_{25}	Ice proxy with 25 carbon atoms
$IPSO_{25}$	Ice proxy for the Southern Ocean with 25 carbon atoms
IRMS	Isotope ratio mass spectrometer
P/S	Predator/scavenger
NECS	Northeast Chukchi Sea
SDF	Surface deposit feeder
SECS	Southeast Chukchi Sea
SLIP	St. Lawrence Island polynya
SSMIS	Special Sensor Microwave Imager/Sounder
SSDF	Subsurface deposit feeder
SUS	Suspension feeder
SUS/SDF	Suspension/Surface deposit feeder
SWL	Canadian Coast Guard *Sir Wilfrid Laurier*

1. Introduction

1.1. Sea ice habitat in the Arctic

Arctic sea ice provides habitat to a wide diversity of organisms (e.g. Horner 1989, Horner et al. 1992, Arrigo 2017, Bluhm et al. 2017, Caron et al. 2017). These organisms range from the smallest of bacteria, archaea and viruses (reviewed by Deming et al. 2017), eukaryotes (Poulin et al. 2011), seabirds (e.g. Divoky et al. 2015, Ramírez et al. 2017), to marine mammals (reviewed by Laidre et al. 2015, Laidre & Regher 2017). Not all Arctic organisms necessarily live in or on the ice but a number of organisms [e.g. amphipods, Arctic cod (*Boreogadus saida*), bowhead whales (*Balaena mysticetus*), narwhals (*Monodon Monoceros*)] are dependent on their association with the ice for key life history events (Gradinger & Bluhm 2004, Carmen et al. 2016, Laidre & Regehr 2017). The sea ice has also been referred to as an inverted benthos because of organisms resembling those on the seafloor and benthic species that spend part of their life cycle in the ice (Arndt & Swadling 2006, Mundy & Meiners 2021). In the shallow seas across the Arctic shelves, this relationship is evident in the tight coupling between the sea ice and the benthos (Grebmeier et al. 2006a, Søreide et al. 2013). With the Arctic predicted to have ice free summers by the 2030s (Wang et al. 2018) these diverse and uniquely adapted organisms are at risk of losing their habitat (Macias-Fauria & Post 2018). This dissertation assesses organisms spanning different trophic levels, habitats and connections with the sea ice, but with a focus on investigating the contributions of ice-associated and pelagic primary producers (*i.e.* ice algae and phytoplankton, respectively) and the implications of declining sea ice habitat in response to climate change.

The structure of sea ice is an important factor in the development of ice-associated primary producers (Horner et al. 1992, Mundy et al. 2007, Arrigo 2017). The interconnected network of brine channels and pockets found within sea ice, particularly at the ice–water interface, provides a complex habitat with access to the nutrients and conditions required to host a variety of endemic species (Horner 1989). Many of these organisms become entrained during sea ice formation (Garrison et al. 1983, Kauko et al. 2018). Small suspended particles in the water column serve as condensation nuclei for ice crystal formation (Krembs et al. 2000, Arrigo 2017). These particles may themselves be vegetative diatoms or resting spores in the water column from a prior bloom or particles resuspended from the sediments during storm events in the autumn (Cota et al. 1991). Another mechanism of entrainment occurs with the formation of small needles of ice (*i.e.* frazil ice), which act like a comb, sweeping up particles from the seawater as the ice crystals aggregate and float to the surface. The aggregation of ice tends to occur horizontally at first and eventually becomes thick enough for ice to begin extending down vertically (Weeks & Ackley 1986). Frazil ice plays a relatively minor role in the Arctic when compared to the Antarctic (Weeks & Ackley 1986, Petrich & Eicken 2017). In the Arctic, congelation ice is more common, where consolidated sheets of columnar ice growth occur at the lower margins (Cota et al. 1991, Petrich & Eicken 2017). The formation of new ice is referred to as first year ice and is typically favored for biological activity (Horner et al. 1992, Gradinger 2009, Kauko et al. 2018). Ice that survives through the summer season and thickens over the winter is referred to as multiyear ice and tends to host fewer microbial sea ice communities (Horner et al. 1992, Olsen et al. 2017, Kauko et al. 2018).

Pack ice typically forms over the continental shelf and central Arctic Ocean, drifting with the wind and currents (Weeks & Ackley 1986). Approximately 75% of diatoms are

incorporated during the first few months of sea ice formation from the surrounding ice and water column while the remainder accumulate with this drifting pack ice (Hop et al. 2020). The actively accreting portion during the formation of congelation or pack ice is full of crevasses within the bottom few centimeters (Horner 1989, Cota et al. 1991). This is referred to as the skeletal layer and is where most of the biological activity occurs (Cota et al. 1991, Horner et al. 1992, Gradinger 2009, Arrigo 2014). As the skeletal layer is forming, seawater is incorporated within its porous structure. This process is increased if the skeletal layer formation occurs under rapid and turbulent conditions (Arrigo 2014). Salts, nutrients, gases and biogenic material within the seawater can thus also be incorporated into the sea ice (Cota et al. 1991). As the temperature decreases and the seawater begins to freeze, ions including salt precipitate out and are rejected from the ice lattice through tubes and channels (Weeks & Ackley 1986, Horner et al. 1992, Krembs et al. 2000). These brine channels create a drainage system where the salinity can exceed 150 near the surface but generally salinities are similar to surrounding sea water (i.e. ~32) at the ice-water interface (Arrigo 2014). Microbial organisms adapted to these extreme salinities, low temperatures and variable conditions are able to thrive in the brine channels (Thomas & Dieckmann 2002).

Horner et al (1992) categorized four vertical layers of sea ice habitat including the surface, interior, bottom and sub-surface communities. The productive bottom layer of the sea ice is typically dominated by pennate diatom assemblages of *Nitzschia frigida* Grunow 1880 (Poulin et al. 2011). As the sea ice begins to thin, melt ponds may form on the surface; these are generally nutrient limited and thus inhibit growth to some degree (Sørensen et al. 2017). However, when seawater floods the surface, a new supply of nutrients is provided (Horner et al. 1992, Sørensen et al. 2017). The sub-surface includes strand (*i.e.* long, colonial) communities of centric diatoms (Cota et al. 1991). These colonial organisms form a

mucilaginous excretion, binding cells together and to the ice, allowing them to extend 2–4 meters into the water column (Gosselin et al. 1997, Boetius et al. 2013, Fernández-Méndez et al. 2015, Wiedmann et al. 2020). The most common taxa with this morphology in the Arctic is the centric sea ice diatom *Melosira arctica* Dickie 1852 (Poulin et al. 2011) but it also occurs with various ice-associated pennate species (Assmy et al. 2013).

There are endemic ice-associated consumers that rely on the sea ice for grazing on algae and to escape predation, examples include Arctic cod (*B. saida*) and several species of gammarid amphipods (Gradinger & Bluhm 2004). Two species of gammarid amphipods, *Gammarus wilkitzkii* and *Apherusa glacialis,* are permanent residents of Arctic sea ice and have adapted their reproductive strategies to the variable conditions of sea ice as a survival mechanism (Poltermann et al. 2000). There are also a number of heterotrophic and mixotrophic protists, including various flagellates (including dinoflagellates) and ciliates, that graze on ice algae (Caron et al. 2017). However, only ~1% of algae biomass is consumed from the ice by these micrograzers (Michel et al. 1996, Mundy & Meiners 2021). A similar proportion of total ice algae standing stock (~1%) is consumed by sea ice meiofauna (e.g. nematodes, rotifers and crustaceans) (Gradinger et al. 2005). A majority of ice algal production is transferred into pelagic and benthic food webs, rather than the sympagic food web (Michel et al. 1996, Grebmeier et al. 2006a, Boetius et al. 2013, Wiedmann et al. 2020).

Sea ice also serves as an important platform for larger organisms including ice seals, walruses, seabirds and polar bears (Moore & Huntington 2008, Kovacs et al. 2011, Divoky et al. 2015, Jay et al. 2017, Laidre & Regehr 2017). These organisms use the sea ice for important life history functions and face great challenges with declining sea ice (Laidre et al. 2015, Macias-Fauria & Post 2018). One of the most iconic examples in the Arctic, the polar bear (*Ursus maritimus*), uses the sea ice for hunting, traveling and mating (Stirling &

Derocher 1993). The decline of sea ice and earlier break up has been linked to the decreased survival of polar bears in Hudson Bay (Regehr et al. 2007) and increased land use ashore from the Chukchi Sea (Rode et al. 2015). Pacific walruses (*Odobenus rosmarus divergens*) haul out on sea ice to forage offshore, rest between dives and long migrations, molt, nurse calves, give birth and for mating (Fay 1982). Declining sea ice has been linked to increased coastal haulouts of walruses numbering in the tens of thousands, which have resulted in large mortality events due to stampedes (Jay et al. 2012). Pacific walruses (*O. rosmarus divergens*) are also expending greater energy swimming to offshore locations when sea ice is scarce (Cooper et al. 2006, Jay et al. 2017). The spectacled eider (*Somateria fischeri)*, a species of diving sea duck, winters in the pack ice of the northern Bering Sea, utilizing surrounding sea ice to forage on bivalves (Lovvorn et al. 2009, Cooper et al. 2013). A reduction in the abundances of their preferred prey, Nuculanid bivalves, and/or access to these sites are linked to the loss of sea ice, potentially resulting in further declines of this species (Grebmeier et al. 2006b, Lovvorn et al. 2009, Grebmeier et al. 2010, Grebmeier et al. 2018). Reductions in benthic and pelagic prey items associated with the loss of sea ice span a number of apex predators in the region (e.g. Bluhm & Gradinger 2008, Divoky et al. 2015, Kędra et al. 2015).

1.2. Sea ice algae

Ice algae have been estimated to contribute 4-26% of primary production in the Arctic (Legendre et al. 1992) and upwards of 50% in the Central Arctic Ocean (Gosselin et al. 1997, Boetius et al. 2013, Fernández-Méndez et al. 2015, Wiedmann et al. 2020). However, this is still an active area of research as Gradinger (2009) showed that contributions from ice algae on the shelves can exceed these estimates. Regardless of the exact proportion of ice algal contributions to primary production overall, the timing of sympagic production for consumers makes it highly valuable (Søreide et al. 2010, Leu et al. 2011, Leu et al. 2015). In addition to

the timing, ice algae have an elevated polyunsaturated fatty acid (PUFA) composition, making it a nutritional resource for grazers (Falk-Petersen et al. 1998, Leu et al. 2010). When ice algae are released from the ice matrix during melt, diatoms are weakly degraded in the water column and contribute a significant supply of rich organic matter to the benthos (Rontani et al. 2018a). Benthic organisms become the beneficiaries of this largely un-degraded, lipid-rich resource (McMahon et al. 2006, Kohlbach et al. 2016).

Sea ice provides a physical substrate and platform for primary producers to remain elevated in the water column where photosynthetically active radiation (PAR) levels are highest (Arrigo 2017). However, ice algae are adapted to very low-light conditions and are able to thrive under thick ice (Hancke et al. 2018). Snow cover over sea ice, rather than ice thickness, tends to have the most significant influence over irradiance levels on ice algal growth (Lund-Hansen et al. 2020) and export (Koch et al. 2020b, Lalande et al. 2020). Sea ice diatoms are able to acclimate to changing light levels throughout the melt season as indicated by increasing levels of photoprotective carotenoids relative to chlorophyll *a* (Leu et al. 2010, Kauko et al. 2018). This response occurs at the expense of PUFA concentrations, lowering the nutritional quality of this food source under thinning sea ice and likely under future Arctic conditions (Leu et al. 2010, Lund-Hansen et al. 2020).

The ice-ocean interface allows for the frequent resupply of nutrients necessary for sustaining ice algal communities (Smith et al. 1990, Gradinger & Ikävalko 1998, Gradinger 2009). Nutrients play an important role in the physiology and metabolism of ice algae, which impacts the lipid content, production of exopolymeric substances used for adhesion and aggregation, sinking rates and overall quality for grazing organisms (Cota et al. 1991, Leu et al. 2010, Meiners & Michel 2017). Lipid production has been shown to increase dramatically with nutrient limitation at the expense of carbohydrate and protein production (Mock &

Gradinger 2000). Nutrient limitation is expected to strongly influence productivity in the Arctic in the future (Carmack et al. 2006). Although irradiance will increase with longer periods of open water, enhanced stratification as a result of increasing meltwater will lead to nutrient limitation (Slagstad et al. 2015) and thus limiting the extent of increasing primary production that has been predicted (Arrigo 2015). In addition to changes associated with the controls on nutrient availability (e.g. stratification, vertical mixing, upwelling and inflow supply on the shelves), the loss of the supply of nutrients within sea ice is a possibility (Carmack et al. 2006, Grebmeier et al. 2006b). For example, iron is currently not considered to be a limiting nutrient in the Arctic (Aguilar-Islas et al. 2008), but could become a limiting nutrient with the loss of the high dissolved iron reservoirs found in drifting sea ice particularly when released during the spring and summer (Carmack et al. 2006, Wang et al. 2014b).

Diatom morphology is an important factor in the colonization of sea ice (Kauko et al. 2018). Ice algae consist primarily of large pennate diatoms (Gosselin et al. 1997, Arrigo 2017), and are estimated to comprise >90% of the sympagic biomass (Smith et al. 1990). In contrast, pelagic phytoplankton are typically dominated by centric and chain forming diatoms in the Arctic (e.g. *Chaetoceros* spp.), as well as dinoflagellates (Horner & Schrader 1982, Poulin et al. 2011, Nelson et al. 2014). However, there can be abundant centric ice-associated species as evident with *M. arctica* Dickie (Poulin et al. 2011), which can account for a significant portion of production in the central Arctic Ocean (Boetius et al. 2013). In the Arctic, *Nitzschia, Fragilariopsis, Entomoneis*, and *Navicula* are common pennate genera found in sea ice communities at the ice-water interface. Other common Arctic diatom genera include *Fragilaria, Cylindrotheca* and *Achnanthes* (Nelson et al. 2014, Arrigo 2017). Assemblages of ice-associated pennate diatoms have commonly been used as a proxy for sea

ice production but there are limitations owing to poor preservation and/or community composition issues (see review by Armand et al. 2017). More specific geochemical markers were needed to discriminate sympagic from pelagic sources for the purposes of both paleo sea ice proxies (de Vernal et al. 2013) and as trophic markers (Gradinger 2009).

The limited gas and inorganic carbon exchange that occurs within the constricted brine channels of the ice matrix leads to less discrimination against ^{13}C during photosynthesis, resulting in organic matter relatively enriched in ^{13}C relative to pelagic phytoplankton as indicated by stable isotope measurements (Hobson et al. 1995, Naidu et al. 2000, Gradinger 2009, Wang et al. 2014a). Typical $\delta^{13}C$ values range from approximately -11 to -24‰ for ice algae compared to -22 to -30‰ in pelagic phytoplankton (Peterson & Fry 1987, Pineault et al. 2013). However, $\delta^{13}C$ values have proven to vary in space and throughout the progression of a bloom and may not always be accurate indicators of sea ice versus pelagic sources alone. Specifically, sympagic particulate organic matter becomes more enriched in ^{13}C as biomass increases (Tremblay et al. 2006, Gradinger 2009, Pineault et al. 2013). More recently, analysis of stable isotopes signatures in amino acids and fatty acids (i.e. compound specific analysis) are improving the capacity of stable isotope measurements to serve as trophic markers by differentiating sea ice from pelagic organic carbon (e.g. Budge et al. 2008, McMahon et al 2006, Schollmeier et al. 2018, Yurkowski et al. 2021).

Fatty acids produced by diatoms are critical fuel for polar food webs (Graeve et al. 2005, Lee et al. 2006). Several classes of microalgae have distinct fatty acid profiles (Volkman et al. 1998, Volkman 2020), making them useful trophic markers and have been used to track sympagic organic carbon pathways in the food web (McMahon et al. 2006, Budge et al. 2008, Schollmeier et al. 2018). The primary fatty acids associated with diatoms are $C_{16:1n-7}$ (palmitoleic acid), $C_{16:0}$ (palmitic acid), $C_{20:5n-3}$ (eicosapentaenoic acid; EPA), C_{16} PUFAs, and

are notably deficient in C_{18} PUFAs (Falk-Petersen et al. 1998, Graeve et al. 2002, Rontani et al. 2018a, Volkman 2020). These fatty acids have been used to track ice algae, based upon the assumptions that diatoms are the primary component of the ice algal community and that pelagic production has a higher proportion of dinoflagellate composition (Budge et al. 2008, Wang et al. 2014). Dinoflagellates have distinct fatty acids including $C_{18:0}$ (stearic acid), $C_{18:5n-3}$ (octadecapentaenoic acid), and particularly $C_{22:6n-3}$ (docosahexaenoic acid; DHA). Dinoflagellates are deficient in $C_{16:0}$, which is therefore a specific diatom marker (Falk-Petersen et al. 1998). DHA and EPA are common lipids found in Arctic zooplankton and therefore important lipid trophic markers in food web ecology (Graeve et al. 2002, Falk-Petersen et al. 2009). Since the diatom markers are not particularly source-specific for distinguishing sympagic from pelagic diatoms, compound specific isotope analyses (CSIA) of fatty acids have been used to further refine these observations (Budge et al. 2008). Additionally, fatty acid profiles are strongly influenced by nutrient limitation, salinity and irradiance (see reviews by Volkman 2020 and Khozin-Goldberg 2016).

The succession of ice algae to phytoplankton throughout the spring and summer in the Arctic is nuanced. Ice algae have been shown to seed the subsequent pelagic phytoplankton blooms with the release of diatoms into the water column with ice melt, as indicated by similar species composition in the ice and in the water column (Szymanski & Gradinger 2016, Selz et al. 2018). Thicker multiyear ice also serves as a seeding repository for ice algae, which is likely to be negatively influenced by the loss of this older ice in the Arctic Ocean (Olsen et al. 2017, Kauko et al. 2018). A substantial under-ice pelagic bloom was observed in the Chukchi Sea in 2011(Arrigo et al. 2012, Arrigo et al. 2014). This was not the first observation of an under-ice bloom, but the scale of the bloom suggested satellite-based observations were not reliable means to estimate biomass and also challenged the paradigm

that pelagic productivity was not significant underneath the ice (Arrigo et al. 2014). While observational data is sparse at this point, models suggest the occurrence of these under-ice pelagic blooms may be increasing (Horvat et al. 2017). The thinning of sea ice over the last 20–30 years has increased the prevalence of melt ponds and therefore increased light transmission that is conducive to these under ice blooms (Frey et al. 2011, Arrigo et al. 2014, Horvat et al. 2017, Ardyna et al. 2020). There has been growing interest in the occurrence and role of under-ice pelagic blooms (see latest review by Ardyna et al. 2020), which have raised questions about the timing of production and community composition in the Arctic. These co-occurring blooms further complicate efforts to distinguish between sympagic and pelagic communities, particularly the timing and relative importance of each.

1.3. Highly branched isoprenoid biomarkers

Paleoclimatic sea ice reconstructions have historically relied on fossil diatoms assemblages (Antarctica) and dinoflagellate cysts (Arctic) in marine sediments as an indicator of sea ice cover or the position of the ice edge at a given location (de Vernal et al. 2013, Armand et al. 2017). The siliceous frustules of diatoms are often not well preserved, particularly in the Arctic, nor are the geochemical signatures that would distinguish a pelagic or sea ice source (Belt et al. 2007, Armand et al. 2017). A need from the paleoclimate community to improve climate models with more accurate sea ice records incentivized researchers to develop a more source-specific biomarker that was stable, well preserved and sensitive to ice coverage (Belt et al. 2007).

Analyzing microalgal lipids from sediments (e.g. sterols, alkenones, fatty acids) has been established for characterizing various sources of organic matter and serving as paleoproxies, albeit with some caveats regarding diagenetic influences, relative abundances and

environmental conditions controlling synthesis (Volkman et al. 1998, Volkman 2020). This approach led to the study of highly branched isoprenoid (HBI) alkenes, which have unusual C_{25} (haslenes) and C_{30} (rhizenes) hydrocarbon skeletons produced solely by diatoms (Volkman et al. 1994, Allard et al. 2001). Approximately thirty diatom species from commonly occurring genera including *Haslea*, *Pleurosigma*, *Navicula*, *Rhizosolenia* and *Berkeleya* have been identified that synthesize these lipids (Volkman et al. 1994, Allard et al. 2001, Massé et al. 2004, Brown et al. 2014c, Belt et al. 2018, Limoges et al. 2018, Brown et al. 2020, Volkman 2020). Rowland et al. (2001) first reported on the degree of unsaturation in HBIs relative to temperature in *H. ostrearia* (Gaillon) Simonsen, which pointed out the possible climatic markers produced by diatoms. This relationship led Belt et al. (2007) to hypothesize the existence of an HBI with a single double bond that could be synthesized by diatoms at the low temperatures found in sea ice, particularly given the occurrence of some ice-associated *Haslea* spp. A monounsaturated HBI, with a double bond in the 23–24 position, was detected in sea ice samples and was termed the "Ice Proxy with 25 carbons", or IP_{25} (Belt et al. 2007, Belt & Müller 2013)(Fig 1-1).

IP_{25} has since been confirmed to be produced by an even smaller number of diatom species found within Arctic sea ice (Brown et al. 2014c, Limoges et al. 2018). This compound was estimated to be produced by approximately 1–5% of Arctic sea ice diatom species, which corresponded with the proportion of *Haslea* species in sea ice samples. This observation provided further evidence that *Haslea* spp. were likely responsible for synthesizing this compound (Belt et al. 2013, Brown et al. 2014c). There were initially three or four species confirmed to produce this compound including, including *H. spicula* (Hickie) Lange-Bergalot and/or possibly *H. crucigeroides* (Hustedt) Simonsen (taxonomic challenges prevented a determination), *H. kjellmani* (Cleve) Simonsen, and *Pleurosigma stuxbergii var.*

rhomboides (Cleve in Cleve and Grunow) Cleve (Brown et al. 2014c). Since then, Limoges et al. (2018) has confirmed *H. spicula* as a source but was unable to detect IP_{25} in *H. crucigeroides*, eliminating this species as a confirmed source – at least in the fjord where it was studied.

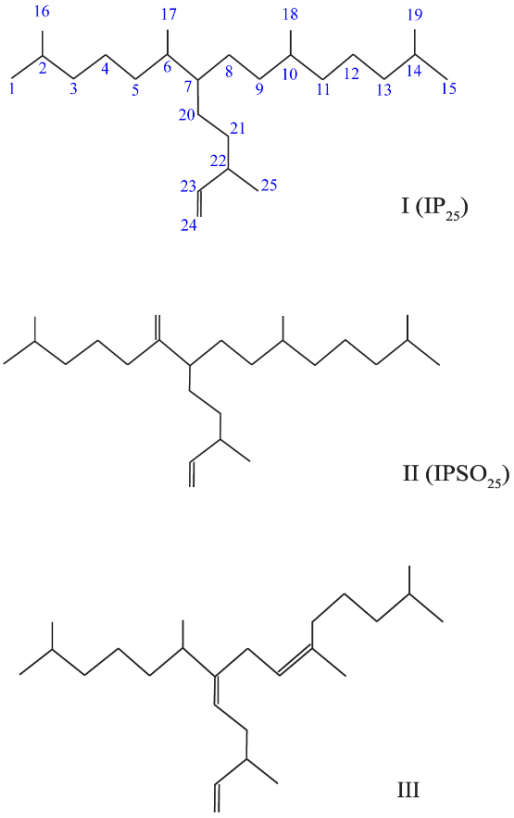

Figure 1-1 Highly branched isoprenoid (HBI) diatom biomarker structures and carbon numbering The HBIs currently utilized in Arctic sea ice reconstructions and trophic markers include the sea ice proxy with 25 carbons (IP25), HBI II – known as $IPSO_{25}$ in Antarctic studies, and HBI III a pelagic and/or marginal ice zone proxy.

There are other di- and tri-unsaturated HBIs produced by diatoms that are considered as complementary sea ice or pelagic biomarkers (Fig 1-1). The diene HBI (II), with a 6–17 double bond, is co-synthesized with IP_{25} and is capable of serving as a surrogate when IP_{25}

levels are below detection limits (Brown et al. 2014c). While *H. crucigeroides* does not apparently synthesize IP_{25}, it does synthesize HBI II (Brown et al. 2014c, Limoges et al. 2018, Brown et al. 2020). Pinpointing a biological source for HBIs, with this $C_{25:2}$ HBI in particular, was initially a result of detecting high abundances of $C_{25:2}$ in Antarctic sediment and sea ice diatom samples (Nichols et al. 1988, Johns et al. 1999). In the Antarctic, *Berkeleya adeliensis* Medlin was confirmed as the sea ice diatom source and was termed the Ice Proxy for the Southern Ocean with 25 carbon atoms, or $IPSO_{25}$ (Belt et al. 2016). This species is widespread and commonly occurring in platelet ice around Antarctica, yet rarely preserved in fossil diatom assemblages (Belt et al. 2016). This $C_{25:2}$ HBI will be hereafter referred to as $IPSO_{25}$ in the Antarctic context, but will otherwise be termed HBI II for the use of this biomarker in the Arctic. IP_{25} has never been detected in the Antarctic, most likely owing to the lack of the species responsible for its synthesis, and remains solely an Arctic sea ice proxy (Belt et al. 2016, Belt 2018).

The tri-unsaturated HBI (III), with *Z* isomerization (Fig 1-1), is a common HBI constituent in marine sediments (Belt et al. 2000b). HBI III and HBI IV (not shown), which is another triene with *E* isomerization, are uniquely both produced by *Pleurosigma* spp. *Haslea* spp. generally have a double bond in the 6-17 and 5-6 positions, while *Pleurosigma* spp. usually have the 7-20 double bond position. Additionally, *Pleurosigma* spp. are not capable of synthesizing HBIs with the 6-17 double bond (Belt et al. 2000b). Studies have shown that HBI III is a suitable proxy for the presence of pelagic diatoms (Massé et al. 2011, Smik et al. 2016) and the compound specific stable isotopic composition of HBI III in Antarctic marine sediments ($\delta^{13}C$=-34‰ to -42‰) supports a pelagic source (Massé et al. 2011). On the other hand, these compounds can be abundant in the highly productive marginal ice zones (MIZ) (Belt 2018). Further analysis of HBI III levels in open water studies are needed to fully

characterize the utility of these compounds as reliable biomarkers of pelagic diatoms. While an increase in abundance suggests greater pelagic production, it may also point to the position of the ice edge owing to elevated production as ice retreats and nutrients are released from the ice matrix. This does not necessarily invalidate HBI III as a pelagic indicator but may require more careful interpretation about the conditions its presence suggests (Belt 2018).

The physiological drivers that influence the production of IP_{25} and other HBIs or the specific environmental conditions that stimulate its production are still not fully understood (Belt and Muller 2013, Brown et al. 2020) and few studies have addressed this point. Recent work has identified nutrient limitation as a trigger for HBI production (Brown et al. 2020). An order of magnitude increase in HBI production was observed in laboratory cultures of *H. vitrea* during low nutrient availability although this response was not observed in *H. crucigeroides*. As previously noted, lipid production is known to increase in response to nutrient limitation and so this HBI response is perhaps not surprising. The elevated production of HBIs may serve as an energy reserve during times of stress (Brown et al. 2020). Yet this species-specific response raises additional questions. Another interesting finding that study highlighted was the production of tri- and tetra-unsaturated HBIs by *H. vitrea*, which were previously assumed to only be produced by pelagic species. Whether this was possible because these were laboratory cultures and not *in situ* observations is unclear. Either way, each of these issues raises important points that have potential implications for how we interpret HBI abundances. HBI synthesis is clearly still an area of research that requires more attention in the future (Brown et al. 2020).

HBIs are subject to some degree of sedimentary diagenesis over time due to autoxidation and biodegradation (particularly in thick oxic layers in the sediment) and may also degrade in samples depending upon storage techniques (Cabedo-Sanz et al. 2016, Rontani et al. 2018b,

Rontani et al. 2019a, Rontani et al. 2019b). However, the degree of degradation in sediments appears to be minor in relation to climatic changes associated with relative abundances (Rontani et al. 2018b). Given the stability of the monounsaturated molecular structure of IP_{25} and its source specific nature, its utility as a proxy for paleoclimate reconstructions has been well established over the last decade or so (see reviews by Belt and Müller, 2013, Belt 2018). Initially it was thought that this biomarker would allow for determining the position of the ice edge through at least the Holocene, but IP_{25} has been identified in sediments dating back to the late Miocene (Stein et al. 2016), far exceeding those original expectations. However, there are caveats, particularly with paleoclimate applications when inferring the past sea ice conditions. IP_{25} inventories can be negligible during periods of both open water and permanent multi-year ice cover, which are both conditions that do no support ice algal production or HBI-producing species. In order to address this complexity, and the often greater abundances of phytoplankton lipids to IP_{25}, a phytoplankton indicator was proposed to normalize and account for open water conditions. This index, called PIP_{25} was initially proposed by Müller et al. (2011):

$$PIP_{25} = \frac{[IP_{25}]}{[IP_{25}]+c[P]} \quad (1)$$

$$c = \frac{mean\,[IP_{25}]}{mean\,[P]} \quad (2)$$

Where P is a phytoplankton biomarker (μg g^{-1} TOC) for a specific dataset or core. The phytoplankton markers used in previous studies include brassicasterol (synthesized by several genera of phytoplankton) and dinosterol (synthesized by dinoflagellates). This has resulted in several variations of this index including P_BIP25 (using brassicasterol), P_DIP25 (using dinosterol), and $P_{III}IP_{25}$ (using HBI III). PIP_{25} has its limitations, given that the phytoplankton sterols are not specific to a single source or environmental condition as IP_{25} is. The correction

factor, *c*, in equation (1) can vary by location and throughout the length of individual cores (Belt and Müller, 2013), based on the phytoplankton population, creating further challenges for consistent measurements throughout the Arctic (Belt 2018). Given the proportionality of the sterols compared to IP_{25}, HBI III has been suggested to be more appropriate to serve as the pelagic or MIZ indicator (Belt et al. 2015). Even with the use of HBI III instead of brassicasterol (the preferred phytoplankton marker), the *c* factor requires scrutiny. Smik et al. (2016) found a strong relationship between spring sea ice concentration and their calculation of PIP_{25} using HBI III and proposed the following equation with a defined *c* factor:

$$P_{III}IP_{25} = \frac{[IP_{25}]}{([IP_{25}]+0.63[III])} \quad (3)$$

In each of the PIP_{25} calculations, values vary between 0 and 1, with 1 representing sea ice cover and 0 representing open water conditions (Müller et al. 2011, Belt & Müller 2013). An equation has also been proposed to infer the spring sea ice concentrations (SpSIC) from this index using HBI III, expressed as a percentage, from these measurements:

$$SpSIC(\%) = \frac{(P_{III}IP_{25}-0.0692)}{(0.0107)} \quad (4)$$

The SpSIC equation was derived from HBI measurements in the Barents Sea (Smik et al 2016) and therefore requires further testing to determine how well it performs in other regions.

While the majority of applied HBI studies to date have focused on their use in paleo-sea ice reconstruction [see reviews by Belt and Müller (2013), Belt (2018)], the use of HBIs as ice algal trophic markers has been emerging. This was made possible by the determination that IP_{25} was stable once grazed and assimilated by consumers (Brown & Belt 2011). In that initial study, IP_{25} was identified in a majority of the benthic macrofauna specimens analyzed

from the Arctic. This study provided the foundation for further investigations into feeding strategies of benthic fauna that incorporate IP_{25} from diatoms. Brown and Belt (2011) also confirmed ice algal sources using compound specific stable carbon isotope measurements of IP_{25}, with a mean $\delta^{13}C$ value of -17‰, which was consistent with previously analyzed sediment trap particle data under sea ice (Belt et al. 2008).

The source-specificity, persistence and stability of HBIs can therefore be used to separate sympagic from pelagic production in Arctic food webs, and likely has advantages over other less specific tracers. By quantifying the relative abundances of the sympagic HBIs (IP_{25} and HBI II) to pelagic HBIs (HBI III), the primary carbon source can be fingerprinted. Brown et al. (2014d) established an HBI fingerprinting index, termed "H-print", that estimates the relative organic carbon contributions of sea ice organic carbon versus pelagic organic carbon sources. The H-print method, is calculated using the relative abundances of IP_{25}, HBI II and HBI III.

$$\text{H-print \%} = \frac{III}{\sum (IP_{25} + II + III)} \text{ x } 100 \qquad (5)$$

The estimated organic carbon contribution resulting from the H-print analysis can vary from 0% (sympagic) to 100% (pelagic).

This biomarker approach was demonstrated by comparing polar (Arctic) and temperate (Atlantic) marine mammal species (Brown et al. 2013a). This study showed that the biomarker signature was unique to Arctic organisms, including those at upper trophic levels. Neither IP_{25} nor HBI II were detected in grey seal (*Halichoerus grypus*), striped dolphin (*Stenella coeruleoalba*), harbor porpoise (*Phocoena phocoena*), fin whale (*Balaenoptera physalus*), and short-beaked common dolphin (*Delphinus delphis*) tissues that were collected from strandings in the United Kingdom, but HBI III was present in each of

these samples. In contrast to these Atlantic samples, ringed seals (*Pusa hispida*) collected during Inuit subsistence harvests in the Arctic, had measurable quantities of IP_{25}, HBI II and HBI III. A growing number of studies have since contributed to the development of the H-print method on a variety of trophic levels and organisms. IP_{25} and other HBIs have now been measured in a number of Arctic and Antarctic consumers (Table 1-1). Since IP_{25} is not present in the Antarctic, a ratio of dienes to trienes are used in a similar way as the H-print approach. The number of studies using the H-print approach with marine mammals are few but are nevertheless revealing the importance of sympagic organic carbon at upper trophic levels. For example, Brown et al. (2018) observed H-print markers consistent with 72-100% sea ice organic carbon composition in polar bears. A recent review of the available trophic markers for Arctic food web analysis (HBIs, fatty acids and stable isotopes) confirmed that HBIs, when compared side-by-side with the other available markers, provided the most robust indicator of sympagic versus pelagic sources (Leu et al. 2020). Moreover, when these markers are used together, interpretations are improved, provided sampling time relative to the bloom progression is known (Leu et al. 2020).

Table 1-1 Summary of HBI food web studies Compilation of studies to-date using HBIs, primarily with the H-print approach (Arctic) or the diene/triene ratio (Antarctic). These studies either measured HBI content in animal tissues or conducted studies on ice algae that have direct implications for food web analyses. This list may not be all inclusive.

Study Region	Sample(s)	Other Measurements	Reference(s)
Arctic			
Arctic Ocean	Amphipods		Brown et al. (2017a)
Barents Sea	Zooplankton		Kohlbach et al. (2021)
Svalbard	Ice algae (sea ice)	CSIA (fatty acids), fatty acids, $\delta^{13}C$	Leu et al. (2020)
	Zooplankton, shrimp, fish, benthic invertebrates		Brown and Belt (2012b)
	Seabirds		Brown et al. (2013b)
NE/E Greenland	Ice algae (sediment traps, sediments)	$\delta^{13}C$, $\delta^{15}N$, biogenic silica	Limoges et al. (2018)

Baffin Bay	Polar bears	Fatty acids, $\delta^{15}N$	Brown et al. (2018)
	Bivalves	Fatty acids	Amiraux et al. (2021)
	Ice algae (sea ice and water column)		Amiraux et al. (2019)
	Ringed seals		Brown et al. (2014b)
Canadian Arctic	Atlantic walrus	CSIA (amino acids)	Yurkowski et al. (2020)
	Beluga whale	$\delta^{15}N$	Brown et al. (2017b)
	Benthic invertebrates	CSIA (IP_{25})	Brown et al. (2011)
	Benthic invertebrates	$\delta^{13}C$, $\delta^{15}N$	Yunda-Guarin et al. (2020)
	Ringed seals, other non-polar marine mammals		Brown et al. (2013a)
	Benthic invertebrates		Brown et al. (2012)
	Ice algae, Zooplankton		Brown and Belt (2012a)
	Benthic invertebrates	Fatty acids, $\delta^{13}C$	Kohlbach et al. (2019)
	Seabirds	$\delta^{13}C$, $\delta^{15}N$	Cusset et al. (2019)
Hudson Bay	Polar bears	Fatty acids, $\delta^{15}N$	Brown et al. (2018)
Bering Sea	Benthic invertebrates		This study (Chapter 3)
	Pacific walrus	$\delta^{13}C$, $\delta^{15}N$	This study (Chapter 4)
Chukchi	Benthic invertebrates		This study (Chapter 3)
	Pacific walrus	$\delta^{13}C$, $\delta^{15}N$	This study (Chapter 4)
Antarctica			
E Antarctica	Euphausiids, fish, seabirds		Goutte et al. (2013)
	Fish		Goutte et al. (2014b)
Sub-Antarctic	Seabirds, seals		Goutte et al. (2014a)
Scotia Sea	Euphausiids		Schmidt et al. (2018)

Overall, HBIs have proven to be useful ice algal trophic markers and show promise for monitoring the contributions of ice algae in past and present food webs. This biomarker index may also provide insights into future scenarios in which summer sea ice is absent and sympagic production diminishes (Fig 1-2). Several studies have hypothesized a shift from benthic-dominated systems on the Arctic shelves, particularly in the highly productive Pacific Arctic region, to pelagic-dominated systems following the loss of sea ice and shifts in organic carbon sources (Kędra et al. 2015, Moore & Stabeno 2015). If and when these ecosystem shifts will occur is complex, owing to possible increases in suitable habitat for ice algae as

first year ice becomes dominant (Arrigo & van Dijken 2015) or if there will be a mismatch in timing of production with life cycles of certain consumers that disrupts the food web (Søreide et al. 2010, Leu et al. 2011, Dezutter et al. 2019, Nadaï et al. 2021). This issue is an active area of research in the Arctic and HBIs may provide one more tool to track sea ice organic carbon flow through food webs with greater specificity than previous approaches.

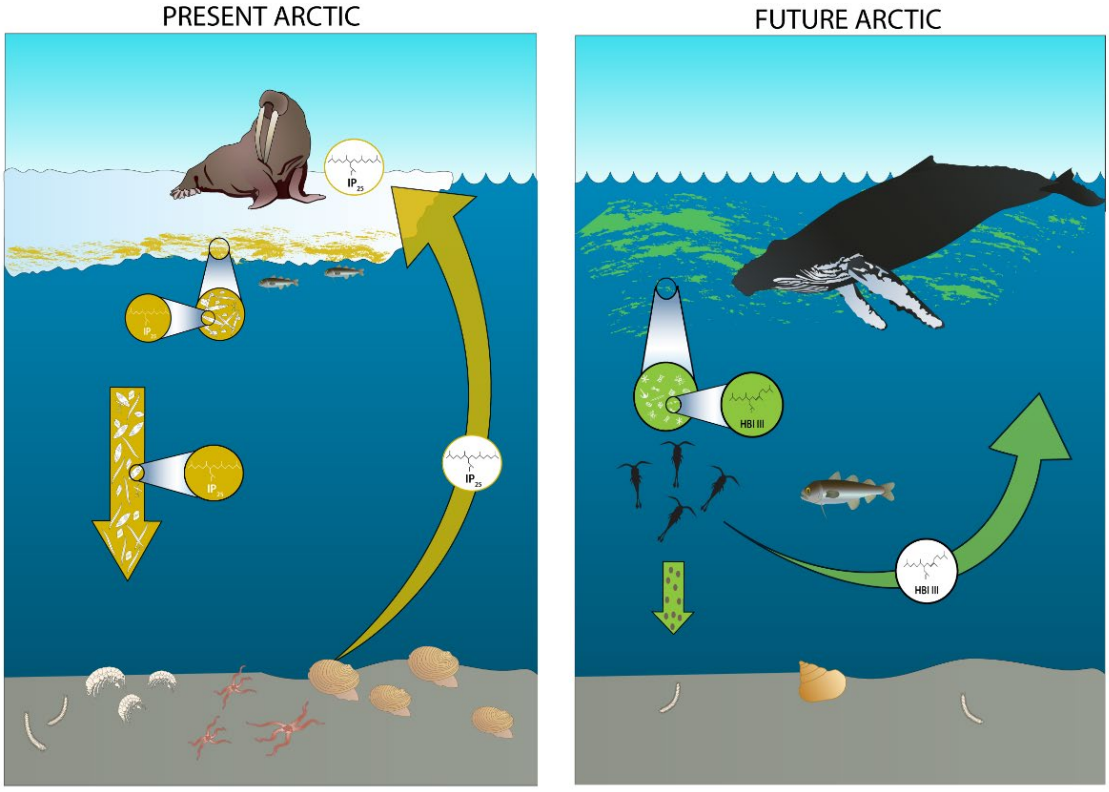

Figure 1-2 HBI biomarkers in Arctic ecosystem studies In the present-day Arctic (left panel), ice algae are prevalent with seasonal spring ice coverage over the shelf supporting rich benthic ecosystems. As a result, there are greater measurable quantities of IP_{25} in the food web. In the future scenario (right panel), pelagic primary production has increased owing to longer open water periods, leading to water column grazing and a decrease in the quality and quantity of organic matter reaching the seafloor. The greater proportions of pelagic phytoplankton result in greater measurable quantities of HBI III in the food web.

1.4. HBI studies in the Pacific Arctic

The use of HBIs in the Pacific Arctic region, defined here as the northern Bering Sea and Chukchi Sea, has so far been limited when compared to other regions of the Arctic (see most recent review by Belt 2018). Most HBI determinations were made from surface sediments and/or sediment cores for the purposes of calibrating the sea ice indices described earlier (Stoynova et al. 2013, Méheust et al. 2015, Xiao et al. 2015, Stein et al. 2017b, Bai et al. 2019, Kim et al. 2019). Stoynova et al. (2013) conducted a more Pan-Arctic study, but some of the reported IP_{25} concentrations were not consistent with prior and subsequent findings, suggesting systematic analytical or methodological errors (Xiao et al. 2015, Belt 2018). Other pan-Arctic assessments have included HBI data from the Bering and Chukchi Seas, including the data review or presented in Chapter 2 (Xiao et al. 2015, Kolling et al. 2020). However, regionally-specific HBI dynamics that would be influenced by the nutrient-rich currents from the north Pacific Ocean and associated differing phytoplankton assemblages have not been thoroughly studied.

Even fewer studies have looked at HBIs in invertebrate or vertebrate tissues for food web studies in the Pacific Arctic (Table 1-1). McTigue et al. (2015) included IP_{25} measurements from surface sediments in the Chukchi Sea as part of an analysis of organic carbon pathways in the food web. However, these HBI measurements were not directly measured by the authors (data provided by K. Taylor and R. Harvey) and the analytical methods were not documented. As the use of HBIs in animal tissues continues to develop, more consistent methodologies are being reported, making direct comparisons feasible. While McTigue et al. (2015) showed a significant relationship among sedimentary IP_{25}, $\delta^{13}C$ and sea ice retreat, which in turn confirms the ice algal origins of their $\delta^{13}C$ measurements, IP_{25} was not measured in macrofaunal tissue samples to track carbon flow. As a result, to the best of my

knowledge, there are currently no other published studies in the Pacific Arctic region utilizing HBIs (vis-à-vis the H-print method) in animal tissues that facilitate tracking sea ice organic carbon in this regional food web.

1.5. The Distributed Biological Observatory – A framework for monitoring change in the Arctic

The Distributed Biological Observatory (DBO, https://dbo.cbl.umces.edu/) was established in the northern Bering, Chukchi, and Beaufort Seas as a change detection array to monitor the rapid changes occurring to this ecosystem (Fig. 1-3). The DBO was established in 2010, but data collection in many of these locations goes back for over thirty years as part of other research programs (Grebmeier et al. 2010) and provides a wealth of prior data. The hydrodynamics and sea ice trends are discussed in greater detail in chapters 2–4. However, a brief overview of this system is important to provide context for my study. The DBO is a region where the physics and biology are tightly coupled, driven by nutrient-rich water from the Pacific Ocean and seasonal ice cover, setting up a region with high productivity both in the water column and the benthos (Moore & Grebmeier 2018, Grebmeier et al. 2019, Stabeno et al. 2019). Five benthic hot spots have been identified throughout the Pacific Arctic –not including those located in the Beaufort Sea (Grebmeier et al. 2015).

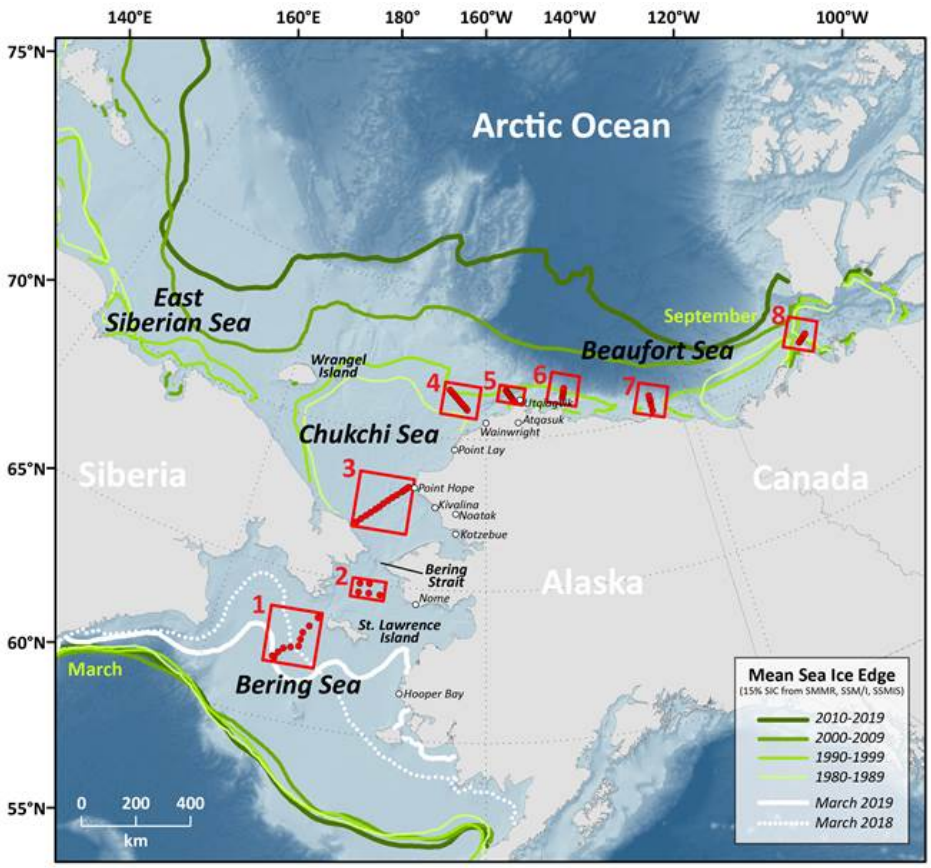

Figure 1-3 The Distributed Biological Observatory The samples collected for this study are part of the Distributed Biological Observatory (DBO) monitoring program. Particular emphasis will be given to DBO regions 1-5, which are areas of high benthic biomass and marine mammal and seabird foraging "hot spots". Map courtesy of Karen Frey (Clark University).

The research design for this dissertation builds off the framework of the DBO, with a particular focus on regions 1–5 (Fig 1-3). The DBO was an ideal sampling mechanism for developing HBI biomarkers for the region, as these five regions are areas of high productivity experiencing rapid rates of change in relation to sea ice along a latitudinal gradient (Moore & Grebmeier 2018), and span sub-Arctic to Arctic marine conditions. During this study, the sea ice edge in the winter extends to approximately the location of DBO 1 in the south, and is associated with the location of a winter polynya south of St. Lawrence Island. The Pacific Arctic region has been experiencing rapid ice loss, with a trajectory of increasing delays in the seasonal formation of sea ice and an earlier break up in the spring, which leads to shifts in

primary production (Grebmeier et al. 2018, Moore & Grebmeier 2018, Frey et al. 2020). These losses are evident in the retreating location of the mean decadal (September) minimum ice extent (Fig 1-3). Not shown in these decadal trends are the record low winter (March) maximum sea ice extents in the Bering Sea that occurred in 2017/2018 and 2018/2019 and the associated ecological responses. These low sea ice events, particularly in 2017/2018, resulted in an unprecedented retraction of the cold pool [a cold and saline layer of bottom water typically formed by brine rejection during sea ice formation; Grebmeier et al. (2018)], leading to increased abundances of Pacific cod and snow crab (*Chionoecetes opilio*) in the northern Bering Sea as opposed to their normal distributions in the southeastern Bering Sea (Siddon et al. 2020, Fedewa et al. 2020). In 2018 there was also an abundance of smaller and lipid-poor copepods and these sea ice conditions were linked to a seabird die-off and "Unusual Mortality Events" of bearded, ring and spotted seals (Duffy-Anderson et al. 2019, Stabeno & Bell 2019, Siddon et al. 2020, Thoman et al. 2020). The reductions in sea ice in the Pacific Arctic are driving changes in all trophic levels of this ecosystem, from the distribution and abundances of phytoplankton and ice algae to changes in foraging and migration patterns in marine mammals (Grebmeier et al. 2019). Shifting and reduced organic carbon sources have been attributed to the ecosystem shifts already underway in the DBO 1 region (Grebmeier et al. 2006b, Grebmeier 2012, Grebmeier et al. 2018). I used these circumstances to help design my study of biomarker distributions in the context of changing sea ice persistence gradients and food web structure.

1.6. Dissertation outline

The goal of my dissertation was to determine the utility of HBI biomarkers in the northern Bering and Chukchi Seas to track the ecosystem response to the rapidly declining sea ice over the past several decades (Grebmeier et al. 2018). Other studies have

hypothesized food web shifts on the broad Arctic shelves as the open water period extends into the fall and northward towards the Arctic basin (Kędra et al. 2015).

Since there was a paucity of HBI measurements in the western Arctic, it was essential to first establish the depositional patterns and timing of HBI production and export throughout the region in order to interpret results at the organismal and ecosystem level. Chapter 2 lays the groundwork for contextualizing the distribution and inventory of the sea ice biomarker (IP_{25}) in the Pacific Arctic region. The export, deposition and burial of IP_{25} can be connected to seasonal sea ice conditions and allows us to use HBIs to interpret ecosystem responses to declining sea ice in more applied studies. One novel finding from this study was that IP_{25} was detected year-round in the particle export to the seafloor, suggesting ice algae is a sustaining energy source for the benthic community even when ice is not present, and in the winter when light is not sufficient to support primary production. This adds to a growing body of evidence that the polar night is more productive than previously thought (Berge et al. 2015). Sea ice biomarker profiles in sediment cores from the Chukchi shelf and slope provided additional evidence of a sediment "food bank" that is comprised of lipid-rich ice algae that can likely sustain the benthic food web. The flux data also highlighted the importance of snowmelt above sea ice as a trigger for production and release of ice algae to the water column, as was observed in other studies in the Chukchi and Beaufort Seas (Lalande et al. 2020, Nadaï et al. 2021). Snow melt allows for sufficient light before ice melt/break up begins, which will have consequences for the magnitude and timing of blooms in the future as the Arctic warms. This chapter was published in the journal *PLOS ONE* in 2020.

Having established the general distribution and timing of HBI fluxes throughout the Bering and Chukchi seas in Chapter 2, Chapter 3 assesses the utilization of ice algae as a resource by benthic communities. HBI biomarkers were used to assess the importance of ice

algae to benthic mega- and macrofauna (e.g. clams, worms, sponges, sea stars, crabs) on the Bering and Chukchi shelves. It has been an ongoing topic of uncertainty whether ice algae are a significant food source in the Arctic given its small proportions overall relative to open water production, and if the increasing open water season will result in increased pelagic primary production and associated carbon fluxes to the seafloor. Given the tight sympagic-pelagic-benthic coupling that occurs on the Pacific Arctic shelves, a mismatch in phytoplankton production and grazing activities is likely to have consequences by altering reproductive and survival strategies by a number of organisms. This study revealed that ice algae are utilized in greater quantities by certain feeding guilds, primarily subsurface deposit feeders, and therefore the reduction of the sympagic-sourced organic carbon pathway may result in a restructuring of the food web. Reductions in sea ice organic carbon could have a cascading effect on the number of higher trophic organisms that are specialized benthic predators by altering the lipid content of their preferred prey. While there are a number of ways the Arctic is threatened by climate change, this study reveals one mechanism that is predicted to result in a decrease in benthic biodiversity and increased competition for specialized benthic-feeding animals such as Pacific walruses (*Odobenus rosmarus divergens*), bearded seals (*Erignathus barbatus*), gray whales (*Eschrichtius robustus*) and the spectacled eider (*S. fischeri*). This study was published in the journal *Marine Ecology Progress Series* in 2020.

Chapter 4 is an applied study to show the potential of HBI biomarkers to assess the trophic transfer of assimilated sea ice carbon to the Pacific walrus (*O. rosmarus divergens*). Pacific walruses have sex-segregated migrations, where females have an apparently obligatory relationship with the sea ice. The most notable outcome of this study is that I was able to show the relationship between sea ice and female walruses appears to extend to their

diets. Females appear to be foraging on different prey items with higher lipid content connected to elevated ice algae consumption by their preferred prey items. This suggests female walruses may be more vulnerable to climate change and therefore the population as a whole, which should be considered for conservation purposes. Walruses are culturally important subsistence resources for Iñupiat and St. Lawrence Island Yupik communities in Alaska. This chapter was submitted to the journal *PLOS ONE* in February 2021 as part of a DBO special collection and undergoing peer-review.

2. Seasonal succession and latitudinal gradients of sea ice algae in the northern Bering and Chukchi Seas determined by algal biomarkers

Published in PLOS ONE, April 2020 https://doi.org/10.1371/journal.pone.0231178

Chelsea Wegner Koch, Lee W. Cooper, Catherine Lalande, Thomas A. Brown, Karen E. Frey, and Jacqueline M. Grebmeier

Contribution: Experimental design, all sample analysis, data analysis and interpretation, and all text and figures; Diatom taxonomy and flux data provided by C. Lalande and sea ice data provided by K. Frey. Text has been edited by all co-authors

Abstract

An assessment of the production, distribution and fate of highly branched isoprenoid (HBI) biomarkers produced by sea ice and pelagic diatoms is necessary to interpret their detection and proportions in the northern Bering and Chukchi Seas. HBIs measured in surface sediments collected from 2012 to 2017 were used to determine the distribution and seasonality of the biomarkers relative to sea ice patterns. A northward gradient of increasing ice algae deposition was observed with localized occurrences of elevated IP_{25} (sympagic HBI) concentrations from 68–70°N and consistently strong sympagic signatures from 71–72.5°N. A declining sympagic signature was observed from 2012 to 2017 in the northeast Chukchi Sea, coincident with declining sea ice concentrations. HBI fluxes were investigated on the northeast Chukchi shelf with a moored sediment trap deployed from August 2015 to July 2016. Fluxes of sea ice exclusive diatoms (*Nitzschia frigida* and *Melosira*

arctica) and HBI-producing taxa (*Pleurosigma, Haslea, and Rhizosolenia* spp.) were measured to confirm HBI sources and ice associations. IP_{25} was detected year-round, increasing in March 2016 (10 ng m^{-2} d^{-1}) and reaching a maximum in July 2016 (1331 ng m^{-2} d^{-1}). Snowmelt triggered the release of sea ice algae into the water column in May 2016, while under-ice pelagic production contributed to the diatom export in June and July 2016. Sea ice diatom fluxes were strongly correlated with the IP_{25} flux, however associations between pelagic diatoms and HBI fluxes were inconclusive. Bioturbation likely facilitates sustained burial of sympagic organic matter on the shelf despite the occurrence of pelagic diatom blooms. These results suggest that sympagic diatoms may sustain the food web through winter on the northeast Chukchi shelf. The reduced relative proportions of sympagic HBIs in the northern Bering Sea are likely driven by sea ice persistence in the region.

2.1. Introduction

Sea ice supports a diverse community of microalgae (primarily diatoms), bacteria, metazoan grazers, heterotrophic and mixotrophic protists, viruses and fungi (Horner 1989, Horner et al. 1992, Steward et al. 1996, Poulin et al. 2011). Sea ice associated (sympagic) algae grow on the underside and bottom few centimeters of sea ice and within brine channels during sea ice formation and eventually decline as sea ice melts (Horner et al. 1992, Gosselin et al. 1997, Fortier et al. 2002, Juul-Pedersen et al. 2008, Szymanski & Gradinger 2016). However, the precise contribution of sea ice algae to total primary production throughout the Arctic is poorly constrained owing to difficulties in measuring production in these communities (Gosselin et al. 1997) and to the overlap in habitat of sea-ice associated species (Szymanski & Gradinger 2016). Estimates of sea ice algae contributions to total primary production in the Arctic are widely variable, ranging from 4 to 26% in seasonally ice covered waters (Legendre et al. 1992) and upwards of 50% in the central Arctic Ocean (Gosselin et al.

1997). Observations of a phytoplankton bloom below melt ponds in the Chukchi Sea indicated that satellite-based estimates of chlorophyll biomass in areas of sea ice may be an order of magnitude too low (Arrigo et al. 2014). The observation of nearly all algal export before complete ice melt in the Eurasian Arctic Ocean further reflects the underestimation by satellite sensor platforms (Lalande et al. 2019). It has been suggested that these ice algae blooms are an important early season source of food to pelagic grazers and benthic communities (Fortier et al. 2002, McMahon et al. 2006, Gradinger 2009, Pirtle-Levy et al. 2009, Grebmeier et al. 2010, Grebmeier et al. 2015). Yet gaps remain in our understanding of the spatial and temporal variability of sea ice primary production in the Arctic and the impact on high latitude food webs. The application of biogeochemical methods to quantify and monitor sea ice algae contributions to pelagic and benthic food webs can be used to address these limitations associated with traditional field and satellite-based observations of sympagic production.

Highly branched isoprenoids (HBI) are a class of lipids with C_{20}, C_{25} and C_{30} hydrocarbon structures comprised of C_5 isoprene units unique to diatoms and can serve as species-specific biomarkers based on the number and position of double bonds (Volkman et al. 1994, Belt et al. 2007). HBIs are produced by several commonly occurring diatoms genera including *Haslea*, *Pleurosigma*, *Navicula* and *Rhizosolenia*, but are limited to a small number of species within these taxa (Volkman et al. 1994, Brown et al. 2014c, Belt et al. 2017). A small subset of these diatoms associated with Arctic sea ice produce a monounsaturated HBI, which has been termed the “Ice Proxy with 25 carbons”, or IP_{25} (Belt et al. 2007) (Fig 2-1). The detection of IP_{25} is presumed to indicate the current or prior presence of sea ice and ice algal production at a given location. The physiological drivers that influence the synthesis of IP_{25} or the specific sea ice and environmental conditions that stimulate its production are not

fully understood and have yet to be synthesized in a laboratory setting (Belt & Müller 2013, Brown et al. 2014c, Belt 2018). HBI II (Fig 2-1), a $C_{25:2}$ alkane co-synthesized with IP_{25} in Arctic sea ice, often occurs in larger relative abundances than IP_{25} and has proven useful as an additional sea ice proxy (Brown et al. 2011, Belt et al. 2013, Belt 2018). HBI III (Fig 2-1), a $C_{25:3}$ alkane, is ubiquitous throughout the world's oceans and serves as an indicator of production in open water and marginal ice zones (Volkman et al. 1994, Brown 2011, Belt et al. 2018). Several sea ice indices have been developed based on the relative proportions of IP_{25} and other HBIs (or phytoplankton sterols) to estimate the relative proportions of sympagic versus pelagic production (Müller et al. 2011, Brown et al. 2014d, Smik et al. 2016).

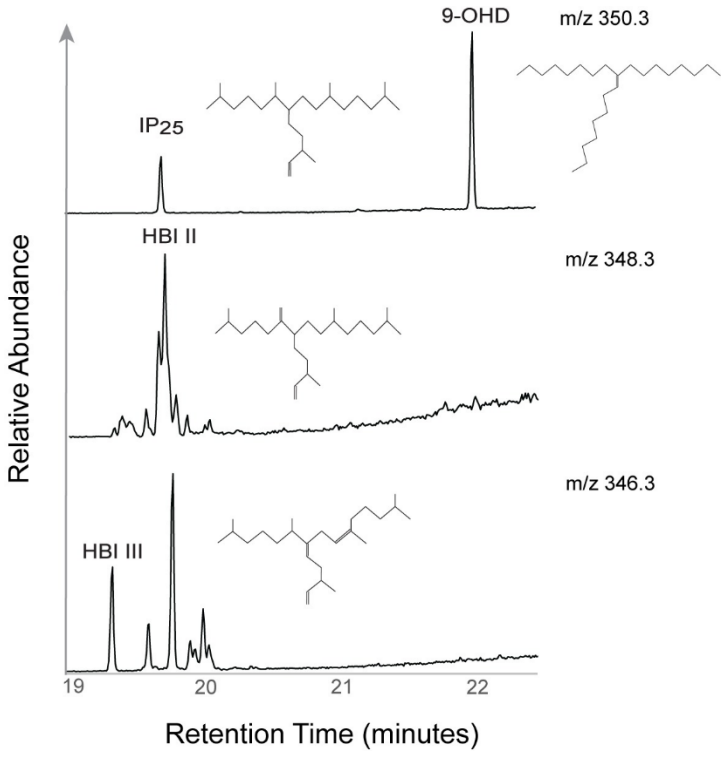

Figure 2-1 Biomarker compounds and chromatograms The highly branched isoprenoid molecular structures for IP_{25}, HBI II, HBI III and the internal standard, 9-OHD. The compounds correspond with an example chromatogram from the surface sediment samples, showing the retention times and relative abundances**.**

Nearly half of summer Arctic sea ice, based on the September minimum extent, has been lost since the start of satellite observations (1979-present) (Arrigo 2014, Serreze & Meier 2018). Therefore, associated changes to ice algal production are to be expected. Trends in sea ice extent and duration are variable from year-to-year and throughout the Arctic (Serreze & Meier 2018). Across the Pacific Arctic region (Bering, Chukchi and Beaufort Seas), sea ice break-up is occurring earlier and forming later, leading to younger and thinner sea ice annually with persistence declining by 9 to 30 days per decade over the satellite record (Frey et al. 2015, Grebmeier et al. 2015, Grebmeier et al. 2018, Serreze & Meier 2018). Two record low maximum winter extent periods for the Bering Sea occurred in 2018 and 2019, along with a record low summer minimum extent for the Chukchi Sea in 2019 (Fetterer 2017, updated daily, Frey et al. 2018, Grebmeier et al. 2018). Recent models suggest that annual sea ice duration in the Bering Strait could be reduced by an additional 20–36 days before 2050 and upwards of 60 days in the Eastern Siberian, Chukchi and Beaufort Seas (Wang et al. 2018). On the continental shelf, August and September are essentially ice-free and the open water period is extending later into the fall.

Few HBI studies have been conducted on the productive shallow shelves of the Pacific Arctic marginal seas relative to the Eurasian and Canadian Arctic (Belt 2018, Bai et al. 2019). Therefore, opportunities exist to improve our understanding of the dynamics of these biomarkers and their applications for ecosystem and paleoclimate studies. These measurements may also supplement existing knowledge from field-based and primarily satellite derived observations. The main goal of this study was first to establish the spatial distribution of IP_{25}, HBI II and HBI III from surface sediments throughout the region and investigate whether interannual variability can be distinguished. Additionally, there was a need to investigate the temporal dynamics of HBI production in the Pacific Arctic through

biomarker fluxes (sediment traps). Finally, the fate or preservation of HBIs in this highly productive region was determined through measurements and comparisons of sediment cores collected from the biological hot spot on the shallow shelf relative to a deeper, less productive region on the Chukchi slope. By assessing the temporal and spatial dynamics of these biomarkers to establish a region-specific baseline, future studies may be able to employ this technique to monitor the rapid changes in sea ice occurring in the Bering and Chukchi seas.

2.1.1. Regional setting

Currents in the Pacific Arctic region are dominated by a northward advection of water crossing the Bering shelf, converging in the Bering Strait and moving into the Chukchi Sea (Fig 2-2A). Different water mass components influence the transfer of associated heat content, organic matter and nutrients to the ecosystem (Weingartner et al. 2005, Woodgate et al. 2005a, Woodgate 2018). There are three primary current pathways during the open water season: the nutrient-rich Anadyr Current to the west, Bering Sea water with summer and winter variants, and the warmer, nutrient-poor and seasonal Alaska Coastal Current to the east (Weingartner et al. 2005, Gong & Pickart 2015, Weingartner et al. 2017). The northward flowing hydrography brings nutrient-rich Pacific waters into the euphotic zone and supports persistent localized *in situ* production and advection and deposition of organic carbon to the benthos, and this productivity plays a role in the maintenance of benthic biological "hot spots" in the Bering Strait region (Grebmeier et al. 2015).

The shallow shelf that spans from the northern Bering Sea to the northeast Chukchi Sea averages 40 meters in depth and has in recent years been seasonally ice covered for 0–3 months in the Bering Sea and 6–9 months in the Chukchi Sea (Frey et al. 2015). The

maximum median sea ice extent (1981–2010) has historically occurred in March in the northern Bering Sea and the minimum ice extent in September in the Chukchi Sea near the shelf break (Fig 2-2A). More recently, the minimum extent has shifted northwards away from the shelf break into the basin. The delayed freeze up in the Chukchi Sea ultimately impacts the winter sea ice extent and shifts the sea ice coverage in this entire region (Wang et al. 2018). Throughout the sea ice cycle, primary production typically initiates with the ice algae bloom prior to sea ice melt, followed by or possibly partially seeding a pelagic phytoplankton bloom (Gradinger 2009, Szymanski & Gradinger 2016, Selz et al. 2018).

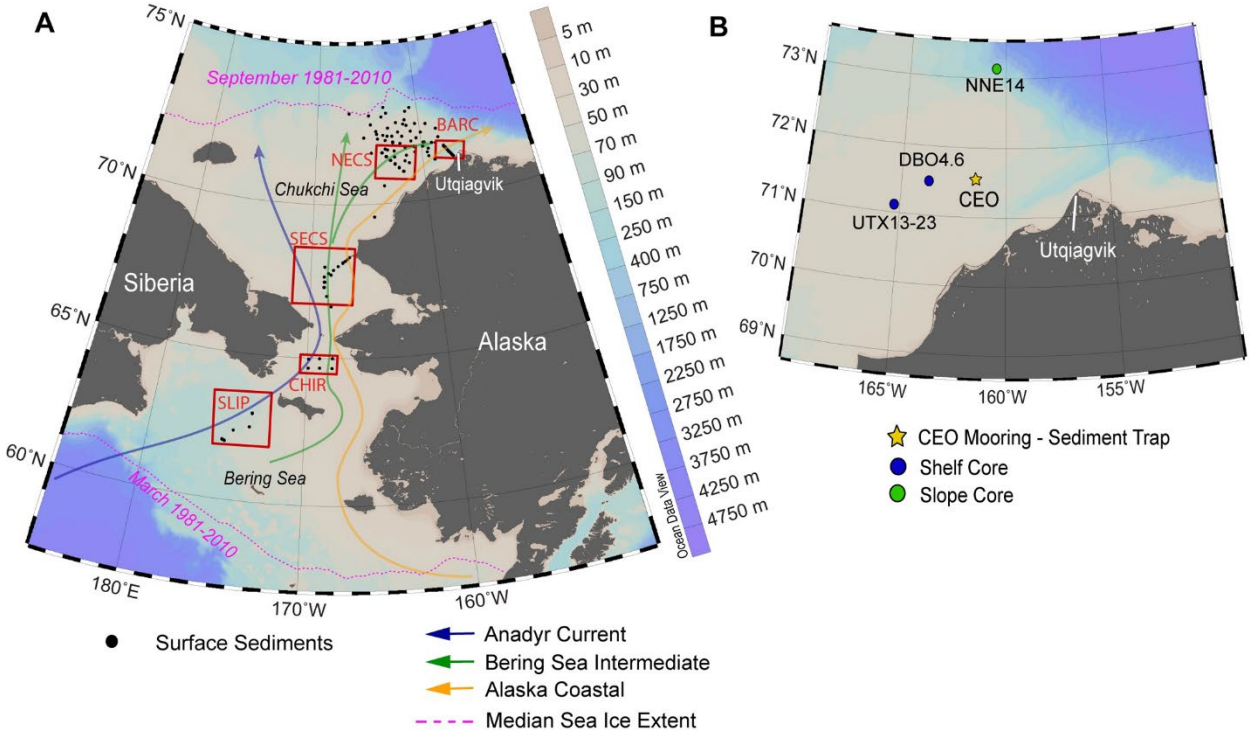

Figure 2-2 Study site in the Pacific Arctic Region A) The surface sediment sampling locations in the northern Bering and Chukchi Seas occurred within the framework of the Distributed Biological Observatory (DBO) regions (black boxes). The DBO regions in this study from south to north include: The St. Lawrence Island polynya (SLIP), Chirikov Basin (CHIR), southeast Chukchi Sea (SECS), northeast Chukchi Sea (NECS) and Barrow Canyon (BARC). **B)** The northeast Chukchi Sea region with the locations of the Chukchi Ecosystem Observatory (CEO) moored sediment trap and Haps core

locations. Reprinted from Ocean Data View under a CC BY license, with permission from R. Schlitzer, original copyright 2020.

2.2. Materials and methods

2.2.1. Permitting

No national or international permitting was required as part of the sample collection efforts. Concerns regarding sampling in waters near Indigenous subsistence hunting areas was addressed by provision of cruise plans to the Arctic Waterways Safety Committee and some samples were imported into the United States from Canada using a US Fish and Wildlife Service Declaration for Importation or Exportation of Fish or Wildlife (USFWS Form 3-177).

2.2.2. Sediment trap deployment

A sequential sediment trap (Hydro-Bios, Germany; 24 cups) was moored at 37 m depth, 8 m above the seafloor, as part of the Chukchi Ecosystem Observatory (CEO) located on the southeastern flank of Hanna Shoal (71.6°N 161.5°W, Fig 2-2B). The sediment trap was deployed in August 2015 and recovered in August 2016. Collection cups rotated at pre-programmed intervals ranging from one week during spring and summer to one month during winter. The last sample was excluded from the study as the sediment trap was recovered before the completion of the last rotation when the cup was still open. Before deployment, collection cups were filled with filtered seawater, adjusted to a salinity of 38 with NaCl to create a solution denser than ambient seawater to ensure material remained in the cup while open, and poisoned with formalin (4% final solution) to preserve samples during deployment and after recovery. In preservation tests of marine samples, formalin did not affect HBI proportions or indices relative to wet/dry freezing (Brown 2018). Trap samples were stored in the dark at room temperature until analysis, but we note that the effects of storage

temperature on HBI degradation in formalin preserved samples have not been investigated (Cabedo-Sanz et al. 2016).

2.2.3. Diatom identification and quantification

Subsamples (0.1–3 mL) from the sediment trap bottles were adjusted to a volume of 3 mL with filtered seawater for the enumeration and identification of algal cells in an Utermöhl chamber (Utermöhl 1931). A minimum of 300 phytoplankton cells were counted and identified to the lowest taxonomic level possible by inverted light microscopy at 100X, 200X or 400X depending on cell size using the Utermöhl method (Utermöhl 1931). Empty algal cells (without chloroplasts) were distinguished from intact cells (with chloroplasts) assumed to be alive at the time of collection and resting spores (Lalande et al. 2019). Algal measurements were converted to daily fluxes depending on the subsampled volume and open cup duration of each sample.

Two sea ice exclusive diatom species, *Nitzschia frigida* and *Melosira arctica*, were selected as indicators of the ice algae bloom. The *Gyrosigma/Pleurosigma/Haslea* group were selected to be the source of sympagic HBIs based on the currently known species that produce these lipids, which include *Pleurosigma stuxbergii var. rhomboides* (Cleve in Cleve and Grunow) Cleve*, Haslea kjellmani* (Cleve) Simonsen, *H. crucigeroides* (Hustedt) Simonsen*,* and *H. spicula* (Hickie) Lange-Bertalot (Brown et al. 2014c, Limoges et al. 2018). This broader group is not exclusively associated with sea ice. Another caveat is that *Pleurosigma* spp. includes species that produce the pelagic HBI III, including *P. intermedium* (Belt et al. 2000a). The diatom genera *Rhizosolenia* was selected as an indicator of the potential sources of HBI III. Species known to produce HBI III include *R. hebetata*, *R.*

polydactyla f. polydactyla and *R. setigera* (Belt et al. 2017). A more detailed analysis of the major diatom taxa and fluxes is discussed in Lalande et al. (2020)

Subsamples for chlorophyll *a* (chl *a*) measurements were filtered onto GF/F filters (0.7 μm), extracted in 90% acetone for 24 h at -20°C and measured on a Turner Design Model 10-AU fluorometer following the methods outlined in Welschmeyer (1994). Samples were kept cool and in the dark prior to chl *a* measurements.

2.2.4. Surface sediment collection

Surface sediment sampling was conducted on six annual expeditions from 2012 to 2017 on board the USCGC *Healy* (HLY; 2012, 2013, 2017) and the CCGS *Sir Wilfrid Laurier* (SWL; 2014, 2015, 2016). Sample collections from 2014 to 2017 were made at Distributed Biological Observatory (DBO) program sites (https://www.pmel.noaa.gov/dbo/), where long-term monitoring has been established in the Bering, Chukchi, and Beaufort seas (Grebmeier et al. 2010, Moore & Grebmeier 2018). These sites are in the vicinity of five DBO long-term sampling station grids that were selected on the basis of having high productivity and/or biodiversity specifically in the north Bering Sea, the St. Lawrence Island polynya (SLIP), and the Chirikov Basin (CHIR), and north of Bering Strait, the southeast Chukchi Sea (SECS), the northeast Chukchi Sea (NECS) and Barrow Canyon (BARC) (Fig 2-2A). Sample collection in 2012 and 2013 focused primarily on the NECS region near Hanna Shoal (Fig 2-2B), but extended to all of the long-term Bering and Chukchi DBO benthic sampling sites in other sampling years. Surface sediments were collected by a van Veen grab (0.1 m^2), with a trap door on the top that was opened prior to opening the grab in order to obtain relatively undisturbed sediments that were assayed for total organic carbon (TOC) and HBIs in the surface sediments. Samples were stored frozen (-20°C) until analysis.

2.2.5. Sediment core collection

Sediment cores were collected using a multi-HAPS corer (area =133 cm^2) with stainless steel barrels and acrylic inserts deployed from the USCGC *Healy* in 2017 at station DBO 4.6 (71.62°N 163.77°W) and station NNE-14 (73.29°N 160.04°W, Fig 2-2B). A single core was collected at station DBO 4.6 on the shelf from a bottom depth of 43 m (Table 1). This core was sectioned shipboard for the first two centimeters at 1-cm intervals and the remaining length of the core at 2-cm intervals. A pair of cores were collected at station NNE-14 (1200 m depth; Table 2-1). Both cores were sectioned in 1 cm intervals at sea. Sections from core sections were immediately frozen and stored at -20°C until analysis.

Table 2-1 Sediment coring locations and parameters

Station	Deployment	Latitude °N	Longitude °W	Bottom depth (m)	Core length (cm)	Distance from CEO (nm)
NNE-14	9/5/2017	73.33	-160.17	1281	20	107
DBO 4.6	8/31/2017	71.62	-163.77	43	18	43
UTX13-23	8/5/2009	71.39	-166.28	46	16	92

Sediment core station names, collection dates, coordinates, station bottom depth, length of the Haps cores and distance from the Chukchi Ecosystem Observatory (CEO) mooring. All sediment cores were collected with a Multi-Haps stainless steel corer. Cores were collected from the northeast Chukchi shelf (DBO 4.6 and UTX13-23) and slope (NNE-14).

2.2.6. Sediment core radiocesium measurements

The sectioned core from NNE-14 was analyzed for radiocesium (^{137}Cs) by gamma spectroscopy using a Canberra GR4020/S reverse electrode closed-end coaxial detector at the Chesapeake Biological Laboratory following established protocols (Cooper & Grebmeier 2018). Sedimentation data from another core collected in 2009 at station UTX13-23 (71.39°N 166.28°W), approximately 50 nautical miles from DBO4.6, was used in lieu of gamma analysis of the single core from DBO4.6 (Cooper & Grebmeier 2018), which was instead used for analysis of IP_{25} and other biomarkers. The ^{137}Cs profile from core UTX13-

23, which has been presented elsewhere (Cooper & Grebmeier 2018) was used as a sedimentation proxy for DBO4.6, based on similarities in deposition (Cooper & Grebmeier 2018). DBO4.6 and UTX13-23 have similar grain sizes (50-75% ≥ 5 phi) and TOC (0.5-1%) (Cooper & Grebmeier 2018), which have been found to be significantly correlated with radiocesium activity in surface sediments (Cooper et al. 1998). Additionally, we expected DBO4.6 to be highly influenced by bioturbation, as are most cores collected from this area of the Chukchi shelf (Cooper & Grebmeier 2018). This substitution was expected to be reasonable for the purpose of comparing cores collected in the biologically productive NECS region on the shelf relative to a core collected on the less productive continental slope (NNE-14).

2.2.7. Biomarker extraction

HBIs were extracted from surface sediment samples (n=184; S1 Table), sediment trap sample cups (n=23), and two sectioned sediment cores. Surface sediment and core samples were freeze dried for 48 hours, homogenized by mortar and pestle, followed by subsampling of approximately 1 g dried sediment. Sample cups from the sediment trap were gently mixed before subsamples were extracted with a modified pipette to enable the collection of larger particles for the measurement of HBIs. Sample volumes varied from 10 to 30 mL to accommodate the fluctuating particle flux through the year. These aliquots were filtered on Whatman GF/F filters (0.7 μm) and rinsed with deionized water. The filters were frozen overnight in petri dishes and placed into 8 mL vials for biomarker extraction.

HBIs were extracted following the methods of Belt et al. (Belt et al. 2012) and Brown et al. (Brown et al. 2014d). An internal standard (10 μL) of 9-octylheptadec-8-ene (9-OHD, 1 μg mL^{-1}) was added to the sample before extraction to facilitate yield quantification. Samples

were first saponified in a methanolic KOH solution and heated at 70°C for one hour. Hexane (4 mL) was added to the saponified solution, vortexed, and centrifuged for 3 minutes at 2500 RPM for three iterations. The supernatant with the non-saponifiable lipids (NSLs) was transferred to clean glass vials and dried under a gentle N_2 stream to remove traces of residual methanolic KOH.

Elemental sulfur was removed from the sediment samples due to analytical interference with HBI III (*m/z* 346.3). This was accomplished by re-suspending the NSLs in 2 mL hexane with the addition of 1 mL of a tetrabutylammonium (TBA) sulfite reagent and 2 mL of 2-propanol. The solution was shaken for one minute and repeated, if necessary, until a precipitate formed. MilliQ water (3 mL) was added and the mixture centrifuged for 2 minutes at 2500 RPM. The hexane layer was removed into a clean vial with the hexane extraction and centrifugation repeated three times. The extract was dried under a gentle N_2 stream at 25°C and removed immediately once the solvent had evaporated.

Following sulfur removal, the extracts were re-suspended in hexane and fractionated using open column silica gel chromatography. The non-polar lipids containing the HBIs were eluted while the polar compounds were retained on the column. The eluted compounds were dried under N_2. 50 µL of hexane was added twice to the dried extract and transferred to amber chromatography vials.

2.2.8. Biomarker analysis

The extracts were analyzed using an Agilent 7890A gas chromatograph (GC) coupled with a 5975 series mass selective detector (MSD) following methods outlined by Belt et al. (Belt et al. 2012). Samples were analyzed on an Agilent HP-5ms column (30 m x 0.25 mm x 0.25 µm). The oven temperature was programmed to ramp up from 40°C to 300°C at

10°C/minute with a 10-minute isothermal period at 300°C. HBIs were identified using both total ion current (TIC) and selective ion monitoring (SIM) techniques. TIC chromatograms and mass spectral output data were used to identify individual HBIs while SIM chromatograms were used to quantify the abundances by peak integration with ChemStation software. A purified standard of known IP_{25} concentration was used to confirm the mass spectra, retention time and retention index (RI). Authentic HBI standards were also measured alongside the internal standard 9-OHD to determine the instrument response factor (RF, Table 2-2). For experimental purposes, samples were reanalyzed on an Agilent DB-5ms column (30 m x 0.25 mm x 0.25 μm) to determine the column-specific retention indices of these compounds. The HBIs were identified by their mass ions and RI including IP_{25} (*m/z* 350.3), HBI II (*m/z* 348.3) and HBI III (*m/z* 346.3). To the best of our knowledge, the RIs for these HBIs have not been previously reported in the literature on a DB-5ms column (Table 2). A procedural blank was run every 9th sample.

Table 2-2 HBI parameters for gas chromatography-mass spectrometry

Biomarker	*m/z*	Response Factor	Retention Index HP-5ms	Retention Index DB-5ms
IP_{25}	350.3	5	2081	2071
HBI II	348.3	12	2082	2075
HBI III	346.3	3	2044	2032

Individual biomarkers and the instrument response factors determined for this study. The known retention indices for the HP-5ms column were used for analysis and the RI for a DB-5ms column were experimentally reported.

Individual HBI concentrations in the surface sediment samples were normalized by TOC on an organic gram weight basis (Table S-1). TOC data from HLY12 (2012), HLY1702 (2017) and SWL 14-16 (2014–2016) cruises were accessed through the National Science Foundation's Arctic Data Center (Grebmeier & Cooper 2019a, Grebmeier & Cooper 2019b, Grebmeier & Cooper 2019c, Grebmeier & Cooper 2019d, Grebmeier & Cooper 2019e). TOC

data from the HLY13 (2013) cruise are available through another data archive, the National Oceanic and Atmospheric Administration National Centers for Environmental Information (Dunton 2014). HBI concentrations from sediment trap samples were converted to daily fluxes depending on the subsampled volume and open cup duration of each sample and integrated over a 365-day period to annual fluxes.

The relative abundances of the sympagic HBIs (IP_{25} and HBI II) to the pelagic HBI (HBI III), were quantified in order to determine the proportions attributable to different organic carbon sources. An HBI fingerprinting index, termed "H-print", was used to estimate the relative organic carbon contributions of sea ice algae versus phytoplankton sources (Brown et al. 2014d). The H-print method (Eq. 1-1), is calculated using the relative abundances of IP_{25}, HBI II and HBI III, as determined by GC-MSD methods:

$$\text{H-print \%} = \frac{\text{HBI III}}{\sum (IP_{25} + \text{HBI II} + \text{HBI III})} \times 100 \qquad \text{(Eq. 1-1)}$$

The estimated organic carbon contribution resulting from the H-print analysis varies from 0% to 100%, with lower values indicative of proportionally greater sympagic inputs and higher values indicative of proportionally lower sympagic inputs (i.e. substantial pelagic diatom sources). Analytical error from replicate control tests was determined to be less than 14% (relative standard deviation, RSD) for HBI quantification and less than 12% (RSD) for H-print values.

2.2.9. Sea ice concentration and snow cover

At the sediment trap location, daily averaged sea ice concentrations were retrieved at a 12.5-km resolution from the National Snow and Ice Data Center (NSIDC, https://nsidc.org) using the Defense Meteorological Satellite Program (DMSP) Special Sensor Microwave

Imager/Sounder (SSMIS) passive microwave data. Snow depth on top of sea ice was retrieved at a 25-km resolution from the Northern Hemisphere snow depth files derived from the SSMIS data. Daily sea ice concentration and snow depth were averaged for a delimited region above the mooring (44 x 44 km; 71.4–71.8°N; 161.4–161.9°W).

The spring sea ice concentration (SpSIC) for each year of the study was averaged from monthly (April-June) sea ice concentration using DMSP SSMIS data (Smik et al. 2016). The mean sea ice concentration at each of the sediment sample locations was extracted from the pixel containing the station location. The sea ice break-up dates were determined at each of the surface sediment sample locations. The sea ice break-up date was defined as the date when the pixel containing the station registered two consecutive days of sea ice concentration ≤15%, a common threshold for open water conditions in sea ice studies (Frey et al. 2015). The sea ice break-up date was then subtracted from the sample collection date to determine the ice-free period prior to sampling at each specific location of interest.

2.2.10. Statistical analysis

Spatial analysis of the biomarker concentrations and H-print values were conducted with ODV using DIVA (Data-Interpolating Variational Analysis) gridding methods (Schlitzer 2016). All other statistical analyses were performed in R v. 3.6.1 (R Core Team 2017) and plots were produced using the package ggplot2 (Wickham 2016). Multiple linear regressions were used to investigate correlations between sea ice data and H-print. One-way ANOVA testing and Tukey Honest Significant Difference (HSD) multiple pairwise comparisons were used to analyze the differences in relative HBI concentrations by DBO region. Principal components analysis (PCA) was used to analyze the impact of individual relative biomarker

abundances at each location. Pearson product moment correlations were used to test for relationships among biomarker, diatom and chl *a* fluxes.

2.3. Results

2.3.1. Annual cycle of sea ice concentration, biomarker and diatom fluxes

At the CEO mooring site, open water conditions persisted from the initial deployment in mid-August through mid-November 2015 (Fig 2-3A). The increase in sea ice concentration in late November 2015 indicated a rapid sea ice freeze-up and the site remained ice-covered through mid-July 2016 (Fig 2-3A). Snowmelt first occurred in May 2016 and sea ice melt initiated in June 2016 (Fig 2-3A). Some sea ice (>15%) however remained present above the sediment trap until the end of deployment.

Chl *a* fluxes ranged from 1.5 to 1.9 mg m^{-2} d^{-1} from August through September 2015. Chl *a* levels remained relatively low (below 0.2 mg m^{-2} d^{-1}) from December 2015 through April 2016. Chl *a* rapidly increased in late June 2016 and the maximum flux occurred in late July 2016 at 4.9 mg m^{-2} d^{-1} (Fig 2-3B). Similarly, POC fluxes were highest from August through September 2015 (1.09 to 1.18 g C m^{-2} d^{-1}), a decline through the winter months and steady increase beginning in April 2016. The POC flux reached 1.04 g C m^{-2} d^{-1} in late July 2016 before the trap was recovered (Fig 2-3B).

The sympagic diatom fluxes are indicated by *N. frigida* and *M. arctica* (Fig 2-3C). *N. frigida* was first detected in the sediment trap in early April 2016, increased through late May 2016 and was no longer detected in early June 2016. *N. frigida* reappeared in mid-June and the maximum flux occurred in late June 2016. *M. arctica* was detected in the trap in early September 2015 and did not reappear until the maximum flux occurred in June 2016, corresponding to the peak flux for the exclusively sympagic species. *M. arctica* resting spores

were present in August and September 2015, reappeared in May and remained consistently present until the end of the deployment. The *Gyrosigma/Pleurosigma/Haslea* group was detected in the trap throughout most of the year with the exception of early September through early November 2015 (Fig 2-3D). This group steadily increased starting in April 2016 and reaches a maximum in early July 2016. *Rhizosolenia* fluxes were only detected as intact cells from September through November 2015 (Fig 2-3E) although there were substantial fluxes of fragments year round (data not shown). The peak flux occurred in mid-November 2015.

IP_{25} was detected throughout the entire sampling period (Fig 2-3F). IP_{25} fluxes in the initial winter months (December 2015 through February 2016) occurred without the corresponding diatom groups recorded in the traps (Figs 2-3D, F). IP_{25} fluxes began to increase in mid-May and reached a maximum in early July 2016 at 1331 ng m^{-2} d^{-1} (Fig 2-3F; Table 2-3). IP_{25} sharply declined to 119 ng m^{-2} d^{-1} in late July (Table 2-3). This precipitous decline coincided with the peak chl *a* flux (Fig 2-3B). Overall, IP_{25} fluxes mirrored the export of the *Gyrosigma/Pleurosigma/Haslea* taxonomic group. HBI III was also detected throughout the year (Fig 2-3G). The HBI III peak flux corresponded to the maximum *Rhizosolenia* spp. flux. HBI III fluxes reached a maximum flux of 799 ng m^{-2} d^{-1} in September 2015 (Fig 2-3G; Table 2-3). As indicated by the H-print index, the sympagic diatom signal was present but low from September 2015 to late November 2015 with H-print values ranging from 48–70% (Table 2-3), representing a mixed to pelagic diatom composition. H-print values indicated a strong sympagic diatom signal in late March through late July 2016, with the strongest sympagic indicators during mid-May, late June and early July. The annual flux of IP_{25} was 60 µg m^{-2} yr^{-1}, HBI II fluxes were 278 µg m^{-2} yr^{-1}, and HBI III fluxes reached 87 µg m^{-2} yr^{-1} (Table 2-3).

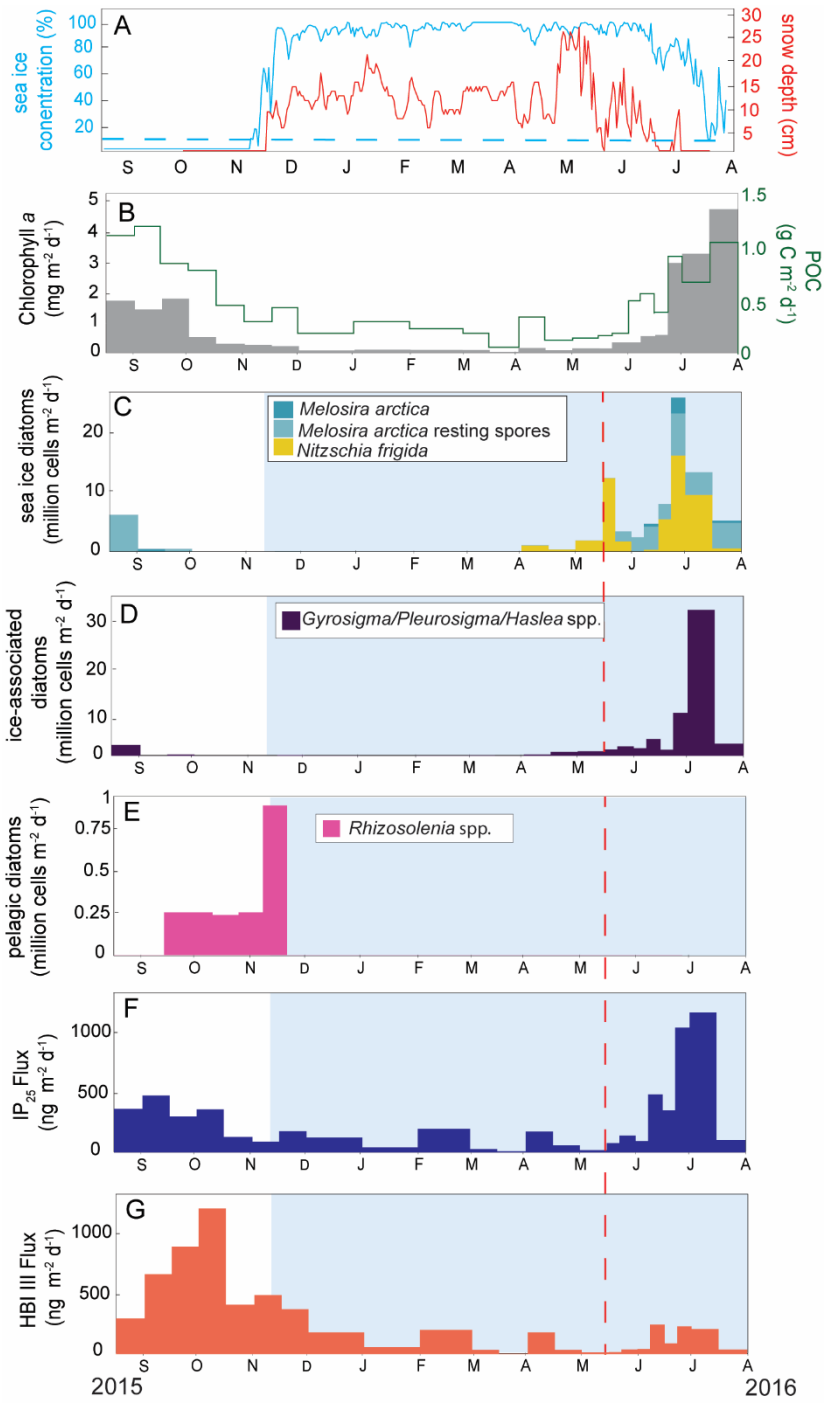

Figure 2-3 Sea ice concentration, snow depth, and annual fluxes of diatoms and biomarkers at the Chukchi Ecosystem Observatory 2015-2016 The parameters measured from the CEO sediment trap from August 2015 – August 2016 included: **A)** sea ice concentration (%) and snow depth (cm). The blue-dashed line indicates the 15% sea ice concentration threshold defining open water, **B)** chlorophyll *a* fluxes (mg $m^{-2}d^{-1}$) and POC fluxes (g C m^{-2} d^{-1}). POC and chl *a* data from Lalande et al. 2020 **C)** *Nitzschia frigida* and *Melosira arctica* fluxes (sea ice exclusive diatoms), **D)**

Gyrosigma/Haslea/Pleurosigma fluxes (group containing HBI-producing species), **E)** *Rhizosolenia* spp. fluxes (group containing HBI III-producing species), **F)** IP_{25} fluxes (ng $m^{-2}d^{-1}$), and **G)** HBI III fluxes (ng $m^{-2}d^{-1}$). All panels indicate the ice-covered period within the blue shaded boxes and the onset of snow melt is depicted by the red-dashed line.

Table 2-3 Sediment trap summary data

Sampling Period	IP_{25} Flux (ng $m^{-2}d^{-1}$)	HBI II Flux (ng $m^{-2}d^{-1}$)	HBI III Flux (ng $m^{-2}d^{-1}$)	H-print (%)
16-31 August 2015	413	2209	495	24
1-15 September 2015	540	2654	799	37
16-30 September 2015	341	1957	732	53
1-15 October 2015	408	1477	673	63
16-31 October 2015	146	496	242	63
1-15 November 2015	103	490	448	70
16-30 November 2015	199	873	380	49
1-31 December 2015	140	627	209	39
1-31 January 2016	47	220	64	37
1-29 February 2016	223	1143	250	29
1-15 March 2016	32	162	31	33
16-31 March 2016	10	44	2	18
1-15 April 2016	197	1067	232	29
16-30 April 2016	65	326	43	20
1-15 May 2016	20	100	25	26
16-22 May 2016	88	420	14	8
23-31 May 2016	160	641	75	11
1-7 June 2016	107	509	70	16
8-15 June 2016	550	2212	366	19
16-22 June 2016	400	1795	154	10
23-30 June 2016	1186	5500	476	9
1-15 July 2016	1331	6903	559	7

16-31 July 2016	119	650	78	12
Total Annual Flux	**60 µg $m^{-2}yr^{-1}$**	**278 µg $m^{-2}yr^{-1}$**	**87 µg $m^{-2}yr^{-1}$**	

Summary of daily (ng $m^{-2}d^{-1}$) and annual (µg $m^{-2}yr^{-1}$) HBI fluxes at the Chukchi Ecosystem Environmental Observatory moored sediment trap. IP_{25} and HBI II are sea ice (sympagic) algae biomarkers and HBI III is a phytoplankton (pelagic) biomarker. The H-print index represents the relative proportion of the pelagic to sympagic contribution of the total HBI flux. Low H-print values indicate elevated sea ice algae contributions while high H-print values indicate higher contributions of pelagic diatoms.

A Pearson correlation test was conducted on the assigned diatom groupings, chl *a* fluxes, and HBI fluxes (Table 2-4). The group containing sympagic-HBI producing species (*Gyrosigma/Pleurosigma/Haslea*) was strongly correlated with IP_{25} fluxes (r=0.80, p<0.001). The group containing pelagic-HBI producing species (*Rhizosolenia spp*.) was not significantly correlated with HBI III fluxes. Chl *a* was positively correlated with IP_{25} fluxes (r=0.60, p<0.01) and *Gyrosigma/Pleurosigma/Haslea* spp. (r=0.56, p< 0.01). IP_{25} and HBI III were also positively correlated (r=0.61, p<0.01). IP_{25} was positively correlated with the sea ice diatom flux (*N. frigida* and M. *arctica*, r=0.58, p<0.05).

Table 2-4 Pearson product-moment correlation matrix for flux data

	Sea ice diatom flux	*Gyrosigma - Pleurosigma- Haslea* flux	*Rhizosolenia* flux	Chlorophyll *a* flux	IP_{25} flux
Gyrosigma/Pleurosigma/Haslea flux	**0.58**				
Rhizosolenia flux	-0.25	-0.16			
Chlorophyll *a* flux	**0.55**	**0.56**	0.13		
IP_{25} flux	**0.73**	**0.80***	-0.09	**0.60**	
HBI III flux	0.11	0.26	0.31	0.35	**0.61**

The Pearson product-moment correlation coefficients for the sediment trap flux parameters including: sympagic diatom flux (*N. frigida* and *M. arctica*), *Gyrosigma/Pleurosigma/Haslea* spp. flux, *Rhizosolenia* spp. flux, chlorophyll *a* flux, IP_{25} and HBI III fluxes. Values in bold indicate significant correlation (r) where $p < 0.05$. An asterisk indicates targeted associations for HBI and diatom comparisons. Sample sizes for all parameters were n=23.

2.3.2. Distribution and variation of biomarker deposition

IP_{25} was detected in all of the surface sediment samples (Fig 2-4). Localized high concentrations occurred in the NECS and BARC regions in 2013 and 2017 and in the Chirikov Basin in 2016. IP_{25} concentrations were generally higher (>3 μg g^{-1} TOC) overall in the NECS and BARC regions relative to the lower latitude DBO regions. The SLIP region in 2015 was an exception with IP_{25} concentrations reaching 12 μg g^{-1} TOC at the SLIP3 station (S1 Table), which was the highest concentration observed of all years and stations. IP_{25} data were only available for the SLIP region from 2015 through 2017, however, the concentration decreased over this time. Values exceeded 6 μg g^{-1} TOC in four samples total (8–12 μg g^{-1} TOC), which were determined statistically to be outliers by the IQR (Interquartile Range) method, and were incorporated as the maximum value (6 μg g^{-1} TOC) rather than omitted for DIVA gridding. HBI III values were relatively consistent from year to year, with the highest concentrations found in the southeast Chukchi Sea (SECS) and northern Bering Sea (SLIP and CHIR) and minimal concentrations in the NECS (Fig 2-4).

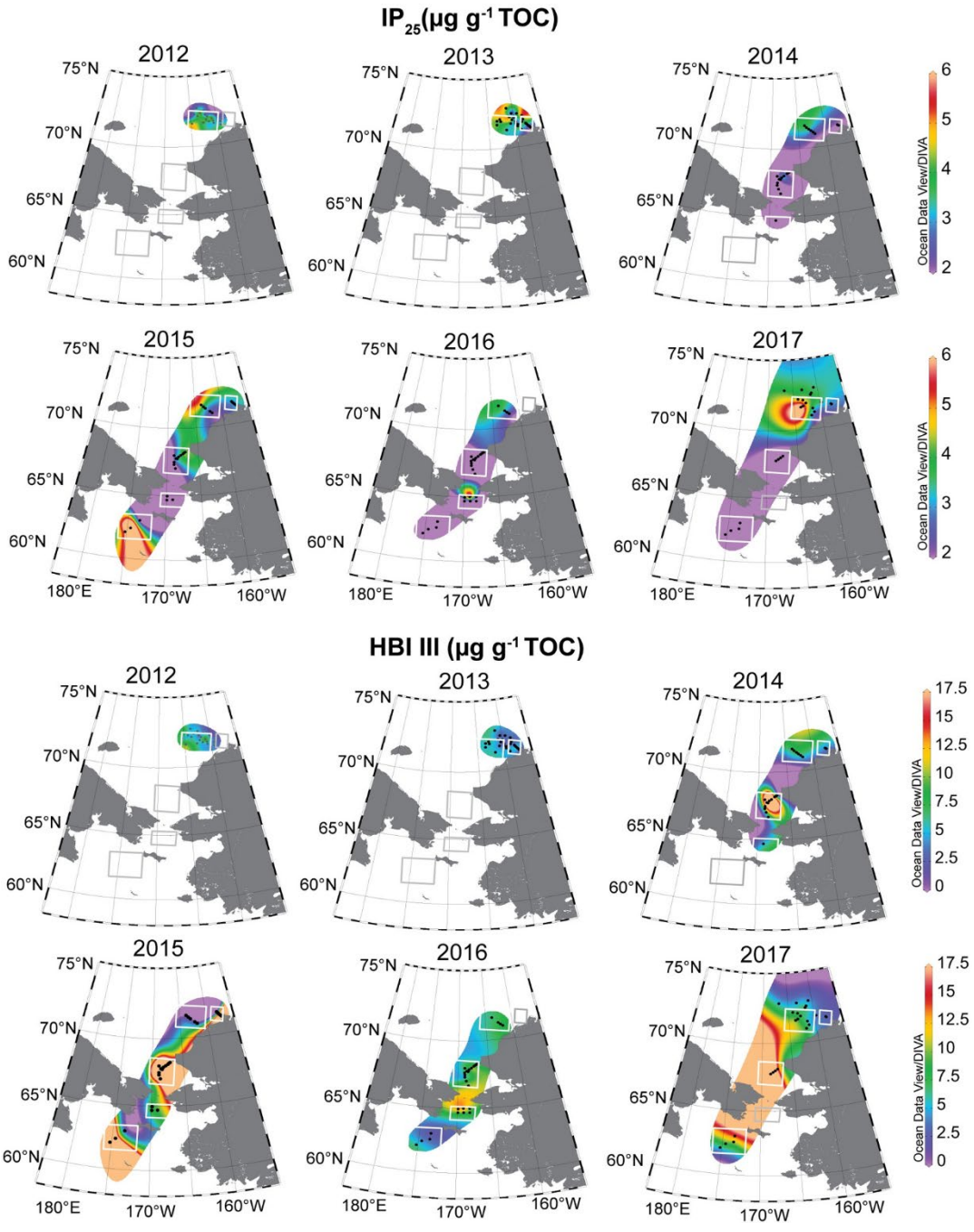

Figure 2-4 IP_{25} and HBI III biomarker distributions Spatial distribution of the relative abundances of IP_{25} and HBI III concentrations (µg g^{-1} TOC) in surface sediments from 2012–2017. The white and grey bounding boxes indicate the DBO regions from south to north (SLIP, CHIR, SECS, NECS and BARC). Not all sampling stations and DBO regions were able to be occupied every year due to sea ice or weather, indicated by grey boxes (no data collected). IP_{25} and HBI III values were used as sympagic and pelagic diatom proxies, respectively, for the H-print analysis. Reprinted from Ocean Data View under a CC BY license, with permission from R. Schlitzer, original copyright 2020.

The spatial distribution of H-print index followed the general pattern of spring sea ice retreat each season, with weaker sympagic signatures (H-print > 60%) in the northern Bering Sea, particularly south of St. Lawrence Island and in the Chirikov Basin (Fig 2-5). The NECS and BARC regions displayed an elevated to moderate sea ice signal each year, with mean H-print values ranging from ~21–59% for NECS and ~38–49% for BARC (Table 2-5). Spring sea ice concentrations derived from satellite data indicated sea ice persistence through July in the northeast Chukchi Sea for 2012 to 2017 and an increasing open water period from the Chirikov Basin north to the southeast Chukchi sea from 2014 to 2017. By the spring months (April-June), the lower latitude stations were consistently ice-free. Four stations in 2017 had duplicate surface sediment samples from HAPS core tops and Van Veen grabs. The maximum difference in H-print was 6%, within the margin of error (12%).

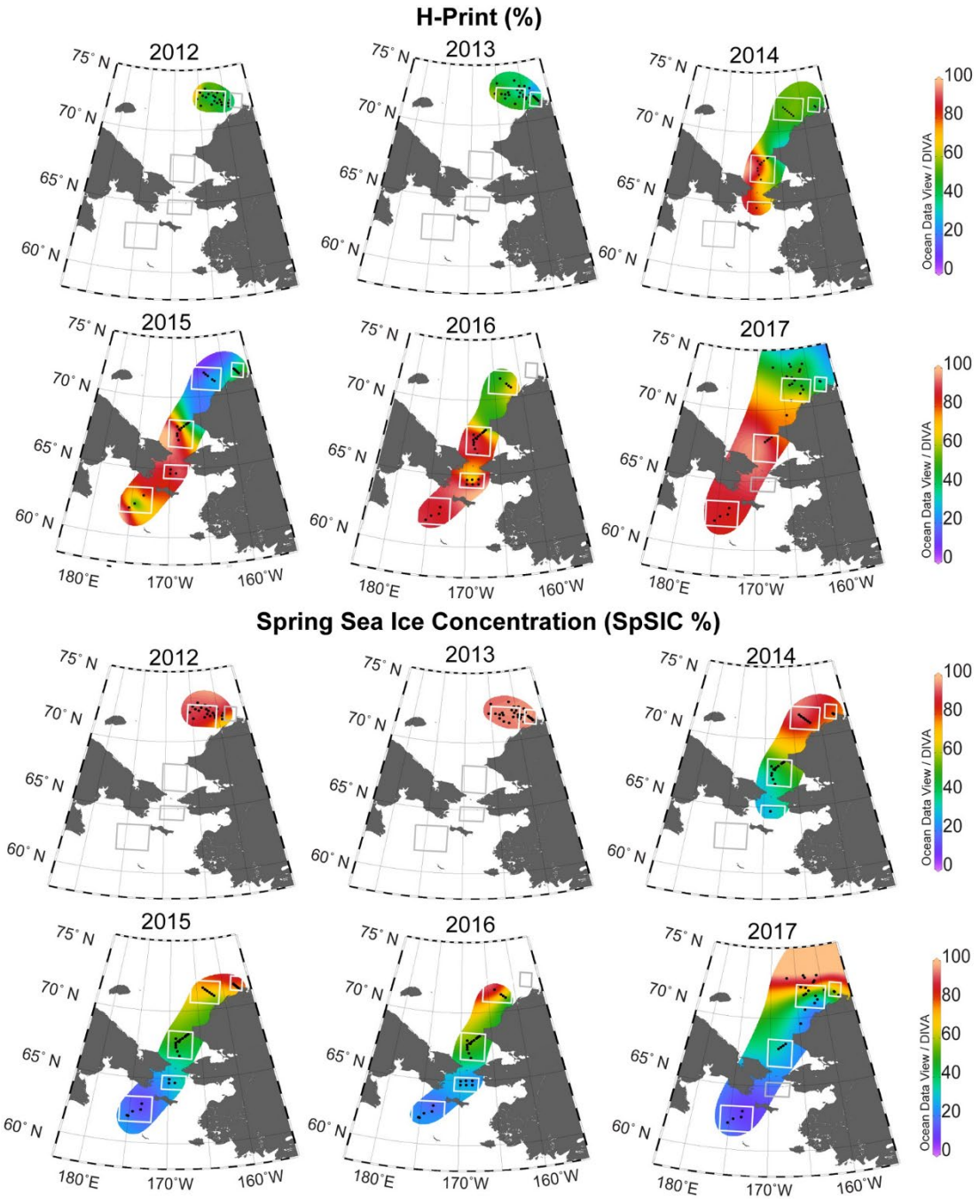

Figure 2-5 H-print index and satellite-derived sea ice concentration The spatial distribution of H-print (%) in surface sediments from 2012–2017 and the spring sea ice concentration (SpSIC%) derived from April–June mean sea ice concentrations collected from SSMIS passive microwave data (NSIDC). The white and grey bounding boxes indicate the DBO regions from south to north (SLIP, CHIR, SECS, NECS and BARC). Not all sampling stations and DBO regions were able to be occupied every year due to sea ice or weather, indicated by grey boxes (no data collected). H-print ranges from 0-100%, where low values indicate elevated sea ice algae contributions while high values indicate higher

contributions of pelagic diatoms. Reprinted from Ocean Data View under a CC BY license, with permission from R. Schlitzer, original copyright 2020.

Table 2-5 Regional summary of H-print sea ice index spatial distributions

	Mean H-print (%) by Year					
DBO Region	**2012**	**2013**	**2014**	**2015**	**2016**	**2017**
St. Lawrence Island Polynya (SLIP)	-	-	-	71 ± 32 (5)	88 ± 2 (5)	86 ± 1 (4)
Chirikov Basin (CHIR)	-	-	82 (1)	88 ± 6 (4)	82 ± 18 (6)	-
Southeast Chukchi (SECS)	-	-	76 ± 16 (12)	71 ± 24 (14)	83 ± 11(14)	87 ± 9 (7)
Northeast Chukchi (NECS)	49 ± 9 (21)	46± 7 (30)	54 ± 3 (6)	21 ± 10 (6)	59 ± 8 (4)	49 ± 11 (18)
Barrow Canyon (BARC)	-	41 ± 9 (10)	49 ± 6 (3)	40 ± 22 (10)	-	37± 4 (4)

Mean H-print (mean ± SD) by DBO region and year of sample collection. Sample sizes (n) are in parentheses.

To assess the relationship between the H-print index and sea ice, linear regressions of two sea ice metrics were examined, including the SpSIC and sea ice break-up date relative to sample collection (Fig 2-5). Both relationships were significant at the 99% confidence level but the SpSIC relationship was a better fit (R^2=0.46 versus R^2=0.34, n=184). The SpSIC and H-print regression shows that the locations with ice-coverage through spring had more substantial sympagic HBI contributions (Fig 2-6A). The number of ice-free days before sampling shows longer relative periods of open water were associated with reduced sympagic and elevated pelagic organic matter inputs (Fig 2-6B). There was a linear gradient and association between higher H-prints and extended open water periods (lower spring sea ice concentration) at lower latitudes and lower H-prints with higher spring sea ice and shorter ice-free periods at higher latitudes. There was a large degree of variability in both relationships.

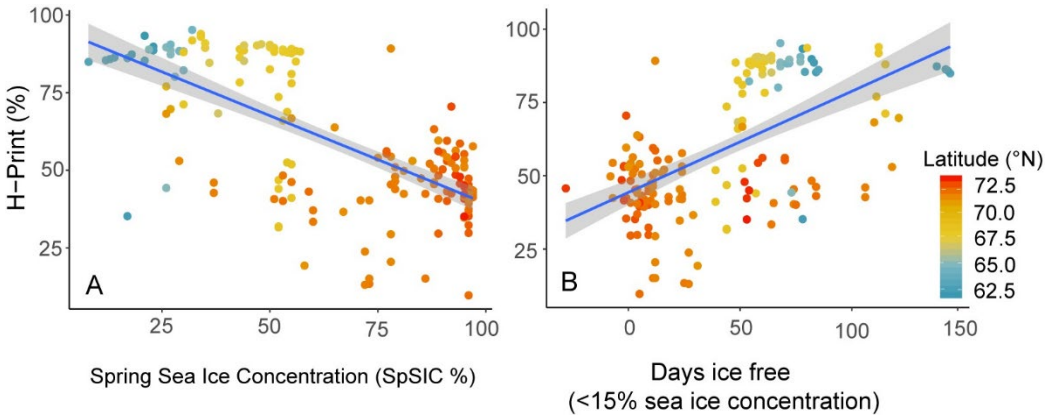

Figure 2-6 Latitudinal variation and correlation of the H-print index with sea ice The 2012–2017 H-print values were compared with two different metrics for sea ice to determine the influence on the biomarkers. A) Linear regression of H-print and the mean Spring Sea Ice Concentration (SpSIC) derived from April-June monthly sea ice concentration values. B) Linear regression of H-print and the ice free period determined by the sea ice break-up date relative to sample collection date. Both relationships are shown with respect to latitude.

To further explore the relationship between latitude and H-print, the H-print values were grouped by DBO region and plotted by latitude (Fig 2-7A). The box-and-whisker plots show the transition of increasing sea ice algal signature from south to north. There is also a greater degree of variability in the Chukchi Sea regions (SECS, NECS and BARC). The principal components analysis with individual HBIs (IP_{25}, HBI II, and HBI III) and grouped by DBO region also depict a divergence between the SLIP-CHIR-SECS and the NECS-BARC regions.

A one-way ANOVA test for the H-print values grouped by DBO region suggests that the mean values were statistically different (p<0.001, F-value=55.97). A Tukey multiple-pairwise comparison indicates that the differences between NECS-BARC, SECS-CHIR, CHIR-SLIP, and SLIP-SECS were not significant. In other words, the northern regions (NECS, BARC) are similar to each other and the southern regions (SLIP, CHIR, SECS) are similar to each other, but both of the northern stations differ from each of the southern stations (p<0.001). The H-print index varied by latitude, with the greatest amount of

variability among NECS and BARC locations in addition to a stronger sea ice carbon signature at the higher latitudes (71–73°N) and stronger pelagic influence at the lower latitudes (62–68°N; Fig 2-7A). The PCA of the relative abundances of individual HBIs grouped by DBO region also supports this divergence in H-print between the northern Bering and northeast Chukchi Seas (Fig 2-7B). The first principal component (PC1) accounted for 83.3% of the variation, with primary contributions from HBI III, and the second principal component (PC2) accounting for 16.6% of the variation, with HBI II and HBI III as the primary contributors (Fig 2-7B).

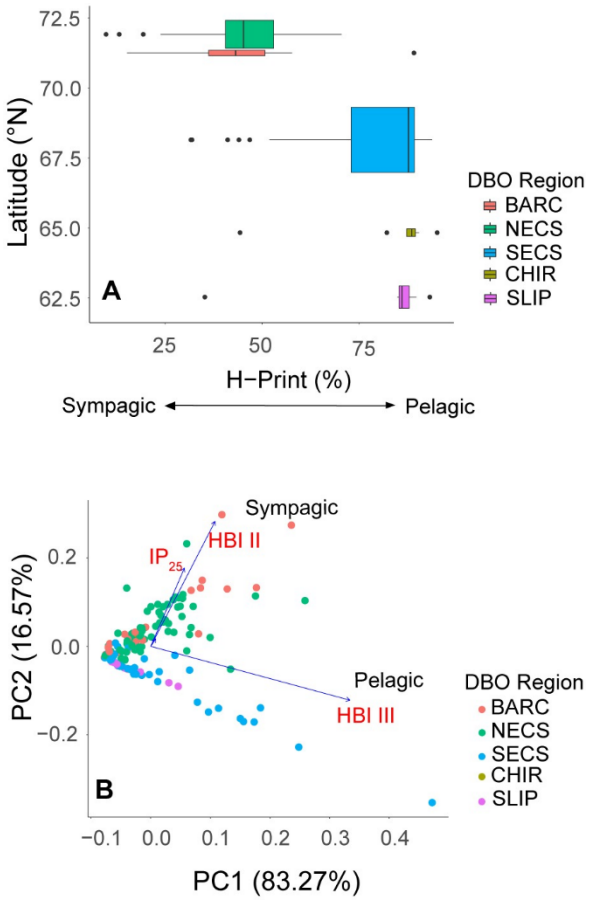

Figure 2-7 H-print index by DBO region Statistical analysis of the H-print values from surface sediments in relation to the location **A)** boxplot of H-print variability by DBO region and latitude **B)** Multivariate separation of surface sediments visualized by principal components analysis (PCA) of individual HBIs (IP_{25}, HBI II isomers, and HBI III) grouped by DBO region.

The annual mean H-print and SpSIC values for the two distinct regions were grouped to assess temporal trends over the study period (Fig 2-8). Based on regression analyses, the only significant trend identified was for the SpSIC in the northeast Chukchi Sea, with a decline of 5.8% per year (p<0.001). However, the patterns are consistent for both regions, where the SpSIC is declining and the H-print is increasing from 2012–2017 in the northeast Chukchi (Fig 2-8A) and from 2014–2017 in the northern Bering and southeast Chukchi Seas (Fig 2-8B).

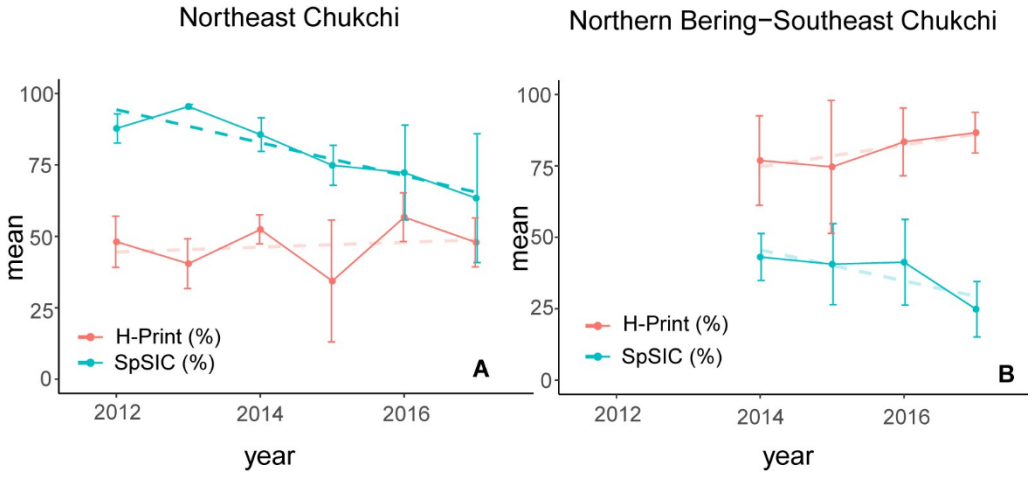

Figure 2-8 Annual trends in H-print and spring sea ice concentration (A) the northern Chukchi DBO regions (NECS and BARC) for 2012–2017 and **(B)** the Bering-southeast Chukchi DBO regions (SLIP, CHIR and SECS) for 2014–2017. The bold dashed line shows the only significant trend (p<0.01).

2.3.3. HBI profiles in sediment cores

The core collected on the Chukchi shelf break, NNE14, showed minimal signs of bioturbation, based visually on three distinct layers of sediment and validated by ^{137}Cs measurements indicating a single subsurface peak in the upper 5 cm (Fig 2-9) that can be interpreted as corresponding to the bomb fallout peak in 1963 (Cooper & Grebmeier 2018). The top 3 cm of the core consisted of oxidized red-brown sediment, the next 5 cm consisted of brown sediments with similar consistency as the shelf sediments, and the remaining length

of the core was composed of grey, fine-grained sediments. The H-print values for this core were generally homogenous and less than 30%, indicating a high and consistent degree of sympagic organic carbon contributions (Fig 2-9). The core collected on the Chukchi shelf, DBO 4.6, on the other hand, was subject to significant bioturbation, including by polychaete worms present in the core when it was sectioned (sometimes spanning multiple core intervals). The H-print values from this core were higher than the slope core, with values ranging from 30–55%, representing a greater pelagic contribution compared to the slope core but still having substantial sympagic inputs.

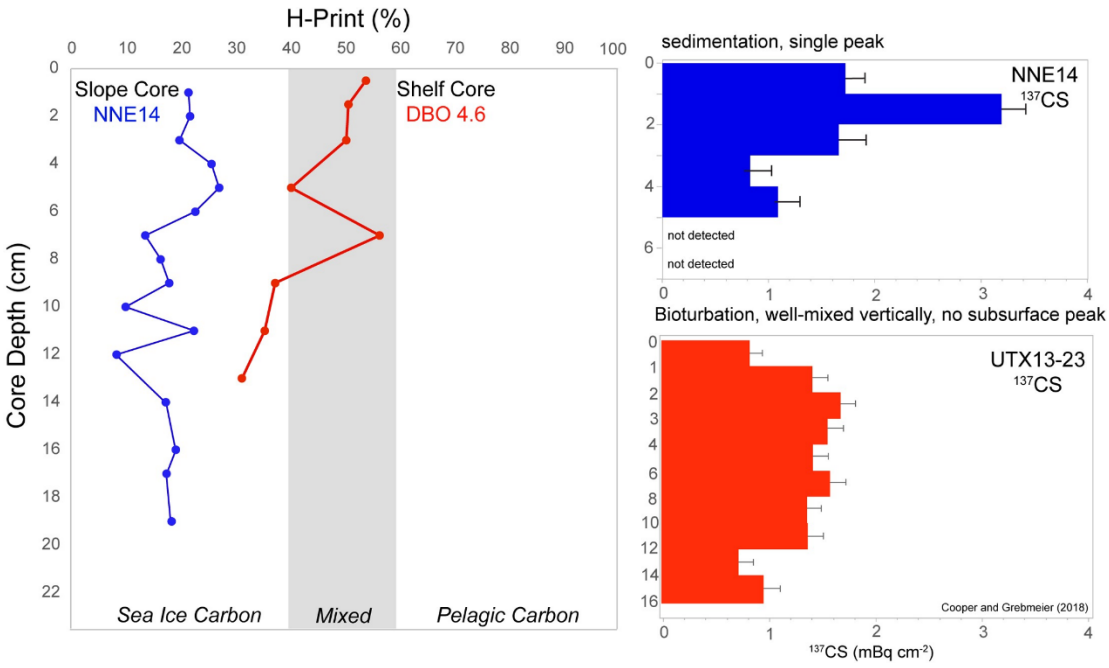

Figure 2-9 H-print and rRadiocesium profiles in sediment cores H-print profiles for a core collected on the Chukchi slope, NNE-14 (blue), and a bioturbated core collected on the shallower Chukchi shelf at DBO 4.6 (red). ^{137}Cs profiles for NNE-14 and UTX13-23, a core collected in close proximity to DBO 4.6, depict the consistent sedimentation or bioturbation of deposited material.

2.4. Discussion

Recent trends in sea ice formation and retreat in the Pacific Arctic include delayed freeze up in the Chukchi Sea, driven by increasing sea surface temperatures, water column heat

content and atmospheric dynamics, which ultimately result in later ice formation and earlier retreat in the Bering Sea (Frey et al. 2015, Frey et al. 2018, Stabeno et al. 2019). These recent higher surface water temperatures, particularly if paired with southerly winds in the winter, lead to conditions where sea ice does not reach the historical (1981–2010) median extent. In particular, the 2017–18 overwinter period was an extreme year for sea ice decline in the northern Bering Sea (Frey et al. 2018, Grebmeier et al. 2018, Stabeno et al. 2019). In 2018, the winter sea ice extent in the Bering Sea was the lowest on record followed by 2019, which was the second lowest maximum extent on record (Fetterer 2017, updated daily, Grebmeier et al. 2018). These areas once recurrently covered by ice in winter and early spring were open waters. In July 2019, the Chukchi Sea also experienced record low sea ice extent, with sea ice retreating off of the shelf by this time (Fetterer 2017, updated daily). Four of the six years analyzed in this study in the Chukchi Sea were among the top ten record low sea ice years based on regional analysis of satellite data (Fetterer 2017, updated daily). Therefore, all of the data examined in this study have occurred in a period of anomalies in the overall record, or a new norm relative to the satellite record.

2.4.1. Seasonal variations of HBI and diatom export in the northeast Chukchi Sea

The IP_{25} and sea ice diatom fluxes observed at the CEO indicated an early summer sea ice algal bloom on the Chukchi shelf. Peak IP_{25} fluxes during early July 2016 (1331 ng m^{-2} d^{-1}), coincided with the largest flux of the diatom group *Gyrosigma/Pleurosigma/Haslea* (Fig 2-2D), which account for ~1% of the relative abundance of major diatom taxa groups (Lalande et al. 2020). This value is higher than maximum values observed in August 2008 and August 2009 in the Chukchi Borderland (46 ng m^{-2} d^{-1} and 33 ng m^{-2} d^{-1}, respectively) (Bai et al. 2019). This is not surprising given that generally shallow Arctic shelves are more

productive than the basin and slope regions (Gradinger 2009, Lalande et al. 2019). The presence of sea ice associated species, such as *N. frigida* and *M. arctica,* provided additional indicators of ice algae release. Export of *N. frigida* was first detected at the CEO sediment trap in early April 2016 (Fig 3C), which was followed by the highest detected relative abundance of *Gyrosigma/Pleurosigma/Haslea* (~5%) in late April (Lalande et al. 2020). The slight increase of IP_{25} fluxes from January to February 2016 (47 to 223 ng m^{-2} d^{-1}, Table 3) corresponds to the reappearance of the *Gyrosigma/Pleurosigma/Haslea* taxonomic group (Lalande et al. 2020). This timing would correspond to the first seasonal deposition by known IP_{25} producers contributing to the algal flux from the CEO site. This period also corresponds to an increase in HBI III (220 to 1143 ng m^{-2} d^{-1}). The sharp decline in IP_{25} in late July, along with an increase in pelagic diatom species (*Chaetoceros* and *Thalassiosira spp.*) (Lalande et al. 2020), likely signified the end of ice associated diatom export as a result of the bottom few centimeters of sea ice melting that contain the most organic material and nearly all sea ice algae (Juul-Pedersen et al. 2008).

There were limitations in this study for comparing the selected diatom fluxes with the HBI fluxes, as taxonomy to the desired level was not feasible. The flux of the *Gyrosigma/Pleurosigma/Haslea* group into the sediment trap was used to compare the IP_{25} fluxes, given the potential inclusion of the three or four known species that produce IP_{25} from the genera *Haslea* and *Pleurosigma* (Brown et al. 2014c). However, this genus cluster also includes species that are not HBI producers and diatoms that are not considered exclusively sympagic. HBI-producing species are minor taxa (ca. 1–5%) and only represent a small fraction of the abundances observed in this group (Brown et al. 2014c). Therefore, these results are presented with caution in regards to being the direct source for IP_{25}. However, the onset of increasing levels of IP_{25} strongly corresponded to the increasing levels of the

sympagic diatoms and the *Gyrosigma/Pleurosigma/Haslea* group as indicated by the Pearson product-moment correlation (r=0.73 and 0.80, p<0.001; Table 2-4). The strong correlation of IP_{25} with the sea ice diatom group and the *Gyrosigma/Pleurosigma/Haslea* genus group strengthens our interpretation that IP_{25} is an appropriate sea ice proxy on the Chukchi shelf. In an example that echoes the complexities we observed in HBI source attribution, in a study conducted in an ice-covered fjord in Greenland, all known HBI-producing species were detected in ice cores and algal fluxes at 37 m but IP_{25} production could only be attributed to *H. spicula* (Limoges et al. 2018). Limoges et al. (2018) also found that *H. crucigeroides* and *H. vitrea* were producing both the diene (HBI II) and triene forms (HBI III), meaning that it is unclear what promotes synthesis of IP_{25}, including the sea ice conditions and other parameters that may promote or depress the synthesis of this compound. A recent study found that sea ice diatoms increase HBI concentration up to ten-fold when nutrients are a limiting factor (Brown et al. 2020). We had to address similar uncertainties in determining the HBI III producing species in this study. The decision to investigate the correlations between *Rhizosolenia* fluxes with HBI III was made as this genus contains several HBI III producing species, but again would not encompass all potential sources. However, we found no correlation between the *Rhizosolenia* spp. and HBI III flux (Table 2-4). It is also noteworthy that the HBI III flux decreased in late July as chl *a* reach a maximum flux during a pelagic under-ice phytoplankton bloom (Fig 2-3B, G). There was also a positive correlation between IP_{25} and HBI III fluxes that we cannot unambiguously interpret. This correlation could be due to the potential overlap of the taxa and broad assignments of possible biomarker producers (i.e. *Pleurosigma*). The weaker correlations with HBI III overall may suggest that HBI III perhaps is not reliable as a pelagic productivity indicator at this location and that *Rhizosolenia* did not adequately capture the source of the HBI III. This finding was also

discussed in a recent study in the sea ice, raising similar complexities in assigning this to a pelagic source or the potential of regional implications (Amiraux et al. 2019). An association of HBI II and HBI III was also observed in the Antarctic where it was suggested that HBI III is an indicator of the intense phytoplankton blooms that emerge in the marginal ice zone (MIZ) rather than open water, meaning that HBI III was more suitable as a proxy for sea ice seasonality or MIZ duration (Collins et al. 2013).

The HBI fluxes obtained at the CEO suggest that a combination of processes including production, resuspension and advection led to the persistent IP_{25} signature in the algal flux recorded on the northeast Chukchi Sea shelf. The high export event at the end of June and beginning of July in 2016 (Fig 2-3 B-G) corresponded to the declining sea ice concentration rather than the early snowmelt in May (Fig 2-3A). This could also mean that IP_{25} producing diatoms were present below the ice, rather than within the ice matrix. While pelagic diatoms were largely responsible for the chl *a* signal in the NECS region from August to October 2015, based upon taxonomic analysis, IP_{25} and HBI II fluxes observed under-ice during April and May 2016 reflected a large proportion of sea ice algae in diatom export. Photosynthetically active radiation (PAR) measured at 33 m depth at the CEO began to increase (>1 uE cm^{-2} s^{-1}) in March 2016, reaching upwards of 15 uE cm^{-2} s^{-1} in May 2016 (Hauri et al. 2018). The onset of increasing PAR, along with snow melt (Fig 2-3A), triggered the initiation of the sea ice algae export, as reflected in the HBI fluxes and the first maxima of the sympagic diatom (*N. frigida*) in the trap material in May 2016. Export occurring prior to melt events was possibly due to the detachment of ice algae by currents and/or grazing processes. Diatoms that may have been incorporated into the ice matrix seeding a phytoplankton bloom (e.g. *Fragilariopsis* spp., *Pseudonitzschia/Nitzschia* spp.) dominated algal fluxes in July before complete sea ice retreat, along with the exclusively pelagic diatom

Chaetoceros spp. (Lalande et al. 2020). A Bering Sea study previously found a fluid reciprocity between sympagic and pelagic diatoms through the melt season, with both groups incorporated into the sea ice matrix and a gradual transition of assemblages throughout the season (Szymanski & Gradinger 2016).

The most notable finding from the sediment trap analysis was the detection of IP_{25} fluxes year round, likely the result of both new production and resuspension events. Our observations are consistent with continuous fluxes of organic matter, which were recorded under land-fast ice from winter through late spring on the Mackenzie Shelf of the Beaufort Sea, although particulate organic carbon fluxes in winter were not consistent with diatom export (Juul-Pedersen et al. 2008). In our samples, there was a lack of chloroplast-containing *Haslea* spp. during most of the winter months (October through February; Fig 3D). The winter sympagic HBI signal may be the result of resuspension, as supported by the low export of diatoms with chloroplasts recorded during winter (Lalande et al. 2020).

Pelagic HBI III fluxes increased from 495 to 799 ng m^{-2} d^{-1} from August to September 2015, reflecting the export of an autumn phytoplankton bloom and/or resuspension due to storm activity (Table 2-2). The large flux of HBI II (2654 ng m^{-2} d^{-1}; Table 3) at this sampling interval suggested resuspension as more likely than *in situ* production given the absence of sea ice. During this period, there was also a large flux of chloroplast-containing *Cylindrotheca closterium*, a rapid growing diatom when resuspended in the euphotic zone and common on shallow shelves, among other diatoms that suggested a resuspension-driven autumn bloom as sea ice was absent and sunlight sufficient for growth (Lalande et al. 2020). In addition, water temperatures, salinity and nutrient data collected at the CEO as well as the meteorological record from the US National Weather Service station in Utqiaġvik indicated an increase in storm frequency and intensity during this period (Hauri et al. 2018). These fall

storms generally lead to a mixing of the water column, bringing remineralized nutrients to the surface, and allowing for the possibility of an autumn bloom (Woodgate et al. 2005b).

2.4.2. Latitudinal gradients of sympagic HBIs and declining sea ice

While core tops can provide more reliable collection of undisturbed surface sediments, comparisons of surface sediments collected by Van Veen grabs and Haps core tops in this biologically productive region were found to have no significant difference in radiocesium activity, suggesting similar recent deposition (Cooper et al. 1998). Therefore, we are confident that the results from the surface sediment analysis present recent deposition with some degree of interannual variability, but unlikely to represent a single year due to the mixing on the shelf.

IP_{25} and HBI II were detected throughout our study sites in the Bering and Chukchi Seas. The range of IP_{25} concentrations in the surface sediments (0–12 μg g^{-1} TOC), are comparable with the range of previously reported pan-Arctic observations (0–10 μg g^{-1} TOC) (Xiao et al. 2015). The largest concentration observed (12 μg g^{-1} TOC), in addition to samples with values exceeding 10 μg g^{-1} TOC (n = 4), suggest there were localized areas of elevated ice algal export in the Pacific Arctic. One prior study of IP_{25} in the Pacific Arctic indicated comparable concentrations (0–5 μg g^{-1} TOC (Bai et al. 2019)). However, direct comparisons with our data may be equivocal because of the less productive location further offshore near the Chukchi Borderlands. In addition, there were methodological differences in the prior study because instrument response factors were not taken into account in their IP_{25} estimates.

When the H-print index was compared with two satellite-derived sea ice metrics (mean spring sea ice concentrations and ice-free period before sample collection), there was general agreement regarding the periods of open water and sea ice cover for each season (Figs 2-5

and 2-6). The H-print was a slightly better predictor of the mean spring sea ice concentration rather than break-up date, likely due to the scale of this measurement and the resolution of the satellite data. As was the case with the sediment trap analysis, the snowmelt period prior to break-up was the event that initiated the biomarker flux consistent with an ice algae bloom. This parameter likely signified melt pond formation and melting of the bottom few centimeters of sea ice. This represents an advantage over satellite-based observations that do not indicate whether there was significant production occurring beneath the ice.

H-print indices from 2014–2017 show significant sea ice algal deposition, and increasing proportions of sympagic inputs on a latitudinal gradient (Figs 2-3, 2-6A). Pelagic influences were significantly greater in the northern Bering Sea and southeast Chukchi Sea than in the northeast Chukchi Sea. However, individual biomarkers provide a more nuanced perspective of localized areas of elevated ice algae markers. Sea ice algal material deposition was increasingly significant throughout the northeast Chukchi shelf, southeast of Hanna Shoal and in upper Barrow Canyon (Fig 2-3).

Northern Bering and Southeast Chukchi Seas

Although the H-print suggests proportionally low ice algae deposition throughout the 68–70°N stations overall, there were occurrences of elevated IP_{25} concentrations relative to all sampling locations. These localized areas were observed in the SLIP, CHIR, and SECS regions and contained some of the highest concentrations observed in this study. For example, in the SECS region in 2015, station SEC6 had an IP_{25} concentration of 11 μg g^{-1} TOC but an H-print of 74%, suggesting greater pelagic influence. These cases in which there are high IP_{25} concentrations with higher H-print values (>50%) can be explained by a significant contribution in mass by sea ice algae but not necessarily the proportion of total

production that may be sustained in the open water season by pelagic production (Grebmeier et al. 2015). This could also be attributed to environmental drivers, such as nutrient limitation increasing HBI production (Brown et al. 2020). Given that the H-print is determined as a ratio of the pelagic HBI to total HBIs, this index may reduce the prominence of the early season input of ice algae in the northern Bering Sea where phytoplankton blooms are substantial in the summer months and can also experience autumn blooms (Hill et al. 2018). The apparent dominance of the pelagic signature is consistent with the longer open water period and more time for pelagic phytoplankton production compared to the study area to the north. However, there were a few notable exceptions to the high IP_{25} coinciding with high H-print scenarios. For example, at the SLIP3 station in 2015 we observed a low H-print (35%) and high concentration of IP_{25} (12 μg g^{-1} TOC; Table S1). This is the general location of the recurring St. Lawrence Island polynya that forms in the winter, enhancing the production of sea ice and late winter production, but these data suggest that summer open water production is not as prominent. HBI profiles in sediments near a polynya have not been widely described or reported, but this could be one explanation for this observation.

Advection through the Pacific Arctic region provides an important source of nutrients and organic matter. Upstream production of ice algae could be a contributing fraction of the material carrying the IP_{25} observed in the sediment trap prior to ice melt in the northeast Chukchi Sea, given the pattern of sea ice retreat. The appearance of IP_{25} in the surface sediments at these lower latitude stations does suggest the sinking of some portion of this production. However, retention of IP_{25} is likely greater in SLIP and SECS than in CHIR based on larger sediment grain size (Grebmeier et al. 2015) and stronger currents in the Chirikov Basin as the flow pathways converge entering Bering Strait (Roach et al. 1995, Gong & Pickart 2015). There is generally limited pelagic grazing by zooplankton at the time

of ice algal production in the SLIP region, allowing for the organic matter to settle largely unaltered to the benthos (Grebmeier et al. 1989, Grebmeier et al. 2010, Szymanski & Gradinger 2016).

The SLIP region has been undergoing a shift in the arrival, retreat and duration of sea ice in the past several years (Frey et al. 2018, Stabeno et al. 2019). There was an unprecedented decrease in sea ice duration in this region in 2014/15, 2016/17 and 2017/18 (Stabeno et al. 2019). H-print values for surface sediments in the 2015–2017 seasons are consistent with these indications of open water productivity. If the current trend in the SLIP region towards more ice-free conditions year round continues, early ice algal production will be increasingly removed from the local food web; water column stratification may not occur until later in the season, which could result in decreased phytoplankton production (Stabeno et al. 2019).

Northeast Chukchi Sea

Among the biomarkers studied here, sympagic HBIs were the dominant contributor in the NECS for all years sampled. Given the insights from data on the ice algal fluxes at the CEO, it is reasonable that ice algal production, export, advection, and resuspension sustain a year round source of sea ice algal material to the benthos of the Chukchi Shelf. However, particulate organic carbon and diatom export have been found to be highly variable on the Chukchi shelf (Lalande et al. 2007). Surface sediments collected at stations nearest the moored CEO sediment trap show some of the highest concentrations of IP_{25} and HBI II observed in this study. In addition, *N. frigida* and *M. arctica* fluxes, which are generally low on Arctic shelves, were higher at the CEO sediment trap in the northeast Chukchi Sea than fluxes observed in the Beaufort Sea and the Eurasian Arctic (Dezutter et al. 2019, Lalande et al. 2019), suggesting elevated sea ice algal export in 2016.

The NECS hotspot is known for high *in situ* production with pelagic and benthic retention in addition to the inputs of upstream productivity (Grebmeier et al. 2015). The flow is variable, paired with a heterogeneous bathymetry that promotes retention of cold and saline water that forms in the winter, carrying relatively high nutrient concentrations (Woodgate et al. 2005a, Weingartner et al. 2017). Hanna Shoal is an important subsurface feature in the NECS, with active ice keeling and sea ice persistence after ice has melted elsewhere on the shelf (Weingartner et al. 2017). Productivity is high along the southeastern flanks of Hanna Shoal, where strong pelagic-benthic coupling results in increased benthic biomass and foraging opportunities for walruses in the late summer (Grebmeier et al. 2010, Jay et al. 2012, Grebmeier et al. 2015, Jay et al. 2017).

Barrow Canyon also appears to be a region of high ice algal material inputs due to the low H-print values and low abundances of HBI III. Much of the current flow from the Chukchi shelf exits through Barrow Canyon, carrying organic matter towards the deeper Canada basin. Export fluxes of particulate matter are high both in the presence and absence of sea ice in Barrow Canyon with more labile, fresh organic matter exported than in other regions of the Chukchi shelf (Lalande et al. 2007). It is probable that there is local production of sea ice algae, given the dominance of sympagic HBIs, but sediments also contain advected material from the shelf. Consequently, sea ice algal material appears to make a significant contribution to the benthos at this study location in addition to also likely forming a source of sympagic production that is exported into the deeper basin.

2.4.3. Sympagic HBI burial through bioturbation and sedimentation

The H-print levels from the sediment core collected on the slope (NNE-14) were dominated by sea ice carbon biomarkers throughout the entire 20 cm core depth (Fig 2-9).

The location of this core, near the median minimum limit of summer sea ice extent (1981–2010, Fig 2-2A), means it is likely representative of late season export and a shorter duration of open water relative to the shelf. Sedimentation rates for this core based on estimates from peak ^{137}Cs activity (0.04 cm yr^{-1}) were similar to the estimate from ^{210}Pb (0.02 cm yr^{-1}, data not shown), suggesting a core spanning centuries of deposition. Based on radiocesium measurements throughout the shelf region, maximum ^{137}Cs activity occurs between 6-10 cm depth, suggesting the surface sediments represent years and not decades or centuries of deposition (Cooper & Grebmeier 2018). While core tops can provide more reliable collection of undisturbed surface sediments, comparisons of surface sediments collected by Van Veen grabs and Haps core tops in this biologically productive region were found to have no significant difference in radiocesium activity, suggesting similar recent deposition (Cooper et al. 1998). The H-print values were slightly higher in the top 6 cm (>20%, Fig 2-9), where the sediment characteristics were similar to the shelf, although still predominantly sympagic, suggesting a possible recent increase in pelagic phytoplankton deposition. In the bottom 8–20 cm of the core, where the composition consisted of grey, fine-grained sediments, the H-print is relatively homogenous and strongly sympagic (8–20 %, Fig 2-9). The ^{137}Cs profile from the station UTX 13-23 on the shelf (Fig 2-9) suggests a well-mixed profile and a somewhat mixed composition of HBIs at nearby DBO4.6 (H-prints between 40 and 60%). However, there is an increasingly sympagic signature (~30 %) at the bottom of the core, suggesting a persistence of the sympagic sourced organic matter at depth or possibly a reduction of sympagic production associated with sea ice declines. Since the shelf has higher nutrient loads, levels of productivity (Gradinger 2009), and an earlier retreat of sea ice, it is not surprising the core collected at DBO4.6 indicates a greater influence of pelagic production than NNE14. The H-print data from NNE14 also reflects the limits of phytoplankton

deposition relative to sea ice algal deposition on the slope, since this core was collected from a slope area that was historically close to the minimum extent of the ice edge or is ice-covered for most of the year.

The sediment core H-print data collected near DBO4.6 supports the assumption that there is rapid burial of sea ice algae relative to phytoplankton. The propensity of ice algae to form aggregates, facilitated by microbial exopolymeric substances and the rapid sinking of the pennate diatom *N. frigida*, may indicate greater relative pulses of ice algae to the seafloor despite a larger relative proportion of pelagic productivity (Riebesell et al. 1991, Riedel et al. 2006). These processes have also been suggested to support the greater burial potential of sympagic lipid biomarkers (Amiraux et al. 2017, Amiraux et al. 2019). The H-print values also suggest there is a greater source of ice algae lipids available to the benthic infaunal communities that occupy these sediment horizons. HBI burial data are not available for cores spanning the entire shelf, but it can be expected from the surface sediment data presented in this study that it is likely that ice algal lipids are stored in sediments throughout the Bering and Chukchi shelf. The persistence and potential availability of labile ice algal lipids mixed to depth in the sediments is an important consideration for assessing the ecosystem response to the loss of seasonal sea ice. It is important to note that despite the high degree of bioturbation, the preservation of these biomarkers is still robust. IP_{25} in particular has proven to be controlled more by climatic conditions rather than degradation processes (Rontani et al. 2018b). According to Rontani et al. (2019a), autoxidation of lipids in the oxic layers of sediments can be particularly important in regions of low accumulation rates, where near-surface sediments can represent decades to centuries of deposition. There is relatively high deposition based on ^{137}Cs sediment profiles throughout the Chukchi Shelf, where the ^{137}Cs maxima associated with peak bomb fallout deposition (1963) averaged 7-8 cm in depth.

Radiocesium based sedimentation estimates determined from these previous studies on the shelf ranged from 0.1 up to 0.3 cm yr^{-1} (Cooper & Grebmeier 2018), suggesting deposition on the scale of years in near-surface sediments.

2.4.4. Mechanisms for HBI distribution throughout the Pacific Arctic

The gradient of HBIs throughout the northern Bering and Chukchi Sea sampling locations and the seasonal succession of sympagic to pelagic diatoms as determined through export fluxes at the CEO (Lalande et al. 2020), suggests a general regionally-specific HBI production mechanism (Fig 2-10). In similarity to the use of HBIs in the Antarctic MIZ (Collins et al. 2013), the HBI distribution in the Pacific Arctic may be a proxy for relative sea ice persistence rather than proportions of production of sea ice algae and phytoplankton organic matter. In the more southerly latitudes of the northern Bering Sea (62-65°N), sea ice persistence typically occurs 0–3 months of the year. Sea ice retreat historically initiated early in the year (March-April), allowing for a spring sea ice algae bloom. The ice algae bloom is thought to seed a phytoplankton bloom as the ice retreats, with a gradual transition of sympagic to pelagic assemblages (Szymanski & Gradinger 2016). The more recent extended open water period in the northern Bering Sea region and a deepening of the mixed layer allows for a second phytoplankton bloom in the fall before sea ice freeze up, which may be particularly relevant during warmer years (North et al. 2014). Therefore, sympagic HBI (IP_{25} and HBI II) production likely occurs during the brief period in early spring with two possible pulses of HBI III production throughout the late spring and fall. This results in a greater relative proportion of the apparent pelagic HBIs relative to the sympagic-origin HBIs. There are also likely to be years with no new IP_{25} or HBI II production due to the timing of sea ice retreat or lack of formation. The current flow over the Bering shelf, through Bering Strait and into the Chukchi shelf promotes the advection of HBIs northward, potentially elevating the

HBI III proportionally in the southeast Chukchi Sea as currents slow north of the Strait. HBI flux data in the northern Bering Sea do not yet exist but could help to refine some of these assumptions.

In the northeast Chukchi Sea, sea ice coverage extends into the summer months (July-August), with some regions of localized persistence throughout the summer, particularly near Hanna Shoal (Weingartner et al. 2017). Sea ice persistence at these higher latitudes typically occurs for 6–9 month intervals. Advection of HBIs from more southerly locations is likely but ultimately may be a minimal source deposited to the northern shelf sediments, due to the aggregation and rapid sinking of diatoms closer to the point of production (Legendre et al. 1992). The sympagic production initiates with increasing PAR followed by the release of ice algae in April-May, and an under-ice bloom composed of sympagic and pelagic diatoms from June to August as open water is initiated (Fig. 10). The presence of exclusively pelagic diatoms reflected the development of an under-ice bloom, as observed in June and July 2016 (Lalande et al. 2020), with HBI III export that coincides with pelagic-sourced production. However, the peak export of HBI III should occur after ice break up during the open water period. In this study, IP_{25} export occurs year-round through both new production and resuspension. The appearance of *M. arctica* resting spores following the ice algae bloom and through the fall months supports the prevalence of sympagic diatom persistence in a sediment "seed bank", which can be resuspended in the fall (Ellegaard & Ribeiro 2018). The presence of IP_{25} throughout the year may suggest that *Haslea* and *Pleurosigma* resting cells persist until the return of sea ice on the Chukchi shelf. Supporting evidence of this was observed in laboratory cultures of *H. crucigeroides* and *H. vitrea* maintained in complete darkness for over six months, where the cells remained viable and with their HBI content the same as when grown in light (unpublished data). Owing to the

shallower conditions on the Chukchi shelf (40–50 m), it seems clear that resuspension during the open-water period plays an important role in the persistent IP_{25} signal.

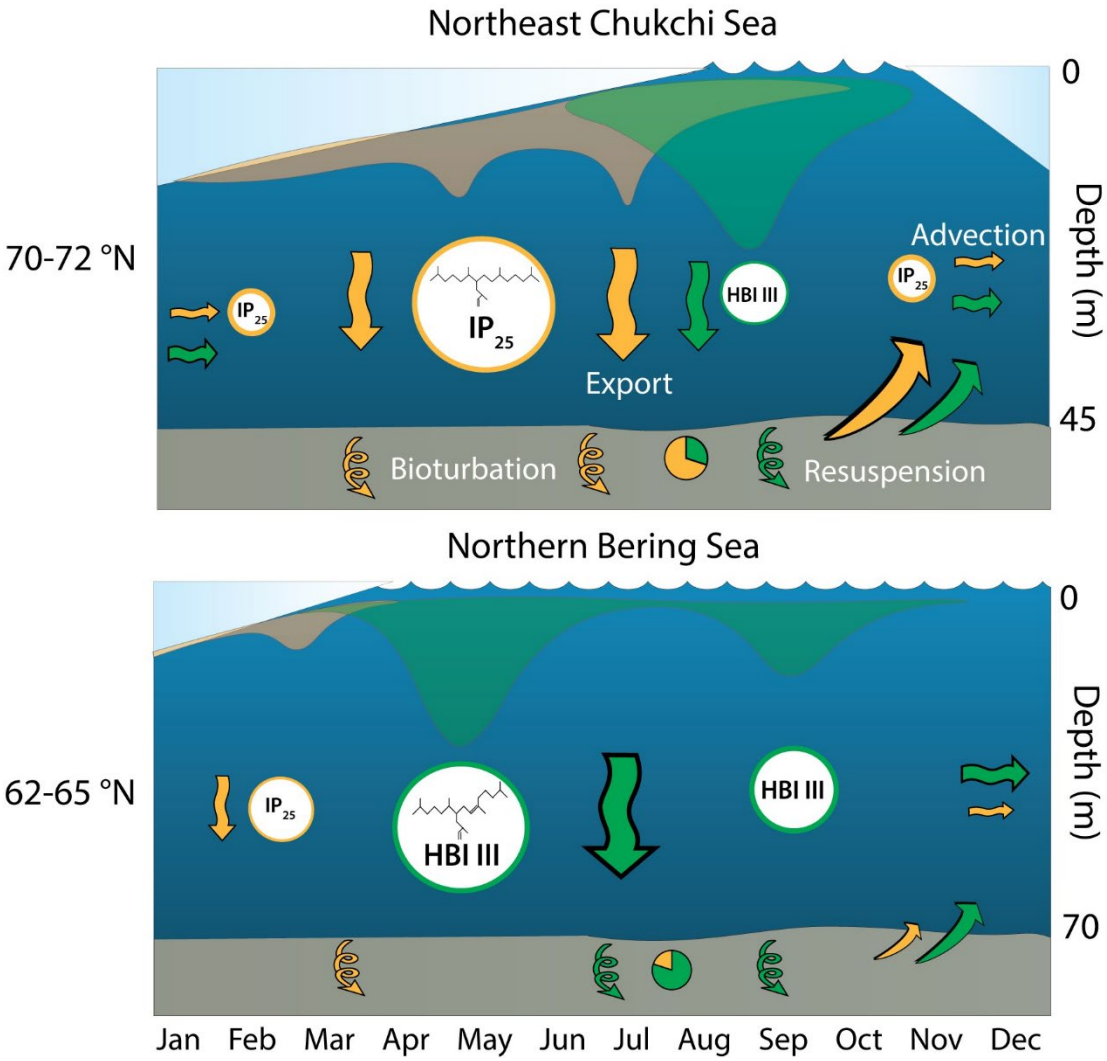

Figure 2-10 Conceptual diagram for the production, flux and fate of HBIs in the Pacific Arctic Sea ice persistence increases from the northern Bering Sea to the northeast Chukchi Sea. There is a brief opportunity for sympagic production (yellow shading) in the Bering Sea due to the timing of sea ice retreat and return of sunlight, followed by extensive ice-edge and open water phytoplankton blooms (green shading) in the spring and fall. Sympagic production can occur over a longer period in the Chukchi Sea. Sympagic IP_{25} production (yellow circles) occurs in much lower proportions to pelagic HBI III (green circles) owing to the extensive open water period in the northern Bering Sea. In the Chukchi Sea, there is a greater proportion of IP_{25} to HBI III. This relative proportionality is observed in the surface sediments when sampled in the summer (pie chart). There is rapid burial of the sympagic HBIs (yellow spiral) owing to aggregation and rapid sedimentation in both regions, with a greater proportion available on the Chukchi shelf. Resuspension (upward arrows) plays a larger role in the Chukchi Sea, sustaining the suspension of IP_{25} and in the water column. Advection (horizontal

arrows) is also likely to be a more prominent contribution to the HBI signal in the Chukchi than the northern Bering Sea. Symbols courtesy of the Integration and Application Network, University of Maryland Center for Environmental Science (ian.umces.edu/symbols/) and reprinted under a CC BY license, permission from B. Walsh, original copyright 2020.

2.5. Conclusions

Based on the results of this study, sea ice algae (or some component of sea ice algal origin i.e. lipids, fatty acids, hydrocarbons) are present year-round in the northeast Chukchi Sea with export events occurring to some degree at all phases of the sea ice cycle, along with seasonal resuspension events. This study also confirms that satellite observations underestimate the ice algal component due to peak export occurring during snow melt that happens before sea ice break up. The presence of IP_{25} without strong indications of the associated diatoms present emphasizes the need for future investigations on IP_{25} synthesis using ice cores from the Bering and Chukchi seas and the possibility of identifying other species that are capable of producing these compounds. Given the overlap of HBI III production with *Pleurosigma* spp., the weaker correlations with *Rhizosolenia* spp., and correlations with sympagic HBIs, the need to determine the fidelity of truly pelagic HBI biomarkers is still an ongoing imperative.

This study presents an assessment of the production, flux and fate of HBI biomarkers using the H-print sea ice index in the Bering-Chukchi Sea inflow shelf system. We found evidence of a northward latitudinal gradient of decreasing pelagic to sympagic production proportionality in the Pacific Arctic system likely driven by sea ice persistence. These data indicate that sea ice algae contribute a significant portion of the organic matter deposited to the seafloor in the NE Chukchi Sea, with a peak early spring pulse and year-round persistence. With a foundational understanding and baseline measurements of the production and distribution mechanisms of HBIs in the Pacific Arctic region, these lipid biomarkers may

serve as an integrating tool to better understand and monitor the rapid changes occurring in this ecosystem, which are associated with shifts in the timing and distributions of primary production with cascading effects in the food web. HBIs provide a targeted approach to isolating the sea ice algae contributions that other methods lack (e.g. stable isotopes, fatty acids). However, there are still limitations as these biomarkers are proxies and may not always faithfully reflect the community composition. Setting the region apart from the rest of the Arctic, the Pacific Arctic is one of the world's most productive ocean ecosystems (Grebmeier et al. 2006a) with nutrient-rich waters allowing for high primary production, emphasizing the importance of regional considerations when applying HBI biomarkers to paleoclimate studies. This includes the influence of physical drivers, nutrient dynamics, primary production rates and phytoplankton community composition that likely influence the abundance and proportion of HBI production.

2.6. Acknowledgements

We thank the science teams, captains and crew aboard the CCGS *Sir Wilfrid Laurier* and USCGC *Healy*. We also thank Carla Ruiz-Gonzalez (Scottish Association for Marine Science) for assistance with sample processing and Laura Gemery (United States Geological Survey) for access to archived frozen sediment samples. We would also like to thank Cheryl Clark and Andrew Heyes for the Organic Analytical Laboratory facilities and support at the Chesapeake Biological Laboratory. We thank two anonymous reviewers for critical comments that improved an earlier version of the manuscript and R. Schlitzer for providing permission to use Ocean Data View images for publication in PLOS ONE under the Creative Commons Attribution License (CCAL) CC BY 4.0.

3. Ice algae resource utilization by benthic macro- and megafaunal communities on the Pacific Arctic shelf determined through lipid biomarker analysis

Published in Marine Ecology Progress Series, October 2020

https://doi.org/10.3354/meps13476

Chelsea Wegner Koch, Lee W. Cooper, Jacqueline M. Grebmeier, Karen E. Frey and Thomas A. Brown

Contribution: Experimental design, all sample analysis, data analysis and interpretation, and all text and figures; Text has been edited by all co-authors

Abstract

We studied ice algae utilization by benthic fauna from the northern Bering and Chukchi Seas using highly branched isoprenoid (HBI) biomarkers. We assessed whether various food acquisition strategies influence the observed HBI signatures. The proportion of phytoplankton to ice algae-sourced HBIs was determined through the H-print approach that is presumed to reflect the percentage of sea ice organic carbon (iPOC) incorporated into tissues, relative to phytoplankton organic carbon. Cluster analysis separated three groups based on location and feeding strategy that were significantly influenced by annual sea ice persistence. Ice algae utilization was most significant in the northeast Chukchi Sea, where seasonal sea ice was present the longest. General feeding strategy was determined to be a significant factor in the degree of ice algae utilization. Predominant deposit feeders (both surface and subsurface) used more ice algae relative to suspension feeders. Organic carbon incorporated by

predominant suspension feeders was primarily phytoplankton-based. The vast majority of all organisms sampled (~90%) incorporated a measureable quantity of iPOC. Sipunculids and brittle stars had the highest relative dependence on ice algae, while other taxa displayed plastic dietary responses, including the suspension/surface deposit feeder *Macoma calcarea*. This study indicates that ice algae are widely utilized in Pacific Arctic benthic food webs, but most benthic organisms displayed flexibility in consuming the available food sources. The elevated utilization of ice algae by deposit feeders may prove to be a disadvantage for these organisms if they cannot adapt to the on-going decline of iPOC as seasonal sea ice declines.

3.1. Introduction

Microalgal primary production on the Pacific Arctic continental shelves is partitioned between ice-associated (sympagic) and pelagic diatoms, and depends on seasonal ice cover dynamics, nutrient availability and water column stratification (Hill et al. 2018, Selz et al. 2018). Strong sympagic-pelagic-benthic coupling has sustained rich benthic ecosystems on this shallow shelf system (Iken et al. 2010, Dunton et al. 2014, Grebmeier et al. 2015). However, declining sea ice cover and persistence along with changes in the timing of the sea ice cycle are likely to disrupt this ecosystem structure (Grebmeier et al. 2006a, Leu et al. 2011, Kędra et al. 2015, Moore et al. 2018). Sea ice has declined overall in the Arctic with pronounced losses in the Bering and Chukchi Seas (Serreze & Meier 2018). The winter of 2017-18 marked the record low maximum sea ice extent for the northern Bering Sea, reaching only 46% (411,500 km^2) of the 1979-2016 mean maximum extent (Thoman et al. 2020). These were levels that were not previously predicted to occur until the 2030s (Stabeno & Bell 2019).

With the increasing open water season for the Pacific Arctic, there are a number of possible outcomes that will impact trophic stability and function as a result of changes in the timing, quality and quantity of the basal food source (Moore & Stabeno 2015). Lower trophic level consumers coordinate life cycles (i.e. spawning, growth, foraging) with the early spring bloom containing sympagic microalgae, where a mismatch in timing could be detrimental to the food web (Søreide et al. 2010, Leu et al. 2011). Ice algae are a high-value food source because of its high polyunsaturated fatty acid composition (Falk-Petersen et al. 1998, McMahon et al. 2006, Søreide et al. 2010, Wang et al. 2014a) and high sinking rates (Legendre et al. 1992, Riedel et al. 2006) relative to phytoplankton. Although overall primary production is predicted to increase in the Arctic with global warming (Arrigo 2015, Lewis et al. 2020), it would likely coincide with an increasing proportion of small pelagic algae with a lower sinking potential (Li et al. 2009) and a decrease in sympagic productivity.

As a result of these changes in primary production, the organic carbon flow in the Pacific Arctic is hypothesized to increase through pelagic trophic chains to the detriment of the benthic ones, which will have a large impact on the whole food web in terms of both quality and standing stock (Kędra et al. 2015, Moore & Stabeno 2015). The shift to a pelagic-dominated food web, together with access to ice-free waters are likely to lead to population increases in foraging pelagic fish, along with water column feeding whales and seabirds (Moore & Huntington 2008, Kędra et al. 2015). As a result, there are expected to be reductions and redistributions of benthic populations that serve as the prey base for higher trophic predators including walruses, bearded seals, spectacled eiders, and gray whales (Grebmeier et al. 2006b, Moore & Huntington 2008, Jay et al. 2014, Moore & Stabeno 2015). A shift has already been observed in the northern Bering Sea benthic communities with northward contractions in dominant species and declines in benthic biomass (Overland &

Stabeno 2004, Grebmeier et al. 2006b, Grebmeier et al. 2018). Therefore, monitoring changes in the functioning of the benthos is critical for identifying a larger ecosystem shift.

Various approaches have been used to assess the benthic response to sea ice retreat and food availability on Arctic shelves. Given that sea ice algae accounts for only 4–26% of overall production on Arctic shelves (Legendre et al. 1992, Arrigo 2014), uncertainties remain about the significance of this food source and its potential decline. However, these values may be an underestimate on the Chukchi shelf, where ice algae has been found to significantly exceed phytoplankton biomass and productivity in the spring (Gradinger 2009). Despite the uncertainty in the actual proportion of sea ice algae that supports the benthic based food web, the pulsed timing and high quality of the largely ungrazed food source is thought to increase its trophic significance (Søreide et al. 2010, Leu et al. 2011, Leu et al. 2015, Dezutter et al. 2019). It has been an ongoing imperative to distinguish the sympagic and pelagic organic matter sources and trace their flow to the benthic and Arctic food webs.

The community composition of ice algae and phytoplankton are complex and have been difficult to unequivocally distinguish since numerous taxa share both environments. Stable isotopes have allowed the detection of an enriched carbon signature in ice algae, yet these values can vary in space and time with bloom progression and may not be reliable indicators alone (Tremblay et al. 2006, Gradinger 2009) and include additional potential sources (e.g. terrestrial, bacterial, etc.). Essential fatty acids are another tool that have advanced our ability to trace organic carbon sources in the Arctic but still lack unambiguous source specificity between the ice and open water regimes (McMahon et al. 2006, Budge et al. 2008, Schollmeier et al. 2018). The use of fatty acids assumes that sea ice organic matter is comprised primarily of diatoms and can best be represented by a fatty acid marker common to diatoms (Budge et al. 2008, Wang et al. 2014a). However, the community composition of

pelagic blooms is complex and is further compounded by the transition from diatoms to dinoflagellates as blooms progress seasonally in the Pacific Arctic (Szymanski & Gradinger 2016, Hill et al. 2018, Selz et al. 2018). Compound-specific stable isotope analyses of these fatty acids have further refined the distinction between organic carbon sources but still remain equivocal (McMahon et al. 2006, Budge et al. 2008, North et al. 2014, Wang et al. 2014a, Kohlbach et al. 2016, Mohan et al. 2016, Kohlbach et al. 2018, Schollmeier et al. 2018).

Highly branched isoprenoids (HBIs) lipids provide an advantage over these other methods to distinguish sympagic and pelagic resources in Arctic food webs. C_{25} HBI lipids are produced by a small number of commonly occurring diatoms and serve as biomarkers based upon the number and position of double bonds (Volkman et al. 1994, Belt et al. 2007). A monounsaturated C_{25} HBI, termed IP_{25} (Ice Proxy with 25 carbon atoms), is synthesized by three or four sympagic diatom species in the Arctic (Belt et al. 2007, Belt & Müller 2013, Brown et al. 2014c, Limoges et al. 2018). Owing to the stability of this compound and its persistence in the environment, IP_{25} is a reliable proxy for paleo sea ice reconstructions (Stein et al. 2016, Belt 2018). Di- and tri-unsaturated structural isomers provide further context for these interpretations. These isomers include a diene (HBI II), associated with sea ice in both polar regions, and a triene (HBI III), found globally in open waters and marginal ice zones (see review by Belt 2018). HBI III has also proven a reliable pelagic biomarker when used in a sea ice index validated by numerous well-resolved paleo sea ice reconstructions (Müller & Stein 2014, Stein et al. 2017a, Kremer et al. 2018). However, modern ecological applications of these HBIs are gaining interest. IP_{25} is chemically stable once grazed and assimilated by consumers, allowing for tracking the trophic transfer of sea ice carbon (Brown & Belt 2012a). Measuring the relative proportion of sympagic (IP_{25} and HBI II) to pelagic HBIs (III), creates

an index termed H-print, which provides further insight into resource utilization in Arctic food webs (Brown et al. 2014d).

As with previously described methods, there are limitations to consider with H-print and the use of HBIs more broadly. In some circumstances, HBI III may be more susceptible to abiotic degradation in the water column based on the extent of algal senescence and the comparative sinking rates of sea ice and open water diatoms, with sea ice diatoms more rapidly removed from the photic zone (Rontani et al. 2019b). There is also evidence that HBI III can at times be co-synthesized within or under sea ice (Amiraux et al. 2019). However, this has been attributed to entrapment of pelagic diatoms, as the identified sources of HBI III (from the genus *Rhizosolenia*) are not ice-associated and may have been a site-specific phenomenon with minimal impacts on HBI indices. Additionally, the specific assimilation and depuration rates of HBIs in primary consumers are largely unknown. Other studies conclude that HBIs do not bioaccumulate in higher trophic organisms and represent seasonal observations (Brown et al. 2014a, Brown et al. 2017b, Brown et al. 2018). However, the advantages of HBIs over previously described methods include the ability to more definitively distinguish sea ice and pelagic carbon sources.

The application of HBI measurements for the Pacific Arctic food web could provide promising new insights into the significance of ice algae on this productive continental shelf system. With this objective in mind, this study applied the H-print method to track ice algae utilization by benthic consumers of the northern Bering and Chukchi Seas to determine which organisms and/or feeding strategies are more reliant on sympagic carbon. Based on observed shifts in benthic biomass and dominant species along with the phenology and quality of algal blooms the northern Bering Sea over the last decade (Grebmeier et al. 2018), we hypothesize that there are differences in ice algae utilization among feeding strategies and taxa. To test

this hypothesis, a range of benthic invertebrates (epifaunal and infaunal) were collected over the summer of 2018 and analyzed for their HBI content with respect to location, feeding strategy and overlying sea ice conditions. Determining the partitioning of sea ice and pelagic organic carbon resources may identify the organisms more vulnerable to a changing food supply as a result of declining sea ice and their ability to adapt to these changes.

Owing to a lack of data on HBI retention and depuration rates in invertebrates, we also conducted a natural depuration experiment using bivalves to determine the turnover rates of HBIs relative to the time of consuming the organic matter. Establishing a baseline of HBI depuration rates is necessary to accurately estimate the time period of foraging reflected in the H-print values. Since HBI III is not specific to polar regions, it was practical to measure depuration rates of this HBI from temperate clams. This experimental design allowed us to fully remove natural introduction and prevent recirculation of HBI III using a flow-through filtration system. We used in-situ temperate conditions in Chesapeake Bay, USA because it was not feasible to maintain the flow through system at sustained Arctic temperatures and therefore this experiment serves as a starting point for addressing these questions. We acknowledge that HBI III and IP_{25} may behave differently, but nevertheless this experiment can serve as a general baseline to measure HBI retention in macrofaunal tissue.

3.2. Materials and methods

3.2.1. Study site

Sampling locations occurred in regions of high benthic biomass influenced by Pacific water inflow across the shallow (<100 m) continental shelf of the northern Bering and Chukchi Seas (Fig. 1). These regions are annually sampled as part of the Distributed Biological Observatory (DBO), which serves as a change detection array and was formally

established in 2010 with time series observations spanning over 30 years (Grebmeier et al. 2010, Moore & Grebmeier 2018). Our sampling spanned five DBO (1-5) regions (https://dbo.cbl.umces.edu) and two additional transects. DBO 1 is located near the winter-only polynya that forms south of St. Lawrence Island in the northern Bering Sea; DBO 2 is in the Chirikov Basin south of Bering Strait; DBO 3 is in the southeast Chukchi Sea, where organic rich material settles out north of Bering Strait; DBO 4 is in the northeast Chukchi Sea on the southeastern flanks of Hanna Shoal; and DBO 5 is a transect across Barrow Canyon (Grebmeier et al. 2015). Icy Cape (IC) has high benthic biomass due to sustained advection of organic carbon from more productive regions (Feder et al. 1994). The Ledyard Bay (LB) transect is in the Chukchi Sea and was only sampled for surface sediments.

3.2.2. Sea ice persistence

Sea ice persistence data were determined from sea ice concentrations obtained from the Special Sensor Microwave Imager/Sounder (SSMIS) on the Defense Meteorological Satellite Program satellites, and compiled by the National Snow and Ice Data Center (http://www.nsidc.org). A 15% ice concentration threshold was set to identify days of sea ice presence in the Pacific Arctic region (Frey et al. 2015). We then summed the number of days with sea ice present (>15%) per pixel, from 14 September 2017 through 15 September 2018. Discrete sea ice persistence values were obtained for each of the sampling locations by extracting the value of the pixel at each location (Fig. 3-1). The use of annual persistence, rather than confined to the sampling period, allowed for the inclusion of winter sea ice conditions that would contribute to the lack of or delay in a spring bloom and account for the deposition of organic matter available in the sediments prior to sampling.

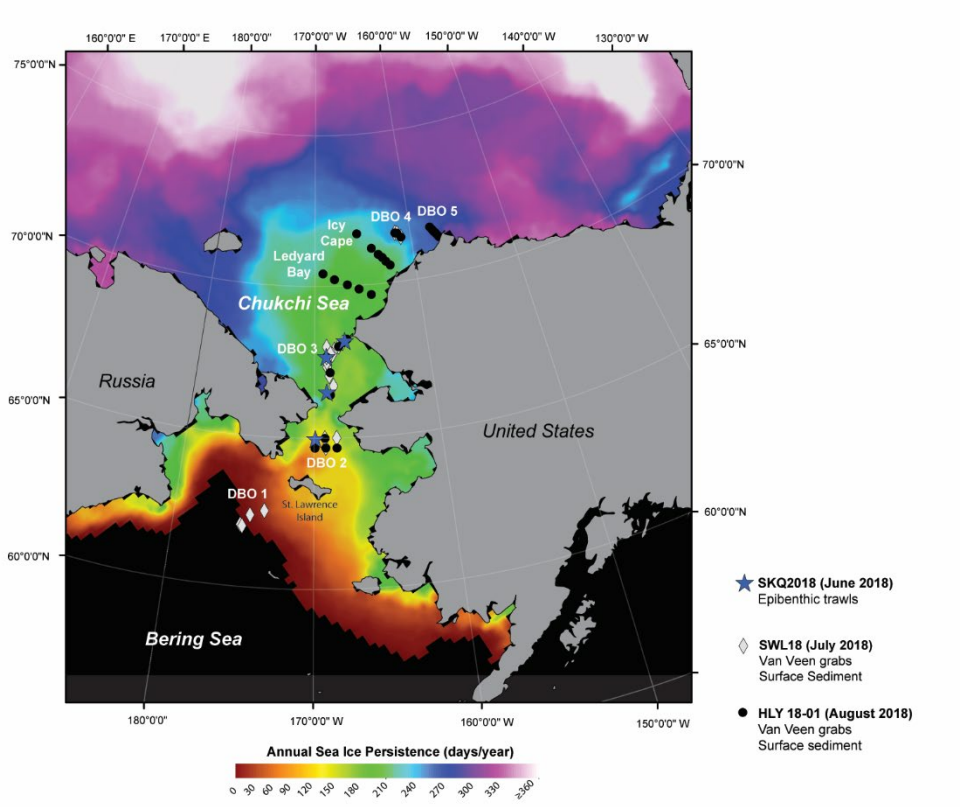

Figure 3-1 Sampling locations and sea ice persistence. Sampling locations in the northern Bering and Chukchi Seas in June (ASGARD, SKQ2018, blue stars), July (DBO, SWL18, black dots), and August (DBO, HLY18-01, gray diamonds) 2018 with corresponding sampling methods. Sea ice persistence is shown as days of sea ice cover (i.e., >15% concentration) per year, which was defined as the sea ice period from 14 September 2017 through 15 September 2018. The areas in black were ice-free throughout the entire year-long period.

3.2.3. Benthic sampling

Organisms were collected on board the CCGS *Sir Wilfrid Laurier* (SWL18; 16–23 July 2018) and the USCGC *Healy* (HLY18-01; 7–24 August 2018) as part of the DBO program (Table 3-1, Fig. 3-1). Additional samples were collected opportunistically on board the R/V *Sikuliaq* (SKQ2018; 4–25 June 2018) as part of the Arctic Shelf Growth, Advection, Respiration and Deposition (ASGARD) Rate Measurements Project of the Arctic Integrated Ecosystem Research Program, which overlapped with the DBO 2 and 3 regions (Table 3-1, Fig. 3-1).

Table 3-1. Station summary for the ASGARD cruise SKQ2018 and the Distributed Biological Observatory (DBO) cruises SWL18 and HLY18-01.

Sampling date (yyyy-mm-dd)	Station ID	Latitude (°N)	Longitude (°W)	Sampling depth (m)	Cruise collected
2018-06-11	DBO 2.4	64.964	-169.889	46	SKQ2018
2018-06-11	Diomede	65.753	-168.871	30	SKQ2018
2018-06-14	DBO 3.8	67.670	-168.951	51	SKQ2018
2018-06-15	DBO 3.3	68.189	-167.308	49	SKQ2018
2018-06-12	CNL3	66.510	-168.959	56	SKQ2018
2018-07-16	SLIP1	62.009	-175.063	80	SWL18
2018-07-16	SLIP2	62.049	-175.206	82	SWL18
2018-07-16	SLIP3	62.391	-174.569	72	SWL18
2018-07-17	SLIP5	62.558	-173.558	66	SWL18
2018-07-18	UTBS2	64.681	-169.100	45	SWL18
2018-07-18	UTBS1	64.992	-169.140	49	SWL18
2018-07-18	DBO2.7	65.000	-168.220	46	SWL18
2018-07-19	UTN1	66.709	-168.398	35	SWL18
2018-07-19	UTN2	67.050	-168.728	46	SWL18
2018-07-19	UTN3	67.331	-168.905	50	SWL18
2018-07-20	UTN4	67.500	-168.909	50	SWL18
2018-07-20	SEC4	68.013	-167.866	54	SWL18
2018-07-21	SEC1	67.672	-168.930	50	SWL18
2018-07-21	UTN6	67.740	-168.441	51	SWL18
2018-07-21	SEC2	67.784	-168.602	50	SWL18
2018-07-21	SEC3	67.899	-168.236	59	SWL18
2018-07-21	UTN7	68.000	-168.929	58	SWL18
2018-07-21	SEC5	68.128	-167.493	51	SWL18
2018-07-22	DBO4.4	71.588	-161.401	49	SWL18
2018-07-22	DBO4.5	71.610	-161.615	44	SWL18
2018-07-23	DBO4.3	71.454	-161.036	49	SWL18
2018-08-08	UTBS2A	64.671	-168.234	39	HLY18-01
2018-08-08	UTBS1	64.991	-169.146	49	HLY18-01
2018-08-09	UTBS5	64.672	-169.926	48	HLY18-01
2018-08-09	T2	67.164	-168.664	47	HLY18-01
2018-08-10	SEC4/DBO3.5	68.015	-167.880	51	HLY18-01
2018-08-10	SEC5/DBO3.4	68.136	-167.492	48	HLY18-01
2018-08-11	SEC1/DBO3.8	67.677	-168.957	51	HLY18-01
2018-08-11	SEC2/DBO3.7	68.246	-167.126	51	HLY18-01
2018-08-12	IC-10	71.705	-165.603	43	HLY18-01
2018-08-13	IC-6	71.195	-164.202	45	HLY18-01
2018-08-13	IC-8	71.449	-164.919	43	HLY18-01
2018-08-13	IC-9	71.601	-165.304	43	HLY18-01

2018-08-14	IC-1	70.580	-162.491	39	HLY18-01
2018-08-14	IC-2	70.717	-162.857	43	HLY18-01
2018-08-14	IC-3	70.849	-163.187	45	HLY18-01
2018-08-15	DBO4.3	71.351	-161.396	49	HLY18-01
2018-08-15	DBO4.4	71.481	-161.505	49	HLY18-01
2018-08-15	DBO4.5	71.610	-161.615	47	HLY18-01
2018-08-17	DBO5.1	71.247	-157.135	45	HLY18-01
2018-08-17	DBO5.2	71.289	-157.221	56	HLY18-01
2018-08-17	DBO5.4	71.373	-157.380	116	HLY18-01
2018-08-17	DBO5.5	71.410	-157.450	131	HLY18-01
2018-08-17	DBO5.6	71.454	-157.553	120	HLY18-01
2018-08-17	DBO5.7	71.495	-157.627	96	HLY18-01
2018-08-17	DBO5.8	71.536	-157.711	75	HLY18-01
2018-08-17	DBO5.10	71.626	-157.901	64	HLY18-01

Epibenthic megafauna were collected from trawl surveys on SKQ2018 using a modified plumb-staff beam trawl (2.26-m opening; 7-mm mesh net; 4-mm cod end liner). Trawl sample biomass was dominated by echinoderms, mollusks, crustaceans, sponges, ascidians and bryozoans. Organisms were either sorted from the full catch or from a well-defined, well-mixed subsample. All samples were sorted by species, genus or distinct morphotype depending on the level of identification possible on board. Surface sediments were not collected on this cruise.

Benthic macrofauna (> 1 mm, included megafauna) were collected on the SWL18 and HLY18-01 cruises using a 0.1 m^2 van Veen grab weighted with 32 kg lead. Grab sample biomass was dominated by bivalves, polychaetes, crustaceans, sipunculids, echinoderms and anthozoans. The grab was gently lowered on to the deck and a trap door on the top was opened prior to the full grab opening in order to sample relatively undisturbed surface sediments for HBI analysis. The sediments were collected by skimming the surface with a metal spatula. Prior studies have established from radiocesium activities that the surface sediments on the Bering and Chukchi shelf (<100 m) reflect recent deposition, and that due to

bioturbation, surface sediments recovered from the tops of cores are as well-mixed as those from the tops of van Veen grabs (Cooper et al. 1998, Cooper & Grebmeier 2018). Organisms were sieved through 1-mm mesh sieve screens, live sorted and identified to the lowest taxonomic level practical on board. Organisms from all three cruises and sediments were placed in individual whirl-pak bags, immediately frozen (-20°C) and stored until analysis. All benthic fauna collected were classified by feeding strategy using the following five categories: suspension (SUS), surface deposit feeder (SDF), sub-surface deposit feeder (SSDF), suspension-surface deposit (SUS/SDF), or predator/scavenger (PS) based on previous studies (Table 3-2).

Table 3-2 Summary of taxa . Summary of taxa collected in 2018 for HBI biomarkers with assigned feeding strategy, cruise (SKQ=SKQ2018, SWL=SWL18, HLY=HLY18-01) and collection method, along with the Distributed Biological Observatory (DBO) sample region (see Fig. 1). Feeding strategies were classified as SUS (suspension), SUS/SDF (suspension/surface deposit), SDF (surface deposit), SSDF (subsurface deposit), and P/S (predator/scavenger). Sample size indicates number of stations with the species analyzed**.**

Species	Sample size (n)	Feeding Strategy	SKQ (trawls)	SWL (grabs)	HLY (grabs)	DBO Sample Regions
Holothuroidea						
Amphideima sp.	1	SUS[a]	X			2
Chiridota sp.	1	SDF[a]	X			2
Ocnus glacialis	2	SUS[b]	X			3
Myriotrochus sp.	1	SUS[a]		X		3
Ascidacea (Tunicata)						
Styela rustica	4	SUS[b]	X	X	X	2, 3, 5
Pelonaia corrugata	2	SUS[b]	X			2, 3
Boltenia ovifera	2	SUS[b]	X			2
Boltenia echinata	3	SUS[b]	X			3
Chelyosoma macleayanum	3	SUS[b]	X			3
Gastropoda						
Neptunea heros	3	P/S[b]	X			2
Neptunea communis	1	P/S[b]	X			2
Buccinum scalariforme	2	P/S[b]	X			2

Buccinum polare	2	P/S[b]	X			3
Cryptonatica affinis	5	P/S[b]	X			2, 3
Bivalvia						
Serripes lamperosii	7	SUS [a,b]	X	X	X	3
Macoma calcarea	37	SUS/SDF[c]	X	X	X	ALL
Ennucula tenuis	18	SSDF[c]		X	X	ALL
Nuculana pernicula	2	SSDF[b]		X		3, 4
Astarte borealis	4	SUS[c]		X	X	IC, 4, 5
Yoldia hyperborea	11	SSDF[c]		X	X	3, IC, 4, 5
Mya truncata	2	SUS[b]		X		3
Mya sp.	1	SUS[b]		X		3
Musculus sp.	2	SUS[b]		X	X	IC, 4
Hiatella arctica	1	SUS[b]	X			3
Pandora sp.	1	SUS[b]			X	IC
Lysianassidae unidentified sp.	1	P/S[b]			X	IC
Nutricola sp.	2	SUS[b]			X	IC, 5
Polychatea						
Gattyana ciliata	1	SSDF[b]	X			2
Gattyana sp.	1	SSDF[b]	X			3
Eunoe sp.	1	P/S[b]	X			3
Nephtys sp.	8	P/S[b]		X	X	2, 3, 5
Pectinaria hyperborea	12	SSDF[b]		X	X	1, 3, 4, IC, 5
Maldane sp.	18	SSDF[b,c]		X	X	ALL
Echiurus	3	SDF[a]	X			3
Lumbrineris sp.	1	SSDF[b]				IC
Sipuncula						
Golfingia margaritacea	6	SDF[d]			X	3, IC, 5
Ophiuroidea						
Ophiura sarsiii	3	SDF[b]		X		1, 4
Gorgonocephalus sp.	1	P/S[b]			X	5
Malacastroca (Decapoda)						
Pandalus eous	1	P/S[b]		X		1
Pagurus trigonocheirus	1	P/S[b]	X			2
Chionoecetes opilio	2	P/S[e]		X		1, 3
Malacastroca (Amphipoda)						

Isaeidae sp.	2	SDF[b]		X		2, 3
Ampelisca sp.	11	SUS[b]		X	X	1,2,4,5
Asteroidea						
Henricia sp.	1	P/S[b]			X	4
Anthozoa						
Gersemia rubiformis	1	SUS[b]	X			2

[a]Encyclopedia of Life 2020
[b]MacDonald et al. 2010
[c]Denisenko et al. 2015
[d]Kędra et al. 2018
[e]Divine et al. 2017

3.2.4. Biomarker extraction

All samples were freeze dried in the laboratory for 48 hours, soft tissues were removed from shells as required, and homogenized by mortar and pestle. Approximately 1 g of dried sediment or 0.1–0.5 g of dried tissue were subsampled for analysis. Owing to the variable sizes and number of organisms per station, where there was often only one individual per taxon per grab, major taxa with more than one individual were grouped for analysis. This was intended to capture a representative HBI composition per species and/or feeding strategy at a particular station. HBI biomarkers were extracted from 78 surface sediment samples and 193 tissue samples. HBIs were extracted following established methods (Belt et al. 2012, Brown et al. 2014d). Briefly, an internal standard (10 µL) of 9-octylheptadec-8-ene (9-OHD, 1 µg mL^{-1}) was added to the sample before extraction to facilitate yield quantification. Samples were saponified in a methanolic KOH solution and heated at 70°C for one hour. Hexane (4 mL) was added to the saponified solution, vortexed, and centrifuged for three minutes at 2500 RPM, three times. The supernatant with the non-saponifiable lipids (NSLs) was transferred to clean glass vials and dried under a gentle N_2 stream. We removed elemental sulfur from the sediment samples following established protocols (Koch et al. 2020b) to prevent analytical

interference with HBI III. The initial extracts were re-suspended in hexane and fractionated using open column silica gel chromatography. The non-polar lipids containing the HBIs were eluted while the polar compounds were retained on the column. The eluted compounds were dried under N_2. 50 µL of hexane was added twice to the dried purified extract and transferred to amber chromatography vials.

3.2.5. Biomarker analysis

The extracts were analyzed using an Agilent 7890A gas chromatograph (GC) coupled with a 5975 series mass selective detector (MSD) using an Agilent HP-5ms column (30 m x 0.25 mm x 0.25 µm), following established methods (Belt et al. 2012). The oven temperature was programmed to ramp up from 40°C to 300°C at 10°C/minute with a 10-minute isothermal period at 300°C. HBIs were identified using selective ion monitoring (SIM) techniques. The SIM chromatograms were used to quantify the HBI abundances by peak integration with ChemStation software. A purified standard of known IP_{25} concentration was used to confirm the mass spectra, retention time and retention index (RI). The HBIs were identified by their mass ions and RI including IP_{25} (*m/z* 350.3), HBI II (*m/z* 348.3) and HBI III (*m/z* 346.3). A procedural blank was run every 9th sample. Individual HBI concentrations in the surface sediment samples were normalized by total organic carbon (TOC) on an organic gram weight basis. Surface sediment TOC data from the SWL18 and HLY18-01 cruises were accessed from the National Science Foundation's Arctic Data Center (Grebmeier & Cooper 2019f,g).

The H-print index was used to provides an estimate of the relative organic carbon contributions of phytoplankton to sea ice algae (Brown et al. 2014c). The H-print (Eq. 3-1), is

calculated using the relative abundances of IP_{25}, HBI II and HBI III, as determined by GC-MS methods:

$$\text{H-print \%} = \frac{\text{HBI III}}{\sum (IP_{25} + \text{HBI II} + \text{HBI III})} \times 100 \quad (3\text{-}1)$$

The estimated organic carbon contribution varies from 0% to 100%, with lower values indicative of proportionally greater sympagic organic carbon and higher values indicative of proportionally greater pelagic organic carbon. Analytical error from replicate control tests was determined to be less than 3% for H-print values in an individual organism from homogenized tissue sample. Sea ice organic carbon (iPOC), as a proportion of marine-origin carbon within samples, was estimated using Eq. 3-1 from a prior H-print calibration from feeding experiments with known algal species ($r^2 = 0.97$, $p < 0.01$; Brown & Belt 2017).

$$\text{iPOC \%} = 101.8 - 1.02 \times \text{H-print} \quad (3\text{-}2)$$

Given our interest in the proportion of sea ice algae utilization, the iPOC calibration is presented referenced to sea ice carbon rather than pelagic carbon, as is the case with the H-print. However, since the calibration was derived and validated from feeding experiments, we retained the H-print values for the sediment data. Therefore, all invertebrate samples were converted and reported as iPOC, while sediments are reported as H-print.

3.2.6. Statistical analysis

All statistical analyses were performed in R v. 3.6.1 (R Core Team 2017). Normality of the data was assessed using a Shapiro-Wilks test and the homogeneity of variance using Levene's test. We used a generalized additive model (GAM) in R using package 'mcgv' to determine the effects of various predictor variables for the sea ice organic carbon content in benthic macrofauna. This included sea ice persistence, sampling location, feeding strategy

and sediment H-print composition. A combination of these variables in seven competing equations was evaluated and the best performing equation was selected based on the lowest AIC (Akaike information criterion) score. Linear regression models were assessed to determine the relationship between the HBI content of invertebrate tissue (iPOC%) and the corresponding surface sediment (H-print %) they were collected from. We conducted k-means clustering analysis to group similar observations and assess potential patterns in the HBI distribution among location, feeding strategy, major taxa and annual sea ice persistence. Owing to the lack of corresponding sediment samples, the samples collected from SKQ2018 (n = 41) were not included in the cluster analysis. We then used the combination of factors that explained the variation within the benthic macrofauna samples by the GAM to define the individual clusters. This analysis was conducted in R using packages 'cluster' and 'factoextra'. Sediment H-print and macrofauna iPOC values were normalized prior to running the cluster analysis and the optimal number of clusters (k) were determined based on the gap statistic (Tibshirani et al. 2001). One-way ANOVA with Tukey Honest Significant Difference (HSD) and Bonferroni corrections were used to analyze the significant differences in relative HBI concentrations.

3.2.7. HBI depuration experiment

In May 2019, bivalves were collected from the pier at the Chesapeake Biological Laboratory (CBL) in Solomons, Maryland, USA using a hand-deployed PONAR grab. The two species collected are widely distributed and also found in parts of the Arctic, *Mya arenaria* (suspension feeder, n= 18) and *Macoma (Limecola)balthica* (suspension and surface deposit feeder n = 50). *M. balthica* (n=10) and *M. arenaria* (n=3) were analyzed immediately (day 0) after collection to determine their initial HBI III content from their natural environment and the remainder (*M. arenaria*, n = 15; *M. balthica*, n = 40) were put in flow

through filtered seawater tanks (5L). The clams were fed every other day with Shellfish Diet 1800 (Instant Algae, Reed Mariculture). The Instant Algae (1 mL) was analyzed prior to feeding to confirm there were no HBIs present.

Clams were removed from the tank and the HBI III abundances were analyzed at 4, 7, 21, and 28 days. Owing to the small size of the individual *M. balthica* collected (~5 mm), individuals had to be grouped (n=10 per collection date) for analysis. The *M. arenaria* samples were a sufficient size (~20–30 mm) for individual analysis (n=3 per collection date). The relative response on the GC-MS was recorded until the response fell below detection limits, indicating complete depuration of the biomarkers. As the depuration rate was the intended measurement, absolute quantification of HBI III was not undertaken.

3.3. Results

Several factors were considered in various combinations to explain the variation observed in sea ice organic carbon utilization among benthic macrofauna. The GAM equation selected was based on the AIC scores, with the lowest AIC indicating the best fit. The combination of sample region, sea ice persistence, sediment H-print, and feeding strategy performed the best (AIC=1140, r^2=0.78). Therefore, the following variables were examined in greater detail.

3.3.1. Surface sediment HBI distributions and relationship with sea ice

IP_{25} was only detected in trace amounts as a fraction of organic carbon (OC; < 1 µg g OC^{-1}) throughout DBO 1–2 in the northern Bering Sea and less than 2 µg g OC^{-1} was observed at DBO 3 in the southern Chukchi Sea (Fig. 3-2A). Ledyard Bay (LB), which was only sampled for sediments, marked a transitional zone where IP_{25} levels increase in the northeast Chukchi Sea. IP_{25} reached maximum concentrations of 14.5 µg g OC^{-1} in the northeast Chukchi Sea at DBO 4 and ranged from 1 to 10 µg g OC^{-1} at the DBO 5 transect across Barrow Canyon. HBI

III (Fig. 3-2B) displayed a more homogenous distribution throughout the region. Localized areas of elevated concentrations were observed in LB, where HBI III reached 18 µg g OC^{-1}. HBI III levels were also considerably lower in the northern Bering Sea at DBO1–2 with values ranging from 2–6 µg g OC^{-1}. H-print (Fig. 3-2C) follows a latitudinal gradient from south to north with decreasing relative pelagic HBI inputs. The mean sea ice extent indicates that the IC transect was ice-covered in June but retreated by July, while the sea ice had fully retreated from DBO 4 and 5 by August.

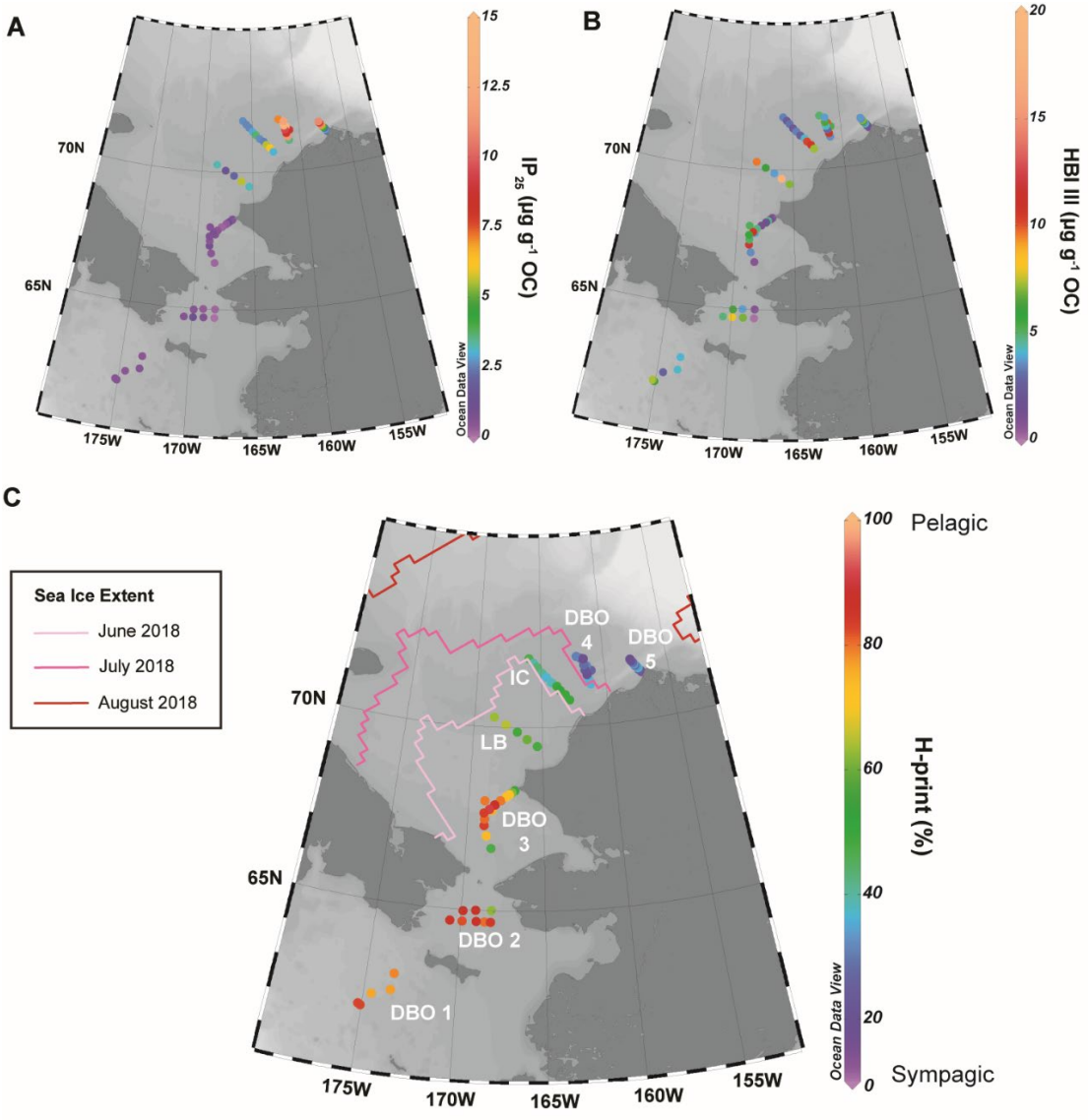

Figure 3-2 Highly branched isoprenoid distributions in the Pacific Arctic Highly branched isoprenoid biomarker analysis from surface sediments collected in July (SWL18) and August (HLY18-01) in the northern Bering and Chukchi Seas. Sampling stations are shown as grey circles. (A) Distribution of the sea ice proxy IP_{25} (µg g OC^{-1}). (B) distribution of the pelagic HBI marker, HBI III (µg g OC^{-1}). (C) The H-print (%) determined from sympagic (IP_{25} and HBI II) and pelagic (HBI III) biomarker proportions. Sample regions included DBO 1, DBO 2, DBO 3, Ledyard Bay (LB), Icy Cape (IC), DBO 4 and DBO 5. Note: LB was only sampled for sediments and not macrofauna. The mean monthly sea ice extent is shown for June, July and August 2018.

There was a significant relationship between sea ice persistence and sediment H-print (r^2=0.61, $p < 0.001$; Fig. 3-3). The DBO 1 stations experienced low (<30 days) sea ice cover in 2018 and were determined to be outliers using a Grubbs' test (Grubbs 1950) (Fig. 3-3 red-dashed box). After removing the subset of DBO 1 samples (n=3), the strength of the relationship increased, indicating a very strong fit (r^2=0.81, $p < 0.001$).

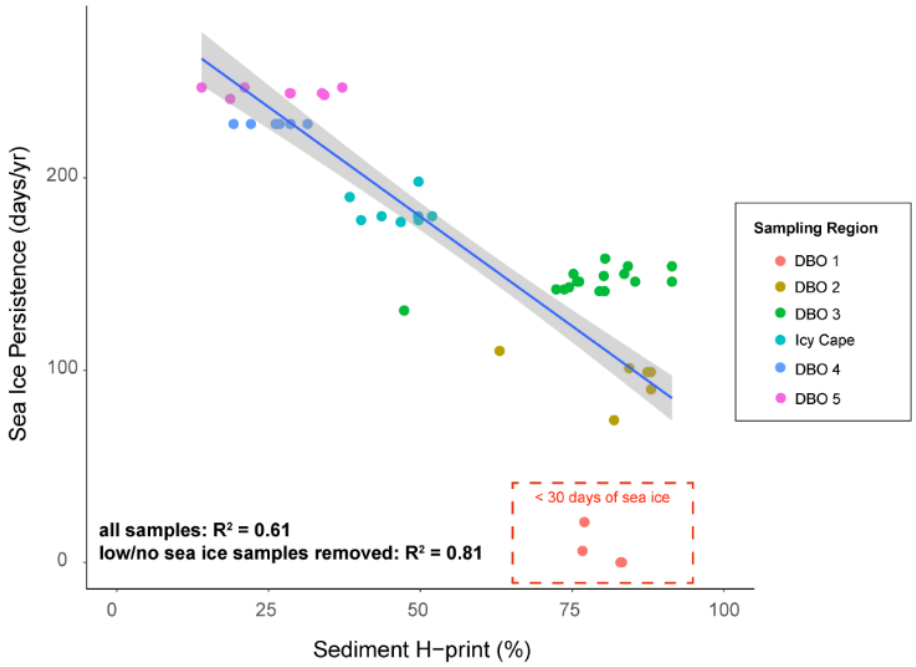

Figure 3-3 Linear regression of sediment H-print and sea ice persistence Linear regression with 95% confidence interval (shaded region) of sea ice persistence (days/year) and sediment H-print (%). Colors indicate the DBO sampling regions. The no/low sea ice stations were deemed outliers and the corresponding r^2 values with and without these outliers are shown.

3.3.2. Sea ice organic carbon (iPOC %) variation by feeding strategy and region

There was an increasing gradient of sympagic utilization by benthic invertebrates from the lower latitude sampling regions (DBO 1–3) to the higher latitude sampling regions (IC and DBO 4–5; Fig. 3-4). The invertebrates classified as deposit feeders (both SDF and SSDF) generally had the highest iPOC and SUS the lowest within each region. The highest iPOC values are observed in the SSDF category. However, the SDF at DBO 5 (most northerly sampling area) reach iPOC levels similar to SSDF. The highest iPOC value observed among the SDF at DBO 5 (78%) was comparable with the SSDF and attributed to sipunculids (*Golfingia margaritacea*). iPOC values increased at the IC transect. iPOC values for SUS fauna were <25% in all sampling regions, with the exception of DBO 4, indicating that they are utilizing predominantly pelagic resources. P/S by comparison have a less clear trophic dependence on sympagic sources relative to the other feeding strategies from DBO 1–3. The SUS/SDF align with SUS but with greater differences at IC and DBO 5. Feeding strategies were significantly different ($p < 0.05$) at all stations but DBO 1 and 2 as determined by one-way ANOVA testing (Table 3-3). Tukey HSD pairwise comparisons indicate SUS were significantly different from deposit feeders (SDF and SSDF) at all four of these sampling regions (see Table S1 for *p*-values).

Table 3-3 ANOVA results for H-print for each of the Distributed Biological Observatory (DBO) regions and clusters.

Group	Factor	DF	*SS*	*MS*	F	p-adj
DBO 1	Feeding strategy	4	113.4	28.36	0.70	0.612
	Residuals	9	365.4	40.60		
DBO 2	Feeding strategy	4	302.7	75.66	1.51	0.23
	Residuals	25	1252.7	50.11		

DBO 3	Feeding strategy	4	267.9	66.98	2.72	0.0358*
	Residuals	73	1796.5	24.61		
Icy Cape	Feeding strategy	4	2898.0	724.60	3.08	0.049*
	Residuals	15	3534.0	235.60		
DBO 4	Feeding strategy	4	2657.0	664.30	5.46	0.002**
	Residuals	27	3288.0	121.80		
DBO 5	Feeding strategy	4	4645.0	1161.30	3.47	0.036*
	Residuals	14	4680.0	334.30		
Cluster 1	Feeding strategy	4	847.8	211.95	2.36	0.0818
	Residuals	24	2154.0	89.75		
Cluster 2	Feeding strategy	4	1814.0	453.40	3.93	0.009**
	Residuals	39	4501.0	115.40		
Cluster 3	Feeding strategy	4	521.5	130.40	7.76	<0.001***
	Residuals	70	1176.2	16.80		

Significant p-values are denoted as <0.05 (*), <0.01 (**) and <0.001 (***).

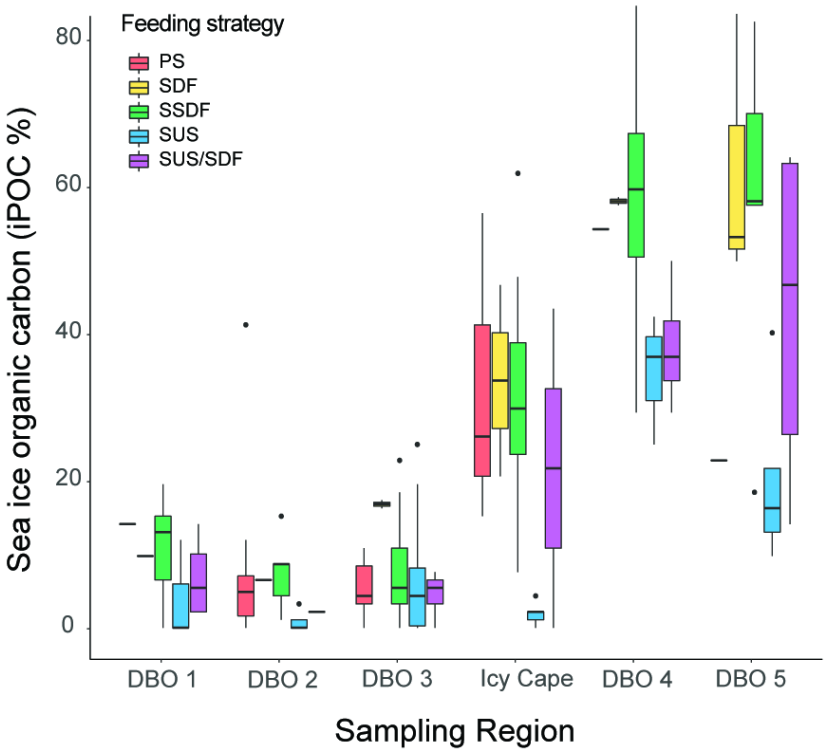

Figure 3-4 Sea ice organic carbon (iPOC %) by feeding strategy across the Distributed Biological Observatory (DBO) sampling regions in 2018 Feeding strategies include: predator/scavengers (P/S), suspension (SUS), surface deposit (SDF), subsurface deposit (SSDF), and suspension/surface deposit feeders (SUS/SDF). Sample regions from south to north included DBO 1, DBO 2, DBO 3, Icy Cape, DBO 4 and DBO 5. The boxes indicate the interquartile range from the first to third quartiles, with the median shown as the line within each box. The minimum and maximum are indicated by the lines and outliers are shown as individual points.

3.3.3. Relationships between macrofauna iPOC and sediment H-print

The linear regression of normalized iPOC values for the invertebrate tissues and corresponding H-print values in surface sediments indicates a significant relationship between these variables ($p < 0.001$, $r^2=0.66$). The samples were grouped into 3 clusters (Fig. 3-5A). The cluster composition took advantage of the prior assessments of the factors determined to be significant (e.g. DBO region and feeding strategy, Figs. 3-5B and 3-5C, respectively). Sea ice persistence patterns and taxa composition were also examined for each of the clusters.

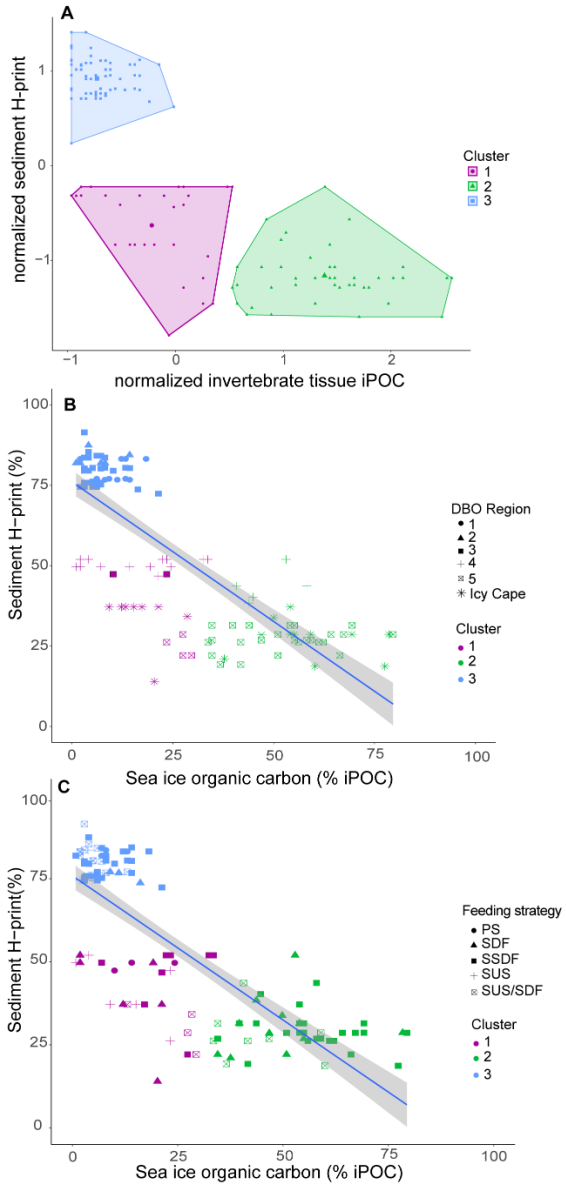

Figure 3-5 Results of the k-means clustering analysis between macrofaunal tissue and the sediment the organisms were collected from (A) normalized sediment H-print and macrofauna tissue iPOC values grouped into the optimal number of clusters (3), **(B)** sediment H-print (%) and macrofaunal tissue iPOC (%) with symbols represented by DBO sampling region and color represent cluster number. The linear regression is shown with a 95% confidence interval. **(C)** sediment H-print (%) and invertebrate tissue iPOC (%) with symbols represented by feeding strategy and color represent cluster number. The linear regression is shown with a 95% confidence interval. Feeding strategies as defined in Table 2.

Cluster 1 samples were found throughout the Chukchi Sea including DBO 3, DBO 4, DBO 5 and IC (Fig. 3-5B) with a majority (52%) from IC (Table 3-4). The difference in

feeding strategy was not significant based on a one-way ANOVA test (Table 3-3). The composition of feeding strategies contained in cluster 1 (Fig. 3-5C) was distributed among SUS (38%), SSDF (28%), SUS/SDF (17%), SDF (3%), and PS (14%; Table 3-4). The SSDF group had the highest mean iPOC (23 ± 9%) and SUS had the lowest (10 ± 9%; Fig. S2-1). This cluster was dominated by bivalves (62%) and polychaete worms (21%). Overall, cluster 1 had a moderate sediment H-print (42 ± 11%) with invertebrate iPOC values indicative of low sea ice organic carbon utilization (mean iPOC 17 ± 10%; Table 3-4). The mean sea ice persistence for this cluster was 205 ± 35 days (Table 3-4)

Table 3-4 Summary parameters for the k-means clustering analysis Summary parameters for the k-means clustering analysis including the cluster composition by DBO region, feeding strategy and dominant taxa, mean sediment H-print (%), mean macrofaunal tissue sea ice organic carbon (iPOC %), and mean sea ice persistence.

	Cluster Composition								
	DBO Region		Feeding Strategy		Dominant Taxa		Mean sediment H-print (%)	Mean sea ice carbon (iPOC %)	Mean Sea Ice Persistence (days)
Cluster 1	1	-	Suspension (SUS)	38%	Bivalvia	62%	mixed composition		
(n=29)	2	-	Subsurface deposit (SSDF)	28%	Polychaeta	21%	42 ± 11	17 ± 10	205 ± 35
	3	7%	Suspension/Surface deposit (SUS/SDF)	17%					
	IC	52%	Surface deposit (SDF)	3%					
	4	14%	Predator/Scavenger (PS)	14%					
	5	28%							
Cluster 2	1	-	Suspension (SUS)	7%	Bivalvia	52%	sympagic		
(n=44)	2	-	Subsurface deposit (SSDF)	57%	Polychaeta	25%	29 ± 7	53 ± 12	227 ± 18
	3	-	Suspension/Surface deposit (SUS/SDF)	18%	Sipuncula	9%			
	IC	6%	Surface deposit (SDF)	14%					
	4	66%	Predator/Scavenger (PS)	5%					
	5	25%							
Cluster 3	1	19%	Suspension (SUS)	27%	Bivalvia	52%	pelagic		
(n=75)	2	19%	Subsurface deposit (SSDF)	35%	Polychaeta	27%	80 ± 5	5 ± 5	111 ± 55
	3	63%	Suspension/Surface deposit (SUS/SDF)	27%	Ampeliscidae	13%			
	IC	-	Surface deposit (SDF)	3%					
	4	-	Predator/Scavenger (PS)	9%					
	5	-							

Cluster 2 stations were located in the northeast Chukchi Sea from IC, DBO 4 and DBO 5 (Fig. 3-5B), with the majority from DBO 4 (66%; Table 3-4). The organisms sampled in this cluster were predominantly SSDF (57%; Table 3-4). Two of the three SUS samples included in this cluster (bivalve *Astarte borealis* and amphipod *Ampelisca* sp.) were from a station in DBO 4 with high IP_{25} deposition (DBO 4.4). Feeding strategy was found to be significant based on the one-way ANOVA test ($p < 0.05$; Table 3-3). The iPOC values in this cluster were highest overall. Values ranged from 37-57%, with SSDF the highest (57 ± 11%) and SUS/SDF the lowest (37 ± 3%; Fig. S2-1). The Tukey HSD pairwise comparison indicated that SUS/SDF–SSDF and SUS–SSDF were significantly different ($p < 0.05$; Table S1). Cluster 2 contained bivalves (52%) and polychaete worms (25%), but also an increased contribution from sipunculids (9%; Table 3-4). The mean sediment H-print was low (i.e. sympagic) at 29 ± 7%, with invertebrate iPOC values ranging from moderate to high with a mean value of 53 ± 12% (Table 3-4). The mean sea ice persistence was the longest of all clusters at 227 ± 18 days of the year (Table 3-4).

Cluster 3 contained the northern Bering Sea (DBO 1 and 2) and southeast Chukchi Sea (DBO 3) stations, immediately north and south of Bering Strait (Fig. 3-5B). 63% of the samples in cluster 3 were from DBO 3, but contained all samples from DBO 1 and 2 (Table 3-4). Feeding strategy was a significant variable for this cluster based on one-way ANOVA tests ($p < 0.001$; Table 3). SUS (27%), SSDF (35%) and SUS/SDF (27%) were the primary feeding strategies within this cluster (Table 4). SDF had the highest mean iPOC value (13 ± 6 %) with SUS the lowest at 1 ± 3%, meaning food sources were nearly completely pelagic (Fig. S2-1). The differences were significant between SUS–PS ($p < 0.05$), SUS–SDF ($p < 0.01$) and SUS–SSDF ($p < 0.001$) based on pairwise comparisons (Table S1). Cluster 3 was dominated by bivalves (52%) and polychaetes (27%), with an increased contribution from

ampeliscid amphipods (13%; Table 3-4). The mean sediment H-print was high (80 ± 5%, i.e. pelagic) and the mean iPOC value in invertebrate tissues was low (5 ± 5%; Table 3-4). The sea ice persistence for cluster 3 was the shortest at 111 ± 55 days (Table 3-4).

3.3.4. Sea ice persistence and sea ice organic carbon (iPOC %)

The clusters were further analyzed using the linear regression of sea ice persistence determined from each of the sampling locations relative to the invertebrate tissue iPOC (Fig. 3-6A). The clusters remain distinctly grouped with the exception of two data points from cluster 1. The relationship between sea ice persistence and sea ice carbon utilization was significant ($p < 0.001$, $r^2 = 0.41$; Fig. 3-6A). However, there was a distinct group from cluster 3 with stations that experienced less than 30 days of sea ice, including several samples where there was no sea ice cover in 2018 (Fig. 3-6A, red-dashed box). By removing this cluster from the linear regression, the fit of the relationship improved ($r^2 = 0.56$, $p < 0.001$). All of the stations with no or low sea ice cover occurred at DBO 1, also known as the St. Lawrence Island polynya (SLIP) region (Fig. 3-6B). Stations SLIP 1 and SLIP 2 had no sea ice cover during the study period in 2017-18, while SLIP 3 and SLIP 5 had less than 30 days of sea ice. The SDF and SUS/SDF iPOC were lowest at SLIP 1 and 2, with values at or near 0%. The SSDF and P/S iPOC values are slightly higher, but still consistent with dominantly pelagic organic carbon acquisition (<20% sea ice organic carbon). The patterns are less clear at SLIP 3 and 5, with both SSDF and SUS sea ice organic carbon sources less than 10% and a group of SSDF, SDF and SUS/SDF falling between 6–18% (Fig 3-6B).

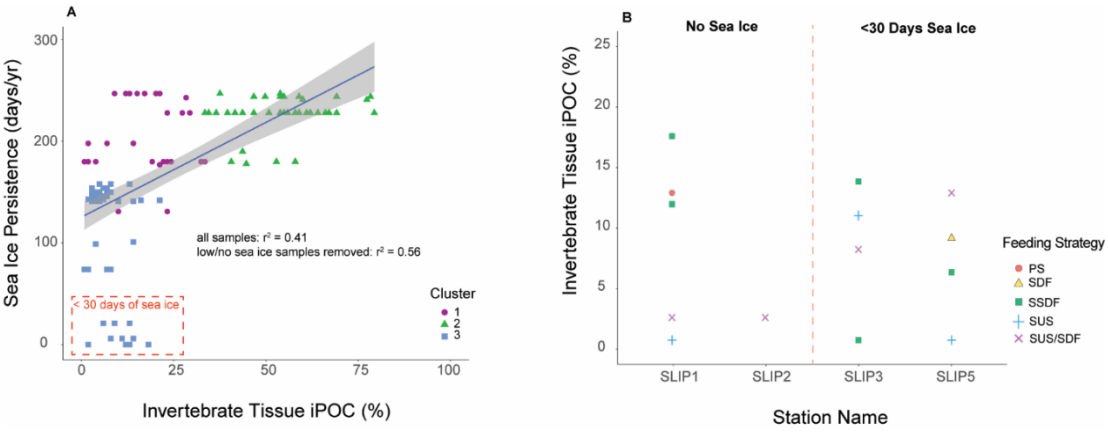

Figure 3-6 Relationships between invertebrate tissue sea ice carbon (iPOC%) and sea ice parameters (A) Linear regression of sea ice persistence and macrofauna sea ice organic carbon (iPOC %). Clusters are represented by corresponding shape/color. The samples that were deemed outliers due to low sea ice persistence or no sea ice cover in 2018 are enclosed in the dashed-red box. The linear regression is shown with a 95% confidence interval. **(B)** The macrofaunal tissue iPOC (%) from the no/low sea ice group by station in the DBO 1/St. Lawrence Island Polynya (SLIP) region. Symbols and corresponding colors represent feeding strategies of individual samples at these locations.

3.3.5. Sea ice organic carbon (iPOC %) utilization by major taxa

The species that contained the highest iPOC values (>75%) included maldanid polychaetes, the sipunculid *G. margaritacae*, and the clam *Ennucula tenuis* (Fig. 3-7A). High levels of iPOC (50–75%) were observed in the clams *Yoldia hyperborea* and *Macoma calcarea*, brittle star *Ophiura sarsiii*, polychaete *Pectinaria hyperborea*, amphipod family Lysianassidae (not practical to identify species at sea), and sea star *Henricia* sp. Moderate iPOC levels (25–50 %) were observed in the clams *Nuculana pernicula* and *Astarte borealis*, gastropod *Buccinum scalariforme*, and amphipod *Ampelisca* sp. The lowest iPOC levels (<25%) occurred in the snow crab *Chionoecetes opilio*, predatory polychaete *Nepthys* sp., bivalves *Serripes laperousii* and *Mya* sp., and all tunicates, holothuroids, ascidians, anthozoans, and the remaining gastropods. Estimates of iPOC by feeding strategy (Fig. 3-7B) reveal a dominance of SSDF in the dominant utilization of sea ice organic carbon (iPOC >50%). The SDF organisms were primarily in the moderate to high range of iPOC, but also

contained the highest mean iPOC values (e.g. sipunculids and brittle stars). None of the suspension feeders exceeded use of more than 25% sea ice carbon.

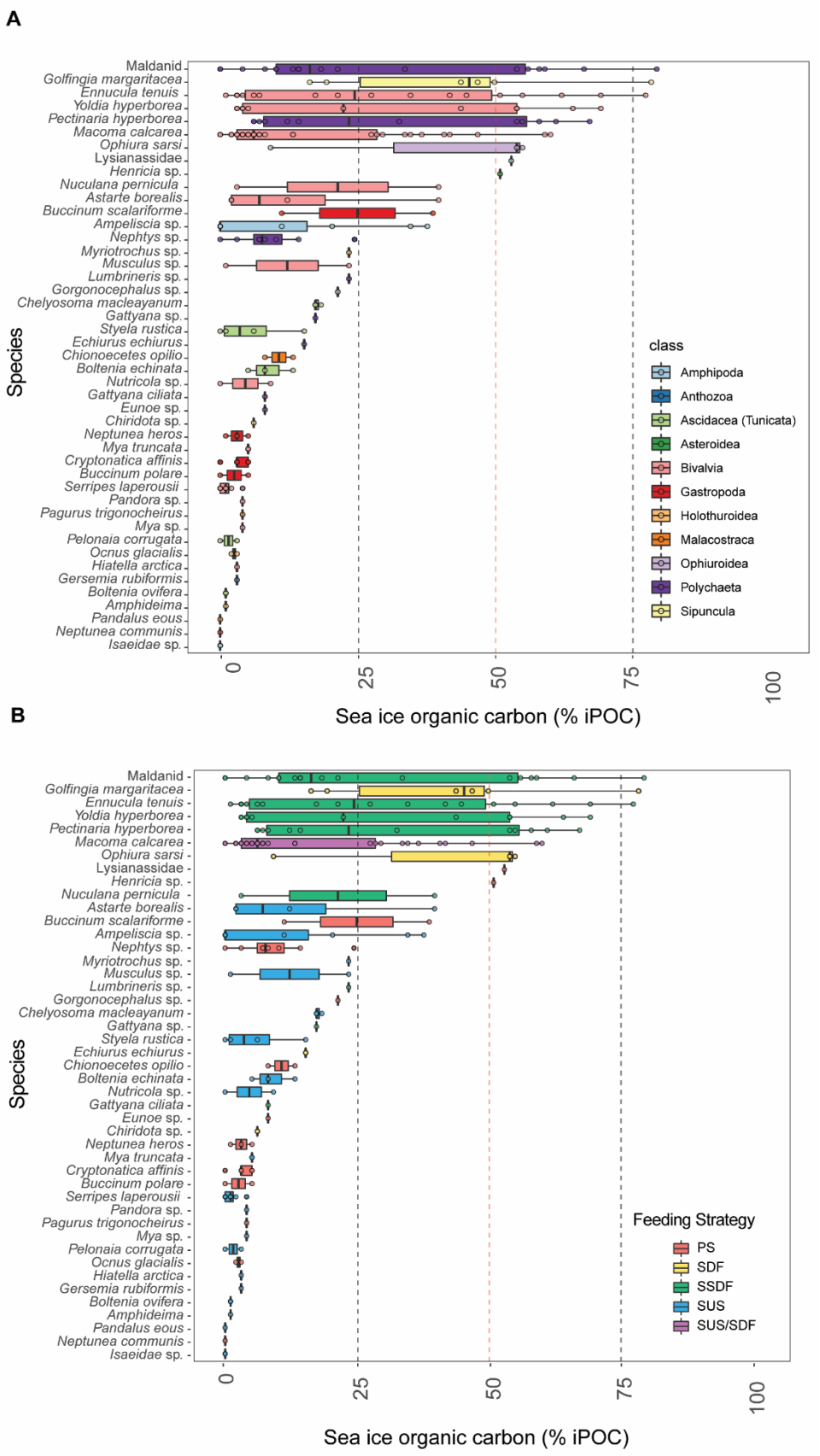
A
Maldanid
Golfingia margaritacea
Ennucula tenuis
Yoldia hyperborea
Pectinaria hyperborea
Macoma calcarea
Ophiura sarsi
Lysianassidae
Henricia sp.
Nuculana pernicula
Astarte borealis
Buccinum scalariforme
Ampeliscia sp.
Nephtys sp.
Myriotrochus sp.
Musculus sp.
Lumbrineris sp.
Gorgonocephalus sp.
Chelyosoma macleayanum
Gattyana sp.
Styela rustica
Echiurus echiurus
Chionoecetes opilio
Boltenia echinata
Nutricola sp.
Gattyana ciliata
Eunoe sp.
Chiridota sp.
Neptunea heros
Mya truncata
Cryptonatica affinis
Buccinum polare
Serripes laperousii
Pandora sp.
Pagurus trigonocheirus
Mya sp.
Pelonaia corrugata
Ocnus glacialis
Hiatella arctica
Gersemia rubiformis
Boltenia ovifera
Amphideima
Pandalus eous
Neptunea communis
Isaeidae sp.
Species
class
Amphipoda
Anthozoa
Ascidacea (Tunicata)
Asteroidea
Bivalvia
Gastropoda
Holothuroidea
Malacostraca
Ophiuroidea
Polychaeta
Sipuncula
0
25
50
75
100
Sea ice organic carbon (% iPOC)
B
Maldanid
Golfingia margaritacea
Ennucula tenuis
Yoldia hyperborea
Pectinaria hyperborea
Macoma calcarea
Ophiura sarsi
Lysianassidae
Henricia sp.
Nuculana pernicula
Astarte borealis
Buccinum scalariforme
Ampeliscia sp.
Nephtys sp.
Myriotrochus sp.
Musculus sp.
Lumbrineris sp.
Gorgonocephalus sp.
Chelyosoma macleayanum
Gattyana sp.
Styela rustica
Echiurus echiurus
Chionoecetes opilio
Boltenia echinata
Nutricola sp.
Gattyana ciliata
Eunoe sp.
Chiridota sp.
Neptunea heros
Mya truncata
Cryptonatica affinis
Buccinum polare
Serripes laperousii
Pandora sp.
Pagurus trigonocheirus
Mya sp.
Pelonaia corrugata
Ocnus glacialis
Hiatella arctica
Gersemia rubiformis
Boltenia ovifera
Amphideima
Pandalus eous
Neptunea communis
Isaeidae sp.
Species
Feeding Strategy
PS
SDF
SSDF
SUS
SUS/SDF
0
25
50
75
100
Sea ice organic carbon (% iPOC)

Figure 3-7 Sea ice organic carbon (% iPOC) composition by species Sea ice organic carbon (% iPOC) composition by species and shown by **(A)** major taxa and **(B)** feeding strategy. See Fig. 3-3 for boxplot descriptions and Table 3-2 for feeding strategies. Shaded points represent individual samples.

3.3.6. HBI depuration rates

The depuration rates determined from the temperate clam experiment suggest similar timing for suspension/deposit feeding *M. balthica* and suspension feeding *M. arenaria* at 21 and 28 days respectively (Fig. 3-8). Relative HBI III abundance indicated reductions by day 7 in both species, however there were detectable levels until the 3 to 4-week sampling events.

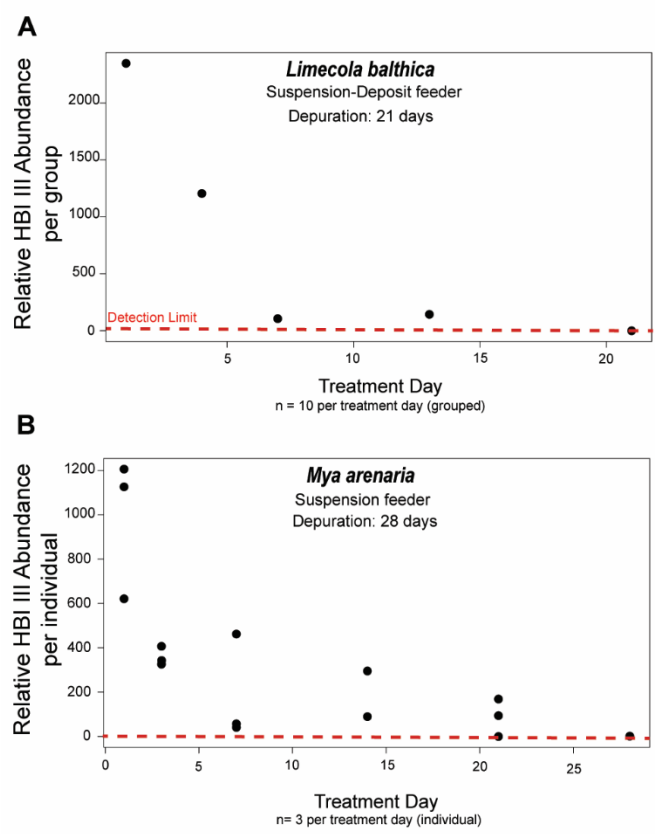

Figure 3-8 Experimental HBI III depuration rates in temperate clam samples **(A)** suspension-surface deposit feeding *Limecola balthica.* Individual points represent n=10 clams. **(B)** suspension feeding *Mya arenaria*. Individual points represent n=1 clam. The red-dashed line indicates the GC-MS detection limit for HBIs.

3.4. Discussion

The spatial distribution of H-print in surface sediments in 2018 (Fig. 3-2C) followed a latitudinal gradient previously observed for the region (Koch et al. 2020). IP_{25} concentrations were relatively high in surface sediments in the northeast Chukchi Sea compared to previous years, exceeding 14 μg g OC^{-1} (Fig. 3-2A). The strong relationship between sea ice persistence and sediment H-print supports the use of these biomarkers in this region as diagnostic of sea ice cover (Fig. 3-3). Based on the distribution of HBIs, we hypothesized that the invertebrate HBI composition would be influenced by the regional HBI patterns in the surface sediments as indicators of available food sources. Linear regressions between sediment H-print and macrofaunal iPOC confirmed that location was a significant influence (Figs. 3-4, 3-5C).

Sea ice persistence, which was correlated with DBO region, appeared to be an important factor in the cluster analysis. The samples in cluster 3 were located in the three southern DBO regions (Table 3-4; Fig. 3-5). Baseline studies of H-print in Pacific Arctic surface sediments suggest that a dominance of pelagic carbon is common throughout these three DBO regions (Koch et al. 2020). However, a defining feature of this region in 2017-2018 was the record low maximum sea ice extent (Grebmeier et al. 2018, Stabeno & Bell 2019). This may be the reason for the outlier iPOC signatures from benthic macrofauna samples collected at SLIP 1 and SLIP 2, where there was no sea ice cover and presumably no freshly deposited ice algae (Fig. 3-6A-B). The large ice-edge bloom that typically occurs in April or May over the northern Bering shelf did not occur in 2018, according to primary production measurements derived from satellite observations of chlorophyll *a* (Frey et al. 2020). The late pelagic bloom and abnormally low chlorophyll in the northern Bering Sea near DBO 1 were observed from fluorescence sensors on the M5 mooring (Duffy-Anderson et al. 2019). The lack of sea ice

also led to bottom water temperatures that were above 0°C for the first time since observations began in 1988 (Grebmeier & Cooper 1995, Grebmeier et al. 2018), eliminating the cold pool that typically serves as a thermal barrier to several pelagic and demersal fish species that could alter benthic food webs (Grebmeier et al. 2018, Duffy-Anderson et al. 2019). An observed ecosystem shift in this region has occurred over the last few decades, including a northward shift in benthic biomass and decline of nuculanid and nuculid bivalves replaced by maldanid polychaetes (Grebmeier et al. 2006b, Grebmeier et al. 2018). There has also been a northward contraction of the bivalve *M. calcarea* within the sampled stations in DBO 1 (Goethel et al. 2019). A recent study concluded that physical oceanographic shifts in this system are largely responsible for driving the changes seen in benthic community structure (Waga et al. 2020), and it seems plausible that these shifts are likely connected to changing food sources in the northern Bering Sea.

Moving northward, cluster 1 had a majority of the IC samples and a subset of samples from DBO 5 (Table 3-4; Fig. 3-5). The IC transect was located at the approximate position of the ice-edge through June and July before the rapid retreat off of the Chukchi shelf by August (Fig. 3-2C). At this location, the ice retreats in an onshore to offshore pattern with sea ice persistence lower by 20–30 days at the onshore sampling locations. This transect is also located at the start of the Central Channel for Bering Sea water transport northwards and current flow increases, as indicated by coarser grain sizes (Grebmeier & Cooper 2019g), suggesting reduced deposition of particulate organic matter including ice algae and phytoplankton. The sea ice persistence patterns, location of the mean ice edge for June and July, and sediment H-print values show a clear delineation between IC and DBO 4 despite their relatively close proximity (Figs. 3-1 and 3-2). There is also a front that forms between these regions, keeping warmer, nutrient-poor Alaska coastal water south and offshore and

nutrient-rich Bering Sea water to the north near DBO 4 (Weingartner et al. 2017). The strong negative correlation between sea ice persistence and H-prints suggest that the additional approximate month of sea ice at DBO 4 driven by the hydrography had an impact on IP_{25} synthesis and deposition. The surface deposit feeders at IC also contributed to the elevated iPOC values associated with this cluster (Fig. 3-4). The DBO 5 line is a transect across Barrow Canyon. The H-prints are elevated in the center of the canyon (~35%), yet still dominantly sympagic, and decrease on the sides (~14-18%). We attribute this cross-sectional pattern to the flow through Barrow Canyon, where currents converge with mean speeds of 15-20 cm/s (Bering water) and surface currents upwards of 70–100 cm/s (Alaska Coastal Current on the eastern flanks) with bottom intensified flows (Aagaard & Roach 1990, Pickart et al. 2005, Pickart et al. 2019). Although Barrow Canyon is on the northeast Chukchi Shelf where ice algae influence is most significant, ice algal aggregates likely do not settle to the bottom of Barrow Canyon as readily because of stronger currents than on the shelf and organic materials are transported towards the basin because of these enhanced current speeds (Lepore et al. 2009). Additionally, the high current speeds in Barrow Canyon favor suspension over deposit feeding (Pisareva et al. 2015). Therefore, the reason for these DBO 5 samples to be clustered with IC is likely due to the apparent increased phytoplankton utilization by suspension feeders relative to DBO 4 (Fig. 3-4).

As previously noted, DBO 4 and 5 dominated the cluster 2 composition in the northeast Chukchi Sea where ice algae deposition and utilization were most substantial. There were fewer SUS and P/S collected within the offshore DBO 4 transect. Macrofaunal biomass at these sites is typically dominated by deposit feeders, primarily sipunculids and maldanid polychaetes, but also brittle stars (Ophiuroidea) and bivalves (Yoldiidae and Astartidae) and occasionally the SUS/SDF bivalve *M. calcarea* (Grebmeier & Cooper 2019h). Depositional

regimes on the Chukchi shelf, such as along DBO 4, tend to favor deposit feeders over suspension feeders (Pisareva et al. 2015). The HBI data show that the pairing of longer sea ice persistence in a depositional environment results in higher ice algae utilization. Recent studies indicated that IP_{25} and diatom export occur year-round at this location (Koch et al. 2020, Lalande et al. 2020). There is currently a lack of HBI flux data available from other DBO regions, but preliminary HBI data from sediment traps at DBO 2 and DBO 3 suggest this steady supply of sympagic HBIs is likely a unique feature at DBO 4 (unpublished data). Although pelagic phytoplankton blooms are greater in the summer as seasonal ice retreats, in addition to the occurrence of under-ice phytoplankton blooms (Arrigo et al. 2014, Assmy et al. 2017), the continuous export of IP_{25} suggests a sustained source of sea ice carbon is transported to the benthos, both when grazing pressure in the water column is minimal and as a result of re-suspension events throughout the year (Koch et al. 2020b). The mean iPOC value in the invertebrate tissue samples suggests an approximate 50:50 mixture of ice algae and phytoplankton, although our analysis does not preclude organic carbon from other possible detrital or terrestrial sources. Feeding experiments providing both ice algae and phytoplankton to benthic consumers have shown that certain organisms may preferentially consume ice algae (McMahon et al. 2006, Sun et al. 2009). It has also been suggested that despite the preference for ice algae, many Arctic macrofauna exhibit dietary plasticity and will respond similarly to availability of either category of organic matter and may not be dependent on ice algae (Mäkelä et al. 2017, Kędra et al. 2019).

Location did not fully account for the variability among the sampled organisms and was the basis for exploring the differences among species and feeding strategies. Deposit feeders have been previously observed to have greater ice algae utilization than suspension feeders based upon fatty acid concentrations in macrofaunal tissues in the Chukchi Sea (Schollmeier

et al. 2018). This was similarly demonstrated through feeding experiments and was attributed to preferential grazing on the higher fatty acid composition of ice algae (McMahon et al. 2006). Our iPOC measurements confirm these findings, with higher values for surface and subsurface deposit feeders than suspension feeders throughout the study area (Fig. 3-4). Our HBI measurements do not mean that suspension feeders do not utilize ice algae from the water column. However, because ice algae aggregates sink rapidly to the seafloor and can overwhelm any pelagic grazers present, it is possible that much of the ice algae is not immediately consumed but is incorporated into the surface sediments (Legendre et al. 1992). By contrast, suspension feeders may more predominantly depend on water column phytoplankton that can be suspended in the water column over longer periods of the seasonal cycle.

Understanding HBI retention in consumers is critical to fully interpreting any transition in food sources as sea ice coverage diminishes. Short residence times (days to weeks) of HBIs in various consumer tissues have been suggested from previous studies (Brown & Belt 2012, Brown et al. 2013b, Brown et al. 2014a). Based on the results from the HBI III depuration experiment (Fig. 3-8), and the assumption that those temperate results are generalizable to higher latitudes, the HBI signal may represent assimilation over the course of approximately one month prior to sampling. Similar assimilation rates (i.e. approximately one month) of organic carbon were determined in Arctic bivalves using isotope labeled ice algae (McMahon et al. 2006). While IP_{25}-specific depuration rates are currently unavailable, a starting point might be to assume that this compound would behave similarly to HBI III, with further experimentation required to confirm this. Complexities include prior studies that suggest that metabolic rates can be quite variable in response to seasonal variations in temperature (Jansen et al. 2007) or that Arctic bivalves use elevated metabolic rates at low temperatures as an

adaptation strategy (Thyrring et al. 2015). The potential influence of temperature on metabolic rates when comparing our experiment using temperate species with Arctic species clearly imposes some limitations on the extent of possible interpretation. However, the results of this experiment demonstrate that very short lipid depuration (i.e. less than 48 hours) or bioaccumulation were not observed. If either were to be the case, relationships between sea ice and organic carbon transfer to higher trophic levels would be more ambiguous to interpret.

Ice algae deposition occurred with the shortest time interval in the northeast Chukchi Sea stations prior to sampling, allowing for the freshest deposition of iPOC at those locations. Owing to the low sea ice conditions in the Bering Strait region in 2018, there would have been little to no opportunity for ice-associated blooms, as was evident in the anomalous timing of maximum chlorophyll biomass in June rather than April–May (Frey et al. 2018). Therefore, the low levels of iPOC in deposit feeders from DBO1 and 2 (Fig. 3-6B) were most likely from previous years' sea ice carbon stored in the sediments. This indicates that this carbon source may serve as a reserve of lipid-rich organic matter in low sea ice years. This "sediment food bank" on polar shelves has been supported by other studies (Mincks et al. 2005, Pirtle-Levy et al. 2009, Sun et al. 2009, McTigue & Dunton 2014, North et al. 2014, Schollmeier et al. 2018). Analysis of HBIs from sediment cores on the Chukchi Shelf indicate that IP_{25} is well-mixed by bioturbation and can increase with depth (Koch et al. 2020). However, biological utilization of stored sea ice carbon and consistent burial through bioturbation will ultimately deplete these reserves, and subsequently the associated sympagic HBIs.

The importance of ice algae to predators and scavengers is not clear in light of our results. The iPOC values of these organisms suggest ice algae may not be a significant

component of their diet, which indicates more about their available prey items. It appears that P/S had comparable sea ice organic carbon levels as deposit feeders at IC (Fig. 3-4). Unfortunately, our sample sizes at DBO 4 and 5 were too low to robustly investigate this relationship where ice algae is incorporated into tissues in greater proportions. Future studies focused in these locations to analyze the progression of iPOC values in P/S and their preferred prey following sea ice retreat would be useful to better understand the significance of ice algae sources to these organisms, as they serve as important trophic links in the Pacific Arctic food web (Bluhm et al. 2009).

The SUS/SDF tellinid clams (e.g. *M. calcarea*), have a wide range of iPOC values. *M. calcarea* are found throughout the Pacific Arctic region and often dominate the macrofaunal biomass (Grebmeier et al. 2018). Their dietary plasticity is advantageous to allow for broader utilization of the available food source. The range of iPOC values of *M. calcarea* were between those of the deposit and suspension feeders, suggesting utilization of dual feeding strategies. Prior work found that *Macoma* species preferred ice algae over phytoplankton (Sun et al. 2009), but compound specific stable isotope analysis of amino acids has also revealed that some deposit feeding benthic species with high feeding plasticity can adjust feeding strategies in response to the quality and availability of organic matter reaching the seafloor (Kędra et al. 2019). One other species in this study, *G. margaritacea* (Sipuncula), is primarily a deposit feeder in the Pacific Arctic but also capable of suspension feeding (Gibbs 1977, Kędra et al. 2018). Sipunculids may utilize this feeding method in high current flow regions like that of Barrow Canyon where sipunculan abundance is high (Kędra et al. 2018).

G. margaritacea was one of two species in which the low end of the interquartile range of iPOC values was in the moderate utilization category for ice algae (25–50%, Fig. 3-7B). It also had one of the highest mean iPOC values overall. This range of iPOC values suggests

that *G. margaritacea* is one of the benthic macrofaunal groups most reliant on ice algae in the Pacific Arctic. *G. margaritacea* abundance is greater in the Chukchi Sea than in the northern Bering Sea, particularly in depositional environments, which may be driven by sea ice persistence and differing food types reaching the seafloor (Kędra et al. 2018). Our results also suggest there may be an association between ice algae deposition and sipunculan distributions. Sipunculids are a known prey item for important higher trophic organisms including the Pacific walrus (Sheffield & Grebmeier 2009, Jay et al. 2014), snow crab (Divine et al. 2017), and possibly others (Kędra et al. 2018). We also found that the brittle star *O. sarsiii* had elevated sea ice algae dependence relative to other species. Elevated ice algae utilization by ophiuroids has been observed in the Canadian Arctic using HBIs, stable isotopes and fatty acids (Kohlbach et al. 2019). *O. sarsiii* are widely distributed throughout the Pacific Arctic, however, they are most abundant in the northern Chukchi Sea than to the south (Ambrose et al. 2001, Bluhm et al. 2009) although they are also abundant in the muddy sediments on the outer shelf-slope southwest of St. Lawrence Island (Grebmeier et al. 2015). Brittle star abundance is associated with finer grain sizes (Grebmeier et al. 2015), but our HBI data suggest that it could also be influenced by the availability of ice algae as a food source in these depositional environments. *O. sarsiii* are also a prey item for snow crab in addition to sea stars and buccinid snails (Bluhm et al. 2009), which are similarly important trophic links to marine mammals. Despite the suggestion of potential plasticity to food quality and availability, based upon biomarker evidence, sipunculids and brittle stars seem to have a preference for ice algae and may face greater impacts to shifting food sources as seasonal sea ice coverage is reduced.

3.5. Conclusions

The main goal of this study was to determine the relative importance of ice algae on the highly productive shelves of the Pacific Arctic. The detection of sea ice source-specific biomarkers IP_{25} and HBI II, in comparison to the pelagic-sourced HBI III biomarker, suggests that both surface and subsurface deposit feeders in this region are more reliant on ice algae, compared to suspension feeders and predators/scavengers. Sea ice carbon is more abundant and utilized in greater proportions in the northeast Chukchi Sea relative to the northern Bering Sea and Bering Strait regions to the south. Our findings indicate that benthic communities of the Pacific Arctic display dietary plasticity for both sea ice and pelagic food sources with elevated ice algae utilization across several taxa and feeding strategies, either driven by elevated lipid content or availability and accessibility of this food source. Changes in quality, quantity and timing of primary production are likely to impact these benthic populations. The concept of a food bank stored within sediments on Arctic shelves is further supported here. This reservoir of organic matter may provide prolonged access to lipid reserves in the sediment in low sea ice years and in the decades to come. If ice algae production becomes much less prominent as the ice edge retreats northward, the sympagic carbon reserves will eventually be depleted and replaced by exclusively pelagic-sourced carbon which may particularly affect those organisms that currently obtain nearly half of their carbon from ice algae. The incorporation of HBI measurements into Arctic benthic food web studies provides advantages as a monitoring tool because of the source-specificity associated with the sea ice origin of organic matter. While the HBI measurements improve our ability to track the utilization of sea ice primary production, they may not fully capture the pelagic primary production and might be best considered complementary measurements to other diagnostic analyses such as stable isotopes and essential fatty acids.

3.6. Acknowledgements

We thank the captains and crew aboard the CCGS *Sir Wilfrid Laurier* and USCGC *Healy*. We also thank Katrin Iken (University of Alaska Fairbanks) for epibenthic sample collection and identification from the ASGARD cruise on the R/V *Sikuliaq*. We thank the four anonymous reviewers for their constructive comments that helped improve an earlier version of the manuscript. Financial support was provided by grants from the U.S. National Science Foundation Arctic Observing Network program (Award # 1917469 to J. Grebmeier and L. Cooper and Award # 1917434 to K. Frey) and NOAA Arctic Research Program (CINAR 22309.07) to J. Grebmeier and L. Cooper. We thank the North Pacific Research Board (NPRB) for additional funding support provided to C. Wegner (Koch) through the NPRB Graduate Research Award.

4. Female Pacific walruses (*Odobenus rosmarus divergens*) show greater partitioning of sea ice organic carbon than males: Evidence from ice algae trophic markers

Submitted to PLOS ONE, February 2021

Chelsea Wegner Koch, Lee W. Cooper, Jacqueline M. Grebmeier, Karen E. Frey, Raphaela Stimmelmayr and Thomas A. Brown

Contribution: Experimental design, all sample analysis, data analysis and interpretation, figure design and writing; Text has been edited by all co-authors; Sea ice persistence figure and sea ice data provided by Karen Frey

Abstract

We analyzed the highly branched isoprenoid lipid biomarker-based index (H-print) to follow the trophic transfer of sympagic (ice-associated) organic carbon to an ice-obligate consumer in the Pacific Arctic. We measured these trophic biomarkers in walrus liver tissues, with residence times of days to weeks, made available by Indigenous subsistence hunters harvested from 1997-2016 and coupled with δ^{15}N tissue measurements. Samples were collected from Bristol Bay (an ice-free summer/autumn male haulout location), the northern Bering Sea (mixed-sex winter breeding grounds with presence of sea ice in the winter and spring), and the Chukchi Sea (predominantly female summer/autumn foraging grounds with the highest persistence of sea ice). The H-print index estimated sympagic carbon contributions to the walrus tissues harvested from the Chukchi Sea to be >50%, significantly greater ($p < 0.001$) than the northern Bering Sea and Bristol Bay. While there was no clear relationship between sympagic carbon and trophic position overall, higher trophic positions

in the Chukchi Sea revealed an increasing complexity of the food web moving northward. Walrus tissues harvested in the northern Bering Sea were significantly different ($p < 0.001$) between males and females with the elevated sympagic carbon found in females. Male walruses from Bristol Bay contained exclusively pelagic carbon (>97%), consistent with minimal sea ice coverage. These patterns are consistent with largely sex-segregated distributions during most of the year and regional sea ice coverage. The elevated sympagic carbon in females in the Bering Sea is likely linked to energetic demands associated with pregnancy and lactation. Sympagic carbon in young walruses was consistent with elevated levels in females. The retreat of seasonal sea ice in recent decades may therefore create a greater vulnerability for female and dependent young Pacific walruses and should be considered in management of the species, including the application of the U.S. Endangered Species Act.

4.1. Introduction

Primary production in the Pacific Arctic region is partitioned between sympagic (sea ice) and pelagic (open water) sources (Nelson et al. 2014). On the continental shelf there is tight sea ice-pelagic-benthic coupling resulting in high benthic biomass (Grebmeier et al. 2006a), which supports a variety of specialized predators of the benthos including spectacled eiders, grey whales, Pacific walruses (*Odobenus rosmarus divergens*) and bearded seals (Grebmeier et al. 2015, Kuletz et al. 2015). This ecosystem is undergoing a shift from a benthic-dominated system to a more pelagic-based one owing in part to changes in ice algal production (Huntington et al. 2020). Ice algae are considered to be an important food source for benthic populations owing to the early timing of the blooms, which are rapidly exported to the benthos (McMahon et al. 2006). However, ice algae may be decreasing and phytoplankton blooms may be increasing in some regions in response to sea ice declines

(Arrigo et al. 2008). It is unclear how this shift will impact food webs in the Pacific Arctic (Grebmeier et al. 2010, Kędra et al. 2015). We selected the Pacific walrus to investigate how sea ice primary production is presently being utilized and incorporated at the upper trophic levels of this benthic-dominated system. Declining sea ice not only affects foraging behavior and access to foraging grounds for the Pacific walrus (Jay et al. 2012, Jay et al. 2017) but it also has the potential to reduce the quality of their diet in response to shifting carbon sources and associated lipid content. Therefore, we attempt to identify another mechanism in which climate change is likely impacting this species.

We used highly branched isoprenoid (HBI) lipids, which are biomarkers produced by diatoms with well-defined sea ice and phytoplankton sources (Brown et al. 2013a, Brown et al. 2014c, Brown et al. 2014d) to track the trophic transfer of these carbon sources. One HBI in particular has made these biomarkers useful for Arctic food web studies (Brown et al. 2013a), which is termed IP_{25} (Belt et al. 2007). IP_{25} is only produced in Arctic sea ice by four ice-associated diatom species (Brown et al. 2014c, Limoges et al. 2018). HBI II, a similar compound with two double bonds, is co-synthesized with IP_{25} and serves as an additional suitable proxy for sea ice organic carbon (Brown et al. 2014d). In contrast, HBI III is produced by pelagic diatoms in open waters and ice-edge blooms (Belt et al. 2017), and serves as a pelagic counterpart. These three HBIs together can be used to estimate the relative sympagic and pelagic organic carbon contributions (Brown et al. 2014d). Based on the relative proportion of ice algae and phytoplankton utilized by primary consumers (Brown & Belt 2011, Brown et al. 2017a), the HBI signal is incorporated into these lower trophic levels (Koch et al. 2020a), and then subsequently into secondary consumer tissues through trophic transfer (Brown et al. 2013a, Brown et al. 2013b, Brown et al. 2017b, Brown et al. 2018). In marine mammals, the liver is metabolically active with high tissue turnover rates on the order

of days to weeks (Vander Zanden et al. 2015). Therefore, by analyzing HBI signatures in walrus livers, we can estimate carbon sources assimilated on short timescales that reflect recent sea ice conditions and associated primary production. Owing to their source specificity, HBIs have the potential to inform how valuable sympagic production is in the Pacific Arctic food web and can hopefully contribute to monitoring the ecosystem response to shifting food sources in the years to come.

The Pacific walrus serves as an interesting test case for several reasons including their geographic range relative to sea ice areal coverage, the migratory behavior of this species, their benthic-based diet and their physical reliance on sea ice. The geographic range of the Pacific walrus females and their dependent young generally follows that of the seasonal ice edge, constrained to the shallow waters over the continental shelf (Fay 1982). Increasingly in recent years, sea ice retreats further north where the ice edge is typically over deep water by late summer, limiting an important platform for foraging walruses (Cooper et al. 2006, Jay et al. 2012). Beginning in 2007, walruses began regularly using coastal haulouts along the Alaskan coast and Chukotka peninsula once sea ice had retreated off of the Chukchi shelf (Jay et al. 2012). Sea ice over the shelf allows walruses to forage further offshore where benthic biomass is high (Jay et al. 2012). Sea ice also provides a platform for female walruses giving birth and nursing their young (Fay 1982). Breeding grounds have historically included the western and southeastern Bering Sea, but the largest is in the northern Bering Sea, south of St. Lawrence Island (Fay 1982, MacCracken et al. 2017). Male haulout locations are prominent on the Kamchatka Peninsula and near Bristol Bay in the southeast Bering Sea where they remain throughout the year (MacCracken et al. 2017). As the sea ice retreats in the early spring, female, dependent young, and some male walruses typically follow the ice

edge north into the Chukchi Sea where they remain (when possible) through the fall until the ice begins to reform (Fay 1982).

Walruses consume a wide range of benthic prey items (Sheffield & Grebmeier 2009, Maniscalco et al. 2020, Sonsthagen et al. 2020). They have the ability to forage on infaunal organisms up to 30 cm deep into the sediments (Oliver et al. 1983). Walruses primarily feed on bivalves but their diet also includes gastropods and polychaetes in the Chukchi and Bering seas (Bluhm & Gradinger 2008, Sheffield & Grebmeier 2009). Most of what is known about the Pacific walrus diet has come from fresh stomach content studies, acknowledging that some prey items are underrepresented with this method (Fay 1982, Sheffield & Grebmeier 2009). Uncertainties remain regarding the breadth of their diets and the flexibility that exists to adapt and partition resources with other benthic predators in the region (Oxtoby et al. 2017). With expanding northward ranges of boreal species, there may also be increasing competition for benthic resources, as has recently been observed for the Atlantic walrus (*Odobenus rosmarus rosmarus*) population (Gebruk et al. 2020). An analysis of the status of the Pacific walrus population indicated the need for understanding walrus diets and potential prey shifts (and quality) as a result of climate change (MacCracken et al. 2017).

South of St. Lawrence Island in the northern Bering Sea is an important wintering ground and breeding area for the Pacific walrus population (Jay et al. 2014, MacCracken et al. 2017). The area is the site of a winter polynya (area of open water in otherwise ice-covered waters) that generates cold bottom water during sea ice formation and elevated nutrient supply, leading to high benthic biomass (Grebmeier & Cooper 1995), resulting in an ideal walrus foraging location (Jay et al. 2014). Tellinid bivalves (i.e. *Macoma* spp.) are historically prevalent in this region and areas of high biomass were determined to be significantly correlated with Pacific walrus foraging site selection (Jay et al. 2014). However, this region is

changing in response to a warming climate and the bivalve communities have been shifting northwards over the past few decades (Goethel et al. 2019). The once dominant Tellinid and Nuculanid bivalves in the southern part of the region have been replaced by polychaete worms, which may be linked to changes at the base of the food web and/or changing sediment characteristics (Grebmeier et al. 2018). As the sea ice retreats earlier in the year, or never reaches previously covered areas (e.g. 2018 and 2019) an early spring ice-edge bloom does not occur (Duffy-Anderson et al. 2019, Stabeno & Bell 2019). Studies have hypothesized that a retreating winter ice edge and shifting benthic populations could lead to a northward shift in the walrus wintering grounds and changes in their prey selection (Jay et al. 2014, Beatty et al. 2016). The northern Bering Sea is transitioning to a pelagic dominated system with a declining benthic standing stock that will have consequences for marine mammals, particularly the benthic-feeding Pacific walrus (Grebmeier et al. 2006b, Grebmeier et al. 2018).

Seasonal segregation of the Pacific walrus population is timed by the advance and retreat of the seasonal ice edge. Walruses segregate into distinct groups where adult males remain in the northern Bering Sea, Bristol Bay and Kamchatka while females, dependent calves and young walruses follow the ice edge north into the Chukchi Sea each spring where they stay until autumn (Fay 1982, MacCracken et al. 2017). Declining sea ice has consequences for these summer and autumn foraging grounds in the Chukchi Sea (Jay et al. 2012, Jay et al. 2017, MacCracken et al. 2017). Walruses require a substantial amount of benthic prey to meet their energetic needs (Fay 1982, Noren et al. 2012). The southeastern flanks of Hanna Shoal in the northeast Chukchi Sea have sufficiently high bivalve biomass, providing the caloric density requirements to sustain walrus foraging activities (Noren et al. 2012, Wilt et al. 2014, Young et al. 2017). However, access to Hanna Shoal is largely

dependent on the presence of sea ice given the distant offshore location, which allows the walruses to haulout on ice to rest and remain offshore (Beatty et al. 2016, Jay et al. 2017). Without sufficient sea ice coverage on the shelf, these walruses are forced to seek out coastal haulouts, either utilizing scarce nearshore resources or traveling much greater distances to reach their preferred foraging grounds (Jay et al. 2012, Beatty et al. 2016, Jay et al. 2017). The benthic communities closer to the Alaskan shore are influenced by the Alaska Coastal Current (Iken et al. 2010), which is warmer, fresher and nutrient-poor compared to the Bering Sea water that flows towards Hanna Shoal in the summer (Gong & Pickart 2015, Woodgate 2018). The nutrient-rich waters of Hanna Shoal, coupled with prolonged presence of sea ice (Weingartner et al. 2017), allow for sustained ice algae blooms that likely fuels the high benthic biomass there (Grebmeier et al. 2015, Hauri et al. 2018). Ice algae are likely a more prominent food source for the benthos in the Chukchi Sea than in the Bering Sea (Koch et al. 2020a) and may be a source of more lipid-rich prey for walruses.

Combining the foraging ecology of the Pacific walrus with its close association to the sea ice, changes in sympagic and pelagic primary production may have an indirect impact on walrus condition and foraging behavior in the future. The objectives of this study were: (1) to investigate the relative contribution of sea ice organic carbon in the Pacific walrus diet to establish a baseline in anticipation of shifting organic carbon sources at the base of the food web, (2) determine regional and sex-specific differences in the utilization of sea ice organic carbon, and (3) evaluate sea ice organic carbon composition alongside trophic position throughout the region to assess possible shifts in walrus diets. Understanding the ecological connections between the Pacific walrus and sea ice, and the associated potential threats owing to climate change, have been an ongoing research imperative (Jay et al. 2011, Udevitz et al.

2017). HBIs provide a novel approach to assess these connections and may be useful monitoring tools in the future.

4.2. Materials and methods

4.2.1. Study Site

The geographic range of the Pacific walrus spans the Bering and Chukchi seas (Fig. 4-1), with coastal haulouts spanning many locations along the coasts of Russia and the United States (Alaska) (Fischbach et al. 2016). Walrus samples in this study originated from three general regions. Bristol Bay is located in the southeastern Bering Sea where several all-male coastal haulouts occur in the summer and autumn months, including the consistently occurring haulouts at Round Island (Fay 1982). The predominantly St. Lawrence Island Yupik villages of Gambell and Savoonga on St. Lawrence Island are positioned at the entrance of the Bering Strait, close to large wintering and breeding grounds in the northern Bering Sea and along the passageway to the Chukchi Sea during the annual northern spring migration route (Fay 1982, Huntington et al. 2016). Subsistence hunts occur here in the spring, typically around May of each year (Fay 1982, Kapsch et al. 2010, Huntington et al. 2016). Walrus hunting occurs in villages across northwestern Alaska but for this study walrus samples from the Chukchi Sea were only available from harvests that occurred near Wainwright and Utqiaġvik. Walrus samples from Point Lay were collected during several walrus mortality haulout investigations (Stimmelmayr et al. 2016). The walruses harvested by hunters in these communities are known to forage near the coast as well as further offshore, near Hanna Shoal in the northeast Chukchi Sea (Garlich-Miller et al. 2011, Jay et al. 2012, Grebmeier et al. 2015, Jay et al. 2017).

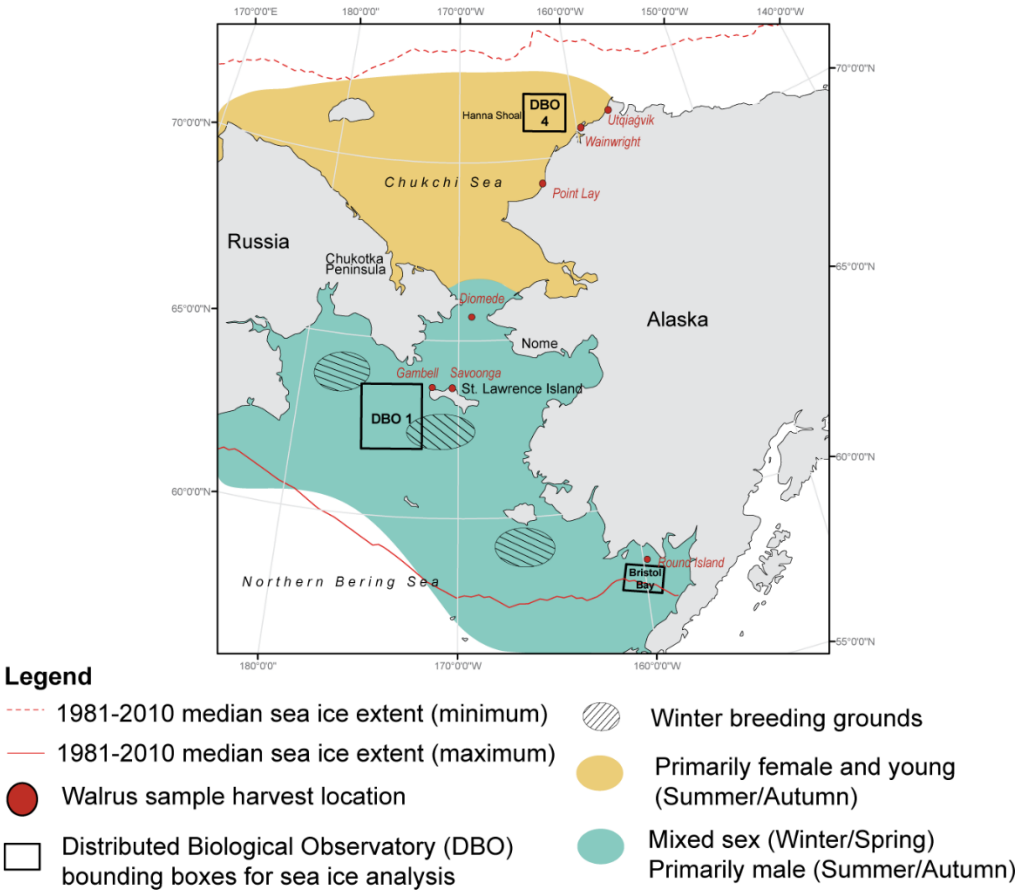

Figure 4-1 Distribution of the Pacific walrus and sample harvest locations. Boxes indicate regions used to determine the sea ice concentration near the time of collection (DBO 1 and 4, Bristol Bay) and for stable isotopes of nitrogen from sediment organic matter (DBO 1 and 4). Walrus range data modified from Garlich-Miller et al. (2011) and Smith (2010).

The Distributed Biological Observatory (DBO) sampling regions occupy five areas of high benthic biomass in the northern Bering and Chukchi sea, which in turn support higher trophic levels (Grebmeier et al. 2010). Several of these DBO regions are hotspots for walrus foraging activities owing to the high benthic biomass (Grebmeier et al. 2015). Our study focuses on DBO regions 1 and 4 (Fig. 1). DBO 1 is located south of the St. Lawrence Island polynya, which is a key area for Pacific walrus wintering and a prominent breeding ground (Fay 1982). DBO 4 is located on the southeastern flanks of Hanna Shoal, a shallow region on the northeast Chukchi shelf with substantial bivalve populations and the location of a

prominent summer foraging ground for walruses (Fay 1982, Jay et al. 2012, Grebmeier et al. 2015). Bristol Bay is not part of the DBO but was included in this study because it is a region of the Pacific walrus range that is ice-free for most of the year and would potentially serve as a pelagic endmember for comparison, as the male walruses there remain in the Bering Sea year-round (Fay 1982).

4.2.2. Sample collection

Subsistence hunted livers were donated to the University of Alaska Museum of the North (permit number: UAM 2018.020.Mamm) and the North Slope Borough Department of Wildlife Management (collected under US Fish and Wildlife Service permit number: MA 80164B-0) (Table 1). Samples from the North Slope Borough also included several walruses found dead from haulout mortality investigations at Point Lay. The collection date, location, sex, and age class of the walruses were identified at the time of collection, or were otherwise marked as unknown. Walrus livers were stored at -80°C prior to processing. The Museum of the North provided 0.5 g tissue plugs, shipped on dry ice; these samples were freeze-dried immediately upon arrival. The North Slope Borough Department of Wildlife Management sent frozen livers to the Chesapeake Biological Laboratory where we sampled 0.5–1 g of tissue using sterilized stainless steel scalpels followed by freeze-drying over 24 hours.

Table 4-1 Walrus liver sample summary

Location	Source	Month	Date	sample size (n)		
				female	*male*	*unknown*
Northern Bering Sea	University of Alaska Museum of the North	May	2002	3	-	-
Savoonga		May	2003	3	-	1
Gambell		May	2004	1	2	-
Diomede		May	2005	3	-	-
		May	2012	21	12	-
		May	2014	9	23	1

		May	2015	-	1	-
		April/May	2016	12	5	-
Bristol Bay	University of Alaska Museum of					
Round Island	the North	September	1997	-	12	-
Chukchi Sea	North Slope	unknown	2007	-	-	1
Utqiaġvik	Borough	unknown	2008	-	-	4
Wainwright	Department of Wildlife	July	2009	1	1	1
Point Lay	Management	July & September	2010	1	2	1
		July	2011	1	2	1
		June/July	2012	5	3	-
		July	2013	2	-	-
		July & October	2014	3	5	-

4.2.3. Biomarker extraction and analysis

After freeze-drying, HBIs were extracted following established methods (Belt et al. 2012, Brown et al. 2014d). Samples were saponified in a methanolic KOH solution and heated at 70°C for one hour. Hexane (4 mL) was added to the saponified solution, vortexed, and centrifuged for three minutes at 2500 RPM, three times. The supernatant with the non-saponifiable lipids (NSLs) was transferred to clean glass vials and dried under a gentle N_2 stream. The initial extracts were re-suspended in hexane and fractionated using open column silica gel chromatography. The non-polar lipids containing the HBIs were eluted while the polar compounds were retained on the column. The eluted compounds were dried under N_2. 50 µL of hexane was added twice to the dried purified extract and transferred to amber chromatography vials.

The extracts were analyzed using an Agilent 7890A gas chromatograph (GC) coupled with a 5975 series mass selective detector (MSD) using an Agilent HP-5ms column (30 m x 0.25 mm x 0.25 µm), following established methods (Belt et al. 2012). The oven temperature was programmed to ramp up from 40°C to 300°C at 10°C/minute with a 10-minute

isothermal period at 300°C. HBIs were identified using selective ion monitoring (SIM) techniques. The SIM chromatograms were used to quantify the HBI abundances by peak integration with ChemStation software (Agilent Technologies, California, USA). A purified standard of known IP_{25} concentration was used to confirm the mass spectra, retention time and retention index (RI). The HBIs were identified by their mass ions and RI including IP_{25} (*m/z* 350.3), HBI II (*m/z* 348.3) and HBI III (*m/z* 346.3). A procedural blank was run every 9th sample.

The relative abundances of the sympagic HBIs (IP_{25} and HBI II) to the pelagic HBI (HBI III), were quantified in order to determine the proportions attributable to different organic carbon sources. The H-print index provides an estimate of the relative organic carbon contributions of phytoplankton to sea ice algae (Brown et al. 2014d). The H-print (Eq. 4-1), is calculated using the relative abundances of IP_{25}, HBI II and HBI III, as determined by GC-MSD methods:

$$\text{H-print \%} = \frac{\text{HBI III}}{IP_{25}+HBI\ II+HBI\ III} \text{ x } 100 \qquad \text{(Eq. 4-1)}$$

The estimated organic carbon contribution varies from 0% to 100%, with lower values indicative of proportionally greater sympagic organic carbon and higher values indicative of proportionally greater pelagic organic carbon. Sea ice organic carbon (iPOC), as a proportion of marine-origin carbon within samples, was estimated using Eq. 4-1 from a prior H-print calibration from feeding experiments with known algal species [$R^2 = 0.97$, $p < 0.01$, df = 23 (Brown & Belt 2017)].

$$\text{iPOC \%} = 101.8 - 1.2 \text{ x H-print} \qquad \text{(Eq. 4-2)}$$

In contrast to the H-print index, higher iPOC values reflect greater proportions of organic carbon derived from ice algae.

4.2.4. Stable isotope analysis

Freeze-dried samples were homogenized with a mortar and pestle. 0.4–0.6 mg of tissue was weighed and introduced into tin capsules. The carbon and nitrogen stable isotope ratios were measured at the stable isotope facilities at the Chesapeake Biological Laboratory using a Costech elemental analyzer coupled to a ThermoFisher Delta V Isotope Ratio Mass Spectrometer in continuous flow mode. Nitrogen isotope ratios are expressed relative to atmospheric nitrogen (N_2) and Vienna-PeeDee Belemnite (VPDB) for carbon isotopes using the following equation:

$$\delta X = \left[\left(\frac{R_{sample}}{R_{standard}}\right) - 1\right] x\ 1000 \qquad (3)$$

where R is the corresponding ratio of $^{15}N/^{14}N$ or $^{13}C/^{12}C$. An internal protein standard was run every 5 samples (for carbon) and an internal standard of black sea bass (*Centropristis striata*) liver and Acetanilide (for nitrogen) were run every 9 samples. Since large amounts of ^{13}C-depleted lipid in liver tissue can affect the $\delta^{13}C$ results, we considered the practicality of removing tissue lipids prior to analysis or undertaking a general stoichiometric correction (Post et al. 2007), which may not be valid for Pacific walrus livers (Clark et al. 2019b). Owing to the limited amount of tissue available for the northern Bering Sea walrus samples at the time of that recommendation, we were unable to re-analyze and extract lipids from these samples to conduct an adequate $\delta^{13}C$ analysis. Therefore, the $\delta^{13}C$ values (with lipids) measured (S3 Table) were not considered in the numerical analysis.

Trophic positions (TP) for Pacific walruses were calculated from the stable nitrogen isotope values of livers using the following three equations (Eq. 4-4 – 4-6):

$$TP_{SPOM} = (\delta^{15}N_{walrus} - \delta^{15}N_{SPOM})/3.4 + 1 \qquad (Eq.\ 4\text{-}4)$$

$$TP_{SS} = (\delta^{15}N_{walrus} - \delta^{15}N_{Surface\ Sediment})/3.4 + 1 \quad \text{(Eq. 4-5)}$$

$$TP_{MC} = (\delta^{15}N_{walrus} - \delta^{15}N_{\textit{Macoma calcarea}})/3.4 + 2 \quad \text{(Eq. 4-6)}$$

The use of an enrichment factor of 3.4 is in agreement among several food web studies in the Pacific Arctic region (Iken et al. 2010, McTigue & Dunton 2014, North et al. 2014) and a standard enrichment factor suitable for marine consumers (Post 2002). We used previously published stable nitrogen isotope values from the northern Bering and Chukchi seas for suspended particulate organic matter (SPOM), surface sediments from DBO 1 and 4, and *Macoma calcarea* (a primary consumer). TP_{SPOM}, TP_{SS}, and TP_{MC} each assumes a different approach to serve as the food web baseline. $TP_{(SPOM)}$ considers particulate matter in the water column before it is reworked in the sediments and nitrogen values are impacted by denitrification processes (Chang & Devol 2009). TP_{SPOM} for the northern Bering Sea were calculated using the mean $\delta^{15}N$ of spring SPOM measurements (North et al. 2014). TP_{SPOM} were calculated for the Chukchi Sea using $\delta^{15}N$ measurements associated with the Bering Sea water mass (Iken et al. 2010), which flows across the Chukchi Shelf near Hanna Shoal (Weingartner et al. 2017). TP_{SS} used the $\delta^{15}N$ of surface sediments collected in July 2016 (Grebmeier & Cooper 2019d), which was intended to represent a cumulative estimate for each region. TP_{MC} utilized mean $\delta^{15}N$ values of *M. calcarea* from prior food web studies in the northern Bering (North et al. 2014) and northeast Chukchi seas (Iken et al. 2010, McTigue & Dunton 2014).

4.2.5. Sea ice analysis

Monthly averaged sea ice concentrations were retrieved at a 12.5-km resolution from the National Snow and Ice Data Center (NSIDC, https://nsidc.org) using the Defense Meteorological Satellite Program (DMSP) Special Sensor Microwave Imager/Sounder

(SSMIS) passive microwave data. We calculated the mean monthly sea ice concentrations within the boundaries of selected DBO regions associated with the month and year of walrus harvest and likely foraging grounds two weeks prior to determine a sea ice index. For example, a walrus harvested from St. Lawrence Island in early May 2016 was assumed to be foraging at DBO 1 in late April 2016. DBO 1 was assigned as the foraging area for the northern Bering Sea walruses harvested in the spring months and DBO 4 for the walruses harvested from the Chukchi Sea in the summer and fall months. However, we note that these assignments may not always accurately represent walruses from more southeastern foraging aggregations in the St. Lawrence Island/Diomede harvest or walruses recently migrating north in the early summer (June) harvests from Utqiaġvik/Wainwright (Jay et al. 2012). Since Bristol Bay is not a part of the DBO, a similarly sized delimited region offshore of Round Island (80 x 124 km, 57.7-58.4°N 158.9-161.3°W) was assigned for the walruses harvested from this location (Fig. 4-1).

Annual sea ice persistence data were calculated from SSMIS sea ice concentrations [using a 15% threshold to determine the presence vs. absence of sea ice cover, as in Frey et al. (2015)] for regional sea ice comparisons between 2012 and 2014. Persistence data were parsed annually from 15 September 2011 through 14 September 2012 and 15 September 2013 through 14 September 2014 to encompass the full seasonal sea ice advance and retreat cycle. Sea ice persistence anomalies were calculated relative to the 1981–2010 average (i.e., the average of all years between 15 September 1980/14 September 1981 through 15 September 2009/14 September 2010).

4.2.6. Numerical analysis

All analyses were conducted using R version 3.6.1. Walrus samples from all years were assigned to one of three regions including Bristol Bay (Round Island), northern Bering Sea (Gambell and Savoonga on St. Lawrence Island, as well as samples originating from Diomede Village (Inalik) on Little Diomede Island), and the northeast Chukchi Sea (village sources were Point Lay, Wainwright, and Utqiaġvik) based on their harvest location (Fig. 4-1). We determined if there were distinctions in carbon source among walruses harvested from these three regions by exploring the sympagic and pelagic HBIs graphically through non-metric multidimensional scaling (NMDS) ordination plots using the R package 'vegan'. Distances were based on Bray-Curtis dissimilarities of three HBIs (IP_{25}, HBI II and HBI III). A two-way ANOVA with interactions was used to determine if there were differences in iPOC between sexes and regions. Significant relationships were identified by post-hoc Tukey pairwise comparison and means adjusted using the R package 'lsmeans'. We opportunistically utilized all available liver samples and as a result, there were unequal and low sample sizes from most years of this study to assess changes in iPOC over time. Adequate sample sizes were available from 2012, 2014 and 2016 (northern Bering Sea only) to allow for limited annual comparisons. Age class data were available for approximately half of the samples. Of the known age classes in the Chukchi Sea samples (n=25), 10 were calves and 15 were adults. Only 6 of 57 walruses were identified as calves in the northern Bering Sea samples. Based on the comparable sample sizes, the effect of age class on sea ice organic carbon was examined for the Chukchi Sea only. A Welch two sample *t*-test was used for comparisons between adults and calves. The sea ice index was not normally distributed as determined by a Shapiro-Wilk test and therefore associations between our sea ice index and iPOC values were assessed using the non-parametric Spearman's (rho) rank correlation. We used one-way ANOVA tests to explore the relationship between sex, region and trophic

position based on stable nitrogen isotope values and sea ice organic carbon in walrus liver tissues.

4.3. Results

4.3.1. Sea ice organic carbon (iPOC%) by region and sex

The NMDS ordination plot indicated there were distinctions in sea ice organic carbon among the three regions (Fig. 4-2A). The iPOC values were normally distributed by region with equal variances, therefore a two-way ANOVA test was conducted with sex and region as factors. Samples with unknown sex were excluded from numerical analysis examining sex as a factor. There were significant differences between sex (DF=1, F=25.30, $p<0.001$) and region (DF=2, F=25.40, $p<0.001$). However, the interaction between sex and region was also significant (DF=1, F=4.5, $p<0.05$), therefore the least square means were reported. The adjusted mean (± SE) iPOC value in livers was highest in the Chukchi Sea with females at 51 ± 5% and males at 54 ± 5%. In the northern Bering Sea, females reached iPOC values of 43 ± 2% and males reached 29 ± 2% (Fig. 4-2b, Table 4-2). In Bristol Bay, male walruses had only 3 ± 5% sympagic carbon (Fig. 4-2B, Table 4-2). iPOC values in livers ranged from 1 – 79 % in the northern Bering Sea, 12 – 96% in the Chukchi Sea and 0 – 15% in Bristol Bay (Fig. 4-2b).

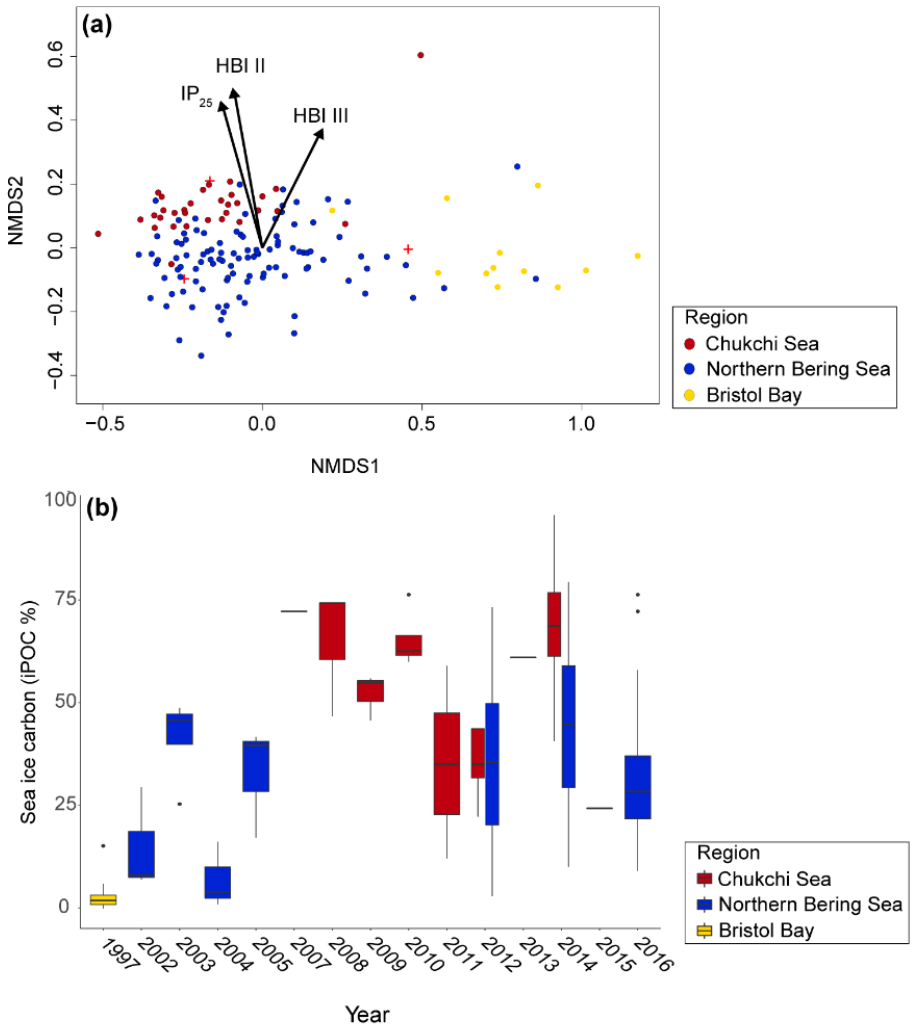

Figure 4-2 Regional analysis of sea ice organic carbon a) Ordination plots of sea ice organic carbon (iPOC%) by region with the influence of individual HBIs shown as vectors and b) Boxplots for iPOC (%) in Bristol Bay, northern Bering Sea and Chukchi Sea by year from 1997-2016. All samples (males, females and unknown sex) are included. Boxes depict the interquartile range from the first to third quartiles, including the median (horizontal line), minimum/maximum (vertical lines) and outliers (individual points).

Table 4-2 Summary of sea ice organic carbon (iPOC %) in Pacific walruses by region and sex

Region	Sex	Mean iPOC(%)*	SE	n
Bristol Bay	*females*	-	-	-
	males	3	5	12
Northern Bering Sea	*females*	43	2	54

	males	29	3	51
Chukchi Sea	*females*	51	5	12
	males	54	5	13

*Means adjusted to account for significant interaction between factors (Sex and Region)

Due to small samples sizes for most years of this study, only 2012, 2014 and 2016 had adequate sample sizes to allow for limited comparisons between sexes in the northern Bering and Chukchi seas (Fig. 4-3; Table 4-3). Post-hoc Tukey tests confirmed sea ice organic carbon was significantly higher in northern Bering Sea females compared to males in 2012, 2014 and 2016 ($p < 0.001$). Sea ice organic carbon was similar between males in females in the Chukchi Sea in 2012 but higher in females in 2014 ($p < 0.001$).

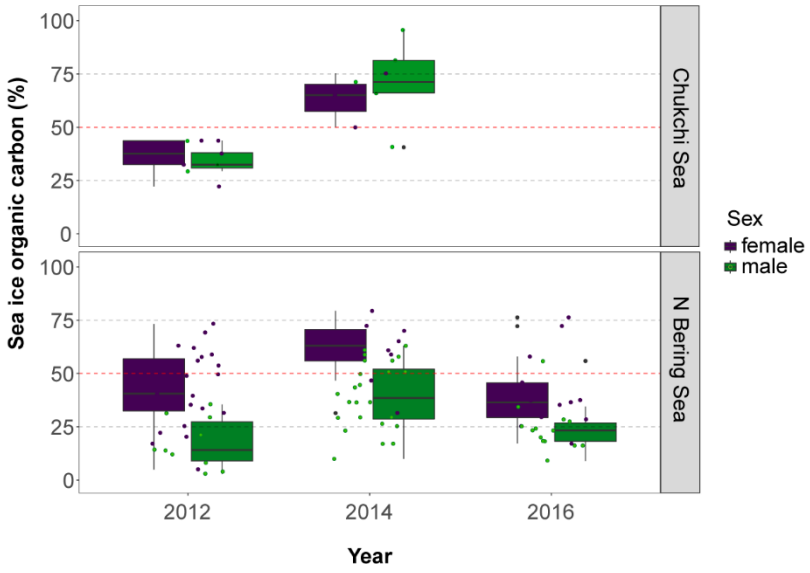

Figure 4-3 Sea ice organic carbon (iPOC%) by region and sex. Sea ice organic carbon by region and sex for 2012, 2014 and 2016 (northern Bering Sea only). The boxplot indicates the interquartile range from the first to third quartiles, with the median shown as the horizontal line within each box for females (purple) and males (green) for each region. All individual data points are shown. The red-dashed line indicates 50% sea ice organic carbon utilization, with values above this level suggesting an elevated sea ice signature.

Table 4-3 Summary of sea ice organic carbon (iPOC%) mean and standard error (SE) by year between male and female Pacific walruses in the northern Bering Sea and Chukchi Sea for 2012, 2014 and 2016.

	2012		2014		2016	
Northern Bering Sea	**Mean iPOC(%)***	**SE**	**Mean iPOC(%)***	**SE**	**Mean iPOC(%)***	**SE**
males	23	4	41	3	24	3
females	40	3	58	4	41	3
Chukchi Sea						
males	25	6	62	4	-	-
females	42	6	80	6	-	-

*Means adjusted to account for significant interaction between factors (Sex and Region)

The only years with overlapping samples collected from both the Bering and Chukchi seas occurred in 2012 and 2014 (Table 4-3). There was no difference between northern Bering Sea males or females compared to Chukchi Sea males and females in 2012 ($p>0.05$). Contrastingly in 2014, females in the Chukchi Sea had greater sea ice organic carbon than females in the northern Bering Sea ($p<0.001$) and males had more sea ice organic carbon in the Chukchi Sea than in northern Bering Sea males ($p<0.001$).

4.3.2. Sympagic carbon (iPOC%) by age class

In the Chukchi Sea, calves had higher sea ice organic carbon than adults (Fig. 4-4). Eight of the 10 calves sampled in this region had iPOC values that exceeded 50%. A Welch two-sample *t*-test indicated the difference in iPOC between calves and adults was significant (t=-2.8, df=13, $p<0.05$).

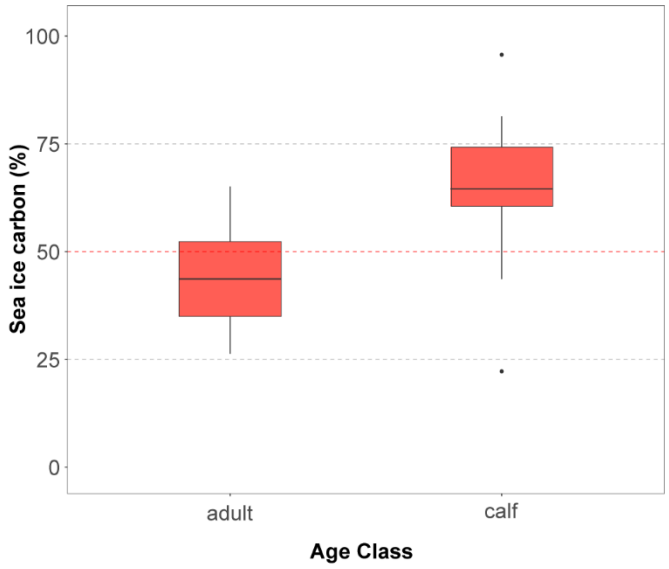

Figure 4-4 Sea ice organic carbon (iPOC%) by age class in the Chukchi Sea Box plots represent the interquartile range of values for adults and calves in the Chukchi Sea. The red-dashed line indicates 50% sea ice organic carbon utilization, with values above this level suggesting an elevated sea ice signature.

4.3.3. Sea ice

There was no significant correlation between the sea ice index and sea ice organic carbon in walrus liver tissues overall. Based on the significant differences of sea ice organic carbon observed between the Bering and Chukchi seas, we ran correlation tests for each region. The sea ice index was significantly correlated with iPOC in the Chukchi Sea ($R=-0.55$ and $p<0.001$), but there was no correlation in the northern Bering Sea.

There was a divergent pattern in sea ice anomalies for 2011/12 in the Pacific Arctic region (Fig. 4-5a). Sea ice persistence in 2011/12 in the northern Bering Sea was above the 1981–2010 average by upwards of 40 days or more, while sea ice persistence was below average in the Chukchi Sea (Fig. 4-5a). In contrast, there was a more uniform pattern of below average sea ice throughout the region in 2013/14 (Fig. 4-5b).

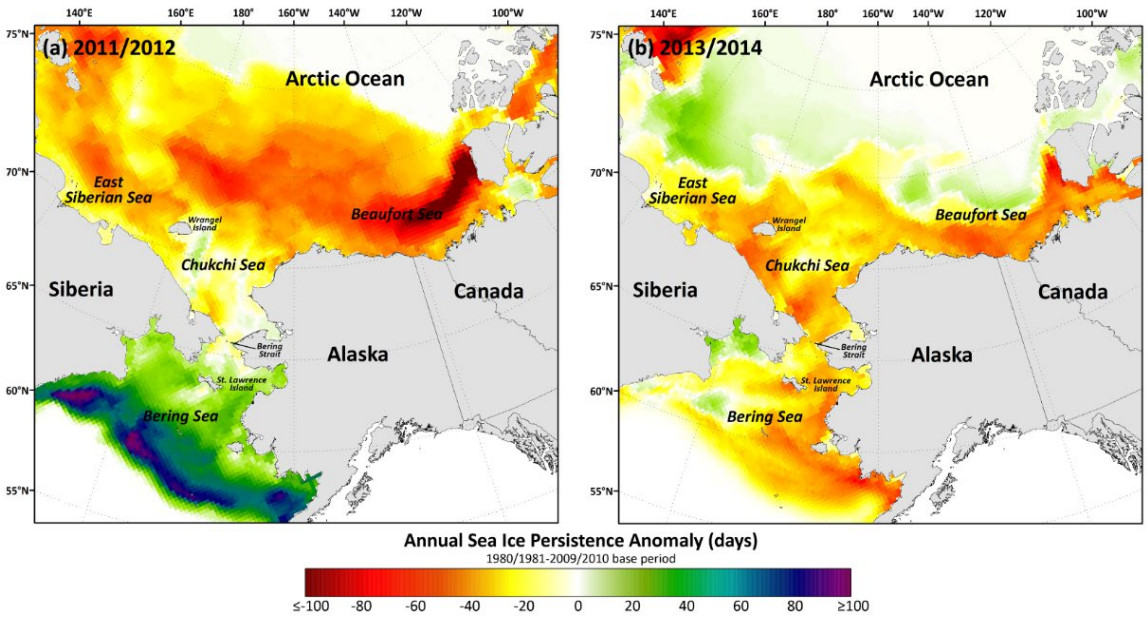

Figure 4-5 Sea ice persistence anomalies for 2011/12 and 2013/14 for the Pacific Arctic. a) Sea ice persistence anomalies for 15 September 2011 – 14 September 2012 and **b)** 15 September 2013 – 14 September 2014 compared to a 1980/1981-2009/2010 base period. These time intervals encompass the full annual sea ice advance and retreat cycle.

4.3.4. Stable nitrogen isotope composition and trophic positions

Overall, there was a significant difference ($p < 0.001$) in $\delta^{15}N$ values (Table S-3) between the northern Bering Sea (13.4 ± 0.9 ‰) and Chukchi Sea (14.9 ± 1.0 ‰) samples as determined by a one-way ANOVA, but there was no significant difference between males (13.6 ± 1.3 ‰) and females (13.9 ± 0.9 ‰). Comparisons were possible between 2012 and 2014, in which the differences between regions were significant in both 2012 (DF=1, F=15.51, $p<0.001$) and 2014 (DF=1, F=58.79, $p<0.001$) as determined by one-way ANOVA testing.

TP_{SPOM} values ranged from 2.2–2.7 in the northern Bering Sea and 3.6–3.9 in the Chukchi Sea (Table 4-4). The mean TP_{SPOM} for Bristol Bay (3.1 ± 0.2, Table 4-4) was more similar to the Chukchi Sea. Trophic positions (TP_{SPOM}) were significantly different among all three regions (DF=2, F=353.7, $p < 0.001$) as determined by ANOVA testing. TP_{MC} (DF=1.

F=116.9, $p < 0.001$) and TP_{SS} (DF=1, F=257.6, $p < 0.001$) were also significantly different between the northern Bering and Chukchi Seas. Differences between males and females were not significant ($p > 0.05$). There was no linear relationship between iPOC and trophic position, however, there was a distinct regional grouping (Fig. 4-6). All three approaches to determine the trophic position are in agreement showing higher values in the Chukchi Sea.

Table 4-4 Stable nitrogen isotope values and trophic levels for Pacific walruses by region and sex

Location	Walrus $\delta^{15}N$ (‰)	SPOM $\delta^{15}N$ (‰)	TP_{SPOM}	Surface Sediment $\delta^{15}N$ (‰)	TP_{SS}	*Macoma calcarea* $\delta^{15}N$ (‰)	TP_{MC}
Northern Bering Sea		8.8[a, b]		8.7[e]		9.9[b]	
females	13.7 ± 0.8		2.4 ± 0.2		2.5 ± 0.2		3.1 ± 0.2
males	13.0 ± 0.7		2.2 ± 0.2		2.3 ± 0.2		2.9 ± 0.2
unknown	14.4 ± 1.6		2.7 ± 0.5		2.7 ± 0.4		3.3 ± 0.4
Chukchi Sea		5.63[c]		7.3[e]		9.4[c]	
females	14.7 ± 0.9		3.7 ± 0.3		3.2 ± 0.3		3.5 ± 0.3
males	15.4 ± 1.2		3.9 ± 0.3		3.4 ± 0.4		3.7 ± 0.3
unknown	14.5 ± 1.6		3.6 ± 0.2		3.1 ± 0.2		3.5 ± 0.2
Bristol Bay		7.4[d]		-		-	
males	14.6 ± 0.4		3.1 ± 0.1		-		-

[a]Lovvorn et al. 2005
[b]North et al. 2014
[c]Iken et al. 2010
[d] Smith et al. 2002
[e]Grebmeier and Cooper 2019

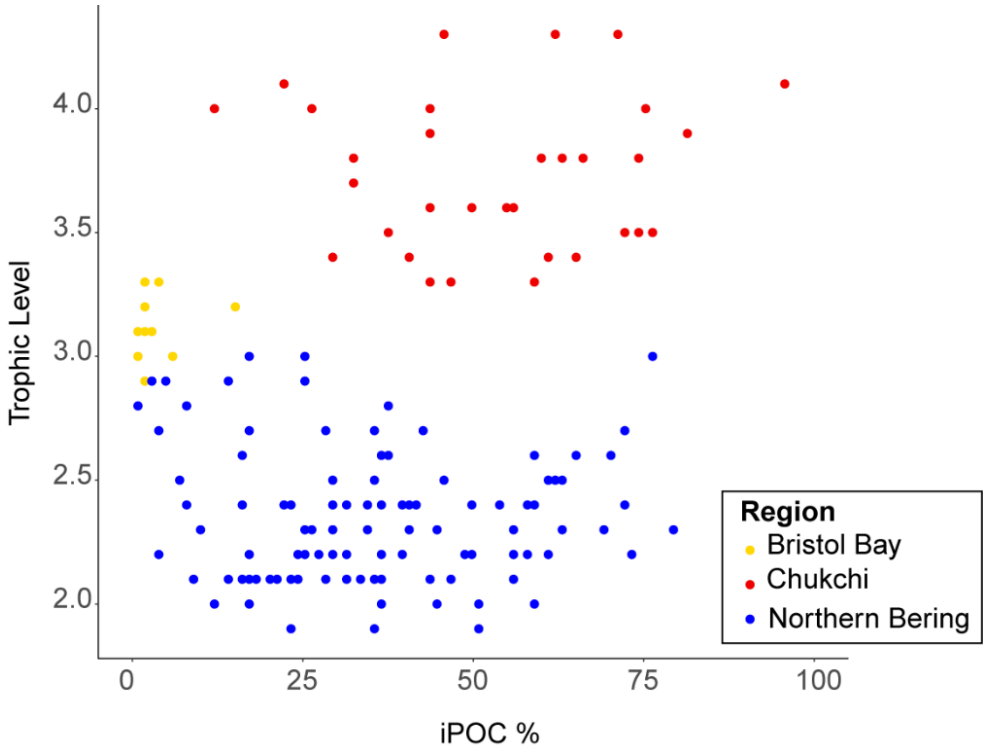

Figure 4-6 Trophic position (TP_{SPOM}) and sea ice organic carbon (iPOC %) by region. Pacific walrus trophic levels were calculated using suspended particulate organic matter (SPOM) values from the southeastern Bering Sea (representing Bristol Bay), northern Bering Sea and Chukchi Sea.

4.4. Discussion

4.4.1. Regional variability in sea ice organic carbon and the sea ice index

The regional patterns observed in this study (Figs. 4-2 and 4-3) are generally consistent with sea ice persistence patterns and HBI distributions determined from surface sediments (Koch et al. 2020b). The iPOC signature in walrus livers are likely more a reflection of the broader HBI distributions and the location of primary foraging activities rather than differences in resource selection. This observation is also supported by the HBI content of benthic invertebrates across the Pacific Arctic, specifically in Tellinid bivalves (Koch et al. 2020a). These bivalves are ubiquitous throughout the entire region and were also generally consistent with the HBI distribution pattern in the surrounding surface sediments,

with elevated iPOC relative to the surface sediments in a few locations (Koch et al. 2020a). Tellinid biomass has proven to be a significant predictor of Pacific walrus resource selection models in both the northern Bering (Jay et al. 2014) and Chukchi (Beatty et al. 2016) seas.

The HBI distributions in the sediments are a reflection of differences in ice algae production throughout the region (Koch et al. 2020b). Sea ice persistence in the Chukchi Sea exceeds that of the northern Bering Sea by 2–4 months (Frey et al. 2015). Recent studies of particle fluxes in the northeast Chukchi Sea indicate a year-round export of diatoms, including ice-associated diatoms, on the shallow shelf (Lalande et al. 2020). Additionally, subsurface chlorophyll alongside disassociated ice algae suggest that ice algae are likely contributing to prolonged periods of productivity on the Chukchi shelf (Stabeno et al. 2020). These data imply that sympagic HBI levels in the northeast Chukchi Sea would be higher than those found in the northern Bering Sea, and therefore the sea ice organic carbon would be higher in the prey items utilized by northerly walrus populations in the summer and autumn.

HBIs have been used to demonstrate dependence on ice-derived resources by upper trophic predators, including seabirds and marine mammals, throughout the polar regions (Goutte et al. 2013, Goutte et al. 2014a, Brown et al. 2017b, Cusset et al. 2019). In one of these studies, a sea ice use index was applied to analyze the reliance on ice-derived resources by two species of seabirds in the Canadian Arctic with different foraging behaviors and dependence on sea ice (Cusset et al. 2019). That prior study concluded ice-obligate thick-billed murres relied heavily on ice-associated prey as indicated by a strong correlation with this species and a sea ice-use index, while contrastingly no such relationship was found for fulmars that are not a sea ice obligate species. Thick-billed murres are restricted in large-scale movements owing to their ice-obligate foraging behavior while fulmars are not (Cusset et al.

2019). Those findings provide an interesting comparison with our results. We found no correlation between the sea ice index and the whole of our Pacific walrus data. As noted previously, this species migrates across a gradient of sub-Arctic to Arctic habitat with distinct sea ice conditions, while also coupling the benthic and pelagic realms along the way. These large-scale movements likely result in both horizontal and vertical habitat integration by these transient marine mammals. This integration across the entire Pacific Arctic region over the course of a few months during the ice melt season is likely why our sea ice index did not robustly match iPOC values in walrus tissues. The negative correlation for the Chukchi Sea walruses relative to the sea ice index was unexpected (*i.e.* more sea ice organic carbon assimilation during open water periods). The few samples that were collected in September when sea ice was absent weighted this negative association. These walruses may have had a longer period of time to forage on more of the prey that had previously assimilated sea ice organic carbon than those harvested earlier in the summer. The relationship is no longer significant if these samples are excluded. These complexities show that direct associations may not always be possible with sea ice indices in secondary consumers. However, our study also indicates that HBIs may still serve as fingerprints of where large marine predators were foraging, similar to the way that carbon isotope distributions have been used to create isoscapes that map differences in primary production throughout a given area (Graham et al. 2010). Additionally, tracking the sympagic carbon in these organisms over time may still be useful in monitoring responses to declining sea ice. HBI measurements of other marine mammals and seabirds in this region with differing foraging ecologies will be potentially useful in further assessing changes in food webs as seasonal sea ice declines.

While there was no association between the sea ice index and sea ice organic carbon values, there were still interesting patterns when assessing the results from 2012 and 2014

within a broader context of sea ice cover during these two seasonal sea ice cycles. In 2012, the northern Bering Sea experienced a cold year in which sea ice persistence was well above average (Fig. 4-5a). However, there was also a geographically divergent pattern in 2012, as sea ice in the Chukchi Sea was a record low year (Frey et al. 2015) (Fig. 4-5a). This geographically divergent sea ice pattern would potentially explain higher than average sea ice algae trophic markers in the Bering Sea and lower abundance in the Chukchi Sea, reflected in comparable values for the two regions (Fig. 4-2b). However, in 2014, sea ice persistence anomalies indicate similarly negative values throughout the region (Fig. 4-5b). Therefore, the default HBI distribution pattern observed for the region (increasing sympagic HBIs from south to north (Koch et al. 2020b)) was reflected in the consumer tissues.

4.4.2. Elevated sea ice organic carbon in female and Chukchi Sea walruses

Sea ice organic carbon was higher in females from the northern Bering Sea and also for the mixed-sex walruses harvested from the Chukchi Sea, relative to those from the northern Bering Sea and Bristol Bay (Fig. 4-3). The elevated sea ice biomarkers in females in the northern Bering Sea samples relative to males, which had no significant difference from tissue values in the Chukchi Sea, could be explained by a few possibilities. The first is that foraging behavior may differ among males and females in this region and during the winter and spring seasons. Resource partitioning between males and females was implicated as the reason for differences in fatty acid profiles in Pacific walrus blubber (Oxtoby et al. 2017). Early studies of walrus stomachs suggested that females and juveniles tended towards smaller bivalves compared to that of males (Fay 1982). Other differences in male and female prey selection have been reported. For example, male Pacific walruses have been reported to opportunistically forage on higher trophic level prey (HTLP), including seals and seabirds, if there is a lack of preferred prey owing to availability or requirements to forage in nearshore

environments (Fay 1982, Seymour et al. 2014). Indications of seals and other HTLP in walrus diets have been suggested through stable isotopes and is supported to some extent with observational data (Lovvorn et al. 2010). However, this behavior, and whether it differs between males and females, remains inconclusive and is also believed to be atypical (Fay 1982, Seymour et al. 2014). Resource partitioning may also be linked to breeding. During the winter breeding season in the northern Bering Sea, male walruses reduce foraging efforts to focus on mating (Ray et al. 2006). The breeding season for the Pacific walrus occurs approximately from January through March (Fay 1982). A majority of the walrus livers from the northern Bering Sea included in this study were collected in April and May. Based on the assumed turnover rate of HBIs in liver, it is possible that the sea ice biomarker signatures are a reflection of this behavior. The results from Oxtoby et al. (2017) suggested an incorporation of lipid-rich resources from the previous season, reflecting turnover rates of several months for blubber. By contrast, the use of liver in this study and a more rapid turnover rate further constrains this possible resource partitioning to the time period close to the subsistence hunt. By reducing the time period of metabolic activity, we conclude the dependence on sea ice organic carbon is not derived from a prior year.

The elevated sea ice organic carbon in females could also be a result of metabolic differences, in which the females have greater lipid stores than males to support lactation and pregnancy and selectively forage on more lipid-rich food sources (Noren et al. 2012, Noren et al. 2014). Pregnant and lactating females have been observed in the water for greater periods than males, suggesting increased foraging efforts (Fay 1982). Lactating females need to increase their lipid stores to support these energetic demands, equivalent to doubling clam consumption during this time (Noren et al. 2014). Owing to the distinct sexual segregation during the summer and autumn seasons, general differences in diet by sex can be anticipated

based on the prey availability in different foraging areas, particularly with males foraging from coastal haulouts and females foraging from offshore sea ice. It had previously been concluded that males and females generally eat the same prey while occupying the same area (Fay et al. 1989, Sheffield & Grebmeier 2009). However, it has been proposed that female walruses may be at greater risk of disturbance than males owing to loss of sea ice habitat (Garlich-Miller et al. 2006, Garlich-Miller et al. 2011, Jay et al. 2011, Noren et al. 2012). The loss of sea ice could impact the females' ability to successfully reproduce and provide adequate nutrition for their offspring (Noren et al. 2012, Noren et al. 2014, Jay et al. 2017). Stress and reproductive biomarkers analyzed from recent and archaeological Pacific walrus bones suggested potential resilience to declining sea ice (Charapata et al. 2021), but ongoing monitoring of this species is necessary to track their response to unprecedented change.

The effects of declining sea ice on walruses may already be evident in the northern Bering Sea. Observations from the southwestern Bering Sea indicate that occupation of land haulouts by males in this region may be shifting to northward locations in the Chukchi Sea on the Chukotka Peninsula (Zagrebelny & Kochnev 2017). There has also been a northward shift in bivalve populations at DBO 1 (Goethel et al. 2019), which is near a prominent walrus breeding ground and a prey base for these walruses (Jay et al. 2014). Negative associations with sea ice declines have also been reported in body condition observations for females and juveniles of other pinniped species in this region (Boveng et al. 2020). These observations together suggest a broader ecosystem shift is underway in response to warming waters, reduced sea ice coverage and timing of ice retreat, and changes in the quality, quantity and timing of primary production (Grebmeier et al. 2018, Huntington et al. 2020).

The HBI signatures from benthic macrofauna in the Bering and Chukchi seas suggested a greater reliance on sea ice organic carbon by subsurface deposit feeders and

predominantly pelagic organic carbon signatures in suspension feeders and predator/scavengers throughout the region (Koch et al. 2020a). If female walruses were foraging on more infaunal organisms deep in the sediments as opposed to more motile epifauna, including predatory gastropods or crustaceans, this may be one explanation for differences in their sea ice organic carbon signatures compared to males. Additionally, the iPOC signatures in benthic prey were highest at the DBO 4 region, which is located at Hanna Shoal, a popular walrus foraging ground in the summer (Grebmeier et al. 2015). Studies in the northern Bering (Jay et al. 2014) and Chukchi (Beatty et al. 2016) seas concluded that Tellinid biomass was a significant predictor of Pacific walrus resource selection. While iPOC data in Tellinid clams that correspond with the timing of the walrus harvests and samples used in this study are currently unavailable, mean iPOC values from both regions in 2018 suggest a significant difference in their sea ice organic carbon content (~6% in the Bering Sea and ~40% in the Chukchi Sea) (Koch et al. 2020a). Given the similarities between males and females in the Chukchi Sea walrus samples, the prey HBI data suggest these walruses likely have similar foraging behaviors. However, the elevated sea ice organic carbon values observed in females from the northern Bering Sea suggest foraging behaviors differ from males during the spring when factoring in mating, pregnancy, and lactation requirements. The study assessing sea ice biomarkers in benthic fauna also revealed elevated sea ice organic carbon use by another common prey item, sipunculid worms (Koch et al. 2020a), which are also more prevalent in the Chukchi Sea than in the northern Bering Sea (Kędra et al. 2018). If these prey items preferred by females and young in the Chukchi Sea are also vulnerable to sea ice declines, this poses another negative potential consequence for walruses.

4.4.3. Trophic position and sea ice organic carbon utilization

Trophic positions were higher overall in the Chukchi Sea (Fig. 4-6). However, it is unlikely that the summer diets of Pacific walruses in the Chukchi Sea are substantially different than those in the northern Bering Sea in the spring and winter (Sheffield & Grebmeier 2009). The distribution and availability of bivalves, their preferred prey item, throughout the Pacific Arctic region supports this argument (Grebmeier et al. 2015). Therefore, the difference in trophic position is likely driven by large-scale processes in the region. The food web in the Chukchi Sea becomes more complex than the northern Bering Sea as a result of the Pacific inflow system, where advective processes deliver substantial organic carbon that is in part degraded and deposited as water moves across the shelf (Feng et al. 2020). As a result, the detrital food web becomes more influential in the northern Chukchi, likely leading to the elevated trophic position estimates. This is also evident in the observed gradation of denitrification from south to north in the region (Brown et al. 2015). The Bristol Bay walrus samples were at a higher trophic position than the northern Bering Sea male walruses, which were more comparable to the Chukchi Sea values (Fig. 4-6). However, this may be a more authentic representation of differences in diets owing to the available prey choices, including an apparent elevated utilization of fish (Maniscalco et al. 2020).

In the northern Bering Sea, higher iPOC levels in males were associated with a lower trophic position. One possibility is that males meeting a majority of their caloric demands from bivalves and invertebrates leads to elevated iPOC levels and are less dependent on HTLP, while foraging on higher trophic level prey results in lower iPOC. Subsurface deposit feeders had elevated iPOC values compared to predatory gastropods, which are considered HTLP (in addition to seals and seabirds) (Koch et al. 2020a). Additionally, the requirement to forage on HTLP could be driven by low sea ice years where access to benthic offshore resources was reduced (Fay 1982). Prior investigations of HTLP in walrus diets concluded

that seals and seabirds were the source of elevated trophic position based on stable isotope mixing models, but suggested this could also be contributions from predatory gastropods and crustaceans which were not adequately represented in the model (Seymour et al. 2014). There was a significant difference in $\delta^{15}N$ between males and females in the Bering Sea, which contradicts previous studies, although these studies were not assessing regional differences across the Pacific Arctic (Seymour et al. 2014, Clark et al. 2019a). Female walruses had a higher mean $\delta^{15}N$ than males (13.7 ± 0.8‰ versus 12.9 ± 0.8‰). Based on the observations of iPOC in benthic macrofauna in the Bering Sea, deposit feeding invertebrates had higher iPOC levels than suspension feeders (Koch et al. 2020a). The iPOC levels in predators and scavengers was potentially dependent on the date of sample collection relative to the ice algae bloom but overall had lower sea ice organic carbon levels than other benthic infauna. Therefore, the variable trophic positions are independent of iPOC values, which suggests foraging on a diversity of benthic invertebrates but still overall having higher mean iPOC values than males (i.e. foraging on more lipid-rich prey items). In 2012 and 2014, TP_{SPOM} were significantly different between the Chukchi and northern Bering Seas. Contrasting this with the sea ice organic carbon (Figs. 4-2 & 4-3), where there was no significant difference in 2012, supports our suggestion that sea ice organic carbon was higher in the Bering Sea during this cold year and/or lower in the Chukchi Sea during a record low sea ice year. The similar trophic positions and divergent patterns suggest there was a shift in the carbon sources at the base of the food web rather than a shift in prey choices.

4.5. Conclusions

There were limitations to this study owing to the opportunistic nature of our samples. Based on the variability observed from year-to-year and no clear annual trends, larger sample sizes with walruses sampled from the northern Bering and Chukchi seas in the same year

would be critical to unambiguously record the changes occurring in the region. Unfortunately, this was not possible with the available archived liver tissues. The available data do suggest there are differences in sea ice organic carbon components serving as food sources throughout the Pacific Arctic region and among the male and female cohorts of this population. Additionally, the lack of a clear relationship between sea ice organic carbon utilization and the satellite-based sea ice index could potentially be improved with a longer time series. Having demonstrated the proof of concept for this approach in walrus livers, coordinated sampling efforts in the future could be valuable in tracking the relationship between sea ice algae and Pacific walruses in response to declining seasonal sea ice.

Our study sought to reveal linkages between sea ice algae and Pacific walrus diets, as shifts in primary production driven by climate change will have cascading effects on the food web. HBI biomarkers revealed distinct differences in sea ice organic carbon among walruses sampled from 2012, 2014 and 2016 that varied among sex, region and season. Sea ice-derived organic carbon was higher in walruses from the Chukchi Sea during subsistence hunting activities in July through September than those harvested from St. Lawrence Island in the northern Bering Sea in April or early spring months. This regional distinction aligns with HBI data from walrus prey items (benthic macrofauna) and the general distribution of HBIs found in the surface sediments throughout the Pacific Arctic (Koch et al. 2020b). There was no significant difference between males and females in the Chukchi Sea, suggesting similar foraging behaviors of the migratory individuals during the summer and autumn. Females indicated greater uptake of ice-derived organic carbon than males in the northern Bering Sea, which may be due to females seeking out lipid-rich prey items and/or different foraging behavior (i.e. reduced foraging by males at this time of the year). Male walruses harvested from Bristol Bay in September displayed a near complete pelagic-based diet (i.e. minimal to

no sea ice-derived organic carbon), which is driven by the absence of sea ice for most of the year and potentially due to differences in prey selection/availability. The sympagic carbon estimates from Round Island in 1997 provide an end member comparison for the exclusively male haulout locations in Bristol Bay, as opposed to the male walruses that migrated into the Chukchi Sea. Sea ice organic carbon increased in both male and female Bering Sea walruses in 2012, which was a cold year in the Bering Sea with above-average sea ice persistence, and decreased in the Chukchi Sea, further supporting the connection between trophic transfer of HBIs and sea ice conditions. Future research on sea ice organic carbon utilization by age class in walruses is needed, but preliminary data suggest that walrus calves may have elevated sea ice organic carbon in their diets, perhaps driven by an enhanced requirement for lipid-rich prey to support their growth and development, or regional influences owing to their time spent foraging in the Chukchi Sea. Overall, we conclude there is a greater dependence on sea ice organic carbon by female Pacific walruses and possibly juveniles which may suggest they are particularly vulnerable as seasonal sea ice continues to diminish in this region.

4.6. Acknowledgements

We would like to thank the subsistence hunters from the communities of St. Lawrence Island, Diomede, Bristol Bay, and the North Slope for sharing the walrus tissues that formed the basis for this study. We thank Dr. Link Olsen and the staff at the University of Alaska Museum of the North for providing sampling support to obtain walrus samples from the Bering Strait communities. We thank Cédric Magen for providing stable isotope measurements. Discussions with Chad Jay from the US Geological Survey were instrumental in improving an earlier version of this manuscript. We recognize and appreciate the Savoonga

Tribal Council and elders for welcoming our team into the village to discuss our findings and share their traditional local knowledge of walrus foraging, mating and migratory behaviors.

5. Conclusion

5.1. Recommendations

5.1.1. Combining trophic markers

Overall, the findings of this work collectively support the further use of HBIs to track sea ice organic carbon flow through the food web and should be considered as a measurement in future Pacific Arctic ecosystem assessments. Yet as noted in Chapter 1, recent studies (Leu et al. 2020) have strongly recommended that pairing multiple trophic markers, including HBIs, is a better approach. There are circumstances in which HBIs will underperform (e.g. if the HBI-producing species is absent or environmental variables suppress its production). Yet their source specificity is highly valuable in confirming sympagic and pelagic sources. While I was able to apply the use of whole tissue, bulk stable isotope measurements in Chapter 4, the pairing of measurements of fatty acids, total lipid content and compound specific stable isotope analysis of amino acids or carbohydrates would likely be more insightful for future studies of Pacific walrus livers. In the end this approach with walruses (or other marine mammals and tissue types) could provide a more holistic assessment of walrus condition relative to declining sea ice. For example, HBIs could be a very useful, complementary measurement to the recent study assessing ribbon and spotted seal body condition in response to sea ice declines in the Pacific Arctic (Boveng et al. 2020). I have also initiated an exploratory project with Dr. Chadwick Jay and Dr. Sarah Sonsthagen (US Geological Survey) to compare the results of DNA metabarcoding clam gut contents collected at DBO 3 and 4 with HBI measurements from clams collected in the same grabs. Ideally, we will be able to identify a proportion of sympagic and pelagic diatoms from both approaches, based on genetic material and lipid content in *Macoma calcarea*.

5.1.2. HBI synthesis

The influence of environmental conditions on HBI synthesis is still an area of research that requires more attention. It was recently proposed that the *Z* (HBI III) and *E* (HBI IV – not shown in Fig. 1-1) isomers of the HBI trienes may have predictive capabilities for the spring pelagic phytoplankton bloom, as expressed in an equation termed HBI TR_{25} (Belt et al. 2019). The TR_{25} equation was initially tested in the Barents Sea and showed a strong correlation with the marginal ice zone. Yet, one of the first studies to try this model elsewhere, specifically in the Fram Strait and Baffin Bay, did not find such a relationship (Kolling et al. 2020). As outlined in Chapter 2, another study identified HBI III that is possibly synthesized within sea ice (Amiraux et al. 2019). The assumption that HBI III is synthesized in open waters or MIZs needs further verification. Despite these discrepancies, Kolling et al. (2020) found a good fit between all sea ice proxies discussed here, and the general distributions of IP_{25} and HBI II, relative to the ice edge and/or perennial ice cover, suggesting the strong sensitivity of these biomarkers to sea ice. Further work is also needed to better understand the role of nutrient dynamics and salinity on HBI synthesis, particularly in the Pacific Arctic region (Brown et al. 2020, Kolling et al. 2020).

5.2. Ongoing and future work

There are still ongoing efforts among the community of HBI researchers to determine the best performing sea ice proxy for paleoclimate sea ice reconstructions (Belt 2018, Kolling et al. 2020). This is especially relevant for calibrating modern sediments to the spring and/or summer sea ice concentrations (SpSIC and SuSIC). As noted in Chapter 1 and 2, the SpSIC equation proposed by Smik et al. (2016) was developed from data in the Barents Sea. The Pacific Arctic hydrography, nutrients, sea ice and productivity are quite different from the

Barents Sea and that equation may not be appropriate. The Barents Sea is influenced by the warm Atlantic inflow, as opposed to the Pacific inflow on the Chukchi Shelf – with an earlier retreat and lower persistence of seasonal sea ice. A Pacific-based SpSIC derived from the data in Chapter 2 needs to be tested on additional samples. The sea ice index P_BIP_{25} was investigated as part of this work, but was not included with the results published in Chapter 2. Some of these preliminary results (2012–2017) are presented here.

5.2.1. Preliminary results

The P_BIP_{25} results were in general agreement with the H-print data. The presence of ice algae in DBO 1 in 2015 is particularly clear, even when using brassicasterol. Further analysis of existing datasets from the St. Lawrence Island polynya in 2015 would be valuable to lend some insight into the conditions that allowed for these higher levels of IP_{25}.

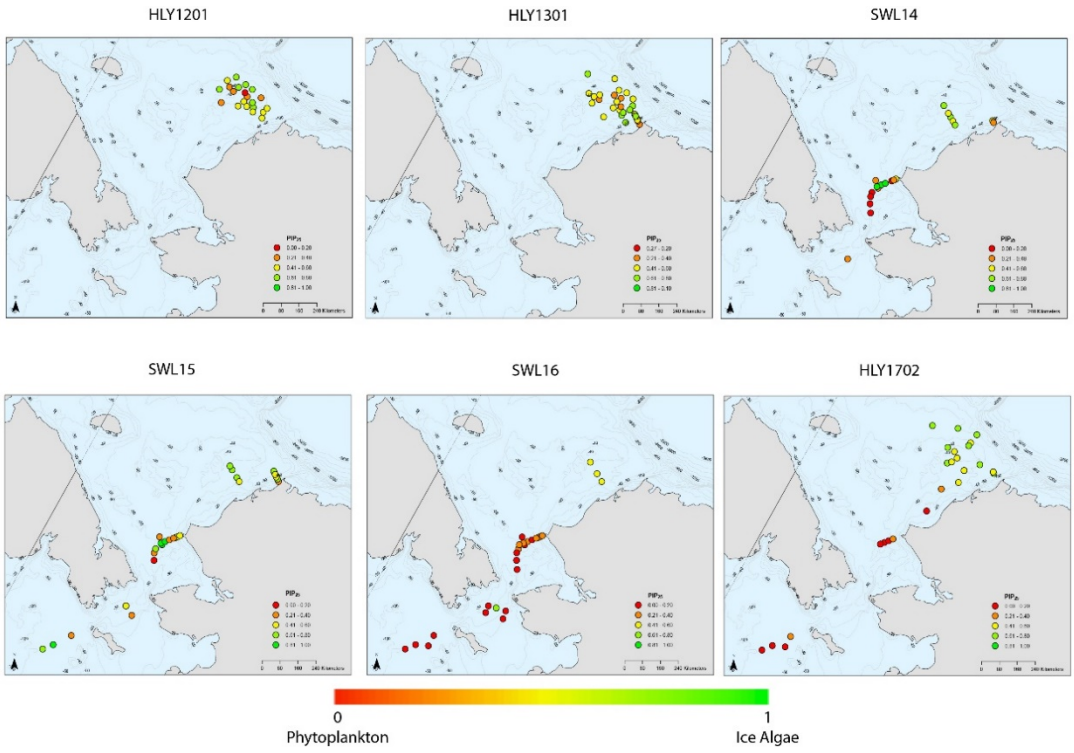

Figure 5-1 P_BIP_{25} index for 2012-2017 The sea ice index PIP_{25} was measured in surface sediments using brassicasterol and HBI III. Surface sediments were collected on the CCGC Sir Wilfrid Laurier (SWL) and the USCGC Healy (HLY). The cruise number signifies the year of samples collection (e.g. SWL15 in 2015, HLY1702 in 2017)

I also tested the effectiveness of each of the sea ice indexes (P_BIP_{25}, $P_{III}IP_{25}$, and H-print) for one year that spanned all DBO regions in 2016 (Fig. 5-2). For this particular dataset, the P_BIP_{25} index performed the best (R^2=0.60), followed by $P_{III}IP_{25}$ (R^2 = 0.41) and then H-print (R^2=0.38). I plan to test these various equations on other datasets and test other sample years using multiple linear regression to determine the most appropriate index and equation for this region.

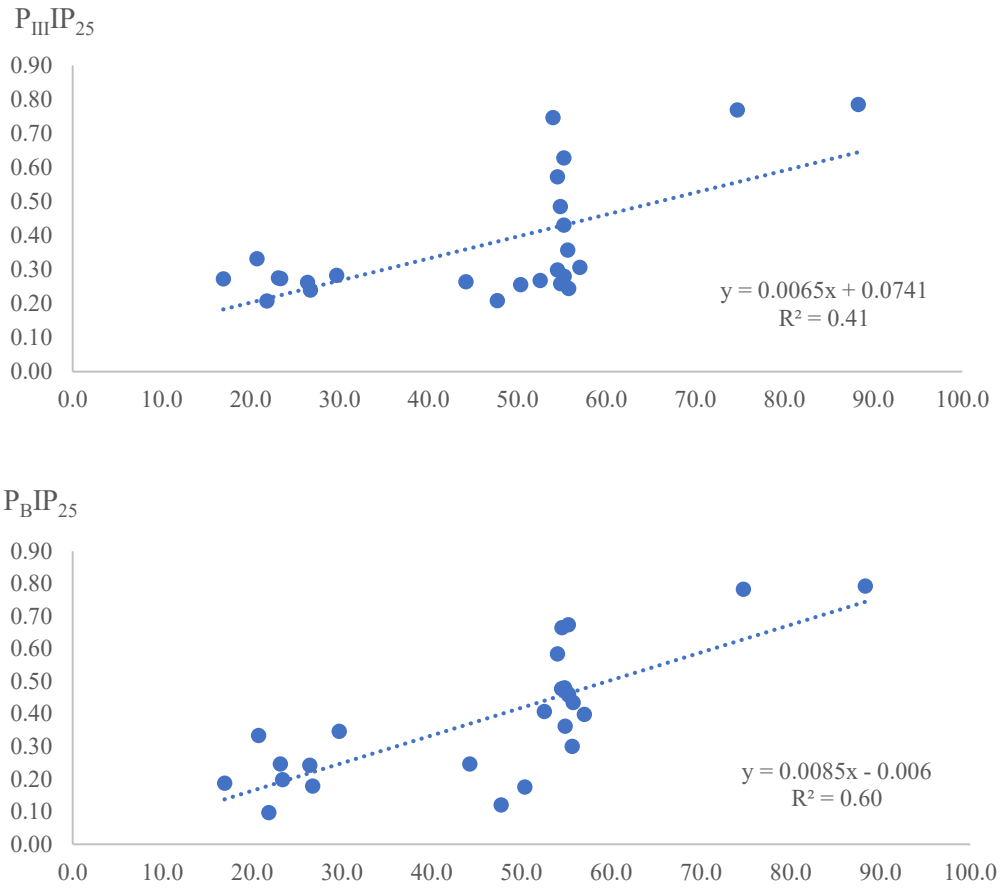

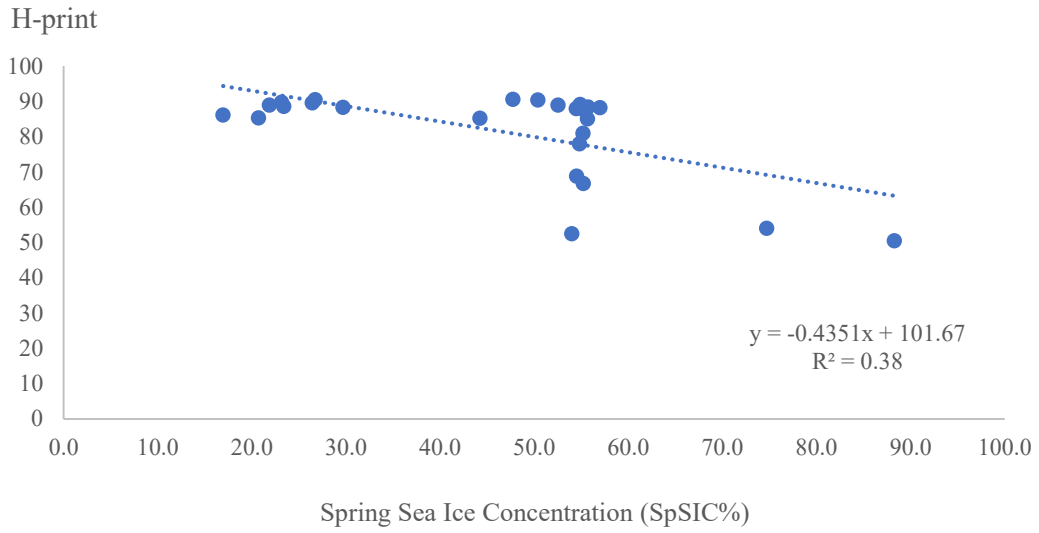

Figure 5-2 Comparison of sea ice indexes in 2016 The three primary versions of the sea ice index using IP_{25} were compared using surface sediments from 2016.

5.3. Ice-associated carbon fluxes

In Chapter 2, I examined ice-associated carbon fluxes in the northeast Chukchi Sea at the Chukchi Ecosystem Observatory (i.e. DBO 4) to inform our understanding of HBI distributions throughout the region. Sediment traps have also been deployed at DBO 2 and DBO 3, and very recently at DBO 1. Sediment traps from DBO 2 and DBO 3 from 2016-17 have been analyzed and will be presented in a future report documenting the succession of HBIs and diatoms in relation to the retreating ice edge. Analyzing overlapping HBI fluxes and diatom taxonomy from a single annual sea ice cycle along a latitudinal gradient from the northern Bering Sea to the northeast Chukchi Sea (DBO 1–4) would be a unique dataset following the ice edge north in a single season. Contemporaneous mooring deployments at all four DBO sites are not yet available. There are sediment trap samples available from DBO 2–4 for 2018–2019 and will be analyzed for HBIs in the future. This analysis has the potential to improve our interpretations of HBIs in marginal ice zones and particularly will refine HBI interpretations in the Pacific Arctic region.

Although this particular deployment will not overlap with other DBO region, it will still be valuable to measure HBIs at the new sediment trap location from DBO 1 [located at the M8 mooring; Stabeno et al. (2019)]. M8 is located at the site of a winter polynya (an area of persistent open water in otherwise ice-covered regions and can be highly productive due to an elevated nutrient supply) in the northern Bering Sea. Analyzing this material provides a unique opportunity to examine the impact of ice cover on particulate carbon fluxes in a region experiencing unprecedented changes in sea ice, benthic biomass, and carbon supply to the seafloor (Grebmeier et al. 2006b, Grebmeier 2012, Stabeno et al. 2019). In 2018 this polynya did not form due to record low winter sea ice extent and this likely impacted the vertical flux of material to the benthos (Grebmeier et al. 2018, Siddon et al. 2020). Given that this rapid change in ice-cover can be considered representative of future ice-free conditions, I plan to compare the Bering Sea mooring samples with those collected in the northeast Chukchi Sea, where sea ice persists throughout the growing season and is characterized by year-round export of ice algae. Using these data alongside a biogeochemical model with explicit representation of ice algae, I hope to predict how future changes in sea ice extent may impact the ice-associated flux rates in the western Arctic.

Supplemental Information

Supplemental figures

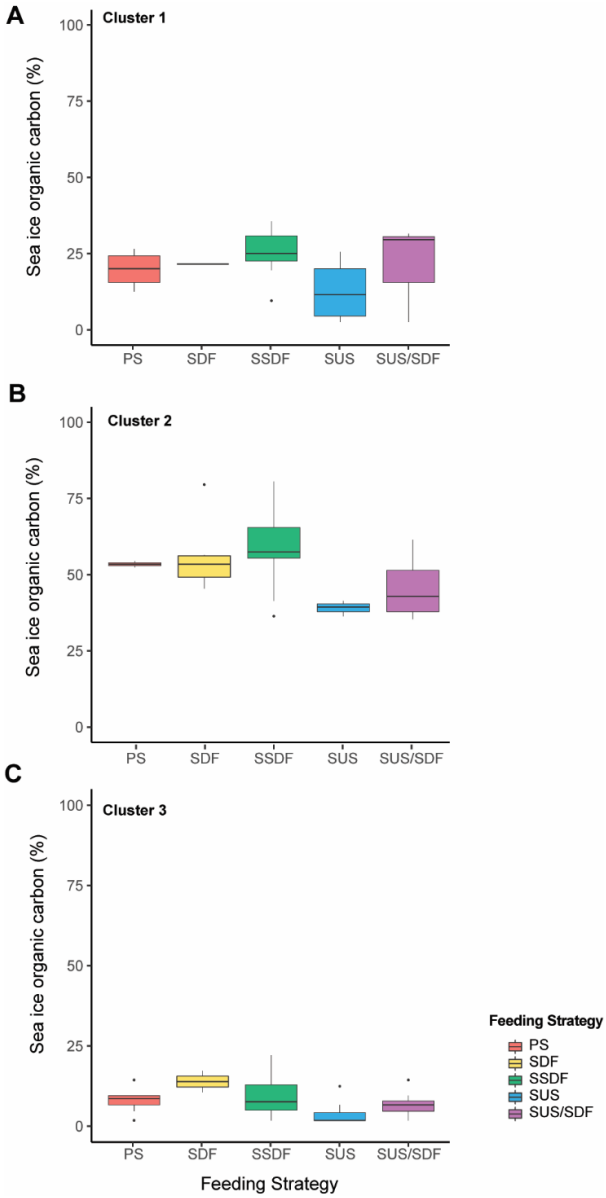

Figure S2-1 Boxplots of sea ice organic carbon (iPOC%) and feeding strategy by cluster A) Cluster 1, B) Cluster 2, C) Cluster 3. Boxes indicate the interquartile range from the first to third quartiles, with the median shown as the line within each box. The minimum and maximum points are indicated by the lines and outliers are shown as individual points.

Supplemental Tables

Table S-1 Surface sediment sample summary Summary of surface sediment sample station names and coordinates (latitude/longitude), dates and cruises collected, TOC (%), and HBI biomarker concentrations including IP_{25} (µg/g TOC), HBI II (µg/g TOC) and HBI III (µg/g TOC) along with H-print (%) values.

Station Name	Cruise	Date	Latitude (°N)	Longitude (°W)	TOC (%)	IP_{25} (µg/g TOC)	HBI III (µg/g TOC)	HBI II (µg/g TOC)	H-print (%)
CBL11	HLY12-01	8/13/2012	72.11	-165.43	0.84	2.3	5.7	10.0	59.5
H24	HLY12-01	8/13/2012	71.63	-164.79	0.35	5.0	10.5	21.7	55.6
H10	HLY12-01	8/14/2012	72.30	-164.25	1.17	2.1	2.4	9.5	40.1
H21	HLY12-01	8/14/2012	72.52	-164.73	1.72	2.5	10.2	11.1	70.5
H30	HLY12-01	8/14/2012	72.74	-163.67	1.61	2.7	4.2	11.3	48.5
H6	HLY12-01	8/16/2012	72.16	-163.60	0.74	3.8	6.6	16.7	50.3
H8	HLY12-01	8/16/2012	72.37	-163.07	0.92	5.2	6.2	21.1	42.5
H14	HLY12-01	8/17/2012	72.41	-161.25	1.59	2.2	4.0	8.8	53.0
H4	HLY12-01	8/17/2012	72.54	-162.25	1.02	3.6	6.7	14.9	53.3
H2	HLY12-01	8/18/2012	72.23	-162.12	0.25	2.0	3.2	9.0	48.3
H3	HLY12-01	8/18/2012	71.87	-162.03	0.55	5.3	6.2	23.1	40.8
H5	HLY12-01	8/18/2012	72.09	-161.74	0.31	2.9	2.1	12.8	29.6
H1	HLY12-01	8/19/2012	71.65	-162.63	1.05	3.5	6.7	16.3	52.1
H19	HLY12-01	8/19/2012	71.71	-161.55	1.13	2.5	3.4	10.0	45.5
H16	HLY12-01	8/20/2012	71.91	-160.93	0.67	5.9	16.8	25.2	63.2
H20	HLY12-01	8/20/2012	72.15	-159.95	1.01	2.0	2.5	8.1	43.2
H32	HLY12-01	8/21/2012	71.78	-158.99	1.36	3.2	3.6	11.9	42.4
H26/CBL14	HLY12-01	8/23/2012	71.37	-159.41	1.19	3.8	4.2	16.0	40.3
H38	HLY12-01	8/23/2012	71.61	-159.36	1.15	2.4	3.4	10.7	45.4
CBL15	HLY12-01	8/24/2012	71.72	-160.70	1.42	3.1	4.3	12.6	46.1
H37	HLY12-01	8/24/2012	71.55	-160.67	1.19	3.4	5.3	15.4	47.4
CBL11	HLY13-01	8/2/2013	72.10	-165.46	*NA*	*NA*	*NA*	*NA*	58.6
UTX1	HLY13-01	8/4/2013	72.06	-164.13	*NA*	*NA*	*NA*	*NA*	55.2
H17	HLY13-01	8/4/2013	71.99	-163.38	0.44	4.0	5.1	15.7	44.6
H7	HLY13-01	8/4/2013	72.12	-162.72	0.53	4.8	6.7	21.6	44.7

HS3	HLY13-01	8/5/2013	71.93	-162.67	0.46	3.9	5.6	17.8	45.1
UTX8	HLY13-01	8/5/2013	71.73	-163.46	0.45	4.5	5.7	21.6	41.5
CBL13	HLY13-01	8/6/2013	71.30	-161.69	1.48	3.3	5.9	14.9	50.9
H109	HLY13-01	8/7/2013	71.50	-159.51	1.30	4.2	5.2	16.5	44.1
H111	HLY13-01	8/7/2013	71.24	-158.89	1.38	3.3	4.6	17.4	42.1
H108	HLY13-01	8/7/2013	71.61	-159.38	1.29	3.4	3.8	14.2	40.5
BARC6	HLY13-01	8/8/2013	71.46	-157.58	1.62	2.4	6.8	14.1	57.7
BARC9	HLY13-01	8/8/2013	71.58	-157.84	1.05	3.4	4.4	14.9	43.5
BARC2	HLY13-01	8/8/2013	71.29	-157.25	0.69	1.8	3.5	12.5	45.4
BARC1	HLY13-01	8/8/2013	71.25	-157.17	0.45	2.2	2.8	15.7	34.7
BARC4	HLY13-01	8/8/2013	71.37	-157.42	0.41	2.8	6.5	18.0	51.3
BARC5	HLY13-01	8/8/2013	71.41	-157.50	1.65	2.1	5.3	13.6	53.2
BARC8	HLY13-01	8/8/2013	71.54	-157.75	1.25	4.8	6.2	22.6	42.0
CBL15	HLY13-01	8/9/2013	71.73	-160.72	1.16	3.0	3.5	11.9	42.0
BARC10	HLY13-01	8/9/2013	71.62	-157.93	1.01	3.8	4.5	14.9	42.8
H29	HLY13-01	8/9/2013	71.93	-158.33	1.28	3.3	0.5	11.9	9.7
H106	HLY13-01	8/9/2013	71.76	-158.60	1.40	3.2	3.5	12.4	41.3
H107	HLY13-01	8/10/2013	71.69	-159.87	1.28	3.0	3.4	12.9	40.6
H33	HLY13-01	8/10/2013	71.82	-159.77	1.12	2.0	1.9	7.0	39.4
H38	HLY13-01	8/10/2013	71.61	-159.36	*NA*	*NA*	*NA*	*NA*	37.4
H20	HLY13-01	8/10/2013	72.15	-159.95	1.28	2.9	4.4	12.3	47.3
H34	HLY13-01	8/11/2013	71.99	-160.40	0.59	3.8	2.9	17.8	29.8
H28	HLY13-01	8/11/2013	72.40	-159.35	1.40	3.8	3.7	13.4	39.5
H15	HLY13-01	8/11/2013	72.45	-160.38	1.43	2.1	2.7	7.9	45.2
H27	HLY13-01	8/11/2013	72.86	-161.22	1.12	4.6	5.6	20.6	41.6
H28	HLY13-01	8/11/2013	72.40	-159.35	1.40	2.8	3.3	11.0	42.8
H27	HLY13-01	8/11/2013	72.86	-161.22	1.12	4.6	5.6	21.7	40.8
H9	HLY13-01	8/11/2013	72.22	-160.87	0.44	5.6	5.1	23.9	35.4
H15	HLY13-01	8/11/2013	72.45	-160.38	1.43	2.3	1.8	7.9	35.2
H34	HLY13-01	8/11/2013	71.99	-160.40	0.59	5.7	5.1	21.4	36.9
H102	HLY13-01	8/13/2013	72.20	-158.41	1.25	5.5	3.7	17.7	32.3
H102	HLY13-01	8/13/2013	72.20	-158.41	1.25	5.1	3.5	20.4	29.8

UTBS2	SWL14	7/16/2014	64.68	-169.10	0.18	0.6	5.6	3.3	82.2
UTN1	SWL14	7/17/2014	66.71	-168.40	1.09	0.5	3.3	4.8	68.3
UTN7	SWL14	7/17/2014	68.00	-168.93	1.37	0.4	6.9	2.7	88.6
UTN4	SWL14	7/17/2014	67.50	-168.90	1.03	0.5	11.3	3.4	90.9
UTN2	SWL14	7/17/2014	67.05	-168.73	0.74	0.4	6.4	3.7	84.6
UTN6	SWL14	7/17/2014	67.74	-168.44	1.18	0.4	5.9	2.8	86.4
UTN3	SWL14	7/17/2014	67.33	-168.91	0.85	0.3	7.7	2.9	89.4
SEC6	SWL14	7/18/2014	68.19	-167.31	0.64	0.9	4.0	6.1	66.0
SEC8	SWL14	7/18/2014	68.30	-166.94	0.62	2.0	3.2	13.4	41.1
SEC7	SWL14	7/18/2014	68.24	-167.12	0.68	1.5	3.8	10.6	51.9
SEC3	SWL14	7/18/2014	67.90	-168.23	1.13	3.7	69.7	25.6	89.0
SEC4	SWL14	7/18/2014	68.01	-167.87	0.65	5.4	61.8	39.6	82.5
SEC2	SWL14	7/18/2014	67.78	-168.60	1.22	2.8	22.5	18.3	78.3
DBO4.3	SWL14	7/20/2014	71.23	-162.64	1.13	2.4	5.1	11.5	54.2
DBO4.2	SWL14	7/20/2014	71.10	-162.26	0.81	2.1	5.8	10.7	59.6
DBO4.1	SWL14	7/20/2014	70.97	-161.90	0.39	2.4	5.4	13.1	53.0
DBO4.6	SWL14	7/21/2014	71.62	-163.77	0.92	3.6	6.9	16.6	52.4
DBO4.5	SWL14	7/21/2014	71.49	-163.39	0.96	3.4	6.0	15.0	50.7
DBO4.4	SWL14	7/21/2014	71.36	-163.01	1.72	4.6	10.5	21.5	56.3
BARC3	SWL14	7/22/2014	71.33	-157.32	0.44	1.7	3.9	11.6	49.8
BARC4	SWL14	7/23/2014	71.36	-157.36	0.34	2.2	3.6	14.4	42.4
BARC5	SWL14	7/23/2014	71.40	-157.46	0.50	1.9	4.7	11.1	54.4
SLIP2	SWL15	7/14/2015	62.05	-175.21	1.18	4.0	89.3	16.3	93.3
SLIP3	SWL15	7/14/2015	62.39	-174.57	0.91	12.1	15.4	84.5	35.2
UTBS5	SWL15	7/15/2015	64.67	-169.92	0.26	0.6	8.7	7.3	80.1
SLIP4	SWL15	7/15/2015	63.03	-173.46	1.48	0.5	5.5	2.7	85.4
UTBS4	SWL15	7/16/2015	64.96	-169.89	0.32	0.3	4.6	2.0	87.3
UTBS2	SWL15	7/16/2015	64.68	-169.11	0.20	0.7	8.3	0.0	95.2
UTBS4	SWL15	7/16/2015	64.96	-169.89	0.20	0.8	14.0	5.4	88.6
SEC6	SWL15	7/17/2015	68.18	-167.31	0.45	11.0	71.5	76.0	73.6
UTN3	SWL15	7/17/2015	67.33	-168.94	0.66	0.5	11.3	3.6	90.2
UTN4	SWL15	7/17/2015	67.50	-168.94	0.96	2.5	63.6	23.4	89.6

SEC7	SWL15	7/17/2015	68.24	-167.12	0.61	1.3	1.3	8.1	31.9
SEC5	SWL15	7/17/2015	68.13	-167.50	0.40	0.7	1.4	4.7	46.8
UTN2	SWL15	7/17/2015	67.05	-168.73	0.57	0.6	14.2	4.8	90.2
SEC8	SWL15	7/17/2015	68.30	-166.94	*NA*	*NA*	*NA*	*NA*	31.6
UTN6	SWL15	7/18/2015	67.74	-168.44	0.96	3.1	67.4	24.4	89.4
SEC2	SWL15	7/18/2015	67.78	-168.60	1.09	3.5	65.2	22.9	89.3
UTN7	SWL15	7/18/2015	68.00	-168.94	0.97	0.4	6.5	2.5	88.2
SEC3	SWL15	7/18/2015	67.90	-168.23	0.83	6.7	100.8	38.2	88.1
SEC4	SWL15	7/18/2015	68.01	-167.87	0.32	1.0	1.2	3.6	44.0
DBO4.6	SWL15	7/19/2015	71.62	-163.79	0.65	5.6	1.4	23.1	13.4
DBO4.4	SWL15	7/19/2015	71.36	-163.03	1.47	3.6	2.1	18.0	23.8
DBO4.5	SWL15	7/19/2015	71.49	-163.41	0.76	3.0	0.7	11.2	13.1
BARC8	SWL15	7/20/2015	71.54	-157.75	1.22	3.1	5.0	14.2	47.9
BARC9	SWL15	7/20/2015	71.58	-157.83	0.99	3.0	3.9	12.6	43.9
DBO4.2	SWL15	7/20/2015	71.10	-162.27	0.79	2.3	2.4	11.0	36.6
BARC10	SWL15	7/20/2015	71.62	-157.91	1.09	3.5	1.0	15.0	15.1
DBO4.1	SWL15	7/20/2015	70.97	-161.90	0.27	2.2	1.0	11.9	19.3
BARC7	SWL15	7/20/2015	71.50	-157.67	1.49	2.6	4.1	12.7	46.4
BARC6	SWL15	7/21/2015	71.46	-157.58	1.47	2.2	4.2	11.1	51.0
BARC2	SWL15	7/21/2015	71.29	-157.25	0.58	7.8	144.5	51.2	89.2
BARC1	SWL15	7/21/2015	71.25	-157.16	1.30	0.6	0.7	5.5	29.4
BARC3	SWL15	7/21/2015	71.33	-157.33	0.29	2.3	1.3	15.2	20.5
BARC5	SWL15	7/21/2015	71.41	-157.49	0.63	2.8	0.9	14.5	15.1
BARC4	SWL15	7/21/2015	71.37	-157.41	0.41	2.4	3.8	16.7	40.3
SLIP5	SWL16	7/13/2016	62.56	-173.55	1.16	0.3	3.4	1.7	85.3
SLIP2	SWL16	7/13/2016	62.05	-175.21	1.07	0.4	6.3	2.0	89.8
SLIP3	SWL16	7/13/2016	62.39	-174.57	0.83	0.3	4.4	1.6	88.6
SLIP4	SWL16	7/13/2016	63.03	-173.46	1.32	0.1	1.6	0.8	86.1
UTBS5	SWL16	7/14/2016	64.67	-169.92	0.28	0.6	9.1	3.4	88.3
UTBS2	SWL16	7/14/2016	64.68	-169.10	0.17	0.5	8.2	3.1	88.4
UTBS2A	SWL16	7/14/2016	64.67	-168.24	0.17	0.4	9.4	2.9	90.5
DBO2.7	SWL16	7/14/2016	65.00	-168.22	0.33	0.4	8.7	3.5	88.9

UTBS1	SWL16	7/14/2016	64.99	-169.14	0.23	11.0	15.0	48.8	44.3
UTBS4	SWL16	7/15/2016	64.96	-169.89	0.29	0.7	12.2	4.0	89.6
UTN1	SWL16	7/15/2016	66.71	-168.40	0.43	0.6	10.2	5.6	85.2
UTN2	SWL16	7/15/2016	67.05	-168.73	0.64	0.4	10.4	3.2	90.6
UTN4	SWL16	7/16/2016	67.50	-168.91	0.80	0.4	6.2	2.2	88.9
UTN3	SWL16	7/16/2016	67.33	-168.95	0.69	0.1	1.9	0.5	90.4
SEC7	SWL16	7/16/2016	68.24	-167.12	0.56	1.8	8.3	10.8	68.8
SEC6	SWL16	7/16/2016	68.19	-167.31	0.54	1.2	8.0	6.2	78.0
SEC8	SWL16	7/16/2016	68.30	-166.94	0.38	2.6	5.6	13.9	52.5
SEC5	SWL16	7/16/2016	68.13	-167.49	0.53	1.3	10.7	7.0	81.0
UTN6	SWL16	7/17/2016	67.74	-168.43	0.99	0.4	6.4	2.3	89.1
SEC3	SWL16	7/17/2016	67.90	-168.23	0.81	0.4	7.0	2.8	88.4
SEC4	SWL16	7/17/2016	68.01	-167.86	0.31	1.3	14.2	7.1	85.0
SEC2	SWL16	7/17/2016	67.78	-168.60	1.00	0.5	7.9	3.3	87.7
UTN7	SWL16	7/17/2016	68.00	-168.93	0.79	0.4	6.1	2.2	88.2
SEC1/UTN 5	SWL16	7/17/2016	67.67	-168.96	0.94	0.5	7.4	2.9	87.9
DBO4.2	SWL16	7/18/2016	71.10	-162.26	0.63	2.3	7.7	11.8	63.8
DBO4.1	SWL16	7/18/2016	70.97	-161.90	0.35	2.3	8.5	11.5	66.7
DBO4.3	SWL16	7/19/2016	71.23	-162.64	0.95	3.9	7.3	15.5	54.0
DBO4.6	SWL16	7/20/2016	71.62	-163.78	0.65	3.8	6.6	16.7	50.5
DBO3.6	HLY17-02	8/29/2017	67.90	-168.23	0.47	1.2	40.1	7.4	93.9
DBO3.7	HLY17-02	8/29/2017	67.78	-168.60	0.54	1.0	31.3	6.2	93.6
DBO3.5	HLY17-02	8/29/2017	68.01	-167.88	0.26	1.0	25.0	6.6	91.8
DBO3.7	HLY17-02	8/29/2017	67.78	-168.60	0.54	1.1	33.6	7.5	93.0
DBO3.4-HAPS	HLY17-02	8/30/2017	68.13	-167.49	0.41	0.9	18.5	7.9	88.0
DBO3.4	HLY17-02	8/30/2017	68.13	-167.49	0.41	1.0	5.8	6.9	71.2
DBO4.1	HLY17-02	8/31/2017	70.97	-161.89	0.44	3.0	11.2	13.7	68.2
DBO4.6	HLY17-02	8/31/2017	71.62	-163.76	0.42	8.7	12.8	33.9	48.3
DBO5.10	HLY17-02	9/1/2017	71.62	-157.90	1.21	0.5	0.6	3.5	33.4
DBO5.9	HLY17-02	9/1/2017	71.58	-157.81	1.25	4.0	4.6	17.1	40.7
DBO5.10	HLY17-02	9/1/2017	71.62	-157.90	1.21	4.3	3.9	16.1	37.1
SW8	HLY17-02	9/2/2017	71.90	-162.68	1.05	4.4	5.1	16.4	43.1

SW6-HAPS	HLY17-02	9/2/2017	71.70	-163.26	0.97	6.2	8.3	23.8	46.2
W2	HLY17-02	9/3/2017	72.12	-163.20	0.77	4.5	8.6	16.3	56.1
W12	HLY17-02	9/3/2017	72.88	-166.85	1.79	4.0	5.4	14.0	47.9
W4	HLY17-02	9/3/2017	72.21	-164.17	0.70	3.4	6.0	11.2	55.3
NNE4	HLY17-02	9/4/2017	72.59	-161.35	1.43	2.9	5.1	10.3	54.4
NNE3	HLY17-02	9/4/2017	72.47	-161.55	1.46	5.0	9.9	19.0	56.1
NW1	HLY17-02	9/4/2017	73.04	-163.42	*NA*	*NA*	*NA*	*NA*	35.1
NW4	HLY17-02	9/4/2017	72.85	-163.18	1.51	4.2	4.5	14.8	42.3
NNE8	HLY17-02	9/5/2017	72.95	-160.75	1.48	3.6	4.3	12.5	45.0
E6	HLY17-02	9/8/2017	71.82	-159.70	1.13	3.9	3.7	12.8	40.1
S4	HLY17-02	9/10/2017	71.22	-161.30	1.05	2.1	3.9	8.8	53.0
S2 (CEO)	HLY17-02	9/10/2017	71.48	-161.52	1.41	4.0	5.7	17.2	46.0
S2-HAPS	HLY17-02	9/10/2017	71.48	-161.52	1.41	2.2	2.7	9.0	42.7
HAB2	HLY17-02	9/10/2017	70.57	-163.74	*NA*	*NA*	*NA*	*NA*	69.7
DBO1.8	HLY17-02	9/12/2017	63.02	-173.46	0.83	1.3	14.9	7.4	84.9
DBO1.4	HLY17-02	9/13/2017	62.39	-174.57	0.52	0.7	9.9	4.7	86.3
DBO1.6	HLY17-02	9/13/2017	62.56	-173.55	0.30	0.7	8.8	4.1	85.8
DBO1.2	HLY17-02	9/13/2017	62.04	-175.21	1.00	0.4	4.7	1.7	87.3

Table S-2 Pairwise comparison results for feeding strategy groupings Tukey honestly significant difference (HSD) test with Bonferroni correction for feeding type comparisons in the station groupings determined to be significant by ANOVA. Feeding strategies were classified as SUS (suspension), SUS/SDF (suspension/surface deposit), SDF (surface deposit), SSDF (subsurface deposit), and P/S (predator/scavenger). Significant p-values are denoted as less than 0.05 (*), 0.01 (**) and 0.001 (***).

DBO Region - Tukey HSD

DBO 3	**p**	**Icy Cape**	**p**	**DBO 4**	**p**	**DBO 5**	**p**
SDF-PS	**0.04 ***	SDF-PS	1	SDF-PS	1	SDF-PS	0.45
SSDF-PS	0.64	SSDF-PS	1	SSDF-PS	1	SSDF-PS	0.49
SUS-PS	0.93	SUS-PS	0.14	SUS-PS	0.63	SUS-PS	1

SUS/SDF-PS	1	SUS/SDF-PS	0.95	SUS/SDF-PS	0.72	SUS/SDF-PS	0.89
SSDF-SDF	0.15	SSDF-SDF	1	SSDF-SDF	1	SSDF-SDF	1
SUS-SDF	0.08	SUS-SDF	0.21	SUS-SDF	0.24	SUS-SDF	0.07
SUS/SDF-SDF	**0.03 ***	SUS/SDF-SDF	0.95	SUS/SDF-SDF	0.26	SUS/SDF-SDF	0.71
SUS-SSDF	0.96	**SUS-SSDF**	**0.04 ***	**SUS-SSDF**	**0.03 ***	**SUS-SSDF**	**0.05 ***
SUS/SDF-SSDF	0.52	SUS/SDF-SSDF	0.92	**SUS/SDF-SSDF**	**0.01 ***	SUS/SDF-SSDF	0.75
SUS/SDF-SUS	0.88	SUS/SDF-SUS	0.63	SUS/SDF-SUS	1	SUS/SDF-SUS	0.46

Clusters - Tukey HSD

Cluster 2	p	Cluster 3	p
SDF-PS	0.99	SDF-PS	0.38
SSDF-PS	0.96	SSDF-PS	0.99
SUS-PS	0.57	**SUS-PS**	**0.05 ***
SUS/SDF-PS	0.89	SUS/SDF-PS	0.87
SSDF-SDF	0.99	SSDF-SDF	0.46
SUS-SDF	0.17	**SUS-SDF**	**0.01 ****
SUS/SDF-SDF	0.38	SUS/SDF-SDF	0.10
SUS-SSDF	**0.03 ***	**SUS-SSDF**	**<0.001 *****
SUS/SDF-SSDF	**0.04 ***	SUS/SDF-SSDF	0.21
SUS/SDF-SUS	0.88	SUS/SDF-SUS	0.09

Table S-3 Pacific walrus sample collection data and analysis summary Supporting information for harvested Pacific walrus livers were supplied by hunters. Not all samples have supporting location, date, age class, etc. Analyses included iPOC (from HBI data), bulk stable isotopes of carbon and nitrogen, and trophic level using baseline values from published suspended particulate organic matter (SPOM), surface sediments (SS) and *Macoma calcarea* (MC; primary consumer) data.

Sample ID	Sex*	Age Class*	Date Collected*	Region	Location	iPOC (%)	$\delta^{13}C$ (‰)	$\delta^{15}N$ (‰)	TL SPOM	TL SS	TL MC
UAM:Mamm: 49567	male	unknown	9/24/1997	Bristol Bay	Round Island	0.82	-16.8	14.5	3.1	-	-
UAM:Mamm: 49566	male	unknown	9/24/1997	Bristol Bay	Round Island	-0.2	-15.8	14.5	3.1	-	-
UAM:Mamm: 49570	male	unknown	9/27/1997	Bristol Bay	Round Island	2.86	-16.1	14.4	3.1	-	-
UAM:Mamm: 49573	male	unknown	9/27/1997	Bristol Bay	Round Island	0.82	-16.8	14.3	3.0	-	-
UAM:Mamm: 49568	male	unknown	9/27/1997	Bristol Bay	Round Island	3.88	-16.3	15.3	3.3	-	-

UAM:Mamm: 49569	male	unknown	9/27/1997	Bristol Bay	Round Island	1.84	-16	15	3.2	-	-
UAM:Mamm: 49575	male	unknown	9/29/1997	Bristol Bay	Round Island	1.84	-17	13.9	2.9	-	-
UAM:Mamm: 49576	male	unknown	9/29/1997	Bristol Bay	Round Island	5.92	-16.3	14.3	3.0	-	-
UAM:Mamm: 49577	male	unknown	9/29/1997	Bristol Bay	Round Island	1.84	-16	14.5	3.1	-	-
UAM:Mamm: 49571	male	unknown	9/29/1997	Bristol Bay	Round Island	1.84	-16.1	15.3	3.3	-	-
UAM:Mamm: 49572	male	unknown	9/29/1997	Bristol Bay	Round Island	15.1	-16	15	3.2	-	-
UAM:Mamm: 49574	male	unknown	9/29/1997	Bristol Bay	Round Island	-0.2	-16.1	14.4	3.1	-	-
NSB:07w021	unknown	unknown	2008	Chukchi Sea	Utqiaġvik	72.22	-18.9	14.2	3.5	3.0	3.4
NSB:08w02	unknown	unknown	2008	Chukchi Sea	Utqiaġvik	74.26	-19.1	14.2	3.5	3.0	3.4
NSB:08W05	unknown	unknown	2008	Chukchi Sea	Utqiaġvik	46.72	-18.8	13.6	3.3	2.9	3.2
NSB:NSB-08-002	unknown	unknown	2008	Chukchi Sea	Utqiaġvik	74.26	-18.1	15.3	3.8	3.4	3.7
NSB:09WW3	unknown	unknown	2008	Chukchi Sea	Wainwright	55.9	-19.2	14.6	3.6	3.1	3.5
NSB:09W1	male	adult	7/11/2009	Chukchi Sea	Utqiaġvik	45.7	-19.5	17	4.3	3.9	4.2
NSB:09W2	female	adult	7/17/2009	Chukchi Sea	Utqiaġvik	54.88	-18.3	14.3	3.6	3.1	3.4
NSB:2010W2	unknown	unknown	2010	Chukchi Sea	Utqiaġvik	76.3	-18.5	14.2	3.5	3.0	3.4
NSB:2010W7	female	calf	9/30/2010	Chukchi Sea	Utqiaġvik	63.04	-21.2	15.3	3.8	3.4	3.7
NSB:2010W4	male	calf	7/17/2010	Chukchi Sea	Utqiaġvik	59.98	-18.5	15	3.8	3.3	3.6
NSB:2010W5	male	calf	9/30/2010	Chukchi Sea	Utqiaġvik	62.02	-20.1	16.7	4.3	3.8	4.1
NSB:2011W2	female	adult	8/6/2011	Chukchi Sea	Utqiaġvik	58.96	-19	13.3	3.3	2.8	3.1
NSB:2011W6	male	adult	2011	Chukchi Sea	Utqiaġvik	43.66	-18.6	15.4	3.9	3.4	3.8
NSB:2011W1	male	adult	6/28/2011	Chukchi Sea	Utqiaġvik	26.32	-20.7	15.7	4.0	3.5	3.9
NSB:2011W045	unknown	unknown	2011	Chukchi Sea	Utqiaġvik	12.04	-19	15.7	4.0	3.5	3.9
NSB:2012W2	male	adult	7/10/2012	Chukchi Sea	Utqiaġvik	43.66	-19.4	13.5	3.3	2.8	3.2
NSB:2012W1	male	adult	7/10/2012	Chukchi Sea	Utqiaġvik	32.44	-18.2	15	3.8	3.3	3.6
NSB:BRW_WALRUS12	male	adult	7/31/2012	Chukchi Sea	Utqiaġvik	29.38	-19.3	13.8	3.4	2.9	3.3
NSB:2012W04	female	adult	7/10/2012	Chukchi Sea	Utqiaġvik	32.44	-18.3	14.7	3.7	3.2	3.6
NSB:2012W06	female	calf	8/3/2012	Chukchi Sea	Utqiaġvik	22.24	-18.7	16.1	4.1	3.6	4.0
NSB:2012W03	female	adult	7/10/2012	Chukchi Sea	Utqiaġvik	37.54	-19.1	14	3.5	3.0	3.4
NSB:2012WWW1	female	calf	6/24/2012	Chukchi Sea	Wainwright	43.66	-20.6	15.8	4.0	3.5	3.9

NSB:2012WWW2	female	adult	6/24/2012	Chukchi Sea	Wainwright	43.66	-18.5	14.3	3.6	3.1	3.4
NSB:2013W27	female	adult	7/26/2013	Chukchi Sea	Utqiaġvik	61	-18.7	13.9	3.4	2.9	3.3
NSB:WALRUS34	female	calf	10/3/2014	Chukchi Sea	Point Lay	75.28	-20.2	15.9	4.0	3.5	3.9
NSB:WALRUS29	male	calf	10/3/2014	Chukchi Sea	Point Lay	66.1	-19	15	3.8	3.3	3.6
NSB:WALRUS22	male	calf	10/3/2014	Chukchi Sea	Point Lay	71.2	-18.5	16.9	4.3	3.8	4.2
NSB:WALRUS31	male	calf	10/3/2014	Chukchi Sea	Point Lay	95.68	-19.1	16.3	4.1	3.6	4.0
NSB:WALRUS32	male	calf	10/3/2014	Chukchi Sea	Point Lay	81.4	-18.8	15.5	3.9	3.4	3.8
NSB:2014W23	male	adult	7/12/2014	Chukchi Sea	Peard Bay	40.6	-19.8	13.8	3.4	2.9	3.3
NSB:2014W25	female	adult	7/12/2014	Chukchi Sea	Peard Bay	65.08	-18.3	13.9	3.4	2.9	3.3
NSB:2014W24	female	adult	7/12/2014	Chukchi Sea	Peard Bay	49.78	-18.9	14.3	3.6	3.1	3.4
UAM:Mamm:116521	female	adult	5/18/2012	Northern Bering	Gambell	57.94	-18.2	13.4	2.4	2.4	3.0
UAM:Mamm:131798	female	adult	5/14/2016	Northern Bering	Savoonga	29.38	-13.2	12.8	2.2	2.2	2.9
UAM:Mamm:125304	male	adult	5/18/2012	Northern Bering	Savoonga	35.5	-18	11.9	1.9	1.9	2.6
UAM:Mamm:99973	unknown	calf	5/13/2003	Northern Bering	Savoonga	25.3	-16.4	15.5	3.0	3.0	3.6
UAM:Mamm:131800	male	calf	5/13/2014	Northern Bering	Savoonga	26.32	-17.7	13.1	2.3	2.3	2.9
UAM:Mamm:84825	female	unknown	5/1/2002	Northern Bering	Diomede	6.94	-16.6	14	2.5	2.6	3.2
UAM:Mamm:84828	female	unknown	5/1/2002	Northern Bering	Diomede	7.96	-17	15	2.8	2.9	3.5
UAM:Mamm:101094	female	adult	5/19/2002	Northern Bering	Savoonga	29.38	-17.3	13.8	2.5	2.5	3.1
UAM:Mamm:99972	female	adult	5/13/2003	Northern Bering	Savoonga	46.72	-16.6	12.7	2.1	2.2	2.8
UAM:Mamm:99990	female	adult	5/17/2003	Northern Bering	Gambell	44.68	-16	13.1	2.3	2.3	2.9
UAM:Mamm:99989	female	adult	5/17/2003	Northern Bering	Gambell	48.76	-16.5	13	2.2	2.3	2.9
UAM:Mamm:97942	male	adult	5/1/2004	Northern Bering	Diomede	3.88	-17.1	14.6	2.7	2.7	3.4
UAM:Mamm:97916	female	adult	5/1/2004	Northern Bering	Diomede	16.12	-17.8	14.2	2.6	2.6	3.3
UAM:Mamm:97936	male	adult	5/1/2004	Northern Bering	Diomede	0.82	-17.5	14.9	2.8	2.8	3.5
UAM:Mamm:101343	female	unknown	5/19/2005	Northern Bering	no specific locality recorded	39.58	-17	13.5	2.4	2.4	3.1

UAM:Mamm: 101376	female	unknown	5/19/2005	Northern Bering	no specific locality recorded	41.62	-17.1	13.4	2.4	2.4	3.0
UAM:Mamm: 101374	female	unknown	5/19/2005	Northern Bering	no specific locality recorded	17.14	-19.3	14.6	2.7	2.7	3.4
UAM:Mamm: 116559	female	unknown	5/8/2012	Northern Bering	Gambell	20.2	-18.1	12.6	2.1	2.1	2.8
UAM:Mamm: 116520	female	unknown	5/9/2012	Northern Bering	Gambell	33.46	-17	12.4	2.1	2.1	2.7
UAM:Mamm: 116495	female	unknown	5/12/2012	Northern Bering	Gambell	36.52	-18.3	12.2	2.0	2.0	2.7
UAM:Mamm: 117033	female	unknown	5/13/2012	Northern Bering	Gambell	39.58	-16.6	13	2.2	2.3	2.9
UAM:Mamm: 116679	female	unknown	5/13/2012	Northern Bering	Gambell	22.24	-18.8	13.4	2.4	2.4	3.0
UAM:Mamm: 116519	female	unknown	5/13/2012	Northern Bering	Gambell	73.24	-18.8	13	2.2	2.3	2.9
UAM:Mamm: 116372	female	unknown	5/13/2012	Northern Bering	Gambell	40.6	-18.4	13.6	2.4	2.4	3.1
UAM:Mamm: 116445	female	unknown	5/13/2012	Northern Bering	Gambell	53.86	-18.3	13.7	2.4	2.5	3.1
UAM:Mamm: 116748	female	unknown	5/13/2012	Northern Bering	Gambell	17.14	-18.8	12.8	2.2	2.2	2.9
UAM:Mamm: 116478	female	unknown	5/13/2012	Northern Bering	Gambell	35.5	-17.6	14.5	2.7	2.7	3.4
UAM:Mamm: 116663	male	unknown	5/17/2012	Northern Bering	Savoonga	29.38	-17.9	13.1	2.3	2.3	2.9
UAM:Mamm: 116581	female	unknown	5/17/2012	Northern Bering	Gambell	63.04	-19	13.8	2.5	2.5	3.1
UAM:Mamm: 116497	female	unknown	5/17/2012	Northern Bering	Gambell	35.5	-18.7	12.6	2.1	2.1	2.8
UAM:Mamm: 116637	male	unknown	5/17/2012	Northern Bering	Savoonga	21.22	-17.8	12.7	2.1	2.2	2.8
UAM:Mamm: 116465	female	unknown	5/18/2012	Northern Bering	Savoonga	25.3	-18.2	12.9	2.2	2.2	2.9
UAM:Mamm: 116446	female	unknown	5/18/2012	Northern Bering	Gambell	42.64	-17.8	14.5	2.7	2.7	3.4
UAM:Mamm: 116487	male	unknown	5/18/2012	Northern Bering	Diomede	7.96	-17.1	13.6	2.4	2.4	3.1
UAM:Mamm: 116616	male	unknown	5/18/2012	Northern Bering	Diomede	14.08	-17.8	12.7	2.1	2.2	2.8
UAM:Mamm: 116498	female	unknown	5/18/2012	Northern Bering	Savoonga	48.76	-19.5	12.9	2.2	2.2	2.9
UAM:Mamm: 116339	female	unknown	5/18/2012	Northern Bering	Savoonga	69.16	-17.6	13.2	2.3	2.3	3.0
UAM:Mamm: 116615	male	unknown	5/18/2012	Northern Bering	Gambell	2.86	-17.6	15.2	2.9	2.9	3.6
UAM:Mamm: 116462	female	unknown	5/18/2012	Northern Bering	Gambell	49.78	-17.6	13.6	2.4	2.4	3.1
UAM:Mamm: 116749	female	unknown	5/18/2012	Northern Bering	Gambell	55.9	-18.7	13.1	2.3	2.3	2.9

UAM:Mamm: 116560	male	unknown	5/18/2012	Northern Bering	Hooper Bay	14.08	-18.6	15.3	2.9	2.9	3.6
UAM:Mamm: 116648	male	unknown	5/18/2012	Northern Bering	Savoonga	3.88	-18	12.9	2.2	2.2	2.9
UAM:Mamm: 116562	female	unknown	5/18/2012	Northern Bering	Hooper Bay	4.9	-18.3	15.2	2.9	2.9	3.6
UAM:Mamm: 117085	male	unknown	5/19/2012	Northern Bering	Savoonga	12.04	-18.4	12.3	2.0	2.1	2.7
UAM:Mamm: 116747	male	unknown	5/19/2012	Northern Bering	Savoonga	31.42	-18	12.6	2.1	2.1	2.8
UAM:Mamm: 116511	female	unknown	5/19/2012	Northern Bering	Savoonga	58.96	-19.7	13.5	2.4	2.4	3.1
UAM:Mamm: 116662	female	unknown	5/20/2012	Northern Bering	Savoonga	62.02	-18.1	13.8	2.5	2.5	3.1
UAM:Mamm: 125311	male	adult	5/3/2014	Northern Bering	Savoonga	25.3	-18.1	12.9	2.2	2.2	2.9
UAM:Mamm: 125305	male	adult	5/3/2014	Northern Bering	Savoonga	50.8	-17.6	12.3	2.0	2.1	2.7
UAM:Mamm: 125290	male	adult	5/4/2014	Northern Bering	Gambell	63.04	-17.6	13.1	2.3	2.3	2.9
UAM:Mamm: 125307	male	unknown	5/4/2014	Northern Bering	Savoonga	43.66	-17.8	12.5	2.1	2.1	2.8
UAM:Mamm: 125314	male	calf	5/4/2014	Northern Bering	Savoonga	29.38	-18.5	13.1	2.3	2.3	2.9
UAM:Mamm: 125322	male	unknown	5/4/2014	Northern Bering	Savoonga	36.52	-17.9	13.6	2.4	2.4	3.1
UAM:Mamm: 125328	female	unknown	5/4/2014	Northern Bering	Savoonga	65.08	-18.1	14.1	2.6	2.6	3.2
UAM:Mamm: 125291	female	adult	5/4/2014	Northern Bering	Gambell	58.96	-18	14.3	2.6	2.6	3.3
UAM:Mamm: 125292	female	adult	5/4/2014	Northern Bering	Gambell	70.18	-18.7	14.2	2.6	2.6	3.3
UAM:Mamm: 125324	male	adult	5/4/2014	Northern Bering	Savoonga	61	-17.9	13	2.2	2.3	2.9
UAM:Mamm: 125325	male	adult	5/4/2014	Northern Bering	Savoonga	29.38	-17.4	13.1	2.3	2.3	2.9
UAM:Mamm: 125327	male	adult	5/4/2014	Northern Bering	Savoonga	29.38	-17.8	13.4	2.4	2.4	3.0
UAM:Mamm: 125321	male	unknown	5/4/2014	Northern Bering	Savoonga	17.14	-17.4	12.4	2.1	2.1	2.7
UAM:Mamm: 125288	male	adult	5/4/2014	Northern Bering	Gambell	57.94	-18.8	13	2.2	2.3	2.9
UAM:Mamm: 125293	female	adult	5/4/2014	Northern Bering	Gambell	61	-19.7	13.8	2.5	2.5	3.1
UAM:Mamm: 125323	male	adult	5/4/2014	Northern Bering	Savoonga	23.26	-18.1	12.5	2.1	2.1	2.8
UAM:Mamm: 125319	male	adult	5/11/2014	Northern Bering	Savoonga	55.9	-18.3	13.3	2.3	2.4	3.0
UAM:Mamm: 125309	unknown	adult	5/16/2014	Northern Bering	Savoonga	44.68	-18.4	13.3	2.3	2.4	3.0
UAM:Mamm: 125330	male	adult	5/16/2014	Northern Bering	Savoonga	49.78	-18.1	12.8	2.2	2.2	2.9

UAM:Mamm: 125301	male	adult	5/16/2014	Northern Bering	Savoonga	36.52	-17.9	12.7	2.1	2.2	2.8
UAM:Mamm: 125317	male	unknown	5/16/2014	Northern Bering	Savoonga	40.6	-18.4	13.2	2.3	2.3	3.0
UAM:Mamm: 125289	female	adult	5/17/2014	Northern Bering	Gambell	79.36	-19.3	13.1	2.3	2.3	2.9
UAM:Mamm: 125316	male	adult	5/22/2014	Northern Bering	Savoonga	50.8	-17.7	11.9	1.9	1.9	2.6
UAM:Mamm: 125310	male	adult	5/22/2014	Northern Bering	Savoonga	17.14	-17.4	12.2	2.0	2.0	2.7
UAM:Mamm: 125312	male	unknown	5/22/2014	Northern Bering	Savoonga	10	-17.8	13.2	2.3	2.3	3.0
UAM:Mamm: 125318	male	adult	5/22/2014	Northern Bering	Savoonga	58.96	-17.1	12.2	2.0	2.0	2.7
UAM:Mamm: 125320	male	adult	5/22/2014	Northern Bering	Savoonga	55.9	-18.3	13	2.2	2.3	2.9
UAM:Mamm: 125302	male	calf	5/22/2014	Northern Bering	Savoonga	36.52	-16.8	12.9	2.2	2.2	2.9
UAM:Mamm: 125308	male	adult	5/22/2014	Northern Bering	Savoonga	44.68	-17.4	12.3	2.0	2.1	2.7
UAM:Mamm: 125306	female	unknown	5/22/2014	Northern Bering	Savoonga	72.22	-16.6	13.5	2.4	2.4	3.1
UAM:Mamm: 125287	female	unknown	5/25/2014	Northern Bering	Gambell	46.72	-15.3	12.4	2.1	2.1	2.7
UAM:Mamm: 131795	male	adult	5/10/2015	Northern Bering	Savoonga	24.28	-17.9	13	2.2	2.3	2.9
UAM:Mamm: 131818	female	adult	4/20/2016	Northern Bering	Gambell	35.5	-18.9	14	2.5	2.6	3.2
UAM:Mamm: 131822	female	adult	4/20/2016	Northern Bering	Gambell	76.3	-18	15.6	3.0	3.0	3.7
UAM:Mamm: 131819	female	adult	4/20/2016	Northern Bering	Gambell	72.22	-18.8	14.5	2.7	2.7	3.4
UAM:Mamm: 131821	female	adult	4/20/2016	Northern Bering	Gambell	45.7	-19.5	13.9	2.5	2.5	3.2
UAM:Mamm: 131817	female	adult	4/21/2016	Northern Bering	Gambell	36.52	-19.3	14.1	2.6	2.6	3.2
UAM:Mamm: 131816	female	adult	4/29/2016	Northern Bering	Gambell	57.94	-17.9	13.5	2.4	2.4	3.1
UAM:Mamm: 131806	male	adult	5/11/2016	Northern Bering	Savoonga	8.98	-18.1	12.7	2.1	2.2	2.8
UAM:Mamm: 131799	male	adult	5/11/2016	Northern Bering	Savoonga	27.34	-17.8	13	2.2	2.3	2.9
UAM:Mamm: 131804	male	adult	5/11/2016	Northern Bering	Savoonga	55.9	-18.2	12.7	2.1	2.2	2.8
UAM:Mamm: 131803	male	adult	5/11/2016	Northern Bering	Savoonga	16.12	-17.8	13.4	2.4	2.4	3.0
UAM:Mamm: 131824	female	adult	5/12/2016	Northern Bering	Gambell	28.36	-17.7	14.7	2.7	2.8	3.4
UAM:Mamm: 131823	female	adult	5/12/2016	Northern Bering	Gambell	37.54	-18.4	15	2.8	2.9	3.5
UAM:Mamm: 131820	female	calf	5/13/2016	Northern Bering	Gambell	25.3	-17.7	15.1	2.9	2.9	3.5

UAM:Mamm: 131814	female	adult	5/13/2016	Northern Bering	Gambell	37.54	-18	14.1	2.6	2.6	3.2
UAM:Mamm: 131796	male	adult	5/14/2016	Northern Bering	Savoonga	16.12	-18.5	12.5	2.1	2.1	2.8
UAM:Mamm: 131805	male	adult	5/14/2016	Northern Bering	Savoonga	25.3	-18.8	13.2	2.3	2.3	3.0
UAM:Mamm: 131808	male	adult	5/14/2016	Northern Bering	Savoonga	20.2	-18.7	12.5	2.1	2.1	2.8
UAM:Mamm: 131807	male	adult	5/14/2016	Northern Bering	Savoonga	18.16	-18.5	12.5	2.1	2.1	2.8
UAM:Mamm: 131809	male	adult	5/14/2016	Northern Bering	Savoonga	18.16	-17.6	12.4	2.1	2.1	2.7
UAM:Mamm: 131797	male	adult	5/14/2016	Northern Bering	Savoonga	28.36	-17.8	12.4	2.1	2.1	2.7
UAM:Mamm: 131802	male	adult	5/20/2016	Northern Bering	Savoonga	24.28	-17.8	12.4	2.1	2.1	2.7
UAM:Mamm: 131810	male	adult	5/20/2016	Northern Bering	Savoonga	23.26	-18.1	13.6	2.4	2.4	3.1
UAM:Mamm: 131811	male	adult	5/20/2016	Northern Bering	Savoonga	34.48	-18.3	13.5	2.4	2.4	3.1
UAM:Mamm: 125315	female	adult	5/6/2014	Northern Bering	Savoonga	31.42	-18.2	13.4	2.4	2.4	3.0
UAM:Mamm: 116496	female	unknown	5/18/2012	Northern Bering	Gambell	31.42	-13.2	12.8	2.2	2.2	2.9
UAM:Mamm: 131801	male	calf	5/14/2016	Northern Bering	Savoonga	23.26	-18	11.9	1.9	1.9	2.6
UAM:Mamm: 131813	female	adult	5/14/2016	Northern Bering	Savoonga	17.14	-16.4	15.5	3.0	3.0	3.6
UAM:Mamm: 131815	female	adult	5/14/2016	Northern Bering	Gambell	34.48	-17.7	13.1	2.3	2.3	2.9
*Samples with unknown sex, age class, or specific date were only used for broad comparisons among regions.											

Method for phytoplankton sterol extraction

Prior to the lipid extraction (see Chapter 2) of surface sediments collected in 2012-2019, 10 µL of 0.01 mg mL^{-1} cholesterol-d6 and 5α-androstan-3β-ol was added as internal standards for sterol quantification. Once the HBIs were eluted during the open column chromatography, I moved the column to a clean vial to elute the polar sterols retained in the column using a methanol rinse, which was repeated three times. The extracts were then dried under a gentle nitrogen stream. Once dried, 50 µL of DCM was added twice to the vial and transferred by syringe into a GC vial. Prior to analysis, 25 µL of BSTFA was added to

derivatize the sterols and placed on a heating block at 70°C for one hour. Sterols were analyzed using an Agilent 7890A coupled to a 5975 series mass selective detector (MSD) with an Agilent DB5-ms column (30 m x 0.25 mm x 0.25 μm). Sample injection (1 μL) was run in splitless mode and helium was used as carrier gas. The GC oven was programmed to heat from 60°C to 150°C at 15°C min^{-1}, then at 3°C min^{-1} to 320°C and held for 20 minutes. brassicasterol (24-methylcholesta-5,22E-dien-3β-ol), dinosterol (4α,23,24-trimethyl-5α-cholest-22E-en-3β-ol), and cholesterol-d6 were identified based on their retention times relative to a standard for *n*-alkanes in selective ion monitoring mode. Molecular ions *m/z* 470, *m/z* 500 and *m/z* 464 were used to identify these compounds, respectively.

Bibliography

Aagaard K, Roach A (1990) Arctic ocean-shelf exchange: Measurements in Barrow Canyon. Journal of Geophysical Research: Oceans 95:18163-18175. https://doi.org/10.1029/JC095iC10p18163

Aguilar-Islas AM, Rember RD, Mordy CW, Wu J (2008) Sea ice-derived dissolved iron and its potential influence on the spring algal bloom in the Bering Sea. Geophysical Research Letters 35. https://doi.org/10.1029/2008GL035736

Allard WG, Belt ST, Massé G, Naumann R, Robert J-M, Rowland S (2001) Tetra-unsaturated sesterterpenoids (Haslenes) from *Haslea ostrearia* and related species. Phytochemistry 56:795-800. https://doi.org/10.1016/S0031-9422(00)00429-5

Ambrose W, Clough L, Tilney P, Beer L (2001) Role of echinoderms in benthic remineralization in the Chukchi Sea. Marine Biology 139:937-949. https://doi.org/10.1007/s002270100652

Amiraux R, Archambault P, Moriceau B, Lemire M, Babin M, Memery L, Massé G, Tremblay J-E (2021) Efficiency of sympagic-benthic coupling revealed by analyses of n-3 fatty acids, IP_{25} and other highly branched isoprenoids in two filter-feeding Arctic benthic molluscs: *Mya truncata* and *Serripes groenlandicus*. Organic Geochemistry 151:104160. https://doi.org/10.1016/j.orggeochem.2020.104160

Amiraux R, Belt ST, Vaultier F, Galindo V, Gosselin M, Bonin P, Rontani J-F (2017) Monitoring photo-oxidative and salinity-induced bacterial stress in the Canadian Arctic using specific lipid tracers. Marine Chemistry 194:89-99. http://dx.doi.org/10.1016/j.marchem.2017.05.006

Amiraux R, Smik L, Köseoğlu D, Rontani J-F, Galindo V, Grondin P-L, Babin M, Belt ST (2019) Temporal evolution of IP_{25} and other highly branched isoprenoid lipids in sea ice and the underlying water column during an Arctic melting season. Elementa: Science of the Anthropocene, 7:38. http://doi.org/10.1525/elementa.377

Ardyna M, Mundy CJ, Mayot N, Matthes LC, Oziel L, Horvat C, Leu E, Assmy P, Hill V, Matrai PA, Gale M, Melnikov IA, Arrigo KR (2020) Under-Ice Phytoplankton Blooms: Shedding Light on the "Invisible" Part of Arctic Primary Production. Frontiers in Marine Science 7. https://doi.org/10.3389/fmars.2020.608032

Armand, L., Ferry, A. and Leventer, A. (2017). Advances in palaeo sea ice estimation. In Sea Ice, D.N. Thomas (Ed.). https://doi.org/10.1002/9781118778371.ch26

Arndt CE, Swadling KM (2006) Crustacea in Arctic and Antarctic sea ice: distribution, diet and life history strategies. Advances in Marine Biology 51:197-315. https://doi.org/10.1016/S0065-2881(06)51004-1

Arrigo KR (2014) Sea ice ecosystems. Annual Reviews in Marine Science 6:439-467. https://doi.org/10.1146/annurev-marine-010213-135103

Arrigo, K.R. (2017). Sea ice as a habitat for primary producers. In Sea Ice, D.N. Thomas (Ed.). https://doi.org/10.1002/9781118778371.ch14

Arrigo KR, and Gert L. van Dijken (2015) Continued increases in Arctic Ocean primary production. Progress in Oceanography 136:60-70. https://doi.org/10.1016/j.pocean.2015.05.002

Arrigo KR, Perovich DK, Pickart RS, Brown ZW, Van Dijken GL, Lowry KE, Mills MM, Palmer MA, Balch WM, Bahr F (2012) Massive phytoplankton blooms under Arctic sea ice. Science 336:1408-1408. https://doi.org/10.1126/science.1215065

Arrigo KR, Perovich DK, Pickart RS, Brown ZW, van Dijken GL, Lowry KE, Mills MM, Palmer MA, Balch WM, Bates NR, Benitez-Nelson CR, Brownlee E, Frey KE, Laney SR, Mathis J, Matsuoka A, Greg Mitchell B, Moore GWK, Reynolds RA,

Sosik HM, Swift JH (2014) Phytoplankton blooms beneath the sea ice in the Chukchi sea. Deep Sea Research Part II: Topical Studies in Oceanography 105:1-16. https://doi.org/10.1016/j.dsr2.2014.03.018

Arrigo KR, van Dijken G, Pabi S (2008) Impact of a shrinking Arctic ice cover on marine primary production. Geophysical Research Letters 35. https://doi.org/10.1029/2008gl035028

Arrigo KR, van Dijken GL (2015) Continued increases in Arctic Ocean primary production. Progress in Oceanography 136:60-70. https://doi.org/10.1016/j.pocean.2015.05.002

Assmy P, Ehn JK, Fernández-Méndez M, Hop H, Katlein C, Sundfjord A, Bluhm K, Daase M, Engel A, Fransson A, Granskog MA, Hudson SR, Kristiansen S, Nicolaus M, Peeken I, Renner AHH, Spreen G, Tatarek A, Wiktor J (2013) Floating ice-algal aggregates below melting Arctic sea ice. PLOS ONE 8:e76599. https://doi.org/10.1371/journal.pone.0076599

Assmy P, Fernández-Méndez M, Duarte P, Meyer A, Randelhoff A, Mundy CJ, Olsen LM, Kauko HM, Bailey A, Chierici M (2017) Leads in Arctic pack ice enable early phytoplankton blooms below snow-covered sea ice. Scientific Reports 7:40850. https://doi.org/10.1038/srep40850

Bai Y, Sicre M-A, Chen J, Klein V, Jin H, Ren J, Li H, Xue B, Ji Z, Zhuang Y, Zhao M (2019) Seasonal and spatial variability of sea ice and phytoplankton biomarker flux in the Chukchi sea (western Arctic Ocean). Progress in Oceanography 171:22-37. https://doi.org/10.1016/j.pocean.2018.12.002

Beatty WS, Jay CV, Fischbach AS, Grebmeier JM, Taylor RL, Blanchard AL, Jewett SC (2016) Space use of a dominant Arctic vertebrate: Effects of prey, sea ice, and land on Pacific walrus resource selection. Biological Conservation 203:25-32. https://doi.org/10.1016/j.biocon.2016.08.035

Belt ST (2018) Source-specific biomarkers as proxies for Arctic and Antarctic sea ice. Organic Geochemistry 125:277-298. https://doi.org/10.1016/j.orggeochem.2018.10.002

Belt ST, Allard G, Massé G, Robert J-M, Rowland S (2000a) Important sedimentary sesterterpenoids from the diatom *Pleurosigma intermedium*. Chemical Communications:501-502. https://doi.org/10.1039/A909670A

Belt ST, Allard WG, Massé G, Robert J-M, Rowland SJ (2000b) Highly branched isoprenoids (HBIs): Identification of the most common and abundant sedimentary isomers. Geochimica et Cosmochimica Acta 64:3839-3851. https://doi.org/10.1016/S0016-7037(00)00464-6

Belt ST, Brown TA, Ringrose AE, Cabedo-Sanz P, Mundy CJ, Gosselin M, Poulin M (2013) Quantitative measurement of the sea ice diatom biomarker IP_{25} and sterols in Arctic sea ice and underlying sediments: Further considerations for palaeo sea ice reconstruction. Organic Geochemistry 62:33-45. https://doi.org/10.1016/j.orggeochem.2013.07.002

Belt ST, Brown TA, Rodriguez AN, Sanz PC, Tonkin A, Ingle R (2012) A reproducible method for the extraction, identification and quantification of the Arctic sea ice proxy IP_{25} from marine sediments. Analytical Methods 4. https://doi.org/10.1039/c2ay05728j

Belt ST, Brown TA, Smik L, Assmy P, Mundy CJ (2018) Sterol identification in floating Arctic sea ice algal aggregates and the Antarctic sea ice diatom *Berkeleya adeliensis*. Organic Geochemistry 118:1-3. https://doi.org/10.1016/j.orggeochem.2018.01.008

Belt ST, Brown TA, Smik L, Tatarek A, Wiktor J, Stowasser G, Assmy P, Allen CS, Husum K (2017) Identification of C_{25} highly branched isoprenoid (HBI) alkenes in diatoms of the genus *Rhizosolenia* in polar and sub-polar marine phytoplankton. Organic Geochemistry 110:65-72. https://doi.org/10.1016/j.orggeochem.2017.05.007

Belt ST, Cabedo-Sanz P, Smik L, Navarro-Rodriguez A, Berben SMP, Knies J, Husum K (2015) Identification of paleo Arctic winter sea ice limits and the marginal ice zone: Optimised biomarker-based reconstructions of late Quaternary Arctic sea ice. Earth and Planetary Science Letters 431:127-139. https://doi.org/10.1016/j.epsl.2015.09.020

Belt ST, Massé G, Rowland SJ, Poulin M, Michel C, LeBlanc B (2007) A novel chemical fossil of palaeo sea ice: IP_{25}. Organic Geochemistry 38:16-27. https://doi.org/10.1016/j.orggeochem.2006.09.013

Belt ST, Massé G, Vare LL, Rowland SJ, Poulin M, Sicre M-A, Sampei M, Fortier L (2008) Distinctive ^{13}C isotopic signature distinguishes a novel sea ice biomarker in Arctic sediments and sediment traps. Marine Chemistry 112:158-167. https://doi.org/10.1016/j.marchem.2008.09.002

Belt ST, Müller J (2013) The Arctic sea ice biomarker IP_{25}: a review of current understanding, recommendations for future research and applications in palaeo sea ice reconstructions. Quaternary Science Reviews 79:9-25. https://doi.org/10.1016/j.quascirev.2012.12.001

Belt ST, Smik L, Brown TA, Kim JH, Rowland SJ, Allen CS, Gal JK, Shin KH, Lee JI, Taylor KWR (2016) Source identification and distribution reveals the potential of the geochemical Antarctic sea ice proxy $IPSO_{25}$. Nature Communications 7:12655. https://doi.org/10.1038/ncomms12655

Belt ST, Smik L, Köseoğlu D, Knies J, Husum K (2019) A novel biomarker-based proxy for the spring phytoplankton bloom in Arctic and sub-arctic settings – HBI T_{25}. Earth and Planetary Science Letters 523:115703. https://doi.org/10.1016/j.epsl.2019.06.038

Berge J, Renaud PE, Darnis G, Cottier F, Last K, Gabrielsen TM, Johnsen G, Seuthe L, Weslawski JM, Leu E (2015) In the dark: a review of ecosystem processes during the Arctic polar night. Progress in Oceanography 139:258-271. https://doi.org/10.1016/j.pocean.2015.08.005

Bluhm B, Iken K, Hardy SM, Sirenko B, Holladay B (2009) Community structure of epibenthic megafauna in the Chukchi Sea. Aquatic Biology 7:269-293. https://doi.org/10.3354/ab00198

Bluhm BA, Gradinger R (2008) Regional variability in food availability for Arctic marine mammals. Ecological Applications 18:S77-S96. https://doi.org/10.1890/06-0562.1

Bluhm, B.A., Swadling, K.M. and Gradinger, R. (2017). Sea ice as a habitat for macrograzers. In Sea Ice, D.N. Thomas (Ed.). https://doi.org/10.1002/9781118778371.ch16

Boetius A, Albrecht S, Bakker K, Bienhold C, Felden J, Fernández-Méndez M, Hendricks S, Katlein C, Lalande C, Krumpen T (2013) Export of algal biomass from the melting Arctic sea ice. Science 339:1430-1432. https://doi.org/10.1126/science.1231346

Boveng P, Ziel H, McClintock B, Cameron M (2020) Body condition of phocid seals during a period of rapid environmental change in the Bering Sea and Aleutian Islands, Alaska. Deep Sea Research Part II: Topical Studies in Oceanography https://doi.org/10.1016/j.dsr2.2020.104904:104904

Brown T (2011) Production and preservation of the Arctic sea ice diatom biomarker IP_{25}. University of Plymouth, PhD Thesis. http://hdl.handle.net/10026.1/314

Brown T, Alexander C, Yurkowski D, Ferguson S, Belt S (2014a) Identifying variable sea ice carbon contributions to the Arctic ecosystem: A case study using highly branched isoprenoid lipid biomarkers in Cumberland Sound ringed seals. Limnology and Oceanography 59:1581-1589. https://doi.org/10.4319/lo.2014.59.5.1581

Brown T, Rad-Menéndez C, Ray J, Skaar K, Thomas N, Ruiz-Gonzalez C, Leu E (2020) Influence of nutrient availability on Arctic sea ice diatom HBI lipid synthesis. Organic Geochemistry:103977. https://doi.org/10.1016/j.orggeochem.2020.103977

Brown TA (2018) Stability of the lipid biomarker H-print within preserved animals. Polar Biology 41:1901-1905. https://doi.org/10.1007/s00300-018-2317-2

Brown TA, Alexander C, Yurkowski DJ, Ferguson SH, Belt ST (2014b) Identifying variable sea ice carbon contributions to the Arctic ecosystem: A case study using highly branched isoprenoid lipid biomarkers in Cumberland Sound ringed seals. Limnology and Oceanography 59:1581-1589. https://doi.org/https://doi.org/10.4319/lo.2014.59.5.1581

Brown TA, Assmy P, Hop H, Wold A, Belt ST (2017a) Transfer of ice algae carbon to ice-associated amphipods in the high-Arctic pack ice environment. Journal of Plankton Research 39:664-674. https://doi.org/10.1093/plankt/fbx030

Brown TA, Belt ST (2011) Identification of the sea ice diatom biomarker IP_{25} in Arctic benthic macrofauna: direct evidence for a sea ice diatom diet in Arctic heterotrophs. Polar Biology 35:131-137. https://doi.org/10.1007/s00300-011-1045-7

Brown TA, Belt ST (2012a) Closely linked sea ice-pelagic coupling in the Amundsen Gulf revealed by the sea ice diatom biomarker IP_{25}. Journal of Plankton Research 34:647-654. https://doi.org/10.1093/plankt/fbs045

Brown TA, Belt ST (2012b) Identification of the sea ice diatom biomarker IP_{25} in Arctic benthic macrofauna: direct evidence for a sea ice diatom diet in Arctic heterotrophs. Polar Biology 35:131-137. https://doi.org/10.1007/s00300-011-1045-7

Brown TA, Belt ST (2017) Biomarker-based H-print quantifies the composition of mixed sympagic and pelagic algae consumed by *Artemia* sp. Journal of Experimental Marine Biology and Ecology 488:32-37. https://doi.org/10.1016/j.jembe.2016.12.007

Brown TA, Belt ST, Ferguson SH, Yurkowski DJ, Davison NJ, Barnett JEF, Jepson PD (2013a) Identification of the sea ice diatom biomarker IP_{25} and related lipids in marine mammals: A potential method for investigating regional variations in dietary sources within higher trophic level marine systems. Journal of Experimental Marine Biology and Ecology 441:99-104. https://doi.org/10.1016/j.jembe.2013.01.020

Brown TA, Belt ST, Philippe B, Mundy CJ, Massé G, Poulin M, Gosselin M (2011) Temporal and vertical variations of lipid biomarkers during a bottom ice diatom bloom in the Canadian Beaufort Sea: further evidence for the use of the IP_{25} biomarker as a proxy for spring Arctic sea ice. Polar Biology 34:1857-1868. https://doi.org/10.1007/s00300-010-0942-5

Brown TA, Belt ST, Piepenburg D (2012) Evidence for a pan-Arctic sea-ice diatom diet in *Strongylocentrotus* spp. Polar biology 35:1281-1287. https://doi.org/10.1007/s00300-012-1164-9

Brown TA, Belt ST, Tatarek A, Mundy CJ (2014c) Source identification of the Arctic sea ice proxy IP_{25}. Nat Commun 5:4197. https://doi.org/10.1038/ncomms5197

Brown TA, Bicknell AWJ, Votier SC, Belt ST (2013b) Novel molecular fingerprinting of marine avian diet provides a tool for gaining insights into feeding ecology. Environmental Chemistry Letters 11:283-288. https://doi.org/10.1007/s10311-013-0402-x

Brown TA, Chrystal E, Ferguson SH, Yurkowski DJ, Watt C, Hussey NE, Kelley TC, Belt ST (2017b) Coupled changes between the H-Print biomarker and $\delta^{15}N$ indicates a variable sea ice carbon contribution to the diet of Cumberland Sound beluga whales. Limnology and Oceanography 62:1606-1619. https://doi.org/10.1002/lno.10520

Brown TA, Galicia MP, Thiemann GW, Belt ST, Yurkowski DJ, Dyck MG (2018) High contributions of sea ice derived carbon in polar bear (*Ursus maritimus*) tissue. PLOS ONE 13:e0191631. https://doi.org/10.1371/journal.pone.0191631

Brown TA, Yurkowski DJ, Ferguson SH, Alexander C, Belt ST (2014d) H-print: a new chemical fingerprinting approach for distinguishing primary production sources in Arctic ecosystems. Environmental Chemistry Letters 12:387-392. https://doi.org/10.1007/s10311-014-0459-1

Brown ZW, Casciotti KL, Pickart RS, Swift JH, Arrigo KR (2015) Aspects of the marine nitrogen cycle of the Chukchi Sea shelf and Canada Basin. Deep Sea Research Part II: Topical Studies in Oceanography 118:73-87. https://doi.org/10.1016/j.dsr2.2015.02.009

Budge SM, Wooller MJ, Springer AM, Iverson SJ, McRoy CP, Divoky GJ (2008) Tracing carbon flow in an arctic marine food web using fatty acid-stable isotope analysis. Oecologia 157:117-129. https://doi.org/10.1007/s00442-008-1053-7

Cabedo-Sanz P, Smik L, Belt ST (2016) On the stability of various highly branched isoprenoid (HBI) lipids in stored sediments and sediment extracts. Organic Geochemistry 97:74-77. https://doi.org/10.1016/j.orggeochem.2016.04.010

Carmack E, Barber D, Christensen J, Macdonald R, Rudels B, Sakshaug E (2006) Climate variability and physical forcing of the food webs and the carbon budget on panarctic shelves. Progress in Oceanography 71:145-181. https://doi.org/10.1016/j.pocean.2006.10.005

Carmen D, Lange B, Krumpen T, Schaafsma F, van Franeker JA, Flores H (2016) Under-ice distribution of polar cod *Boreogadus saida* in the central Arctic Ocean and their association with sea-ice habitat properties. Polar Biology 39:981-994. https://doi.org/10.1007/s00300-015-1774-0

Caron, D.A., Gast, R.J. and Garneau, M.-È. (2017). Sea ice as a habitat for micrograzers. In Sea Ice, D.N. Thomas (Ed.). https://doi.org/10.1002/9781118778371.ch15

Chang BX, Devol AH (2009) Seasonal and spatial patterns of sedimentary denitrification rates in the Chukchi Sea. Deep Sea Research Part II: Topical Studies in Oceanography 56:1339-1350. https://doi.org/10.1016/j.dsr2.2008.10.024

Charapata P, Horstmann L, Misarti N (2021) Steroid hormones in Pacific walrus bones collected over three millennia indicate physiological responses to changes in estimated population size and the environment. Conservation Physiology 9. https://doi.org/10.1093/conphys/coaa135

Clark CT, Horstmann L, de Vernal A, Jensen AM, Misarti N (2019a) Pacific walrus diet across 4000 years of changing sea ice conditions. Quaternary Research https://doi.org/10.1017/qua.2018.140

Clark CT, Horstmann L, Misarti N (2019b) Lipid normalization and stable isotope discrimination in Pacific walrus tissues. Sci Rep 9:5843. https://doi.org/10.1038/s41598-019-42095-z

Collins LG, Allen CS, Pike J, Hodgson DA, Weckström K, Massé G (2013) Evaluating highly branched isoprenoid (HBI) biomarkers as a novel Antarctic sea-ice proxy in deep ocean glacial age sediments. Quaternary Science Reviews 79:87-98. https://doi.org/10.1016/j.quascirev.2013.02.004

Cooper LW, Ashjian CJ, Smith SL, Codispoti LA, Grebmeier JM, Campbell RG, Sherr EB (2006) Rapid Seasonal Sea-Ice Retreat in the Arctic Could Be Affecting Pacific Walrus (*Odobenus rosmarus divergens*) Recruitment. Aquatic Mammals 32:98-102. https://doi.org/10.1578/am.32.1.2006.98

Cooper LW, Grebmeier JM (2018) Deposition patterns on the Chukchi shelf using radionuclide inventories in relation to surface sediment characteristics. Deep Sea Research Part II: Topical Studies in Oceanography 152:48-66. https://doi.org/10.1016/j.dsr2.2018.01.009

Cooper LW, Grebmeier JM, Larsen IL, Dolvin SS, Reed AJ (1998) Inventories and distribution of radiocaesium in Arctic marine sediments: Influence of biological and physical processes. Chemistry and Ecology 15:27-46. https://doi.org/10.1080/02757549808037619

Cooper LW, Sexson MG, Grebmeier JM, Gradinger R, Mordy CW, Lovvorn JR (2013) Linkages between sea-ice coverage, pelagic–benthic coupling, and the distribution of spectacled eiders: Observations in March 2008, 2009 and 2010, northern Bering Sea. Deep Sea Research Part II: Topical Studies in Oceanography 94:31-43. https://doi.org/10.1016/j.dsr2.2013.03.009

Cota G, Legendre L, Gosselin M, Ingram R (1991) Ecology of bottom ice algae: I. Environmental controls and variability. Journal of Marine Systems 2:257-277. https://doi.org/10.1016/0924-7963(91)90036-T

Cusset F, Fort J, Mallory M, Braune B, Massicotte P, Massé G (2019) Arctic seabirds and shrinking sea ice: egg analyses reveal the importance of ice-derived resources. Scientific reports 9:1-15. https://doi.org/10.1038/s41598-019-51788-4

de Vernal A, Gersonde R, Goosse H, Seidenkrantz M-S, Wolff EW (2013) Sea ice in the paleoclimate system: the challenge of reconstructing sea ice from proxies–an introduction. Quaternary Science Reviews 79:1-8. https://doi.org/10.1016/j.quascirev.2013.08.009

Deming, J.W. and Eric Collins, R. (2017). Sea ice as a habitat for Bacteria, Archaea and viruses. In Sea Ice, D.N. Thomas (Ed.). https://doi.org/10.1002/9781118778371.ch13

Denisenko SG, Grebmeier JM, Cooper LW, Denisenko SG, Skvortsov VV (2015) Assessing bioresources and standing stock of zoobenthos (key species, high taxa, trophic groups) in the Chukchi Sea. Oceanography 28:146-157. https://www.jstor.org/stable/24861907

Dezutter T, Lalande C, Dufresne C, Darnis G, Fortier L (2019) Mismatch between microalgae and herbivorous copepods due to the record sea ice minimum extent of 2012 and the late sea ice break-up of 2013 in the Beaufort Sea. Progress in Oceanography 173:66-77. https://doi.org/10.1016/j.pocean.2019.02.008

Divine LM, Bluhm BA, Mueter FJ, Iken K (2017) Diet analysis of Alaska Arctic snow crabs (Chionoecetes opilio) using stomach contents and δ13C and δ15N stable isotopes. Deep Sea Research Part II: Topical Studies in Oceanography 135:124-136. https://doi.org/10.1016/j.dsr2.2015.11.009

Divoky GJ, Lukacs PM, Druckenmiller ML (2015) Effects of recent decreases in arctic sea ice on an ice-associated marine bird. Progress in Oceanography 136:151-161. https://doi.org/10.1016/j.pocean.2015.05.010

Duffy-Anderson JT, Stabeno P, Andrews III AG, Cieciel K, Deary A, Farley E, Fugate C, Harpold C, Heintz R, Kimmel D (2019) Responses of the northern Bering Sea and southeastern Bering Sea pelagic ecosystems following record-breaking low winter

sea ice. Geophysical Research Letters 46:9833-9842. https://doi.org/10.1029/2019GL083396
Dunton KH, Ashjian C, Campbell RG, Cooper LW, Grebmeier JM, Konar B, Maidment DM, Trefry JH, Weingartner TJ, Whiteaker TL (2014) Ecosystem monitoring information collected in Hanna Shoal in the Chukchi Sea for the COMIDA CAB project from August 2012 to August 2013 (NCEI Accession 0123220). https://doi.org/10.7289/v5gx48mn. http://arcticstudies.org/hannashoal/data.html
Dunton KH, Grebmeier JM, Trefry JH (2014) The benthic ecosystem of the northeastern Chukchi Sea: An overview of its unique biogeochemical and biological characteristics. Deep Sea Research Part II: Topical Studies in Oceanography 102:1-8. https://doi.org/10.1016/j.dsr2.2014.01.001
Ellegaard M, Ribeiro S (2018) The long-term persistence of phytoplankton resting stages in aquatic 'seed banks'. Biological Reviews 93:166-183. https://doi.org/10.1111/brv.12338
Encyclopedia of Life (2020) Accessed 07/28/2020. http://eol.org.
Falk-Petersen S, Mayzaud P, Kattner G, Sargent JR (2009) Lipids and life strategy of Arctic Calanus. Marine Biology Research 5:18-39. https://doi.org/10.1080/17451000802512267
Falk-Petersen S, Sargent J, Henderson J, Hegseth E, Hop H, Okolodkov Y (1998) Lipids and fatty acids in ice algae and phytoplankton from the Marginal Ice Zone in the Barents Sea. Polar Biology 20:41-47. https://doi.org/10.1007/s003000050274
Fay F, Hills S, Quakenbush L (1989) Determination of the age of walruses taken in the Alaskan subsistence catch, 1985–1987, together with the analysis of reproductive organs and stomach contents from the 1985 sample. US. Fish and Wildlife Service. In: Service USFaW (ed) Final Report, contract 70181-13097-87, Anchorage, AK https://ecos.fws.gov/ServCat/DownloadFile/110854?Reference=70281 [Accessed 04/11/2021]
Fay FH (1982) Ecology and biology of the Pacific walrus, *Odobenus rosmarus divergens* Illiger. North American Fauna https://doi.org/10.3996/nafa.74.0001:1-279.
Feder HM, Naidu AS, Jewett SC, Hameedi JM, Johnson WR, Whitledge TE (1994) The northeastern Chukchi Sea: benthos-environmental interactions. Marine Ecology Progress Series https://www.jstor.org/stable/24847621:171-190.
Fedewa EJ, Jackson TM, Richar JI, Gardner JL, Litzow MA (2020) Recent shifts in northern Bering Sea snow crab (*Chionoecetes opilio*) size structure and the potential role of climate-mediated range contraction, Deep Sea Research Part II: Topical Studies in Oceanography 181:104878, https://doi.org/10.1016/j.dsr2.2020.104878.
Feng Z, Ji R, Ashjian C, Zhang J, Campbell R, Grebmeier JM (2020) Benthic Hotspots on the Northern Bering and Chukchi Continental Shelf: Spatial variability in production regimes and environmental drivers. Progress in Oceanography https://doi.org/10.1016/j.pocean.2020.102497:102497.
Fernández-Méndez M, Katlein C, Rabe B, Nicolaus M, Peeken I, Bakker K, Flores H, Boetius A (2015) Photosynthetic production in the Central Arctic during the record sea-ice minimum in 2012. Biogeosciences Discussions 12. https://doi.org/10.5194/bgd-12-2897-2015
Fetterer F, Knowles K, Meier WN, Savoie M, Windnagel AK (2017, updated daily) Sea Ice Index, Version 3. Sea Ice Concentration. Boulder, Colorado USA. NSIDC: National Snow and Ice Data Center. doi: https://doi.org/10.7265/N5K072F8. [Accessed 11/05/2019].

Fischbach AS, Kochnev AA, Garlich-Miller JL, Jay CV (2016) Pacific walrus coastal haulout database, 1852-2016—Background report. US Geological Survey https://doi.org/10.3133/ofr20161108.

Fortier M, Fortier L, Michel C, Legendre L (2002) Climatic and biological forcing of the vertical flux of biogenic particles under seasonal Arctic sea ice. Marine Ecology Progress Series 225:1-16. https://doi.org/10.3354/meps225001

Frey KE, Perovich, DK, Light B (2011) The spatial distribution of solar radiation under melting Arctic sea ice cover. Geophysical Research Letters 38:22 https://doi.org/10.1029/2011GL049421

Frey K, Comiso J, Cooper L, Grebmeier J, Stock LV (2018) Arctic ocean primary productivity: The response of marine algae to climate warming and sea ice decline. Arctic Report Card 2018. https://www.arctic.noaa.gov/Report-Card

Frey K, Comiso J, Cooper L, Grebmeier J, Stock LV (2020) Arctic ocean primary productivity: The response of marine algae to climate warming and sea ice decline. Arctic Report Card 2020 https://doi.org/10.25923/vtdn-2198

Frey KE, Moore G, Cooper LW, Grebmeier JM (2015) Divergent patterns of recent sea ice cover across the Bering, Chukchi, and Beaufort seas of the Pacific Arctic Region. Progress in Oceanography 136:32-49. https://doi.org/10.1016/j.pocean.2015.05.009

Garlich-Miller J, MacCracken JG, Snyder J, Meehan R, Myers M, Wilder JM, Lance E, Matz A (2011) Status review of the Pacific walrus (*Odobenus rosmarus divergens*). US Fish and Wildlife Service. https://www.researchgate.net/publication/285715467_Status_review_of_the_Pacific_walrus_Odobenus_rosmarus_divergens [Accessed 06/01/2020].

Garlich-Miller JL, Quakenbush LT, Bromaghin JF (2006) Trends in age structure and productivity of Pacific walruses harvested in the Bering Strait region of Alaska, 1952–2002. Marine Mammal Science 22:880-896. https://doi.org/10.1111/j.1748-7692.2006.00081.x

Garrison DL, Ackley SF, Buck KR (1983) A physical mechanism for establishing algal populations in frazil ice. Nature 306:363-365. https://doi.org/10.1038/306363a0

Gebruk A, Mikhaylyukova P, Mardashova M, Semenova V, Henry LA, Shabalin N, Narayanaswamy BE, Mokievsky V (2020) Integrated study of benthic foraging resources for Atlantic walrus (*Odobenus rosmarus rosmarus*) in the Pechora Sea, south-eastern Barents Sea. Aquatic Conservation: Marine and Freshwater Ecosystems https://doi.org/10.1002/aqc.3418.

Gibbs P (1977) On the status of *Golfingia intermedia* (Sipuncula). Journal of the Marine Biological Association of the United Kingdom 57:109-112. https://doi.org/10.1017/S0025315400021275

Goethel CL, Grebmeier JM, Cooper LW (2019) Changes in abundance and biomass of the bivalve *Macoma calcarea* in the northern Bering Sea and the southeastern Chukchi Sea from 1998 to 2014, tracked through dynamic factor analysis models. Deep Sea Research Part II: Topical Studies in Oceanography 162:127-136. https://doi.org/10.1016/j.dsr2.2018.10.007

Gong D, Pickart RS (2015) Summertime circulation in the eastern Chukchi Sea. Deep Sea Research Part II: Topical Studies in Oceanography 118:18-31. https://doi.org/10.1016/j.dsr2.2015.02.006

Gosselin M, Levasseur M, Wheeler PA, Horner RA, Booth BC (1997) New measurements of phytoplankton and ice algal production in the Arctic Ocean. Deep Sea Research Part

II: Topical Studies in Oceanography 44:1623-1644. https://doi.org/10.1016/S0967-0645(97)00054-4
Goutte A, Charrassin J-B, Cherel Y, Carravieri A, De Grissac S, Massé G (2014a) Importance of ice algal production for top predators: new insights using sea-ice biomarkers. Marine Ecology Progress Series 513:269-275. https://doi.org/10.3354/meps10971
Goutte A, Cherel Y, Houssais M-N, Klein V, Ozouf-Costaz C, Raccurt M, Robineau C, Massé G (2013) Diatom-specific highly branched isoprenoids as biomarkers in Antarctic consumers. PLOS ONE 8:e56504. https://doi.org/10.1371/journal.pone.0056504
Goutte A, Cherel Y, Ozouf-Costaz C, Robineau C, Lanshere J, Massé G (2014b) Contribution of sea ice organic matter in the diet of Antarctic fishes: a diatom-specific highly branched isoprenoid approach. Polar Biology 37:903-910. https://doi.org/10.3354/meps10971
Gradinger R (2009) Sea-ice algae: Major contributors to primary production and algal biomass in the Chukchi and Beaufort Seas during May/June 2002. Deep Sea Research Part II: Topical Studies in Oceanography 56:1201-1212. https://doi.org/10.1016/j.dsr2.2008.10.016
Gradinger R, Bluhm B (2004) In-situ observations on the distribution and behavior of amphipods and Arctic cod (*Boreogadus saida*) under the sea ice of the High Arctic Canada Basin. Polar Biology 27. https://doi.org/10.1007/s00300-004-0630-4
Gradinger R, Ikävalko J (1998) Organism incorporation into newly forming Arctic sea ice in the Greenland Sea. Journal of Plankton Research 20:871-886. https://doi.org/10.1093/plankt/20.5.871
Gradinger RR, Meiners K, Plumley G, Zhang Q, Bluhm BA (2005) Abundance and composition of the sea-ice meiofauna in off-shore pack ice of the Beaufort Gyre in summer 2002 and 2003. Polar Biology 28:171-181. https://doi.org/10.1007/s00300-004-0674-5
Graeve M, Albers C, Kattner G (2005) Assimilation and biosynthesis of lipids in Arctic *Calanus* species based on feeding experiments with a ^{13}C labelled diatom. Journal of Experimental Marine Biology and Ecology 317:109-125. https://doi.org/10.1016/j.jembe.2004.11.016
Graeve M, Kattner G, Wiencke C, Karsten U (2002) Fatty acid composition of Arctic and Antarctic macroalgae: indicator of phylogenetic and trophic relationships. Marine Ecology Progress Series 231:67-74. https://doi.org/10.3354/meps231067
Graham BS, Koch PL, Newsome SD, McMahon KW, Aurioles D (2010) Using Isoscapes to Trace the Movements and Foraging Behavior of Top Predators in Oceanic Ecosystems. In: West JB, Bowen GJ, Dawson TE, Tu KP (eds) Isoscapes: Understanding movement, pattern, and process on Earth through isotope mapping. Springer Netherlands, Dordrecht. https://doi.org/10.1007/978-90-481-3354-3_14.
Grebmeier JM (2012) Shifting Patterns of Life in the Pacific Arctic and Sub-Arctic Seas. Annual Review of Marine Science 4:63-78. https://doi.org/10.1146/annurev-marine-120710-100926
Grebmeier JM, Bluhm BA, Cooper LW, Danielson SL, Arrigo KR, Blanchard AL, Clarke JT, Day RH, Frey KE, Gradinger RR (2015) Ecosystem characteristics and processes facilitating persistent macrobenthic biomass hotspots and associated benthivory in the Pacific Arctic. Progress in Oceanography 136:92-114. https://doi.org/10.1016/j.pocean.2015.05.006

Grebmeier JM, Cooper LW (1995) Influence of the St. Lawrence Island polynya upon the Bering Sea benthos. Journal of Geophysical Research: Oceans 100:4439-4460. https://doi.org/10.1029/94JC02198
Grebmeier JM, Cooper LW (2019a) Surface sediment samples collected from the United States Coast Guard Ship (USCGS) Healy, Northern Bering Sea to Chukchi Sea, 2017. https://doi.org/10.18739/A2804XK1F.
Grebmeier JM, Cooper LW (2019b) Ocean sediment grain size, nutrient, and chrolophyll data from the United States Coast Guard Cutter Healy (HLY1201), Barrow Canyon, Chukchi Sea, 2012. https://doi.org/10.18739/A2BR8MG32
Grebmeier JM, Cooper LW (2019c) Surface sediment samples collected from the Canadian Coast Guard Ship (CCGS) Sir Wilfrid Laurier, Northern Bering Sea to Chukchi Sea, 2014. https://doi.org/10.18739/A2WH2DF2X
Grebmeier JM, Cooper LW (2019d) Surface sediment samples collected from the Canadian Coast Guard Ship (CCGS) Sir Wilfrid Laurier, Northern Bering Sea to Chukchi Sea, 2016. https://doi.org/10.18739/A2XD0QX8B
Grebmeier JM, Cooper LW (2019e) Surface sediment samples collected from the CCGS Sir Wilfrid Laurier, Northern Bering Sea to Chukchi Sea, 2015. https://doi.org/10.18739/A2HH6C58X
Grebmeier JM, Cooper LW (2019f) Surface sediment samples collected from the CCGS Sir Wilfrid Laurier 2018, Northern Bering Sea to Chukchi Sea. https://doi.org/10.18739/A2C824F2J
Grebmeier JM, Cooper LW (2019g) Surface sediment samples collected from the United States Coast Guard Cutter Healy (HLY1801), Northern Bering Sea to Chukchi Sea https://doi.org/10.18739/A2H12V769
Grebmeier JM, Cooper LW (2019h) Benthic macroinfaunal samples collected from the Canadian Coast Guard Ship (CCGS) Sir Wilfrid Laurier, Northern Bering Sea to Chukchi Sea, 2015. Arctic Data Center https://doi.org/10.18739/A28W3827B.
Grebmeier JM, Cooper LW, Feder HM, Sirenko BI (2006a) Ecosystem dynamics of the Pacific-influenced Northern Bering and Chukchi Seas in the Amerasian Arctic. Progress in Oceanography 71:331-361. https://doi.org/10.1016/j.pocean.2006.10.001
Grebmeier JM, Feder HM, McRoy CP (1989) Pelagic-benthic coupling on the shelf of the northern Bering and Chukchi Seas. 1 Benthic community structure. Marine Ecology Progress Series 51:253-268. https://doi.org/10.3354/meps051253
Grebmeier JM, Frey KE, Cooper LW, Kędra M (2018) Trends in benthic macrofaunal populations, seasonal sea ice persistence, and bottom water temperatures in the Bering Strait region. Oceanography 31:136-151. https://www.jstor.org/stable/26542660
Grebmeier JM, Moore SE, Cooper LW, Frey KE (2019) The Distributed Biological Observatory: A change detection array in the Pacific Arctic – An introduction. Deep Sea Research Part II: Topical Studies in Oceanography 162:1-7. https://doi.org/10.1016/j.dsr2.2019.05.005
Grebmeier JM, Moore SE, Overland JE, Frey KE, Gradinger R (2010) Biological response to recent Pacific Arctic sea ice retreats. Eos, Transactions American Geophysical Union 91:161-162. https://doi.org/10.1029/2010EO180001
Grebmeier JM, Overland JE, Moore SE, Farley EV, Carmack EC, Cooper LW, Frey KE, Helle JH, McLaughlin FA, McNutt SL (2006b) A Major Ecosystem Shift in the Northern Bering Sea. Science 311:1461-1464. https://doi.org/10.1126/science.1121365

Hancke K, Lund-Hansen LC, Lamare ML, Højlund Pedersen S, King MD, Andersen P, Sorrell BK (2018) Extreme low light requirement for algae growth underneath sea ice: A case study from Station Nord, NE Greenland. Journal of Geophysical Research: Oceans 123:985-1000. https://doi.org/10.1002/2017JC013263

Hauri C, Danielson S, McDonnell AMP, Hopcroft RR, Winsor P, Shipton P, Lalande C, Stafford KM, Horne JK, Cooper LW, Grebmeier JM, Mahoney A, Maisch K, McCammon M, Statscewich H, Sybrandy A, Weingartner T (2018) From sea ice to seals: A moored marine ecosystem observatory in the Arctic. Ocean Science 14:1423–1433. https://doi.org/10.5194/os-14-1423-2018

Hill V, Ardyna M, Lee SH, Varela DE (2018) Decadal trends in phytoplankton production in the Pacific Arctic Region from 1950 to 2012. Deep Sea Research Part II: Topical Studies in Oceanography 152:82-94. https://doi.org/10.1016/j.dsr2.2016.12.015

Hobson KA, Ambrose Jr WG, Renaud PE (1995) Sources of primary production, benthic-pelagic coupling, and trophic relationships within the Northeast Water Polynya: insights from δ^{13}C and δ^{15}N analysis. Marine Ecology Progress Series 128:1-10. https://doi.org/10.3354/meps128001

Hop H, Vihtakari M, Bluhm BA, Assmy P, Poulin M, Gradinger R, Peeken I, von Quillfeldt C, Olsen LM, Zhitina L, Melnikov IA (2020) Changes in sea-ice protist diversity with declining sea ice in the Arctic Ocean From the 1980s to 2010s. Frontiers in Marine Science 7. https://doi.org/10.3389/fmars.2020.00243

Horner R, Ackley SF, Dieckmann GS, Gulliksen B, Hoshiai T, Legendre L, Melnikov IA, Reeburgh WS, Spindler M, Sullivan CW (1992) Ecology of sea ice biota. Polar Biology 12:417-427. https://doi.org/10.1007/BF00243113

Horner R, Schrader G (1982) Relative contributions of ice algae, phytoplankton, and benthic microalgae to primary production in nearshore regions of the Beaufort Sea. Arctic, https://www.jstor.org/stable/40509382:485-503.

Horner RA (1989) Arctic sea-ice biota. In: Herman Y (ed) The Arctic Seas. Springer, Boston, MA 123-146, https://doi.org/10.1007/978-1-4613-0677-1_5

Horvat C, Jones DR, Iams S, Schroeder D, Flocco D, Feltham D (2017) The frequency and extent of sub-ice phytoplankton blooms in the Arctic Ocean. Science Advances 3:e1601191. https://doi.org/10.1126/sciadv.1601191

Huntington HP, Danielson SL, Wiese FK, Baker M, Boveng P, Citta JJ, De Robertis A, Dickson DM, Farley E, George JC (2020) Evidence suggests potential transformation of the Pacific Arctic ecosystem is underway. Nature Climate Change 10:342-348. https://doi.org/10.1038/s41558-020-0695-2

Huntington HP, Quakenbush LT, Nelson M (2016) Effects of changing sea ice on marine mammals and subsistence hunters in northern Alaska from traditional knowledge interviews. Biology Letters 12:20160198. https://doi.org/10.1098/rsbl.2016.0198

Iken K, Bluhm B, Dunton K (2010) Benthic food-web structure under differing water mass properties in the southern Chukchi Sea. Deep Sea Research Part II: Topical Studies in Oceanography 57:71-85. https://doi.org/10.1016/j.dsr2.2009.08.007

Jansen JM, Pronker AE, Kube S, Sokolowski A, Sola JC, Marquiegui MA, Schiedek D, Bonga SW, Wolowicz M, Hummel H (2007) Geographic and seasonal patterns and limits on the adaptive response to temperature of European *Mytilus* spp. and *Limecola balthica* populations. Oecologia 154:23-34. https://doi.org/10.1007/s00442-007-0808-x

Jay CV, Fischbach AS, Kochnev AA (2012) Walrus areas of use in the Chukchi Sea during sparse sea ice cover. Marine Ecology Progress Series 468:1-13. https://doi.org/10.3354/meps10057
Jay CV, Grebmeier JM, Fischbach AS, McDonald TL, Cooper LW, Hornsby F (2014) Pacific walrus (*Odobenus rosmarus divergens*) resource selection in the Northern Bering Sea. PLOS ONE 9:e93035. https://doi.org/10.1371/journal.pone.0093035
Jay CV, Marcot BG, Douglas DC (2011) Projected status of the Pacific walrus (*Odobenus rosmarus divergens*) in the twenty-first century. Polar Biology 34:1065-1084. https://doi.org/10.1007/s00300-011-0967-4
Jay CV, Taylor RL, Fischbach AS, Udevitz MS, Beatty WS (2017) Walrus haulout and in water activity levels relative to sea ice availability in the Chukchi Sea. Journal of Mammalogy 98:386-396. https://doi.org/10.1093/jmammal/gyw195
Johns L, Wraige EJ, Belt ST, Lewis CA, Massé G, Robert JM, Rowland SJ (1999) Identification of a C25 highly branched isoprenoid (HBI) diene in Antarctic sediments, Antarctic sea-ice diatoms and cultured diatoms. Organic Geochemistry 30:1471-1475. https://doi.org/10.1016/S0146-6380(99)00112-6
Juul-Pedersen T, Michel C, Gosselin M, Seuthe L (2008) Seasonal changes in the sinking export of particulate material under first-year sea ice on the Mackenzie Shelf (western Canadian Arctic). Marine Ecology Progress Series 353:13-25. https://doi.org/10.3354/meps07165
Kapsch M-L, Eicken H, Robards M (2010) Sea ice distribution and ice use by indigenous walrus hunters on St. Lawrence Island, Alaska. SIKU: Knowing Our Ice https://doi.org/10.1007/978-90-481-8587-0_5.
Kauko HM, Olsen LM, Duarte P, Peeken I, Granskog MA, Johnsen G, Fernández-Méndez M, Pavlov AK, Mundy CJ, Assmy P (2018) Algal colonization of young Arctic sea ice in spring. Frontiers in Marine Science 5. https://doi.org/10.3389/fmars.2018.00199
Kędra M, Cooper LW, Zhang M, Biasatti D, Grebmeier JM (2019) Benthic trophic sensitivity to on-going changes in Pacific Arctic seasonal sea ice cover – Insights from the nitrogen isotopic composition of amino acids. Deep Sea Research Part II: Topical Studies in Oceanography 162:137-151. https://doi.org/10.1016/j.dsr2.2019.01.002
Kędra M, Grebmeier JM, Cooper LW (2018) Sipunculan fauna in the Pacific Arctic region: a significant component of benthic infaunal communities. Polar Biology 41:163-174. https://doi.org/10.1007/s00300-017-2179-z
Kędra M, Moritz C, Choy ES, David C, Degen R, Duerksen S, Ellingsen I, Górska B, Grebmeier JM, Kirievskaya D, van Oevelen D, Piwosz K, Samuelsen A, Węsławski JM (2015) Status and trends in the structure of Arctic benthic food webs. Polar Research 34. https://doi.org/10.3402/polar.v34.23775
Khozin-Goldberg I. (2016) Lipid Metabolism in Microalgae. In: Borowitzka M., Beardall J., Raven J. (eds) The physiology of microalgae. Developments in Applied Phycology, vol 6. Springer, Cham. https://doi.org/10.1007/978-3-319-24945-2_18
Kim J-H, Gal J-K, Jun S-Y, Smik L, Kim D, Belt ST, Park K, Shin K-H, Nam S-I (2019) Reconstructing spring sea ice concentration in the Chukchi Sea over recent centuries: insights into the application of the PIP 25 index. Environmental Research Letters 14:125004. https://doi.org/10.1088/1748-9326/ab4b6e
Koch CW, Cooper LW, Grebmeier JM, Frey K, Brown TA (2020a) Ice algae resource utilization by benthic macro-and megafaunal communities on the Pacific Arctic shelf

determined through lipid biomarker analysis. Marine Ecology Progress Series 651:23-43. https://doi.org/10.3354/meps13476
Koch CW, Cooper LW, Lalande C, Brown TA, Frey KE, Grebmeier JM (2020b) Seasonal and latitudinal variations in sea ice algae deposition in the Northern Bering and Chukchi Seas determined by algal biomarkers. PLOS ONE 15:e0231178. https://doi.org/10.1371/journal.pone.0231178
Kohlbach D, Ferguson SH, Brown TA, Michel C (2019) Landfast sea ice-benthic coupling during spring and potential impacts of system changes on food web dynamics in Eclipse Sound, Canadian Arctic. Marine Ecology Progress Series 627:33-48. https://doi.org/10.3354/meps13071
Kohlbach D, Graeve M, A. Lange B, David C, Peeken I, Flores H (2016) The importance of ice algae-produced carbon in the central Arctic Ocean ecosystem: Food web relationships revealed by lipid and stable isotope analyses. Limnology and Oceanography 61:2027-2044. https://doi.org/10.1002/lno.10351
Kohlbach D, Graeve M, Lange BA, David C, Schaafsma FL, van Franeker JA, Vortkamp M, Brandt A, Flores H (2018) Dependency of Antarctic zooplankton species on ice algae-produced carbon suggests a sea ice-driven pelagic ecosystem during winter. Global Change Biology 24:4667-4681. https://doi.org/10.1111/gcb.14392
Kohlbach D, Hop H, Wold A, Schmidt K, Smik L, Belt ST, Keck Al-Habahbeh A, Woll M, Graeve M, Dąbrowska AM, Tatarek A, Atkinson A, Assmy P (2021) Multiple trophic markers trace dietary carbon sources in Barents Sea zooplankton during late summer. Frontiers in Marine Science 7. https://doi.org/10.3389/fmars.2020.610248
Kolling HM, Stein R, Fahl K, Sadatzki H, de Vernal A, Xiao X (2020) Biomarker Distributions in (Sub)-Arctic surface sediments and their potential for sea ice reconstructions. Geochemistry, Geophysics, Geosystems 21:e2019GC008629. https://doi.org/10.1029/2019GC008629
Kovacs KM, Lydersen C, Overland JE, Moore SE (2011) Impacts of changing sea-ice conditions on Arctic marine mammals. Marine Biodiversity 41:181-194. https://doi.org/10.1007/s12526-010-0061-0
Krembs C, Gradinger R, Spindler M (2000) Implications of brine channel geometry and surface area for the interaction of sympagic organisms in Arctic sea ice. Journal of Experimental Marine Biology and Ecology 243:55-80. https://doi.org/10.1016/S0022-0981(99)00111-2
Kremer A, Stein R, Fahl K, Ji Z, Yang Z, Wiers S, Matthiessen J, Forwick M, Löwemark L, O'Regan M (2018) Changes in sea ice cover and ice sheet extent at the Yermak Plateau during the last 160 ka–Reconstructions from biomarker records. Quaternary Science Reviews 182:93-108. https://doi.org/10.1016/j.quascirev.2017.12.016
Kuletz KJ, Ferguson MC, Hurley B, Gall AE, Labunski EA, Morgan TC (2015) Seasonal spatial patterns in seabird and marine mammal distribution in the eastern Chukchi and western Beaufort seas: Identifying biologically important pelagic areas. Progress in Oceanography 136:175-200. https://doi.org/10.1016/j.pocean.2015.05.012
Laidre, K.L. and Regehr, E.V. (2017). Arctic marine mammals and sea ice. In Sea Ice, D.N. Thomas (Ed.). https://doi.org/10.1002/9781118778371.ch21
Laidre KL, Stern H, Kovacs KM, Lowry L, Moore SE, Regehr EV, Ferguson SH, Wiig Ø, Boveng P, Angliss RP (2015) Arctic marine mammal population status, sea ice habitat loss, and conservation recommendations for the 21st century. Conservation Biology 29:724-737. https://doi.org/10.1111/cobi.12474

Lalande C, Grebmeier JM, Hopcroft RR, Danielson SL (2020) Annual cycle of export fluxes of biogenic matter near Hanna Shoal in the northeast Chukchi Sea. Deep Sea Research Part II: Topical Studies in Oceanography https://doi.org/10.1016/j.dsr2.2020.104730:104730

Lalande C, Grebmeier JM, Wassmann P, Cooper LW, Flint MV, Sergeeva VM (2007) Export fluxes of biogenic matter in the presence and absence of seasonal sea ice cover in the Chukchi Sea. Continental Shelf Research 27:2051-2065. https://doi.org/10.1016/j.csr.2007.05.005

Lalande C, Nöthig EM, Fortier L (2019) Algal export in the Arctic Ocean in times of global warming. Geophysical Research Letters. https://doi.org/10.1029/2019gl083167

Lee RF, Hagen W, Kattner G (2006) Lipid storage in marine zooplankton. Marine Ecology Progress Series 307:273-306. https://doi.org/10.3354/meps307273

Legendre L, Ackley SF, Dieckmann GS, Gulliksen B, Horner R, Hoshiai T, Melnikov IA, Reeburgh WS, Spindler M, Sullivan CW (1992) Ecology of sea ice biota. Polar Biology 12:429-444. https://doi.org/10.1007/BF00243114

Lepore K, Moran S, Smith J (2009) ^{210}Pb as a tracer of shelf–basin transport and sediment focusing in the Chukchi Sea. Deep Sea Research Part II: Topical Studies in Oceanography 56:1305-1315. https://doi.org/10.1016/j.dsr2.2008.10.021

Leu E, Brown TA, Graeve M, Wiktor J, Hoppe CJM, Chierici M, Fransson A, Verbiest S, Kvernvik AC, Greenacre MJ (2020) Spatial and temporal variability of ice algal trophic markers—with recommendations about their application. Journal of Marine Science and Engineering 8:676. https://doi.org/10.3390/jmse8090676

Leu E, Mundy CJ, Assmy P, Campbell K, Gabrielsen TM, Gosselin M, Juul-Pedersen T, Gradinger R (2015) Arctic spring awakening – Steering principles behind the phenology of vernal ice algal blooms. Progress in Oceanography 139:151-170. https://doi.org/10.1016/j.pocean.2015.07.012

Leu E, Søreide JE, Hessen DO, Falk-Petersen S, Berge J (2011) Consequences of changing sea-ice cover for primary and secondary producers in the European Arctic shelf seas: Timing, quantity, and quality. Progress in Oceanography 90:18-32. https://doi.org/10.1016/j.pocean.2011.02.004

Leu E, Wiktor J, Søreide J, Berge J, Falk-Petersen S (2010) Increased irradiance reduces food quality of sea ice algae. Marine Ecology Progress Series 411:49-60. https://doi.org/10.3354/meps08647

Lewis K, van Dijken G, Arrigo K (2020) Changes in phytoplankton concentration now drive increased Arctic Ocean primary production. Science 369:198-202. https://doi.org/10.1126/science.aay8380

Li WK, McLaughlin FA, Lovejoy C, Carmack EC (2009) Smallest algae thrive as the Arctic Ocean freshens. Science 326:539-539. https://doi.org/10.1126/science.1179798

Limoges A, Massé G, Weckström K, Poulin M, Ellegaard M, Heikkilä M, Geilfus N-X, Sejr MK, Rysgaard S, Ribeiro S (2018) Spring succession and vertical export of diatoms and IP_{25} in a seasonally ice-covered high Arctic fjord. Frontiers in Earth Science 6. https://doi.org/10.3389/feart.2018.00226

Lovvorn JR, Grebmeier JM, Cooper LW, Bump JK, Richman SE (2009) Modeling marine protected areas for threatened eiders in a climatically changing Bering Sea. Ecological Applications 19:1596-1613. https://doi.org/10.1890/08-1193.1

Lovvorn JR, Wilson JJ, McKay D, Bump JK, Cooper LW, Grebmeier JM (2010) Walruses attack spectacled eiders wintering in pack ice of the Bering Sea. Arctic https://www.jstor.org/stable/40513369:53-56.

Lund-Hansen LC, Hawes I, Hancke K, Salmansen N, Nielsen JR, Balslev L, Sorrell BK (2020) Effects of increased irradiance on biomass, photobiology, nutritional quality, and pigment composition of Arctic sea ice algae. Marine Ecology Progress Series 648:95-110. https://doi.org/10.3354/meps13411

MacCracken JG, Beatty WS, Garlich-Miller JL, Kissling ML, Snyder JA (2017) Final species status assessment for the Pacific walrus (*Odobenus rosmarus divergens*), May 2017 (Version 1.0). US Fish and Wildlife Service, Marine Mammals Management 1011. https://ecos.fws.gov/ServCat/DownloadFile/132114?Reference=86869

Macdonald, T.A., Burd, B.J., Macdonald, V.I., and van Roodselaar, A (2010) Taxonomic and feeding guild classification for the marine benthic macroinvertebrates of the Strait of Georgia, British Columbia. Can. Tech Rep. Fish. Aquat. Sci. 2874: iv + 63 p. http://publications.gc.ca/pub?id=9.571522&sl=0

Macias-Fauria M, Post E (2018) Effects of sea ice on Arctic biota: An emerging crisis discipline. Biology Letters 14:20170702. https://doi.org/10.1098/rsbl.2017.0702

Mäkelä A, Witte U, Archambault P (2017) Ice algae versus phytoplankton: resource utilization by Arctic deep sea macroinfauna revealed through isotope labelling experiments. Marine Ecology Progress Series 572:1-18. https://doi.org/10.3354/meps12157

Maniscalco JM, Springer AM, Counihan KL, Hollmen T, Aderman HM, Toyukak Sr M (2020) Contemporary diets of walruses in Bristol Bay, Alaska suggest temporal variability in benthic community structure. PeerJ 8:e8735. https://doi.org/10.7717/peerj.8735

Massé G, Belt ST, Crosta X, Schmidt S, Snape I, Thomas DN, Rowland SJ (2011) Highly branched isoprenoids as proxies for variable sea ice conditions in the Southern Ocean. Antarctic Science 23:487-498. http://dx.doi.org/10.1017/S0954102011000381

Massé G, Belt ST, Guy Allard W, Anthony Lewis C, Wakeham SG, Rowland SJ (2004) Occurrence of novel monocyclic alkenes from diatoms in marine particulate matter and sediments. Organic Geochemistry 35:813-822. https://doi.org/10.1016/j.orggeochem.2004.03.004

McMahon KW, Ambrose Jr WG, Johnson BJ, Sun M-Y, Lopez GR, Clough LM, Carroll ML (2006) Benthic community response to ice algae and phytoplankton in Ny Ålesund, Svalbard. Marine Ecology Progress Series 310:1-14. https://doi.org/10.3354/meps310001

McTigue ND, Bucolo P, Liu Z, Dunton KH (2015) Pelagic-benthic coupling, food webs, and organic matter degradation in the Chukchi Sea: Insights from sedimentary pigments and stable carbon isotopes. Limnology and Oceanography 60:429-445. https://doi.org/10.1002/lno.10038

McTigue ND, Dunton KH (2014) Trophodynamics and organic matter assimilation pathways in the northeast Chukchi Sea, Alaska. Deep Sea Research Part II: Topical Studies in Oceanography 102:84-96. https://doi.org/10.1016/j.dsr2.2013.07.016

Méheust M, Stein R, Fahl K, Max L, Riethdorf J-R (2015) High-resolution IP_{25}-based reconstruction of sea-ice variability in the western North Pacific and Bering Sea during the past 18,000 years. Geo-Marine Letters 36:101-111. https://doi.org/10.1007/s00367-015-0432-4

Meiners, KM and Michel, C. (2017). Dynamics of nutrients, dissolved organic matter and exopolymers in sea ice. In Sea Ice, D.N. Thomas (Ed.). https://doi.org/10.1002/9781118778371.ch17

Michel C, Legendre L, Ingram RG, Gosselin M, Levasseur M (1996) Carbon budget of sea-ice algae in spring: Evidence of a significant transfer to zooplankton grazers. Journal of Geophysical Research: Oceans 101:18345-18360. https://doi.org/10.1029/96JC00045

Mincks SL, Smith CR, DeMaster DJ (2005) Persistence of labile organic matter and microbial biomass in Antarctic shelf sediments: evidence of a sediment 'food bank'. Marine Ecology Progress Series 300:3-19. https://doi.org/10.3354/meps300003

Mock T, Gradinger R (2000) Changes in photosynthetic carbon allocation in algal assemblages of Arctic sea ice with decreasing nutrient concentrations and irradiance. Marine Ecology Progress Series 202:1-11. https://www.int-res.com/abstracts/meps/v202/p1-11/

Mohan SD, Connelly TL, Harris CM, Dunton KH, McClelland JW (2016) Seasonal trophic linkages in Arctic marine invertebrates assessed via fatty acids and compound-specific stable isotopes. Ecosphere 7. https://doi.org/10.1002/ecs2.1429

Moore SE, Grebmeier JM (2018) The Distributed Biological Observatory: linking physics to biology in the Pacific Arctic Region. Arctic 71:1-7. https://doi.org/10.14430/arctic4606

Moore SE, Huntington HP (2008) Arctic marine mammals and climate change: impacts and resilience. Ecological Applications 18:S157-S165. https://doi.org/10.1890/06-0571.1

Moore SE, Stabeno PJ (2015) Synthesis of Arctic Research (SOAR) in marine ecosystems of the Pacific Arctic. Progress in Oceanography 136:1-11. https://doi.org/10.1016/j.pocean.2015.05.017

Moore SE, Stabeno PJ, Grebmeier JM, Okkonen SR (2018) The Arctic Marine Pulses Model: linking annual oceanographic processes to contiguous ecological domains in the Pacific Arctic. Deep Sea Research Part II: Topical Studies in Oceanography 152:8-21. https://doi.org/10.1016/j.dsr2.2016.10.011

Müller J, Stein R (2014) High-resolution record of late glacial and deglacial sea ice changes in Fram Strait corroborates ice–ocean interactions during abrupt climate shifts. Earth and Planetary Science Letters 403:446-455. https://doi.org/10.1016/j.epsl.2014.07.016

Müller J, Wagner A, Fahl K, Stein R, Prange M, Lohmann G (2011) Towards quantitative sea ice reconstructions in the northern North Atlantic: A combined biomarker and numerical modelling approach. Earth and Planetary Science Letters 306:137-148. https://doi.org/10.1016/j.epsl.2011.04.011

Mundy, CJ and Meiners, KM (2021) Ecology of Arctic Sea Ice. In Arctic Ecology, D.N. Thomas (Ed.). https://doi.org/10.1002/9781118846582.ch10

Mundy CJ, Barber DG, Michel C, Marsden RF (2007) Linking ice structure and microscale variability of algal biomass in Arctic first-year sea ice using an in situ photographic technique. Polar Biology 30:1099-1114. https://doi.org/10.1007/s00300-007-0267-1

Nadaï G, Nöthig E-M, Fortier L, Lalande C (2021) Early snowmelt and sea ice breakup enhance algal export in the Beaufort Sea. Progress in Oceanography 190:102479. https://doi.org/10.1016/j.pocean.2020.102479

Naidu AS, Cooper LW, Finney BP, Macdonald RW, Alexander C, Semiletov IP (2000) Organic carbon isotope ratios (δ^{13}C) of Arctic Amerasian continental shelf sediments. International Journal of Earth Sciences 89:522-532. https://doi.org/10.1007/s005310000121

Nelson RJ, Ashjian CJ, Bluhm BA, Conlan KE, Gradinger RR, Grebmeier JM, Hill VJ, Hopcroft RR, Hunt BPV, Joo HM, Kirchman DL, Kosobokova KN, Lee SH, Li

WKW, Lovejoy C, Poulin M, Sherr E, Young KV (2014) Biodiversity and Biogeography of the Lower Trophic Taxa of the Pacific Arctic Region: Sensitivities to Climate Change. In: Grebmeier JM, Maslowski W (eds) The Pacific Arctic Region: Ecosystem Status and Trends in a Rapidly Changing Environment. Springer Netherlands, Dordrecht, https://doi.org/10.1007/978-94-017-8863-2_10

Nichols PD, Palmisano AC, Volkman JK, Smith GA, White DC (1988) Occurrence of an isoprenoid C_{25} diunsaturated alkene and high neutral lipid content in Antarctic sea-ice diatom communities. Journal of Phycology 24:90-96. https://doi.org/10.1111/j.1529-8817.1988.tb04459.x

Noren S, Udevitz MS, Jay C (2012) Bioenergetics model for estimating food requirements of female Pacific walruses *Odobenus rosmarus divergens*. Marine Ecology Progress Series 460:261-275. https://doi.org/10.3354/meps09706

Noren SR, Udevitz MS, Jay CV (2014) Energy demands for maintenance, growth, pregnancy, and lactation of female Pacific walruses (*Odobenus rosmarus divergens)*. Physiological and Biochemical Zoology 87:6, 837-854. https://doi.org/10.1086/678237

North CA, Lovvorn JR, Kolts JM, Brooks ML, Cooper LW, Grebmeier JM (2014) Deposit-feeder diets in the Bering Sea: potential effects of climatic loss of sea ice-related microalgal blooms. Ecological Applications 24:1525-1542. https://doi.org/10.1890/13-0486.1

Oliver J, Slattery P, O'Connor E, Lowry L (1983) Walrus, *Odobenus rosmarus*, Feeding in the Bering Sea: A Benthic Perspective. Fishery Bulletin 81:501-512. https://spo.nmfs.noaa.gov/content/walrus-odobenus-rosmarus-feeding-bering-sea-benthic-perspective

Olsen LM, Laney SR, Duarte P, Kauko HM, Fernández-Méndez M, Mundy CJ, Rösel A, Meyer A, Itkin P, Cohen L, Peeken I, Tatarek A, Różańska-Pluta M, Wiktor J, Taskjelle T, Pavlov AK, Hudson SR, Granskog MA, Hop H, Assmy P (2017) The seeding of ice algal blooms in Arctic pack ice: The multiyear ice seed repository hypothesis. Journal of Geophysical Research: Biogeosciences 122:1529-1548. https://doi.org/10.1002/2016jg003668

Overland JE, Stabeno PJ (2004) Is the climate of the Bering Sea warming and affecting the ecosystem? Eos, Transactions American Geophysical Union 85:309-312. https://doi.org/10.1029/2004EO330001

Oxtoby L, Horstmann L, Budge S, O'Brien D, Wang S, Schollmeier T, Wooller M (2017) Resource partitioning between Pacific walruses and bearded seals in the Alaska Arctic and sub-Arctic. Oecologia 184:385-398. https://doi.org/10.1007/s00442-017-3883-7

Peterson BJ, Fry B (1987) Stable isotopes in ecosystem studies. Annual Review of Ecology and Systematics 18:293-320. https://doi.org/10.1146/annurev.es.18.110187.001453

Petrich, C. and Eicken, H. (2017). Overview of sea ice growth and properties. In Sea Ice, D.N. Thomas (Ed.). https://doi.org/10.1002/9781118778371.ch1

Pickart RS, Nobre C, Lin P, Arrigo KR, Ashjian CJ, Berchok C, Cooper LW, Grebmeier JM, Hartwell I, He J (2019) Seasonal to mesoscale variability of water masses and atmospheric conditions in Barrow Canyon, Chukchi Sea. Deep Sea Research Part II: Topical Studies in Oceanography 162:32-49. https://doi.org/10.1016/j.dsr2.2019.02.003

Pickart RS, Weingartner TJ, Pratt LJ, Zimmermann S, Torres DJ (2005) Flow of winter-transformed Pacific water into the Western Arctic. Deep Sea Research Part II:

Topical Studies in Oceanography 52:3175-3198. https://doi.org/10.1016/j.dsr2.2005.10.009
Pineault S, Tremblay J-É, Gosselin M, Thomas H, Shadwick E (2013) The isotopic signature of particulate organic C and N in bottom ice: Key influencing factors and applications for tracing the fate of ice-algae in the Arctic Ocean. Journal of Geophysical Research: Oceans 118:287-300. https://doi.org/https://doi.org/10.1029/2012JC008331
Pirtle-Levy R, Grebmeier JM, Cooper LW, Larsen IL (2009) Chlorophyll a in Arctic sediments implies long persistence of algal pigments. Deep Sea Research Part II: Topical Studies in Oceanography 56:1326-1338. https://doi.org/10.1016/j.dsr2.2008.10.022
Pisareva MN, Pickart RS, Iken K, Ershova EA, Grebmeier JM, Cooper LW, Bluhm BA, Nobre C, Hopcroft RR, Hu H, Wang J, Ashjian CJ, Kosobokova KN, Whitledge TE (2015) The relationship between patterns of benthic fauna and zooplankton in the Chukchi Sea and physical forcing. Oceanography 28:68-83. www.jstor.org/stable/24861902
Poltermann M, Hop H, Falk-Petersen S (2000) Life under Arctic sea ice – reproduction strategies of two sympagic (ice-associated) amphipod species, *Gammarus wilkitzkii* and *Apherusa glacialis*. Marine Biology 136:913-920. https://doi.org/10.1007/s002270000307
Post DM (2002) Using stable isotopes to estimate trophic position: models, methods, and assumptions. Ecology 83:703-718. https://doi.org/10.1890/0012-9658(2002)083[0703:USITET]2.0.CO;2
Post DM, Layman CA, Arrington DA, Takimoto G, Quattrochi J, Montana CG (2007) Getting to the fat of the matter: models, methods and assumptions for dealing with lipids in stable isotope analyses. Oecologia 152:179-189. https://doi.org/10.1007/s00442-006-0630-x
Poulin M, Daugbjerg N, Gradinger R, Ilyash L, Ratkova T, von Quillfeldt C (2011) The pan-Arctic biodiversity of marine pelagic and sea-ice unicellular eukaryotes: a first-attempt assessment. Marine Biodiversity 41:13-28. https://doi.org/10.1007/s12526-010-0058-8
R Core Team (2017) R: A language and environment for statistical computing. R Foundation for Statistical Computing. Vienna, Austria https://www.R-project.org
Ramírez F, Tarroux A, Hovinen J, Navarro J, Afán I, Forero MG, Descamps S (2017) Sea ice phenology and primary productivity pulses shape breeding success in Arctic seabirds. Scientific Reports 7:1-9. https://doi.org/10.1038/s41598-017-04775-6
Ray GC, McCormick-Ray J, Berg P, Epstein HE (2006) Pacific walrus: benthic bioturbator of Beringia. Journal of Experimental Marine Biology and Ecology 330:403-419. https://doi.org/10.1016/j.jembe.2005.12.043
Regehr EV, Lunn NJ, Amstrup SC, Striling I (2007) Effects of Earlier Sea Ice Breakup on Survival and Population Size of Polar Bears in Western Hudson Bay. The Journal of Wildlife Management 71:2673-2683. https://doi.org/https://doi.org/10.2193/2006-180
Riebesell U, Schloss I, Smetacek V (1991) Aggregation of algae released from melting sea ice: implications for seeding and sedimentation. Polar Biology 11:239-248. https://doi.org/10.1007/BF00238457
Riedel A, Michel C, Gosselin M (2006) Seasonal study of sea-ice exopolymeric substances on the Mackenzie shelf: implications for transport of sea-ice bacteria and algae. Aquatic Microbial Ecology 45:195-206. https://doi.org/10.3354/ame045195

Roach A, Aagaard K, Pease C, Salo S, Weingartner T, Pavlov V, Kulakov M (1995) Direct measurements of transport and water properties through the Bering Strait. Journal of Geophysical Research: Oceans 100:18443-18457. https://doi.org/10.1029/95JC01673
Rode KD, Wilson RR, Regehr EV, St. Martin M, Douglas DC, Olson J (2015) Increased land use by Chukchi Sea polar bears in relation to changing sea ice conditions. PLOS ONE 10:e0142213. https://doi.org/10.1371/journal.pone.0142213
Rontani J-F, Amiraux R, Lalande C, Babin M, Kim H-R, Belt ST (2018a) Use of palmitoleic acid and its oxidation products for monitoring the degradation of ice algae in Arctic waters and bottom sediments. Organic Geochemistry 124:88-102. https://doi.org/10.1016/j.orggeochem.2018.06.002
Rontani J-F, Belt ST, Amiraux R (2018b) Biotic and abiotic degradation of the sea ice diatom biomarker IP_{25} and selected algal sterols in near-surface Arctic sediments. Organic Geochemistry 118:73-88. https://doi.org/10.1016/j.orggeochem.2018.01.003
Rontani J-F, Smik L, Belt ST (2019a) Autoxidation of the sea ice biomarker proxy IPSO25 in the near-surface oxic layers of Arctic and Antarctic sediments. Organic Geochemistry 129:63-76. https://doi.org/10.1016/j.orggeochem.2019.02.002
Rontani J-F, Smik L, Belt ST, Vaultier F, Armbrecht L, Leventer A, Armand LK (2019b) Abiotic degradation of highly branched isoprenoid alkenes and other lipids in the water column off East Antarctica. Marine Chemistry 210:34-47. https://doi.org/10.1016/j.marchem.2019.02.004
Rowland SJ, Belt ST, Wraige EJ, Massé G, Roussakis C, Robert JM (2001) Effects of temperature on polyunsaturation in cytostatic lipids of *Haslea ostrearia*. Phytochemistry 56:597-602. https://doi.org/10.1016/S0031-9422(00)00434-9
Schlitzer R (2016) Ocean Data View. http://odv.awi.de/
Schmidt K, Brown TA, Belt ST, Ireland LC, Taylor KWR, Thorpe SE, Ward P, Atkinson A (2018) Do pelagic grazers benefit from sea ice? Insights from the Antarctic sea ice proxy $IPSO_{25}$. Biogeosciences 15:1987-2006. https://doi.org/10.5194/bg-15-1987-2018
Schollmeier T, Oliveira A, Wooller M, Iken K (2018) Tracing sea ice algae into various benthic feeding types on the Chukchi Sea shelf. Polar Biology 41:207-224. https://doi.org/10.1007/s00300-017-2182-4
Selz V, Laney S, Arnsten AE, Lewis KM, Lowry KE, Joy-Warren HL, Mills MM, van Dijken GL, Arrigo KR (2018) Ice algal communities in the Chukchi and Beaufort Seas in spring and early summer: Composition, distribution, and coupling with phytoplankton assemblages. Limnology and Oceanography 63:1109-1133. https://doi.org/10.1002/lno.10757
Serreze MC, Meier WN (2018) The Arctic's sea ice cover: trends, variability, predictability, and comparisons to the Antarctic. Annals of the New York Academy of Sciences. https://doi.org/10.1111/nyas.13856
Seymour J, Horstmann-Dehn L, Wooller MJ (2014) Proportion of higher trophic-level prey in the diet of Pacific walruses (*Odobenus rosmarus divergens*). Polar Biology 37:941-952. https://doi.org/10.1007/s00300-014-1492-z
Sheffield G, Grebmeier JM (2009) Pacific walrus (*Odobenus rosmarus divergens*): Differential prey digestion and diet. Marine Mammal Science 25:761-777. https://doi.org/10.1111/j.1748-7692.2009.00316.x
Siddon EC, Zador SG, Hunt GL (2020) Ecological responses to climate perturbations and minimal sea ice in the northern Bering Sea. Deep Sea Research Part II: Topical

Studies in Oceanography 181-182:104914. https://doi.org/10.1016/j.dsr2.2020.104914
Slagstad D, Wassmann PFJ, Ellingsen I (2015) Physical constrains and productivity in the future Arctic Ocean. Frontiers in Marine Science 2. https://doi.org/10.3389/fmars.2015.00085
Smik L, Cabedo-Sanz P, Belt ST (2016) Semi-quantitative estimates of paleo Arctic sea ice concentration based on source-specific highly branched isoprenoid alkenes: A further development of the PIP 25 index. Organic Geochemistry 92:63-69. https://doi.org/10.1016/j.orggeochem.2015.12.007
Smith MA (2010) Arctic Marine Synthesis: Atlas of the Chukchi and Beaufort Seas. Audubon Alaska and Oceana, Anchorage, AK, https://ak.audubon.org/conservation/arctic-marine-synthesis-atlas-chukchi-and-beaufort-seas
Smith REH, Harrison WG, Harris LR, Herman AW (1990) Vertical fine structure of particulate matter and nutrients in sea ice of the high Arctic. Canadian Journal of Fisheries and Aquatic Sciences 47:1348-1355. https://doi.org/10.1139/f90-154
Sonsthagen SA, Jay CV, Cornman RS, Fischbach AS, Grebmeier JM, Talbot SL (2020) DNA metabarcoding of feces to infer summer diet of Pacific walruses. Marine Mammal Science 36:1196-1211. https://doi.org/10.1111/mms.12717
Søreide JE, Carroll ML, Hop H, Ambrose Jr WG, Hegseth EN, Falk-Petersen S (2013) Sympagic-pelagic-benthic coupling in Arctic and Atlantic waters around Svalbard revealed by stable isotopic and fatty acid tracers. Marine Biology Research 9:831-850. https://doi.org/10.1080/17451000.2013.775457
Søreide JE, Leu EV, Berge J, Graeve M, Falk-Petersen S (2010) Timing of blooms, algal food quality and *Calanus glacialis* reproduction and growth in a changing Arctic. Global Change Biology 16:3154-3163. https://doi.org/10.1111/j.1365-2486.2010.02175.x
Sørensen HL, Thamdrup B, Jeppesen E, Rysgaard S, Glud RN (2017) Nutrient availability limits biological production in Arctic sea ice melt ponds. Polar Biology 40:1593-1606. https://doi.org/10.1007/s00300-017-2082-7
Stabeno PJ, Bell SW (2019) Extreme conditions in the Bering Sea (2017–2018): Record-breaking low sea-ice extent. Geophysical Research Letters 46:8952-8959. https://doi.org/10.1029/2019GL083816
Stabeno PJ, Bell SW, Bond NA, Kimmel DG, Mordy CW, Sullivan ME (2019) Distributed biological observatory region 1: physics, chemistry and plankton in the northern Bering sea. Deep Sea Research Part II: Topical Studies in Oceanography 162:8-21. https://doi.org/10.1016/j.dsr2.2018.11.006
Stabeno PJ, Mordy CW, Sigler MF (2020) Seasonal patterns of near-bottom chlorophyll fluorescence in the eastern Chukchi Sea: 2010–2019. Deep Sea Research Part II: Topical Studies in Oceanography 177:104842. https://doi.org/10.1016/j.dsr2.2020.104842
Stein R, Fahl K, Gierz P, Niessen F, Lohmann G (2017a) Arctic Ocean sea ice cover during the penultimate glacial and the last interglacial. Nature Communications 8:1-13. https://doi.org/10.1038/s41467-017-00552-1
Stein R, Fahl K, Schade I, Manerung A, Wassmuth S, Niessen F, Nam S-I (2017b) Holocene variability in sea ice cover, primary production, and Pacific-Water inflow and climate change in the Chukchi and East Siberian Seas (Arctic Ocean). Journal of Quaternary Science 32:362-379. https://doi.org/10.1002/jqs.2929

Stein R, Fahl K, Schreck M, Knorr G, Niessen F, Forwick M, Gebhardt C, Jensen L, Kaminski M, Kopf A (2016) Evidence for ice-free summers in the late Miocene central Arctic Ocean. Nature Communications 7:1-13. https://doi.org/https://doi.org/10.1038/ncomms11148

Steward GF, Smith DC, Azam F (1996) Abundance and production of bacteria and viruses in the Bering and Chukchi Seas. Marine Ecology Progress Series 131:287-300. https://doi.org/10.3354/meps131287

Stimmelmayr R, Bryan A, Lampe WH, Ferrera L, Hepa T (2016) Mortality due to trampling and mesenteric root torsion in Pacific walrus. Alaska Marine Science Symposium, Anchorage, Alaska. http://www.north-slope.org/assets/images/uploads/Mesenteric_torsion_walrus_AMSS2016_RSTdraft.pdf

Stirling I, Derocher AE (1993) Possible impacts of climatic warming on polar bears. Arctic 46:240-245. http://www.jstor.org/stable/40511411

Stoynova V, Shanahan TM, Hughen KA, de Vernal A (2013) Insights into Circum-Arctic sea ice variability from molecular geochemistry. Quaternary Science Reviews 79:63-73. https://doi.org/10.1016/j.quascirev.2012.10.006

Sun M-Y, Clough LM, Carroll ML, Dai J, Ambrose Jr WG, Lopez GR (2009) Different responses of two common Arctic macrobenthic species (*Limecola balthica* and *Monoporeia affinis*) to phytoplankton and ice algae: Will climate change impacts be species specific? Journal of Experimental Marine Biology and Ecology 376:110-121. https://doi.org/10.1016/j.jembe.2009.06.018

Szymanski A, Gradinger R (2016) The diversity, abundance and fate of ice algae and phytoplankton in the Bering Sea. Polar Biology 39:309-325. https://doi.org/10.1007/s00300-015-1783-z

Thoman RL, Bhatt US, Bieniek PA, Brettschneider BR, Brubaker M, Danielson SL, Labe Z, Lader R, Meier WN, Sheffield G (2020) The record low Bering Sea ice extent in 2018: Context, impacts, and an assessment of the role of anthropogenic climate change. Bulletin of the American Meteorological Society 101:S53-S58. https://doi.org/10.1175/BAMS-D-19-0175.1

Thomas DN, Dieckmann GS (2002) Antarctic sea ice – a habitat for extremophiles. Science 295:641. https://doi.org/10.1126/science.1063391

Thyrring J, Rysgaard S, Blicher ME, Sejr MK (2015) Metabolic cold adaptation and aerobic performance of blue mussels (*Mytilus edulis*) along a temperature gradient into the High Arctic region. Marine Biology 162:235-243. https://doi.org/10.1007/s00227-014-2575-7

Tibshirani R, Walther G, Hastie T (2001) Estimating the number of clusters in a data set via the gap statistic. Journal of the Royal Statistical Society: Series B (Statistical Methodology) 63:411-423. https://doi.org/10.1111/1467-9868.00293

Tremblay J-E, Michel C, Hobson KA, Gosselin M, Price NM (2006) Bloom dynamics in early opening waters of the Arctic Ocean. Limnology and Oceanography 51:900-912. https://doi.org/10.4319/lo.2006.51.2.0900

Udevitz MS, Jay CV, Taylor RL, Fischbach AS, Beatty WS, Noren SR (2017) Forecasting consequences of changing sea ice availability for Pacific walruses. Ecosphere 8:e02014. https://doi.org/10.1002/ecs2.2014

Utermöhl vH (1931) Neue Wege in der quantitativen Erfassung des Planktons. (Mit besondere Beriicksichtigung des Ultraplanktons). Verh Int Verein Theor Angew Limnol, 5, 567–595. (in German)

Vander Zanden MJ, Clayton MK, Moody EK, Solomon CT, Weidel BC (2015) Stable isotope turnover and half-life in animal tissues: a literature synthesis. PLOS ONE 10:e0116182. https://doi.org/10.1371/journal.pone.0116182

Volkman JK (2020) Lipids of geochemical interest in microalgae. In: H. Wilkes (ed.) Hydrocarbons, Oils and Lipids: Diversity, Origin, Chemistry and Fate, Handbook of Hydrocarbon and Lipid Microbiology:159-191. https://doi.org/10.1007/978-3-319-90569-3_10

Volkman JK, Barrett SM, Blackburn SI, Mansour MP, Sikes EL, Gelin F (1998) Microalgal biomarkers: a review of recent research developments. Organic Geochemistry 29:1163-1179. https://doi.org/10.1016/S0146-6380(98)00062-X

Volkman JK, Barrett SM, Dunstan GA (1994) C25 and C30 highly branched isoprenoid alkenes in laboratory cultures of two marine diatoms. Organic Geochemistry 21:407-414. https://doi.org/10.1016/0146-6380(94)90202-X

Waga H, Hirawake T, Grebmeier JM (2020) Recent change in benthic macrofaunal community composition in relation to physical forcing in the Pacific Arctic. Polar Biology, https://doi.org/10.1007/s00300-020-02632-3:1-10.

Wang M, Yang Q, Overland JE, Stabeno P (2018) Sea-ice cover timing in the Pacific Arctic: The present and projections to mid-century by selected CMIP5 models. Deep Sea Research Part II: Topical Studies in Oceanography 152:22-34. https://doi.org/10.1016/j.dsr2.2017.11.017

Wang SW, Budge SM, Gradinger RR, Iken K, Wooller MJ (2014a) Fatty acid and stable isotope characteristics of sea ice and pelagic particulate organic matter in the Bering Sea: tools for estimating sea ice algal contribution to Arctic food web production. Oecologia 174:699-712. https://doi.org/10.1007/s00442-013-2832-3

Wang, S, Bailey, D, Lindsay, K, Moore, JK, Holland, M (2014b). Impact of sea ice on the marine iron cycle and phytoplankton productivity. Biogeosciences, 11(17), 4713-4731. https://doi.org/10.5194/bg-11-4713-2014

Weeks WF, Ackley SF (1986) The Growth, Structure, and Properties of Sea Ice. In: Untersteiner N. (eds) The Geophysics of Sea Ice. NATO ASI Series (Series B: Physics): 9-164. Springer, Boston, MA. https://doi.org/10.1007/978-1-4899-5352-0_2

Weingartner T, Aagaard K, Woodgate R, Danielson S, Sasaki Y, Cavalieri D (2005) Circulation on the north central Chukchi Sea shelf. Deep Sea Research Part II: Topical Studies in Oceanography 52:3150-3174. https://doi.org/10.1016/j.dsr2.2005.10.015

Weingartner T, Fang Y-C, Winsor P, Dobbins E, Potter R, Statscewich H, Mudge T, Irving B, Sousa L, Borg K (2017) The summer hydrographic structure of the Hanna Shoal region on the northeastern Chukchi Sea shelf: 2011–2013. Deep Sea Research Part II: Topical Studies in Oceanography 144:6-20. https://doi.org/10.1016/j.dsr2.2017.08.006

Welschmeyer NA (1994) Fluorometric analysis of chlorophyll a in the presence of chlorophyll b and pheopigments. Limnology and Oceanography 39:1985-1992. https://doi.org/10.4319/lo.1994.39.8.1985

Wickham H (2016) ggplot2: Elegant Graphics for Data Analysis. Springer-Verlag, New York

Wiedmann I, Ershova E, Bluhm BA, Nöthig E-M, Gradinger RR, Kosobokova K, Boetius A (2020) What feeds the benthos in the Arctic basins? Assembling a carbon budget for the deep Arctic Ocean. Frontiers in Marine Science 7. https://doi.org/10.3389/fmars.2020.00224

Wilt LM, Grebmeier JM, Miller TJ, Cooper LW (2014) Caloric content of Chukchi Sea benthic invertebrates: Modeling spatial and environmental variation. Deep Sea Research Part II: Topical Studies in Oceanography 102:97-106. https://doi.org/10.1016/j.dsr2.2013.09.025

Woodgate RA (2018) Increases in the Pacific inflow to the Arctic from 1990 to 2015, and insights into seasonal trends and driving mechanisms from year-round Bering Strait mooring data. Progress in Oceanography 160:124-154. https://doi.org/10.1016/j.pocean.2017.12.007

Woodgate RA, Aagaard K, Weingartner TJ (2005a) Monthly temperature, salinity, and transport variability of the Bering Strait through flow. Geophysical Research Letters 32:n/a-n/a. https://doi.org/10.1029/2004gl021880

Woodgate RA, Aagaard K, Weingartner TJ (2005b) A year in the physical oceanography of the Chukchi Sea: Moored measurements from autumn 1990–1991. Deep Sea Research Part II: Topical Studies in Oceanography 52:3116-3149. https://doi.org/10.1016/j.dsr2.2005.10.016

Xiao X, Fahl K, Müller J, Stein R (2015) Sea-ice distribution in the modern Arctic Ocean: Biomarker records from trans-Arctic Ocean surface sediments. Geochimica et Cosmochimica Acta 155:16-29. https://doi.org/10.1016/j.gca.2015.01.029

Young JK, Black BA, Clarke JT, Schonberg SV, Dunton KH (2017) Abundance, biomass and caloric content of Chukchi Sea bivalves and association with Pacific walrus (*Odobenus rosmarus divergens*) relative density and distribution in the northeastern Chukchi Sea. Deep Sea Research Part II: Topical Studies in Oceanography 144:125-141. https://doi.org/10.1016/j.dsr2.2017.04.017

Yunda-Guarin G, Brown TA, Michel LN, Saint-Béat B, Amiraux R, Nozais C, Archambault P (2020) Reliance of deep-sea benthic macrofauna on ice-derived organic matter highlighted by multiple trophic markers during spring in Baffin Bay, Canadian Arctic. Elementa: Science of the Anthropocene 8. https://doi.org/10.1525/elementa.2020.047

Yurkowski DJ, Brown TA, Blanchfield PJ, Ferguson SH (2020) Atlantic walrus signal latitudinal differences in the long-term decline of sea ice-derived carbon to benthic fauna in the Canadian Arctic. Proceedings of the Royal Society B 287:20202126. https://doi.org/10.1098/rspb.2020.2126

Zagrebelny SV, Kochnev AA (2017) Influence of climate change on summer-fall distribution of pacific walrus in the western Bering Sea: analysis of reasons and consequences // Izv. TINRO. 190:62–71. https://doi.org/10.26428/1606-9919-2017-190-102-11 (in Russian). Available from: https://www.researchgate.net/publication/320901039_Influence_of_climate_change_on_summer-fall_distribution_of_pacific_walrus_in_the_western_Bering_Sea_analysis_of_reasons_and_consequences [accessed Mar 11 2021].